Capacity Analysis of Signalised Intersections in Motorcycle Dependent Cities

M.Eng. Huynh Duc Nguyen

TECHNISCHE UNIVERSITÄT DARMSTADT

A dissertation submitted in fulfilment of the requirements for the Degree of Doktor-Ingenieur (Dr.-Ing.) of the Department of Civil and Environmental Engineering, Technische Universität Darmstadt.

Supervisor: Prof. Dr.-Ing. Manfred Boltze
Technische Universität Darmstadt, Germany

Co-supervisor: Prof. Dr. Eng. Hideki Nakamura
Nagoya University, Japan

Date of submission: 16.10.2018 Date of oral examination: 11.02.2019

D17 Darmstadt 2018

Nguyen, Huynh Duc

Capacity Analysis of Signalised Intersections in Motorcycle Dependent Cities

Herausgeber:
Technische Universität Darmstadt
Institut für Verkehrsplanung und Verkehrstechnik
Otto-Berndt-Str. 2
64287 Darmstadt

www.tu-darmstadt.de/verkehr
fgvv@verkehr.tu-darmstadt.de

Schriftenreihe der Instituts für Verkehr
Institut für Verkehrsplanung und Verkehrstechnik
Heft V43

ISSN 1613-8317

Year thesis published in Tuprints 2020
Date of the viva voce 11.02.2019

Acknowledgement

First, I would like to express my sincere appreciation to the co-operation program between Vietnamese-German Transport Research Centre, Vietnamese-German University, Vietnam and Technische Universität Darmstadt, Germany. I had an opportunity to conduct this study thanks to this program.

I also would like to express my thanks to the Ministry of Education and Training of Vietnam (MOET) and relevant agencies for supporting me with the 911 scholarship during my study at Darmstadt University of Technology.

Especially, I would like to express my sincere gratitude to Professor Dr.-Ing. Manfred Boltze, Head of the Institute of Transport Planning and Traffic Engineering, Technische Universität Darmstadt, Germany, as the first supervisor of my work. Without his supervision, I would not have completed this research. It is also very lucky for me to send my sincere thanks to the co-supervisor, Prof. Dr. Eng. Hideki Nakamura, as the second supervisor of my work. He discussed and gave me valuable recommendations with his experiences.

I would like to appreciate Dr. Vu Anh Tuan, director of the VGTRC, for his support in discussing and giving comments of my research. I also want to give grateful thanks to Dr. Chu Cong Minh, the former executive manager of VGTRC, and Dr. Khuat Viet Hung, the former co-director of VGTRC. They introduced me to the doctoral program and supported me to fulfil the requirements and the acceptance by Professor Dr.-Ing. Manfred Boltze.

My sincere gratitudes are directed to my colleagues in VGTRC, TU Darmstadt and other friends from Nagoya University, Tongji University and Indian Institute of Technology Kharagpur. They never hesitated to give me feedbacks and discussions from their point of view. That great working environment is a success factor to my completion.

I'm very lucky to have help from the secretary, students and other relevant people at Darmstadt during my stay there. I would like to give my thanks for all their help.

Finally, I would like to express my appreciation towards my family members. Without their encouragement, sympathy and support, I cannot complete my dream and finish this dissertation.

Abstract

The capacity of a traffic stream is one of the most significant parts of traffic performance analysis. Particularly, capacity analysis of signalised intersections has been studied in developed countries where the primary transportation mode is the private car usage. In some developing countries, however, there are several distinctive traffic flow characteristics in contrast with those in developed countries such as 80% of traffic composition being motorcycles, which is leading to the term 'Motorcycle Dependent City (MDC)'. Moreover, motorcycle driving behaviour in MDCs is entirely different from four-wheeled vehicle driving behaviour in car dependent cities. Therefore, we cannot use models defined for car traffic in developed countries to analyse performances of motorcycle traffic and to evaluate the capacities of signalised intersections in developing countries such as Vietnam.

This research focuses on proposing suitable models which can explain the specific characteristics of traffic streams in MDCs and the intersection capacities in different traffic situations. This goal can be divided into objectives: finding factors that affect the capacity of signalised intersections significantly; proposing a suitable capacity calculation method; developing a capacity calculation guideline for signalised intersections in MDCs. However, the research area of this study is limited to the concept of MDCs in which the motorcycle occupies a high share in traffic composition.

The comprehensive literature review on the capacity of signalised intersections is conducted in both, car dependent cities and motorcycle dependent cities, to understand the calculation method throughout various countries. Several methods and manuals in car traffic-based conditions such as German Highway Capacity Manual (HBS) (FGSV, 2015), American Highway Capacity Manual (HCM) (TRB 2010), Indonesia Highway Capacity Manual 1997 (IHCM 1997), Malaysia Highway Capacity Manual 2011 (MHCM 2011) and the Manual on Traffic Signal Control in 2006 (JSTE 2006) are introduced. Besides, some models from researched projects in MDCs are mentioned to indicate the difference in traffic situations between these cities and others. Basically, the capacity of signalised intersections includes two main components: the saturation flow rate and the effective green ratio. The saturation flow rate would be calculated by the base saturation flow rate and is adjusted by some influencing factors. Depending on the characteristics of each location and the selected method, the saturation flow rate analysis process may differ from car traffic-based flow to motorcycle traffic-based flow. In this study, the saturation flow rate models would also follow the common concept of previous studies. The base saturation flow rate will be investigated, and the motorcycle unit will be used as the basic unit. Then some main adjustment factor will be applied for the model such as approach width, vehicle type, turning activities, etc. On the other hand, the effective green ratio shows the correlation between the effective green time and the cycle time. In car traffic-based flow, the effective green time has been proved to be 1 s higher than the displayed green time. However, in MDCs, this outcome is still a controversial question and is needed to be evaluated because of its unique traffic characteristics.

The traffic characteristics at signalised intersections in MDCs are analysed to figure out how they affect the intersection capacity. The traffic characteristics are categorised into several factors: vehicle characteristics, volume characteristics, speed characteristics, lane allocation characteristics, traffic signal systems, and driver behaviour. From the literature review and the traffic characteristics which are mentioned, the overall capacity model for MDCs is built up as the combination of the saturation flow rate model, the effective green time model, and the intergreen time model. The normal capacity and the maximum capacity are estimated depending on the different effective green times. Besides the proposed theoretical models, field observations are also conducted in Ho Chi Minh City, Vietnam for the model calibration process. The contents and the researching results of each model can be summarised as follows:

- The saturation flow rate is estimated by the motorcycle saturation flow rate and adjustment factors. In the model, the term 'normalised saturation flow rate' which is defined as the saturation flow rate passing over one-meter approach width is introduced. Observation results showed that the normalised saturation flow rate was calculated at 3,058 mcu/(h*m) when the green time was higher or equal to 16 s. That rate was estimated at 3,178 mcu/(h*m) when the green time was lower than 16 s.
- Motorcycle equivalent unit (MCU) is chosen as a basic unit to apply the conversion of heterogeneous streams to homogeneous motorcycle streams. The MCU values may vary depending on the share of passenger cars in the flow. The MCU value changes from 5.5 to 6.8 corresponding with the car share value of 5% to 100%. The recommended MCU values for cars, middle heavy vehicles and heavy vehicles for normal calculation are 6, 9 and 14.4, respectively.
- Besides the adjustment factor for the approach width, the adjustment factors for vehicle types and turning movements are considered as the main affecting factors of the saturation flow rate model. The numerical results indicated that the impact of vehicle type was the primary factor and contributed to reducing the approach capacity significantly. As regards the effect of turning movements, different turning types have different effects on the approach capacity. Right-turning motorcycles do not influence the discharge flow rate because they are assigned to run on the right side of the flow. Right-turning cars, however, affect the through-flow significantly because of their left-side position. Left-turning motorcycles interfere through-discharging cars and left-turning cars, and they would reduce the discharging speed of through-vehicles.
- The effective green time model applies a method to count the number of motorcycles passing the stop line during certain time periods. Two models are classified: model 1 when the rule 'no red-light running' is strictly obeyed and model 2 when the rule 'no red-light running' is ignored. In the first model, the effective green time was proven to be equal to the displayed green time. In the second model, the effective green time was estimated to be equal to the displayed green time plus 2 s.
- The intergreen time model in MDCs applies the German method with some modifications. The crossing time was recommended to be equal to the amber time which is set up at 3 s for most cases. The clearing time was increased by the addition of the interaction time between clearing through-vehicles and clearing opposing left-turning movements. The interaction time depends on vehicle types at each stream and was suggested as 1 s. The entering time was calculated by the entering distance which was defined from the middle point of the stop line to the centre of the conflict area between the entering route and the clearing route, and the entering speed was observed as 5 m/s.
- The normal capacity and the maximum capacity are estimated depending on the different effective green times. The normal capacity is presented along with the rule 'no red-light running' which drivers must obey. Besides, the maximum capacity is given along with weak acceptance of the rule 'no red-light running' which is ignored by many drivers, in practice. In this thesis, the normal capacity is recommended for the capacity analysis. The maximum capacity is considered as an adaption to the current traffic situation while the illegal driving behaviour could not be controlled.

After proposing the comprehensive capacity model of signalised intersections, a procedure for application of that model and a sample calculation are introduced. The procedure for application is presented as a guideline which depicts step by step capacity calculation at signalised intersections in MDCs for operational and planning purposes. Finally, this research concludes with recommendations, limitations, and further studies.

Kurzfassung

Die Kapazität eines Verkehrsstroms ist einer der Hauptbestandteile zur Analyse der Leistungsfähigkeit im Verkehr. In entwickelten Ländern, in denen das primäre Verkehrsmittel das private Automobil ist, wurde insbesondere die Kapazitätsanalyse von signalisierten Knotenpunkten analysiert. In einigen Entwicklungsländern gibt es mehrere Besonderheiten gegenüber entwickelten Ländern im Verkehrsablauf, wie ein 80-prozentiger Verkehrsanteil von Motorrädern. Daher wurde der Begriff der motorradabhängigen Stadt / Motorcycle Dependent City (MDC) eingeführt. Außerdem unterscheidet sich das Fahrerverhalten von Kraftradfahrern in MDC sehr stark von dem Fahrerverhalten vierrädriger Fahrzeuge in autoabhängigen Städten. Deshalb können Modelle, die für die Analyse des Autoverkehrs bestimmt sind, nicht verwenden werden um die Leistungsfähigkeit des Motorradverkehrs zu analysieren und die Kapazität von signalisierten Knotenpunkten in Entwicklungsländern wie Vietnam zu beurteilen.

Diese Arbeit soll geeignete Modelle erarbeiten, die spezifische Charakteristika von Verkehrsströmen in MDCs berücksichtigen und Kapazitäten von Knotenpunkten in verschiedenen Verkehrssituationen erklären können. Das Ziel der Arbeit kann in folgende Unterziele aufgeteilt werden: Vorschlag einer geeigneten Kapazitätsberechnungsmethode; Identifizierung von Faktoren, durch die die Kapazität von signalisierten Knotenpunkten signifikant beeinflusst wird; Datenerhebung durch Feldbeobachtungen; Analyse von Knotenpunktkapazitäten in MDCs; Entwicklung eines Leitfadens für signalisierte Knotenpunkte in MDCs. Das Untersuchungsgebiet dieser Arbeit beschränkt sich auf MDCs in denen Motorräder einen sehr hohen Verkehrsanteil einnehmen.

Die umfassende Literaturrecherche zur Kapazitätsbetrachtung von signalisierten Knotenpunken wurde sowohl für autoabhängige Städte als auch für motorradabhängige Städte durchgeführt, um ein Verständnis für die Berechnungsmethoden in verschiedenen Ländern zu entwickeln. Eine Vielzahl von Methoden und Handbüchern für Autoverkehr, wie das deutsche Handbuch für die Bemessung von Straßenverkehrsanlagen (HBS) (FGSV, 2015), das US-amerikanische Highway Capacity Manual (HCM) (TRB 2010), das indonesische Highway Capacity Manual 1997 (IHCM 1997), das malaysische Highway Capacity Manual 2011 (MHCM 2011), und das Manual on Traffic Signal Control von 2006 (JSTE 2006) werden vorgestellt. Zudem werden Modelle von Forschungsprojekten in MDCs dargestellt, um die Unterschiede der verschiedenen Verkehrssituationen in diesen und anderen Städten zu verdeutlichen. Grundsätzlich umfasst die Kapazität von signalisierten Knotenpunkten zwei Hauptkomponenten: Die resultierende Sättigungsverkehrsstärke und den effektiven Freigabezeitanteil. Die resultierende Sättigungsverkehrsstärke wird berechnet über die Sättigungsverkehrsstärke bei Standardbedingungen und zugehörige Abminderungsfaktoren. Abhängig von örtlichen Gegebenheiten und der verwendeten Methode kann sich der Prozess zur Bestimmung der Sättigungsverkehrsstärke zwischen autobasiertem Verkehrsfluss und motorradbasiertem Verkehrsfluss unterscheiden. In dieser Arbeit sollen die Modelle zur Bestimmung der Sättigungsverkehrsstärke dem grundlegenden Konzept früherer Studien folgen. Die Sättigungsverkehrsstärke bei Standardbedingungen wird untersucht, und Motorräder werden als Basiseinheit zur Homogenisierung des Verkehrsflusses verwendet. Danach wurde einige primäre Anpassungsfaktoren, wie Zufahrtsbreite, Fahrzeugtyp, Abbiegevorgänge auf das Modell angewendet. Der effektive Freigabezeitanteil beschreibt das Verhältnis zwischen der effektiven Freigabezeit und der Umlaufzeit. Im autobasierten Verkehrsfluss wurde nachgewiesen, dass die effektive Freigabezeit 1s höher ist als die angezeigte Grünzeit. Allerdings ist dieses Ergebnis für MDCs noch umstritten, und es besteht aufgrund der besonderen Verkehrscharakteristika die Notwendigkeit, dies zu evaluieren.

Die Verkehrseigenschaften an signalisierten Knotenpunkten in MDCs werden analysiert, um herauszufinden, welchen Effekt sie auf die Kapazität von Knotenpunkten haben. Die Verkehrseigenschaften werden wie folgt kategorisiert: Fahrzeugeigenschaften, Verkehrstärken, Geschwindigkeiten, Fahrstreifenzuordnung, Lichtsignalsysteme und Fahrerverhalten. Auf Grundlage

der Literaturanalyse und den Verkehrseigenschaften wird das übergreifende Kapazitätsmodel für MDCs aus einer Kombination des Sättigungsverkehrsstärkenmodells, des Modells der effektiven Freigabezeit und des Zwischenzeitenmodells aufgebaut. Die Standardkapazität und die maximale Kapazität werden abhängig von den unterschiedlichen effektiven Freigabezeiten geschätzt. Neben dem vorgeschlagenen theoretischen Modell werden Feldbeobachtungen für den Kalibrierungsprozess des Modells in Ho Chi Minh City (Vietnam) durchgeführt. Die Inhalte und die Forschungsergebnisse zur Modellierung können wie folgt zusammengefasst werden:

- Die Sättigungsverkehrsstärke wird über die Sättigungsverkehrsstärke der Motorräder und die Anpassungsfaktoren bestimmt. Im Modell wird der Term „normalisierte Sättigungsverkehrsstärke' eingeführt als die Sättigungsverkehrsstärke für einen Meter Zufahrtsbreite, da die Sättigungsverkehrsstärke pro Fahrstreifen in MDCs nicht geeignet für die Berechnung ist. Beobachtungsergebnisse haben gezeigt, dass sich eine normalisierte homogene Flussrate von Krafträdern von 3058 mcu/(h*m) während einer Freigabezeit größer oder gleich 16 s ergibt. Bei einer Freigabezeit von weniger als 16 s ergibt sich ein Wert von 3178 mcu/(h*m).

- Die Motorradeinheit (MCU) wurde als Basiseinheit in dieser Arbeit gewählt, um heterogene Ströme in homogene Ströme von Krafträdern umzurechnen. Die MCU-Äquivalenzwerte können aufgrund der Anteile von Autos im Verkehrsstrom variieren. Der MCU-Äquivalenzwert schwankt zwischen 5,5 und 6,8 in Abhängigkeit vom Verkehrsanteil der Autos von 5% bis 100%. Der empfohlene MCU-Äquivalenzwert für Autos, Minibusse und Busse beträgt jeweils 6,9 und 14,4.

- Neben dem Anpassungsfaktor für die Zufahrtsbreite zählen der Anpassungsfaktor für die Fahrzeugtypen und der Anpassungsfaktor für Abbiegevorgänge zu den primären Einflussfaktoren im Sättigungsverkehrsstärkenmodell. Die numerischen Ergebnisse zeigen, dass der Fahrzeugtyp der primäre Einflussfaktor ist und dazu beiträgt, die Kapazität einer Zufahrt signifikant zu verringern. In MDCs hängt der Effekt von abbiegenden Fahrzeugen, welche geradeausfahrende Fahrzeuge blockieren, von der Position im Verkehrsstrom ab. Unterschiedliche Abbiegearten haben unterschiedliche Effekte auf die Zufahrtskapazität. Rechts abbiegende Motorräder haben keinen Einfluss auf den Abfluss des Verkehrs, weil sie bereits auf der rechten Seite des Verkehrsstroms angeordnet sind. Rechtsabbiegende Autos haben jedoch einen signifikanten Einfluss auf den Abfluss anderer Fahrzeuge, da sie im Verkehrsstrom links angeordnet sind. Linksabbiegende Krafträder beeinträchtigen geradeaus abfließende Autos und links abbiegende Autos und reduzieren die Abflussgeschwindigkeit geradeausfahrender Fahrzeuge.

- Das Modell der effektiven Freigabezeit wendet eine Verkehrsdichteerfassung an, um die Anzahl der Fahrzeuge, die die Haltelinie in einer definierten Zeitperiode überfahren, zu zählen. Zwei Modelle wurden entwickelt: Modell 1, bei dem die Regel 'kein Fahren über Rot' streng befolgt wurde, und Modell 2, bei dem die Regel „kein Fahren über Rot' nicht eingehalten wurde, was in Vietnam leider von vielen Fahrern getan wird. Im ersten Modell konnte festgestellt werden, dass die effektive Freigabezeit der angezeigten Grünzeit entspricht. Im zweiten Modell wurde festgestellt, dass die effektive Freigabezeit annähernd der angezeigten Grünzeit entspricht und diese lediglich um 2s überschreitet.

- Das Zwischenzeitenmodell in MDCs ist vergleichbar mit der deutschen Methode, jedoch mit einigen Modifikationen. Es wird empfohlen, für die Überfahrzeit die Gelbzeit anzusetzen, welche in den meisten Fällen 3s beträgt. Die Räumzeit wurde um einen Interaktionszeitraum zwischen dem räumenden Geradeausstrom und dem jeweils entgegenkommenden räumenden Linksabbiegerstrom verlängert. Die Interaktionszeit ist abhängig von den Fahrzeugtypen im jeweiligen Verkehrsstrom und wurde mit 1s angenommen. Die Einfahrzeit wurde kalkuliert über den Einfahrweg, welcher definiert wurde als Distanz vom Mittelpunkt der Haltelinie bis zum Konfliktpunkt zwischen den einfahrenden und den räumenden Fahrzeugtrajektorien, und der beobachteten Einfahrgeschwindigkeit von 5 m/s.

- Die Standardkapazität und die Maximalkapazität wurden abhängig von den unterschiedlichen effektiven Freigabezeiten geschätzt. Die normale Kapazität wird gemeinsam mit der Regel „nicht über Rot fahren', welche die Fahrer befolgen müssen, angenommen. Die maximale Kapazität wird unter der Annahme ermittelt, dass Fahrer sich nicht an die Regel „nicht über Rot fahren' halten, was in Vietnam häufig zu beobachten ist. In dieser Arbeit wird die Standardkapazität für die Kapazitätsanalyse empfohlen. Die Maximalkapazität wird zur Widerspiegelung der aktuellen Verkehrssituation, in der das illegale Fahrverhalten nicht kontrolliert werden kann, herangezogen.

Nach der Vorstellung des umfassenden Kapazitätsmodells für signalisierte Knotenpunkte werden ein Verfahren zur Anwendung des Modells und eine Beispielkalkulation vorgestellt. Das Verfahren zur Anwendung des Modells wird in Form eines Leitfadens für operative und planerischer Zwecke ausgearbeitet, welcher eine schrittweise Kapazitätsberechnung für signalisierte Knotenpunkte in MDCs enthält. Die Arbeit schließt mit Empfehlungen, Einschränkungen und einem Ausblick auf weiteren Forschungsbedarf ab.

Table of Contents

1 Introduction

1.1 Background of the Study

The capacity of a traffic stream is one of the most significant parts of traffic performance analysis. Particularly, capacity analysis of signalised intersections has been studied in developed countries where the primary transportation mode is the private car usage. In some developing countries, however, there are much distinctive traffic flow characteristics in contrast with those in developed countries such as 80% of the traffic composition being motorcycles, leading to the term 'Motorcycle Dependent City (MDC)' (Figure 1-1). Moreover, motorcycle driving behaviour in MDCs is entirely different from four-wheeled vehicle driving behaviour in car-dependent cities. Therefore, we cannot use models defined for car traffic in developed countries to analyse performances of motorcycle traffic and to evaluate the capacities of signalised intersections in developing countries such as Vietnam.

Figure 1-1: Traffic Operation at a Signalised Intersection in MDCs

Note. Own Picture

This research focuses on proposing suitable models which can explain the specific characteristics of traffic streams in MDCs and the intersection capacities in different traffic situations.

1.2 The Concept of Motorcycle Dependent Cities

The term 'Motorcycle Dependent City (MDC)' has been presented by Khuat (2006). The motorcycle dependence is defined by three groups of indicators: vehicle ownership, availability of alternatives to motorcycle and car, and use of the motorcycle. The rating system (high, medium, low) of grading motorcycle dependence is shown in Table 1-1.

Table 1-1: Indicators of the Motorcycle Dependence

Indicators			Level					
			Low		Medium		High	
Main Criteria	**Sub-criteria**	**Measurements**	**Value**	**Grade Point**	**Value**	**Grade Point**	**Value**	**Grade Point**
Vehicle Ownership	Motorcycle ownership	MCs/1000 inhabitants	< 150	1	150-350	2	> 350	3
	Private car ownership	PCs/1000 inhabitants	< 150	3	150-350	2	> 350	1
Availability of Alternatives to Motorcycle and Car	Bus transport availability	Buses/ 1000 inhabitants	< 1	3	1- 2	2	> 2	1
	Bicycle availability	Bicycles / 1000 inhabitants	<150	1	150-350	2	>350	3
Use of Motorcycle	Motorcycle share in the traffic flow	% of MCs in the traffic flow (in vehicle unit)	<30%	1	30 – 50%	2	> 50%	3
	Modal split of motorcycle	% of trips by motorcycles	<20%	1	20 -40%	2	> 40%	3
	Modal split of public transport	% of trips by public transport	< 20%	3	20-40%	2	> 40%	1
	Modal split of private car	% of trips by cars	< 20%	3	20- 40%	2	> 40%	1
	Modal split of non-motorised traffic	% of trips by non-motorised traffic	< 20%	3	20 – 40%	2	> 40%	1

Note. Adapted from Khuat (2006), p. 36.

In Table 1-1, the rate of motorcycle dependence is defined based on the grade points average (GPA). The motorcycle dependence is 'high' if the GPA is higher than 2.5; the 'medium' motorcycle dependence is rated for the GPA that falls in-between 2.0 and 2.5, and the 'low' motorcycle dependence is defined for the GPA lower than 2.0 (Khuat, 2006).

Even though the motorcycle dependence is defined as a high level when the motorcycle share is higher than 50% in Table 1-1, the observed data in this study show that the real motorcycle share in the mixed flow at any signalised intersection in the urban area is always higher than 70%. Thus, the traffic flow is considered as motorcycle dependent flow when the motorcycle share is higher than 50%, and the percentage of other four-wheeled vehicles are lower than 50%.

1.3 Research Questions

The primary mission of this thesis is to establish a proper capacity calculation procedure for signalised intersections within MDCs. To do so, issues should be investigated such as the traffic flow characteristics, the affecting factors for the capacity calculation procedure, the performance of a traffic signal, and the specific driving behaviour of motorcyclists. These issues have been brought into focus using the following research questions.

Research Question 1:

What is the state-of-the-art in signalised intersection capacity analysis?

Research Question 2:

What are the specific characteristics of the traffic flow in MDCs?

Research Question 3:

What factors affect the capacity and the saturation flow rate in MDCs?

Research Question 4:

How could the capacity model be built up?

Research Question 5:

How could the recommended capacity model be applied in MDCs?

1.4 Goal and Objectives

The major goal of this study is to find out a measure that analyses the capacity of each stream at a signalised intersection and overall intersection capacity in MDCs. This goal can be divided into objectives as follows:

- Finding factors that affect the capacity of signalised intersections significantly.
- Developing a suitable capacity calculation method.
- Proposing a capacity calculation guideline for signalised intersections in MDCs.

1.5 Scope of Work

The research area of this study is limited to the concept of MDCs in which motorcycle occupies a high share in traffic composition. Therefore, this study is conducted only within the framework of traffic characteristics under the specific traffic conditions in MDCs.

The intersection approach capacity is the primary purpose of this study. Thus, the approach width should remain the same. The approach width with a short left-turning lane or right-turning lane would not be considered in this thesis.

Most of the signal programs in this study are two-phase signal programs. Therefore, this study focuses on signalised intersection under the condition of the two-phase signal program.

Field observation are solely conducted in one place, Ho Chi Minh City, where the motorcycle dependence reaches extreme share in the traffic composition.

1.6 Structure of the Study

The beginning point for the research is a literature review on capacity calculation methods and affecting factors on the capacity of signalised intersections (Chapter 2). The chapter starts with a basic capacity calculation equation for a signalised intersection and introduction of some factors affecting the capacity and the saturation flow. The next section is the state-of-the-art of capacity analysis. Several capacity methods and capacity manuals in selected countries are introduced. Capacity models related to MDC condition from the previous studies are also be mentioned.

In Chapter 3, the specific traffic characteristics such as the vehicle characteristics, the volume characteristics, the speed characteristics, the lane use distribution characteristics, the signal programs, and the driver behaviours are analysed to understand the traffic stream performance at signalised intersections in MDCs. The vehicle characteristics refer to the diversity of vehicle types and vehicle dimensions. The volume characteristics, emphasise the extreme motorcycle rate in the traffic composition. Then, the speed characteristics point out how flows operate in different traffic situations. The lane use distribution characteristics show how lanes are assigned to vehicle types. After that, the

signal programs which are being applied in MDCs are also introduced to analyse how they influence the intersection capacity. Finally, the specific behaviours of drivers are mentioned as unique affecting factors to the intersection capacity.

In Chapter 4, a capacity model structure and a capacity calculation procedure are developed. This model starts with introducing modules that create the whole capacity model. The input module includes input data needed for the capacity calculation. The saturation flow rate module shows the method and calculation steps for the saturation flow rate of each approach at a signalised intersection. The traffic signal module refers to the effective green time and other traffic signal program elements. The capacity analysis module describes the difference in capacity calculation including normal capacity and maximum capacity.

After introducing the theory capacity model in Chapter 4, empirical data is gathered to apply the model and to serve for the calibration process (Chapter 5). The surveys are conducted at urban signalised intersections in Ho Chi Minh City, Vietnam. Video observations such as traffic volume, speed, timing period, and traffic composition are implemented. The calibration process provides the plausibility of the theoretical model and the complete capacity model in MDCs.

Chapter 6 presents the model application. In this chapter, a completed capacity model, and a detailed procedure are depicted as a capacity calculation guideline. The guideline format is organised based on both the calculation form in the German Highway Capacity Manual (FGSV, 2015) and the U.S. Highway Capacity Manual (TRB, 2010). In Chapter 7, a sample calculation is introduced, by applying the guideline in Chapter 6. A typical four-leg signalised intersection is selected to calculate the intersection capacity by using the suggested guideline.

Conclusions and recommendations are summarised in Chapter 8 concerning the research objectives.

2 Capacity Calculation

2.1 Introduction

The comprehensive literature review is performed in this chapter. The primary method for the capacity analysis of signalised intersections is discussed. This part also highlights the importance of the saturation flow rate in the capacity analysis. Section 2.2 refers to the capacity and saturation flow rate models with some influencing factors. Section 2.3 is the state-of-the-art of capacity analysis. From this section, several methods and manuals in car traffic-based condition such as German Highway Capacity Manual (HBS) (FGSV, 2015), American Highway Capacity Manual (HCM) (TRB 2010), Indonesia Highway Capacity Manual 1997 (IHCM 1997), Malaysia Highway Capacity Manual 2011 (MHCM 2011), and the Manual on Traffic Signal Control in 2006 (JSTE 2006) are introduced. Besides, some models from research projects in MDCs are mentioned to show different traffic situations between these cities and others. Section 2.4 and section 2.5 refer to the effective green time and the intergreen time calculation which are the primary part of the comprehensive capacity model. Some conclusions from the literature are abridged in section 2.6 to conclude essential issues for the next steps.

2.2 Capacity and Saturation Flow Rate at Signalised Intersections

The capacity of signalised intersections is based on the lane group capacity and its relationship to demand flow rate. TRB (2010) defines capacity as 'the maximum number of vehicles that can reasonably be expected to pass through the intersection under prevailing traffic, roadway, and signalisation conditions during a 15-min period'. The capacity of a lane or a lane group may be stated as shown in Equation 2-1:

$$C = \frac{t_g}{t_C} \cdot S \tag{2-1}$$

where	C	=	Lane capacity	[veh/h]
	t_g	=	Effective green time	[s]
	t_C	=	Cycle length	[s]
	S	=	Saturation flow rate	[veh/h]

The saturation flow rate is defined as the maximum number of vehicles which pass through an intersection approach when the signal is green, and enough vehicles exist to achieve a continuous flow to the end of the queue. The unit of the saturation flow rate is 'vehicle per effective-green-hour'.

The saturation flow rate is calculated by adjusting the base saturation flow rate to the specific conditions present on the subject intersection approach through adjustment factors. Equation 2-2 is used to compute the adjusted saturation flow rate per lane for the subject lane group:

$$S = S_0 \cdot f_x \tag{2-2}$$

where	S	=	Lane saturation flow rate	[veh/h]
	S_0	=	Base saturation flow rate	[s]
	f_x	=	Adjustment factors	[s]

The adjustment factors may vary across countries depending on their specific traffic conditions. Table 2-1 shows the adjustment factors for the saturation flow rate of a signalised intersection. These factors do not influence the saturation flow or the capacity independently but in the way of combining with each other.

Table 2-1: Adjustment Factors for Saturation Flow Rate at Signalised Intersections

		Application Field				
		HBS 2015	**HCM 2010**	**JSTE 2006**	**IHCM 1997**	**MHCM 2006**
Road conditions	Lane width	✓	✓	✓	✓	✓
	Grade	✓	✓	✓	✓	✓
	Intersection geometry (radius of turn, angle, visibility, etc.)	✓	✓	✓	✓	✓
Traffic conditions	Vehicle type (heavy vehicles, motorcycles, etc.)	✓	✓	✓	✓	✓
	Parking		✓	✓	✓	
	Bus stop		✓		✓	
	Lane utilisation		✓			
	Pedestrians crossing	✓	✓	✓	✓	
Control conditions	Turning movements	✓	✓	✓	✓	
	Opposing movements		✓	✓	✓	
	Duration of green time	✓	✓		✓	
Behaviour conditions	Motorcyclist behaviour					✓
	Regional characteristics (urban, rural)		✓		✓	✓

Note. Factors are retrieved from FGSV (2015), TRB (2010), JSTE (2006), IHCM (1997), and MHCM (2006)

2.2.1 Road Conditions

2.2.1.1 Lane Width

Lane width is the most influential parameter for the saturation flow rate. Apparently, when the lane width rises, the saturation flow rate also increases in correspondence and vice versa. The lane width adjustment factor accounts for the negative impact of narrow lanes on the saturation flow rate and allows for an increased flow rate on wide lanes (TRB, 2010). When determining the saturation flow rate, the lane width adjustment factors reflect the effect of lane width on free-flow speed.

Typically, a standard lane width value will be determined with an influenced degree by 1 to the saturation flow rate. The saturation flow rate will rise or goes down respectively depending on increasing or decreasing of the lane width. The standard lane width varies among different specifications (Table 2-2).

Table 2-2: Standard Lane Width

Specification	HBS 2015	HCM 2010	JSTE 2006	IHCM 1997	MHCM 2006
Standard Lane Width (m)	3	3.6	3	3	3.6

Note. Adapted from FGSV (2015), TRB (2010), JSTE (2006), IHCM (1997), and MHCM (2006)

2.2.1.2 Grade

The vertical grade factor has also the primary effect on vehicle performance. The vertical grade at an intersection increases start-up lost time and diminishes vehicle running speed because it influences acceleration and deceleration of vehicles. As a result, the saturation flow rate is reduced by the vertical grade. Besides that, the effect of the grade is more significant during winter or wet conditions.

2.2.1.3 Intersection Geometry

The geometric characteristics of an intersection are effective factors for the saturation flow rate and the performance when loaded with traffic. The interaction of lane width with other geometric elements, shoulder width, curb, and media, also affect the traffic performance. Apparently, the saturation flow rate and speed at a given flow have higher values for wider shoulder conditions. The saturation flow rate is reduced if there is a fixed obstruction close to the edge of the carriageway, whether the road has a curb or a shoulder. Presence or absence of median also affects the saturation flow, and well-designed median contributes to increasing the saturation flow rate.

2.2.2 **Traffic Conditions**

2.2.2.1 Vehicle Type

Traffic flows comprise various kinds of vehicles such as heavy vehicles, small-sized commercial vehicles, cars, vehicles with small engines, motorcycles, bicycles and so on. The proportion of these vehicles has an influence on the lane or lane group's saturation flow rate. In car traffic-based condition, the ideal saturation flow rates are given to passenger cars and the impact of other vehicles is considered usually based on passenger car units.

Heavy vehicles are considered as the most influential vehicle type for saturation flow rate. TRB (2000) defined heavy vehicles as those with over four tires touching the pavement. The heavy vehicles require additional spaces while operating compared with passenger cars. Thus, heavy vehicles in the traffic flow reduce the saturation flow rate.

2.2.2.2 Parking

Parking factor is important for the frictional effect of a parking lane on flow in an adjacent lane group and for the occasional blocking of an adjacent lane by vehicles moving into and out of parking spaces (TRB, 2010). In addition, on-street parking reduces the effective approach width, narrows down the queuing and discharge space, and influences the saturation flow rate of that approach.

2.2.2.3 Bus Blockage

Bus blockage factor represents the impacts of activities of buses at the stop station for picking up passengers at a near-side or far-side bus stop within the stop line. Usually, the impact of bus stops on saturation flow is significant only when buses regularly block traffic lanes during the green interval or its portion. This factor should be considered when the total expected waiting time occupies a considerable proportion of the green interval.

2.2.2.4 Lane Utilisation

The demand flow rate usually varies on the lanes in a lane group and reduce the saturation flow rate of that lane group. Thus, the lane utilisation factor is introduced to explains the unequal distribution of traffic among lanes in a lane group with more than one lane (TRB, 2000). In car traffic-based cities, this factor may adjust the base saturation flow rate. In motorcycle dependent cities, however, this factor cannot be applied because motorcycles do not operate under lane discipline rule.

2.2.2.5 Pedestrian Crossing

Pedestrian crossing factor only affects left-turning movements in case of permissive left turns with pedestrians. If the pedestrian flow rate operates during a part of the green interval when left-turning movements must wait for the opposing queue to discharge. It may cause a significant underestimation of the left-turning saturation flow rate.

Right-turning flows are affected by pedestrians using parallel crosswalks during the same phase. In areas of higher pedestrian activity, some pedestrians walking on the sidewalks may suddenly enter the crosswalks, and drivers, therefore, proceed cautiously. This movement causes reduce the saturation flow rate of the right-turning lane. On the other hand, where a few pedestrians are presented, or sidewalks are not provided, pedestrians have virtually no effect on the right-turning saturation flow rate (Teply et al., 2008).

2.2.3 **Control Conditions**

The control conditions are represented by the phasing structure as the composition of individual phases and specific green intervals. These conditions have a significant impact on the saturation flow (Teply, 1988).

2.2.3.1 Turning Movements

Turning effects are related to the effect of geometry. The right-turning adjustment factor depends on many variables such as exclusive lane or shared lane and proportion of right-turning movements in the shared lanes. In case of the existence of right-turning lanes with a protected right-turning phase, the saturation flow rate of right-turning lanes is influenced just by road conditions. In case of the existence of right-turning lanes without a protected right-turning phase, the saturation flow rate of right-turning lanes decreases because of the interactions between turning movements and crossing pedestrians.

The left-turning adjustment factor is based on the variables similar to those for the right-turning adjustment factor, including exclusive or shared lanes, left-turning proportion, and opposing flow rate. Exclusive left-turning lanes should be given to left-turning traffic in principle. In car traffic dependent condition, sometimes through and left-turning movements share the same lane because of various conditions. Lanes shared by through and left-turning movements are considered as through lanes and their saturation flow rates are adjusted for left-turning movements because through traffic are disturbed by left-turning traffic.

2.2.3.2 Opposing Movements

Left-turning movements which traverse stop lines during an unprotected left-turning phase is influenced by the opposing through-traffic. During the same phase, left-turning movements must find time gaps during which they can safely complete their turning movements in the opposing through-traffic. In car traffic-based cities, vehicles can only pass the intersection through the unsaturated opposing flow. In motorcycle traffic, real observations show that motorcycles even can pass the intersection through the saturated opposing flow under some certain conditions which can be explained in the next chapters.

2.2.3.3 Duration of Green Time

The first 5-7 vehicles crossing the stop line during the initial period of a green interval usually require longer headways than subsequent parts (Teply et al., 2008). As a result, the maximum saturation flow is not fully developed in this situation. Moreover, some drivers in the long queues become less attentive and do not move immediately after the preceding vehicle where long green intervals with fully a saturated flow. Therefore, their headways are longer than the minimum saturation flow headway during the steady flow portion of the green interval.

2.2.4 **Behaviour conditions**

2.2.4.1 Motorcyclist Behaviour

Motorcycles have the capability to move through queues in congested areas. Motorcycles are capable of zigzag manoeuvres and non-lane-based movements. They likely change their positions to more convenient areas to move forward or turn right/left. Inside the intersections, motorcycles tend to make groups to cross the intersection makes drivers feel safer and more confident (Huynh, Boltze, Vu, 2013). Obviously, motorcyclist behaviour through its unique characteristics was proven to affect the saturation flow rate.

2.2.4.2 Regional Characteristics

The area type has to be taken into account for the relative inefficiency of intersections in business districts in comparison with those in other locations (TRB, 2000). The saturation flow rate of signalised intersections in central business district (CBD) is lower than the one in other areas because there are many traffic activities operate in CBD area such as parking movements, taxi and bus operations, and high pedestrian activities.

2.3 State of the Art in Capacity and Saturation Flow Rate at Signalised Intersections

The capacity analysis is a set of procedures used to estimate the traffic carrying capacity of transportation facilities over a range of defined operational conditions. Different applied procedures through out countries have slightly different approaches to conducting capacity analysis. These procedures have been developed according to the respective countries' traffic behaviour. Therefore, to come up with the best procedure for the country, local studies must be conducted.

The Intersection capacity is calculated based on the saturation flow rate and the signal timing parts, such as the effective green time and the cycle time. The saturation flow rate is computed by multiplying the base saturation flow rate under standard condition by affecting factors.

2.3.1 **Capacity Analysis in Car Traffic-Based Cities**

2.3.1.1 Webster and Cobbe

Webster and Cobbe (1966) defined the saturation flow rate as the flow, which would be obtained If there was a continuous queue of vehicles and they were given a 100 per cent green time'. It is expressed in vehicles per hour of green (vphg).

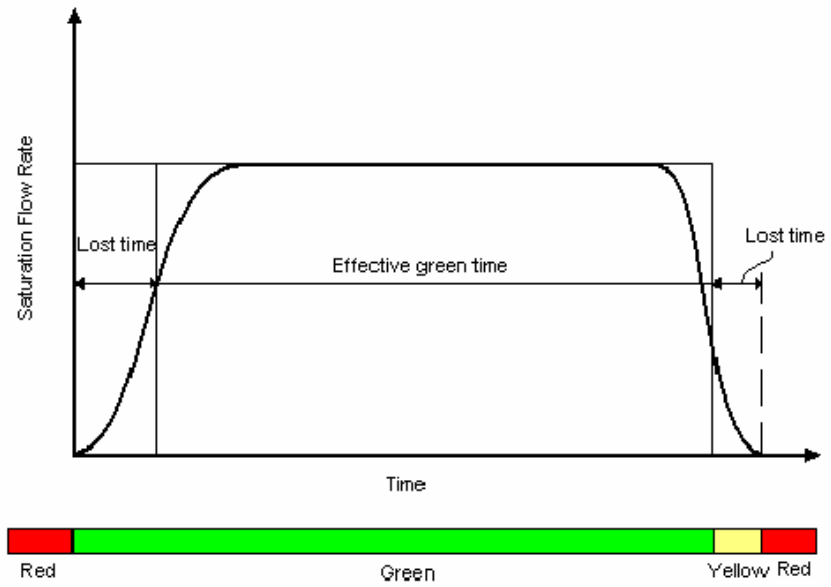

Figure 2-1: The Flow of Traffic during the Green Period from a Saturated Approach

Note. Adapted from Webster amd Cobbe (1966)

The concept 'effective green' period is shown in Figure 2-1 to have the constant value of the saturation rate. It means that the curve in Figure 2-1 is replaced by an equal area rectangle. Therefore, the effective green time is equal to the green time minus the start-up lost time, then plus a part of the amber time.

The unit of pcu/h (passenger car unit per hour) is used to express the saturation flow rate. The saturation flow rate is affected by approach width, gradients of approach, traffic composition (each vehicle type is equivalent to some private cars respect its road-capacity requirements), right-turning traffic, left-turning traffic, pedestrians, parked vehicles, and site characteristics.

Table 2-3: The Effect of Lane Width on Saturation Flow

Lane Width (m)	3.05	3.35	3.66	3.96	4.27	4.57	4.87	5.18
Saturation Flow (pcu/h)	1,850	1,875	1,900	1,950	2,075	2,250	2,475	2,700

Note. Adapted from Webster and Cobe (1966)

2.3.1.2 Germany

According to the Germany Highway Capacity Manual (FGSV, 2015), the basic saturation flow rate S_0 is 2,000 pcu/(h*ln). A basic saturation headway $t_{H,0}$=1.8 s/(veh*ln) is used for the base condition. In the manual, heavy vehicles influence the value of saturation flow rate significantly and it is considered as a separated factor. The saturation flow rate has an inverse ratio to this factor. Moreover, some affecting factors are also computed such as lane width, turning radius, and grade. Considering external conditions, the saturation flow rate is computed as:

$$S = \frac{3,600}{t_H} = \frac{3,600}{t_{H,0} \cdot f_{HV} \cdot f_1 \cdot f_2} \tag{2-3}$$

Where S = Adjusted saturation flow rate [veh/(h*ln)]
t_H = Adjusted saturation headway [s/(veh*ln)]
$t_{H,0}$ = Base saturation headway [s/(veh*ln)]

f_{HV}	=	Adjustment factor for heavy vehicles in the traffic stream	[-]
f_1	=	Max (f_b, f_R, f_S)	[-]
f_2	=	Min (1, f_S)	[-]
f_b	=	Adjustment factor for lane width	[-]
f_R	=	Adjustment factor for turning radius	[-]
f_S	=	Adjustment factor for approach grade	[-]

2.3.1.3 United States of America

The Highway Capacity Manual (TRB, 2010) is developed as a comprehensive revision of the previous manuals in the U.S. As explained in previous sections, the first step taken in the capacity analysis is to determine the saturation flow for the single lanes in the intersection. TRB (2010), a saturation flow rate for each lane group is calculated according to Equation2-4 where the ideal saturation flow for this method is 1,900 pc/(h*ln). The saturation flow rate is the flow in vehicles per hour that can be accommodated by the lane group assuming that the green phase is displayed 100 per cent of the time (i.e., g/C= 1.0).

$$S = S_0 f_w f_{HV} f_g f_p f_{bb} f_a f_{LU} f_{LT} f_{RT} f_{Lpb} f_{Rpb} \quad (2\text{-}4)$$

Where	S	=	Saturation flow rate for subject lane group, expressed as a total for all lanes in lane group	[veh/h]
	S_0	=	Base saturation flow rate per lane S_0=1,900 pcu/(h*ln)	[pcu/(h*ln)]
	f_w	=	Adjustment factor for lane width	[-]
	f_{HV}	=	Adjustment factor for heavy vehicle in the traffic stream	[-]
	f_g	=	Adjustment factor for approach grade	[-]
	f_p	=	Adjustment factor for existence of a parking lane and parking activity adjacent to lane group	[-]
	f_{bb}	=	Adjustment factor for blocking effect of local buses that stop within intersection area	[-]
	f_a	=	Adjustment factor for area type	[-]
	f_{LU}	=	Adjustment factor for lane utilisation	[-]
	f_{LT}	=	Adjustment factor for left turns in a lane group	[-]
	f_{RT}	=	Adjustment factor for right turns in a lane group	[-]
	f_{Lpb}	=	Pedestrian adjustment factor for left-turning groups	[-]
	f_{Rpb}	=	Pedestrian-bicycle adjustment factor for right-turning groups	[-]

2.3.1.4 Japan

In Japan, the Manual on Traffic Signal Control (JSTE, 2006) determined the saturation flow rate based on the ideal saturation flow rate multiplying several adjustment factors.

$$S_a = S_B \times \alpha_w \times \alpha_G \times \alpha_T \times \alpha_{RT} \times \alpha_{LT} \quad (2\text{-}5)$$

Where	S_a	=	Saturation flow rate for subject lane group, expressed as a total for all lanes in lane group	[veh/h]
	S_B	=	Ideal saturation flow rate	[pcu/(h*l)]
	α_w	=	Adjustment factor for lane width	[-]
	α_G	=	Adjustment factor for vertical grade	[-]
	α_T	=	Adjustment factor for heavy vehicles	[-]
	α_{RT}	=	Adjustment factor for right-turning movements	[-]
	α_{LT}	=	Adjustment factor for left-turning movements	[-]

The ideal saturation flow rate means the departure rate from each vehicle queue during an hour of green time where road and traffic conditions are ideal. According to the actual measurement, the saturation flow rate of through lane is from 1,800 veh/h to 2,200 veh/h, left-turning lane is from 1,660 veh/h to 1,840 veh/h, and right-turning lanes is from 1,870 veh/h to 2,120 veh/h.

2.3.1.5 Indonesia

According to the Indonesia Highway Capacity Manual (IHCM, 1997), the saturation flow S can be expressed as a product between a base saturation flow S_0 for a set of standard conditions, and correction factors F for deviation of the actual conditions from a set of pre-determined (ideal) conditions. The equation of saturation flow is given as:

$$S = S_0 \times F_{CS} \times F_{SP} \times F_G \times F_P \times F_{RT} \times F_{LT} \quad (2\text{-}6)$$

The base saturation flow S is determined as a function of an approach width W_e and the flow of right-turning traffic in the own approach and in the opposing approach since the influence of these factors is non-linear. Corrections are then made for actual conditions regarding city size, side friction, gradient, and parking as in formula 2-8 below:

$$S_0 = 600 \times W_e \quad (2\text{-}7)$$

Where	S_0	=	Base saturation flow rate per lane S_0 = 1,900 pcu/(h*ln)	[pcu/(h*ln)]
	W_e	=	Effective approach width	[m]
	F_{CS}	=	The city size correction factor	[-]
	F_{SP}	=	The side friction correction factor	[-]
	F_G	=	The gradient correction factor	[-]
	F_P	=	The parking correction factor	[-]
	F_{RT}	=	The right turn correction factor	[-]
	F_{LT}	=	The left turn correction factor	[-]

2.3.1.6 Malaysia

The effect of motorcycle traffic on the saturation flow rate is considered for the capacity estimation based on the Malaysia Highway Capacity Manual (MHCM, 2011). Motorcyclists' behaviour at the intersection can be regrouped into two categories namely motorcycles outside flow and motorcycles within the flow. Motorcycles outside flow are motorcycles that do not follow the first-in-first-out rule. This group includes motorcycles in front of the stop line and motorcycles beside other vehicles. Motorcycles inside flow are motorcycles that follow the first-in-first-out rule implying that they either travel in front of or behind other vehicles within a traffic stream. Both categories affect the value of saturation flow and consecutively affects the capacity of the road (Ministry of Works Malaysia, 2011). Figure 2-3 shows the distribution of motorcycles inside flow and motorcycles outside flow which are common in Malaysia.

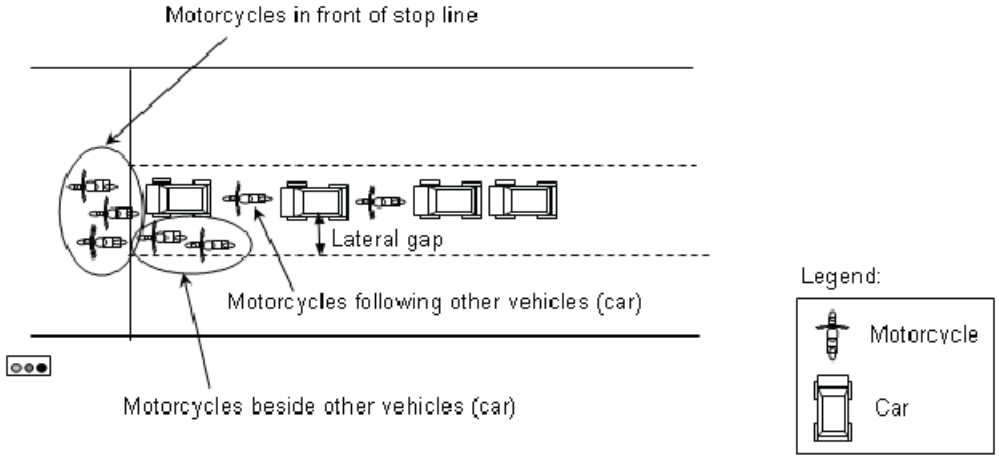

Figure 2-2: The Distribution of Motorcycles inside Flow and Motorcycles outside Flow

Note. Retrieved from Vien et al. (2008), p.03

The saturation flow rate S can be expressed as a product between a base saturation flow rate S_0 for a set of standard conditions, and correction factors f for deviation of the actual conditions from a set of pre-determined (ideal) conditions. The equation of saturation flow is shown by:

$$S = S_0 \times f_w \times f_g \times f_a \times \left(\frac{1}{f_c}\right) \tag{2-8}$$

Where	S_0	=	Base saturation flow rate per lane, 1930 pcu/(h*ln)	[pcu/(h*ln)]
	f_w	=	The lane width factor	[m]
	f_g	=	The grade factor	[-]
	f_a	=	Type of area factor	[-]
	f_c	=	The vehicle composition factor	[-]

2.3.2 Capacity Analysis in Motorcycle Dependent Cities

2.3.2.1 Chu's Method

Chu and Sano (2003) proposed saturation flow rate models in which the effects of the motorcycle both heterogeneous traffic and car traffic at signalised intersections in developing countries. The data was collected in Bangkok, Thailand, and Hanoi, Vietnam by using video method, manual counting and measurement. A comparison of two traffic situations was conducted to get suitable results.

In Hanoi, four intersections were surveyed at the morning peak period (7 am- 9 am) and the afternoon peak period (4 pm–6 pm). The study approaches were similar characteristics. They were fixed time signalised control and have 3.5m-5m lane widths. The proportion of motorcycles was an average of 90% of all transportation modes.

In Bangkok, the traffic data was collected during peak period from 11 am to 1 pm and 4 pm to 6 pm. The lane widths were varied from 3.2 m to 5 m, and the motorcycle shared average 20% of total traffic flow.

Traffic compositions were classified into three groups: group 1 includes motorcycle, mopeds, and scooters; group 2 includes passenger cars, vans and taxis; group 3 includes buses. The different saturated green times from 5 s to 45 s were recorded to estimate the equivalent factor of the motorcycles into passenger car units, the average saturation headway, and the saturation flow rate.

Chu assumed that the saturated green time is a function of the number of vehicles passing the stop line during the green time in which the relationship between dependent variables is linear.

$$t = a_1.n_1 + a_2 \cdot n_2 + a_3.n_3 \quad (2\text{-}9)$$

where	t	=	Saturated green time	[s]
	a_1, a_2, a_3	=	Coefficients of motorcycle, private car, and bus	[s/veh]
	n_1, n_2, n_3	=	The number of vehicles in each group crossing the approach	[veh]

Chu converted all the vehicles passing the stop line to passenger car equivalent during each five-second interval. Then, in every five seconds in green time, if more than three PCUs passing through the stop line, that time is considered as saturated green time and the traffic is saturated.

Table 2-4: Passenger Car Unit (PCU)

Vehicle	PCU
Motorcycle, moped, scooter	0.25
Passenger car, van, taxi	1.00
Bus	2.00

Note. Adapted from Chu (2003), p.1215

The saturated green time is divided by the total number of vehicles (PCU) to the average headway. The formula is shown below:

$$H = \frac{t}{n_1 \cdot p_1 + n_2 \cdot p_2 + n_3 \cdot p_3} \quad (2\text{-}10)$$

where	H	=	Average headway	[s/pcu]
	$p_1; p_2; p_3$	=	The PCU values for motorcycles, passenger cars, and buses respectively	[-]
	$n_1; n_2; n_3$	=	The number of vehicles in each group crossing the	[veh]

From the average saturation headway H, the saturation flow rate is then determined by the Formula: $\frac{3600}{H}$ [pcu/h].

After regression analyses from the collected data, Chu achieved the results as:

In Hanoi: $t = 0.207 \cdot n_1 + 0.85 \cdot n_2 + 1.918 \cdot n_3$ with R^2=0.99
In Bangkok: $t = 0.281 \cdot n_1 + 1.603 \cdot n_2 + 3.487 \cdot n_3$ with R^2=0.99

Table 2-5: Passenger Car Unit (PCU) for Other Vehicles

City	Motorcycle	Car, van, taxi	Bus
Ha Noi	0.24	1.00	2.26
Bangkok	0.18	1.00	2.18

Note. Adapted from Chu (2003), p.1215

Table 2-6: Estimated Saturation Flow Rate

City	Average Headway Statistics		Saturation Flow Rate (PCU/egh)
	Mean [s]	Standard Deviation [s]	
Ha Noi	0.88	0.11	4,092
Bangkok	1.6	0.12	2,253

Note. Adapted from Chu (2003), p.1216

The regression model considers the influence of two main factors (lane width, number of motorcycles) on saturation flow rate S (pcu/h).

$$S = 1965 + 105 \cdot (w - 3.5) + 0.12 \cdot mc \quad (2\text{-}11)$$

Where S = Saturation flow rate [pcu/h]
w = Lane width [m]
mc = Number of motorcycles passing the stop line in one hour. [veh/h]

2.3.2.2 Nguyen 's Method

The second research is conducted by Nguyen et al. (2007) about the saturation flow in traffic dominated by motorcycles. Authors proposed a methodology to study the variation of saturation flow and vehicle equivalence factors simultaneously, and the motorcycle was selected as the basis to study other categories of the vehicle as well as the whole traffic flow.

The regression analysis was also used for this study. Twelve approaches which have 3.9 m -13 m width were collected in Hanoi, Vietnam. The traffic compostion included private cars, light van, minibus, bus, coach, motorcycle, and bicycle. The motorcycle proportion was varying from 80% to 95%.

The Road Note 34 method (Webster, 1963) was applied in this study. In this method, a 6 s period was selected normally. However, Nguyen (2007) decided to count in every consecutive 4 seconds in case traffic dominated by motorcycles. For every 4 s period, vehicles were classified according to turning movements (straight, left turn and right turn) and vehicle categories.

At a starting point, they assumed that S is the motorcycle saturation flow rate during a specific period T (for example, 4 s). If the traffic flow includes N_{mc} motorcycles N_c passenger cars, then the saturation flow rate is expressed as.

$$S = N_{mc} + MCU_c \cdot N_c \quad (2\text{-}12)$$

where S = Saturation flow rate [MCU/4s]
$N_{mc}; N_c$ = The numbers of motorcycles and passenger car crossing the stop line within 4 s periods [veh/4s]
MCU_c = Equivalent factor of one passenger car into motorcycles [MCU]

It is assumed that MCU_c varies depending on the number of cars in the stream, the variation would be linearly related to the number of cars in the stream, as presented in Equation 2-13:

$$MCU_c = m + n \cdot N_c \quad (2\text{-}13)$$

By using both Equations 2-12 and 2-13, a multiple linear regression equation with explanatory variables N_c and N_c^2 was created.

$$N_{mc} = S - m \cdot N_c - n \cdot N_c^2 \quad (2\text{-}14)$$

A model to estimate the saturation flow rate is shown in the equation below:

$$N_{mc} = a + b \cdot (W - 3.5) + c \cdot P_{rt}/R_{rt} + d \cdot P_{lt}/R_{lt} \quad (2\text{-}15)$$

where	W	=	Approach width	[m]
	P_{rt}; P_{lt}	=	Proportion of right-turning and left-turning motorcycles	[-]
	R_{rt}; R_{lt}	=	Right-turning and left-turning radius	[m]
	a; b; c; d	=	Coeffiecients	[-]

By combining of Equation 2-14 and 2-15, an equation representing the relationship between N_{mc} and other factors can be written as in Equation 2-16:

$$N_{mc} = a + b \cdot (W - 3.5) + c \cdot P_{rt}/R_{rt} + d \cdot P_{lt}/R_{lt} - m \cdot N_c - n \cdot N_c^2 + \varepsilon \quad (2\text{-}16)$$

When traffic contains all types of vehicles, i.e. motorcycles, passenger cars, vans and buses and all turning movements, i.e. straight, right turners and left turners, Equation 2-16 needs to be changed to reflect the effect of turning movements. Therefore, their effects are represented by three different factors as described in Equation 2-17.

$$\begin{aligned} N_{mc} &= a + b \cdot (W - 3.5) + c \cdot P_{rt} / R_{rt} + d \cdot P_{lt} / R_{lt} \\ &- m_1 \cdot N_{cst} - n_1 \cdot N_{cst}^2 - m_2 \cdot N_{crt} - n_2 \cdot N_{crt}^2 - m_3 \cdot N_{clt} - n_3 \cdot N_{clt}^2 \\ &- p_1 \cdot N_{vst} - q_1 \cdot N_{vst}^2 - p_2 \cdot N_{vrt} - q_2 \cdot N_{vrt}^2 - p_3 \cdot N_{vlt} - q_3 \cdot N_{vlt}^2 \\ &- r_1 \cdot N_{bst} - s_1 \cdot N_{bst}^2 - r_2 \cdot N_{brt} - s_2 \cdot N_{brt}^2 - r_3 \cdot N_{blt} - s_3 \cdot N_{blt}^2 \\ &+ \varepsilon \end{aligned} \quad (2\text{-}17)$$

Where	N_{cst}; N_{crt}; N_{clt}	=	The numbers of straight, right-turning, and left-turning cars	[veh/4s]
	N_{vst}, N_{vrt}, N_{vlt}	=	The numbers of straight, right-turning and left-turning vans,	[veh/4s]
	N_{bst}, N_{brt}, N_{blt}	=	The numbers of straight, right turning and left-turning buses	[veh/4s]
	m_i, n_i, p_i, q_i, r_i, s_i	=	Coefficients	[-]

The mixed traffic streams need to be converted to homogeneous flow before calculating proportions of vehicle stream. To do so, a pre-defined set of MCU values need to be known. However, MCU values are coefficients of regression models, their exact values can only be obtained after these regression models are calibrated. Hence an iteration approach was introduced to deal with the situation. MCU values for 4.0 for passenger cars, 8.0 for vans and minibuses and 10 for buses as used in Vietnam were used as the initial value. These were used to convert a mixed flow to an equivalent homogeneous stream, and proportions of turning motorcycles were computed. The models were run and revised MCU values were obtained. Then, these MCU values were used to recalculate the portions of right and left turners. The process was repeated until the differences of MCU values from two consecutive loops were smaller than 1%.

$$\begin{aligned} N_{mc} &= 12.28 + 2.15 \cdot (W - 3.5) + 62.60 \cdot P_{rt} / R_{rt} + 34.05 \cdot P_{lt} / R_{lt} \\ &- 3.81 \cdot N_{cst} - 5.70 \cdot N_{crt} - 5.81 \cdot N_{clt} \\ &- 4.82 \cdot N_{vst} - 8.56 \cdot N_{vrt} - 6.67 \cdot N_{vlt} \\ &- 7.96 \cdot N_{bst} - 9.07 \cdot N_{brt} - 10.21 \cdot N_{blt} \end{aligned} \quad (2\text{-}18)$$

From Equation 2-18, the standard saturation flow of a 3.5 m wide approach is 12.28 MCU per 4 seconds. This figure is equal to 11,052 motorcycles per hour of green time. During the time of data collection in Hanoi, an average occupancy value of motorcycles of 1.14 was obtained. Therefore, it is easy to work out that in one hour, a homogeneous flow of motorcycles can accommodate around 13,000 people (11,000 x 1.14) to pass through a 3.5 m approach width.

2.3.2.3 Do's Method

Do (2009) proposed a concept of '**fictitious saturation flow**' to simplify the traffic situation at a signalised intersection. According to that 'fictitious saturation flow' during the green time, the number of fictitious vehicles is equal to the real number of cars and motorcycles passing the stop line.

Three typical cases of traffic situation at signalised intersections were introduced, and corresponding to each case, a saturation flow rate equation was set up.

Case 1: The first layout of the approach is illustrated in Figure 2-3. The green time of the phase is divided into two parts, the first one is used for motorcycles ahead, and the second one is used for cars following.

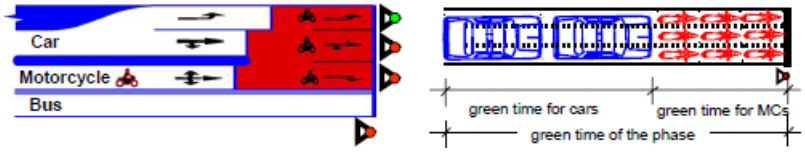

Figure 2-3: Approach at Intersection, Case 1

Note. Adapted from Do (2009), p. 64

The green time of the phase includes the green time for motorcycles and the green time for cars separately:

$$\begin{cases} t_F = t_F^{mc} + t_F^{car} \\ t_F^{mc} : t_F^{car} = \dfrac{q^{mc}}{q_s^{mc}} : \dfrac{q^{car}}{q_s^{car}} \end{cases} \quad (2\text{-}19)$$

Where	t_F	=	The green time of the 'fictitious flow'	[s]
	$t_F^{mc}; t_F^{car}$	=	The green time of motorcycles and cars	[s]
	$q^{mc}; q^{car}$	=	The traffic volume of motorcycles and cars	[veh/s]
	$q_s^{mc}; q_s^{car}$	=	The homogeneous saturation flow rate for motorcycles, and cars	[veh/s]

During the green time of the phase, the number of vehicles passing the stop line is:

$$t_F . q_S = t_F^{mc} \cdot q_s^{mc} + t_F^{car} \cdot q_s^{car} \quad (2\text{-}20)$$

From combining two Equations 2-19 and 2-20, the author calculated the fictitious saturation flow rate according to Case 1:

$$q_S = \frac{q^{mc} + q^{car}}{\frac{q^{mc}}{q_s^{mc}} + \frac{q^{car}}{q_s^{car}}} \tag{2-21}$$

Case 2: In the second case, the green time of the phase is divided into three parts: the first one is for motorcycles, the second one is for cars, and the third one is for mixed traffic.

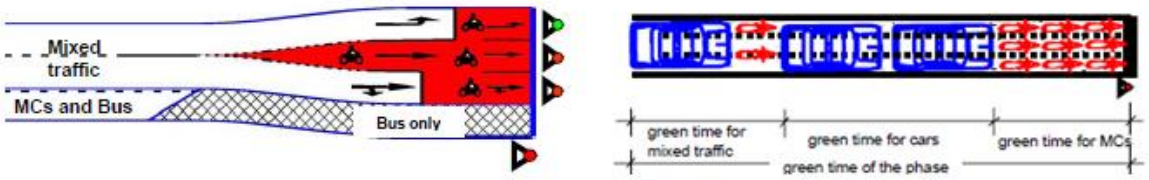

Figure 2-4: Approach at Intersection, Case 2

Note. Adapted from Do (2009), p. 66

In this case, the fictitious saturation flow rate is impaired compared to case 1 because of the mixed traffic operated during the third part of the green interval. The longer green time for mixed traffic is, the lower traffic saturation flow will be. Therefore, the saturation flow in formula 2-21 is adjusted by an adjustment factor $f_1 < 1$.

$$q_S = f_1 \cdot \frac{q^{mc} + q^{car}}{\frac{q^{mc}}{q_s^{mc}} + \frac{q^{car}}{q_s^{car}}} \tag{2-22}$$

The adjustment factor f_1 represents the reduction level because of the mixed traffic state in the third part of the green interval ($f_1 < 1$). f_1 equals the real number of vehicles by investigation divide the fictitious saturation flow. However, the author suggested that $f = [0.9, 0.95]$.

Case 3: In the third case, the green time of the phase is divided for mixed traffic

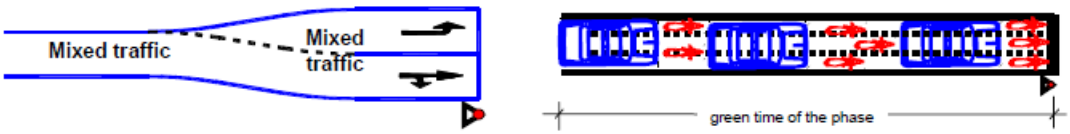

Figure 2-5: Approach at Intersection Case 2

Note. Adapted from Do (2009), p. 67

In this case, the method for determining the saturation flow is similar to that of case 2. However, the adjustment factor is much lower, the author assumed that $f_2 = [0.8,0.9]$ for operating mixed traffic on lanes.

$$q_S = f_2 \cdot \frac{q^{mc} + q^{car}}{\frac{q^{mc}}{q_s^{mc}} + \frac{q^{car}}{q_s^{car}}} \quad (2\text{-}23)$$

2.4 Effective Green Time Calculation

Effective green time is one of the essential inputs to calculate the capacity of signalised intersections. The effective green time t_g is determined by subtracting the start-up lost time from the display green time t_G, and adding the time gained by vehicles making use of amber period (Figure 2-6). The effective green time can be expressed as follow:

$$t_g = t_G - l_1 + (t_A - l_2) = t_G - l_1 + \lambda_2 \quad (2\text{-}24)$$

where	t_g	=	Effective green time	[s]
	t_G	=	Displayed green time	[s]
	l_1	=	Start-up lost time	[s]
	t_A	=	Amber time	[s]
	l_2	=	Clearance lost time	[s]
	λ_2	=	Green end-lag time, $\lambda_2 = (t_A - l_2)$	[s]

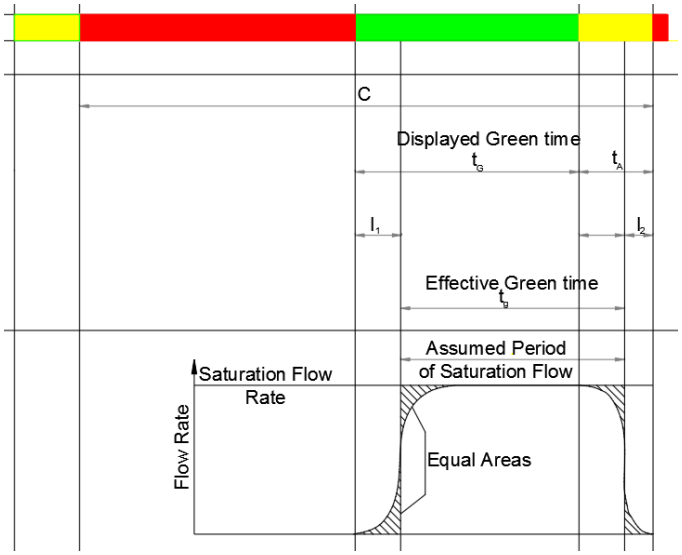

Figure 2-6: Effective Green Time Calculation Model

Note. Adapted from TRB (2010), Chapter 31, p. 07

Start-up lost time occurs when a traffic signal changes from red to green. It is is defined as the additional time, in seconds, consumed by the first few vehicles in a queue at a signalised intersection above and beyond the saturation headway, because of the need to react to the initiation of the green phase and to accelerate (TRB, 2010). There are many factors that affect the start-up lost time such as reaction time of drivers, psychological factors, vehicle type, countdown timer (if any), opposing traffic,

TRB (1985) recommends that the start-up lost time can be calculated as the sum of the differences between the headways for the first four vehicles in the queue and the average headway through the intersection at the saturation flow rate. This approach indicates that start-up lost time is about 2 s. Not like in TRB (1985), Shikata et al. (2003) assumed that only the first three vehicles in the queue were considered experiencing start-up lost time.

Researchers also considered the impact of headway and countdown timers on the start-up lost time. Chu and Sano (2003) proved that when the car headway increases from 2 s to 5 s for the case in Hanoi, and from 2 s to 5.8 s for the case in Bangkok, the start-up lost time increases from 3.2 s to 7.0 s and from 3 s to 6.2 s respectively. Limanond et al. (2009) concluded that using countdown timers, the start-up lost time is reduced by 22%-32%.

The clearance lost time occurs when a traffic signal change from green to red. It is defined as the time at the end of a signal phase during which the movements served by that phase are not used by any traffic because drivers decelerate and stop in response to the presentation of an amber indication (TRB). Clearance lost time is difficult to measure because we can only collect appropriate data during completely saturated green interval.

Through several studies, the values of clearance lost time are suggested. Webster and Cobbe (1966) recommended the clearance lost time to be one second less than the clearance interval period. Miller (1968) suggested considering a half second shorter clearance interval as a clearance lost time. Maini (1997) suggest the clearance lost time is the sum of the all-red clearance interval and a portion (50% to 75%) of the amber change interval.

In the U.S, the effective green time could be equal to the displayed green time if the start-up lost time equals the extension of effective green. In Germany, start-up lost times are small because of the occurrence of Red-Amber signal. Tang (2008) observed that start-up lost times at German urban intersections is around one second while crossing times commonly being more than one second, effective green time can be expected to be greater than the displayed green time. FGSV (2015) defines that the effective green is equal to the displayed green time plus 1 s.

2.5 Intergreen Time Calculation

Intergreen time is a part of the signal program which aims to avoid conflicts between vehicles during the change of stages (Wolfermann, 2009). In the German Guideline for Traffic Signals (FGSV, 1992) the intergreen time is defined as the interval between the end of green for one clearing traffic stream, and the start of green for another entering traffic stream.

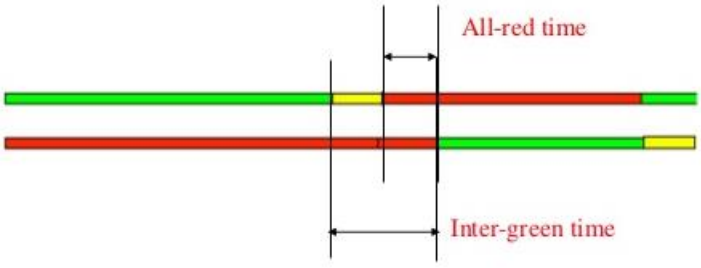

Figure 2-7: Intergreen Time

Note. Own Drawing

Although the aim of intergreen time is the same, the calculation methods are different around the world. There are three different methodologies for the intergreen interval calculation. (i) the method from the German Guideline for Traffic Signals (RiLSA1992) recommended by (Retzko, Boltze, 1987); (ii) the method from the Institute of Transport Engineers (ITE, 1999); (iii) the probabilistic approach recommended by (Easa, 1993).

2.5.1 German Method

In Germany, the shortest necessary intergreen time t_z is estimated by using the RiLSA (1992) guideline shown as Equation 2-26, where the crossing time, the clearing time, and the entering time are represented by $t_{ü}$, t_r, and t_e , respectively.

$$t_z = t_{ü} + t_r - t_e \tag{2-25}$$

The crossing time $t_{ü}$ is the interval between the end of the green time, and the start of the clearing time, determined for the intergreen time calculation. The clearing time t_r is the time needed to cover the clearing distance s_r at a clearing speedv_r. The entering time t_e is the time needed to cover the entering distance s_e at an entering speed v_e (RiLSA, 1992).

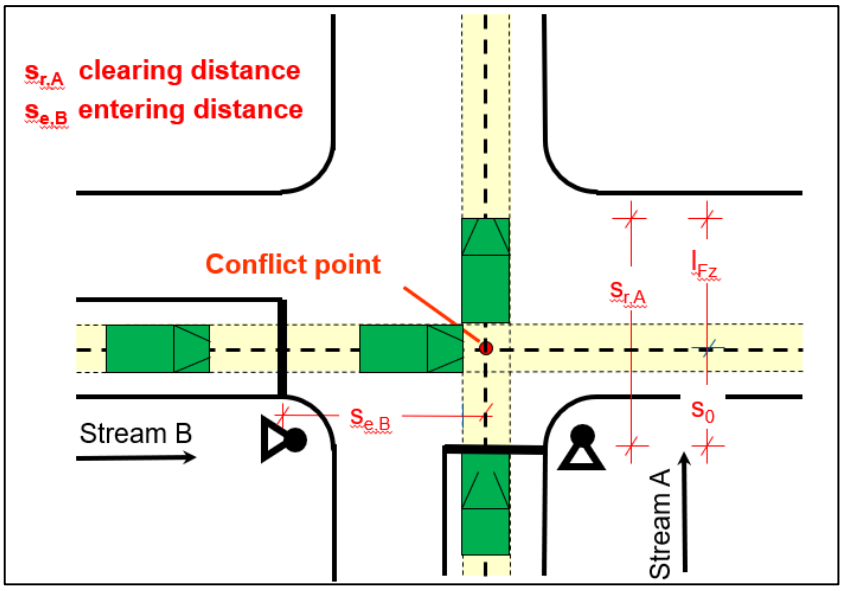

Figure 2-8: Intergreen Time Calculation by German Method

Note. Adapted from Arasan and Boltze (2004), p. 105

RiLSA (1992) defines that the clearing distance s_r is composed of the basic clearing distance s_0 and a fictitious vehicle length l_{Fz}. The basic clearing distance for vehicles is the distance between the stop line and the conflict point with the entering route of the starting traffic stream. The entering distance s_e is the distance from the stop line to the point of intersection with the clearing distance of the ending traffic stream or up to the crossing. Figure 2-8 shows distances which need to be defined for intergreen time calculation.

According to the RilSA (1992) guideline, there are six different cases of crossing and clearing. In each case, assumed values of relevant parameters are defined and lead to different calculation results of intergreen time.

2.5.2 ITE Recommended Method

The equation for intergreen time calculation, as recommended by ITE, is as:

$$y = t + \frac{V}{2a + 64.4g} + \frac{W + L}{V} \tag{2-26}$$

Where	y	=	Intergreen interval	[s]
	t	=	Reaction time of driver	[s]
	V	=	Approach speed of vehicle	[ft/s]
	a	=	Deceleration rate	[ft/s^2]
	g	=	Grade of approach expressed as a decimal	[-]
	W	=	Width of the intersection	[ft]
	L	=	Length of the vehicle	[ft]

In ITE recommended method, the green signal of an entering stream is activated after the tail of clearing vehicle crossing the intersection area. In fact, the safety requirement would be fulfilled when the intergreen interval enabled the tail of clearing vehicle just to pass the conflict area before the head of entering vehicle reach to the conflict area (Retzko and Boltze, 1987). So, the ITE recommended method gives a higher value of intergreen time.

2.5.3 Probabilistic Method

In this method, all factors affecting the intergreen time such as the speed, reaction time, deceleration rate, and vehicle length are random variables (Easa, 1993). The intergreen interval is estimated with the assumption that the dilemma zone occurs with a specified probability. Then, the difference between the clearing and stopping distances is determined as a safety margin based on the first-order second-moment analysis. Finally, the required intergreen interval for a specified reliability index is then derived based on the means, variances, and correlation coefficients of the speed, reaction time, deceleration rate, and vehicle length.

2.5.4 The relationship between intergreen time and lost times

Intergreen times are taken generally as lost times, while they are in fact partly used by vehicles to cross the intersection (Wolfermann, 2009). Because the determinations of intergreen time are different through countries, the relationship between intergreen time and lost times may vary accordingly.

In the U.S, TRB (2010) indicates that that lost time varies with the length of the inter-green. It recommends the lost time of the phase is equal to the inter-green time if start-up lost time equals the extension of effective green. In UK, the lost time equals the intergreen time subtract 1 s because the amber-and-red signal indicated before the onset of the green signal, which can significantly reduce the start-up lost time (ITE, 2009). In Germany, the crossing time of clearing vehicles describes what part of the amber time is used by vehicles and what part represents the clearance lost time (Wolfermann, 2009). The clearance lost time is influenced by the intergreen time. Because of the clearing process, some portion of intergreen intervals is normally left unused by traffic, leading to a clearance lost time. Long intergreen times may cause high lost time and unnecessarily long cycle time.

2.6 Conclusions

The capacity analysis is one of the essential tasks to investigate the signalised intersection performance. Models for capacity and saturation flow rate have been reviewed through the aforementioned sections. The saturation flow rate would be calculated by the base saturation flow rate and is adjusted by some influencing factors. Depending on the characteristics of each location, and the selected method, the saturation flow rate analysis process may differ from car-based flow to motorcycle-based flow.

The base saturation flow rate differs among countries and depends on the actual measurement. TRB (2010) gives the value of 1,900 pcu/(h*ln) while FGSV (2015) suggested the value of 2,000 pcu/(h*ln) for the base saturation flow rate. These figures in Japan, Malaysia and Indonesia are 1,800-2,200 pcu/(h*ln), 1,900 pcu/(h*ln) and 1,930 pcu/(h*ln) respectively. In MDCs, there are two trends of using the PCU or the MCU as the basic unit for the saturation flow rate. For example, Minh's method pointed out the base saturation flow rate in MDCs was 1965 pcu/(h*ln) while Nguyen et al. (2007) calculated this value should be 11,052 mcu/(h*ln).

According to most of the reviewed methods within this chapter, Passenger Car Unit (PCU) is a standard unit for the calculation progress. This assumption is only suitable when passenger cars have a high proportion of the traffic flow and represent traffic characteristics of that flow. However, in MDCs, conversion of all vehicle types to passenger cars seems unsuitable because of the significant differences in terms of traffic behaviour between motorcycles and four-wheeled vehicles.

Some adjustment factors for the saturation flow rate have been reviewed. Even though there are differences in applying adjustment factors throughout various countries, some main factors should remain the same for all, such as lane width, vehicle composition, turning activities, grade.

In this study, the saturation flow rate models would also follow the common concept of previous studies. The base saturation flow rate will be investigated, and the motorcycle unit will be the basic unit. Then some main adjustment factors will be applied for the model, such as approach width, vehicle type, turning activities, etc.

Effective green time is considered as a main part for the capacity calculation. In the U.S, the effective green time is assumed to be equal to the displayed green time because the start-up lost time equals the extension of effective green. In Germany, the effective green time has been proved to be 1 s higher than the displayed green time. However, in MDCs, this outcome is still a controversial question and needs to be evaluated.

Intergreen time is also an important part of the intersection capacity evaluation. Three main methods have been applied over the world. Regards the MDCs condition, however, it seems better to apply the German guidelines for designing the intergreen interval in MDCs.

3 Specific Characteristics of Traffic Streams at Signalised Intersections in MDCs

3.1 Introduction

Intersections, the points of the potential vehicle conflict, play a crucial role in the road network. Traffic flows at a signalised intersection are impeded by several factors, such as different flows running at the same phase, turning activities, disturbance by pedestrians, signal programs, vehicle types, traffic composition, geometric characteristics, driving behaviour and so on. Traffic flow capacity of a signalised intersection is much lower than that of their approach links. Thus, signalised intersections are usually considered as bottlenecks of a network and reasons for traffic congestions and traffic accidents.

Unlike car traffic-based flow where the characteristics have been studied through several studies, the flow characteristics in MDCs are still controversial issues. Study on traffic flow characteristics may help to understand how mixed traffic in MDCs affects capacities at intersections.

A fundamental characteristic of traffic flow in MDCs is mainly the mixed flows with a larger percentage of motorcycles. Such mixed flows bring chaos to traffic operation in the city. It is considered as the main reason for traffic congestion, traffic accidents, and environmental pollution. However, besides the disadvantages, mixed traffic flows with motorcycle majority still have advantages when comparing with car traffic-based flows in developed countries. Because of their small size and their high mobility, the road-space use of motorcycles is more efficient, the road capacity would be higher, and the interaction among motorcycle flows in conflict areas are rather flexible.

In this chapter, the traffic characteristics at signalised intersections in MDCs are described by several factors: vehicle characteristics, volume characteristics, speed characteristics, lane allocation characteristics, traffic signal systems, and driver behaviour.

3.2 Vehicle Characteristics

In MDCs, two-wheeled motor vehicles mainly have small dimensions of 1.7 m length and 0.7 m width, and their engine sizes fluctuate from 50cc to 150cc. The term ‘motorcycle’ is used to represent two-wheeled motor vehicles; however, this is not correct for MDCs because motorcycles in developed countries have larger dimensions than the two-wheel vehicles in MDCs and the engine size starts from 250cc. The term ‘scooter’ may represent these vehicles much better for this case. However, the term ‘motorcycle’ is used to define two-wheeled motor vehicles for the sake of simplicity.

Several vehicle types are operating in the road network in MDCs from two-wheeled vehicles, such as bicycles, motorcycles, scooters to four-wheeled vehicles, such as cars, middle buses, middle trucks, heavy buses, and heavy trucks. They vary in terms of dimensions and engine powers. This situation makes the traffic flow capacity computation rather complex. Thus, all vehicles should be converted to primary vehicle groups. Each vehicle group includes several vehicle types which have similar dimensions, and vehicle characteristics.

Table 3-1 describes typical vehicles in MDCs based on the range of their dimensions (length × width). Four typical vehicle types are defined. Motorcycles/bicycles are grouped as motorcycles and their dimensions are assumed at 2 m length, 0.7 m width. Cars, small trucks, 3-wheeled vehicles, minibuses are grouped as cars and their dimensions are assumed at 5 m length, 2 m width. Middle vehicles, middle trucks are grouped as middle vehicles and their dimensions are assumed at 8 m length, 2 m

width. Large buses and large trucks are defined as heavy vehicles and their dimensions are assumed at 12 m length, 2.5 m width.

Table 3-1: Vehicle Dimensions in MDCs

Vehicle Group	Vehicle Type	Image	Dimension Length x Width		Assumed Dimension Length x Width	
			L [m]	W [m]	L [m]	W [m]
Motorcycle (MC)	Motorcycle		1.8-2.0	0.65-0.75	2	0.7
	Bicycle		1.7-1.9	0.6		
Car (C)	Car		3.29-5.35	1.4-2.2	5	2
	Small Truck		3.24-5.18	1.4-2.18		
	3-wheel Vehicle		4.5	3.0		
	Minibus (16 seat)		5.33-5.78	1.86-2.0		
Middle Vehicle (MV)	Middle vehicle (21-31 seat)		7.01-8.29	2.01-2.31	8	2
	Middle Truck		6.52-6.85	2-2.34		
Heavy Vehicle (HV)	Heavy Bus		10.5-12.2	2.49-2.5	12	2.5
	Heavy Truck		9.5-11.7	2.26-2.5		

Note. Own Table

Although the dimension of a bicycle matches with a motorcycle, the bicycle's speed is much slower than the motorcycle's speed. Obviously, bicycles and motorcycles have different effects on the saturation flow rate and the capacity. Bicycles, however, have a low share in the traffic composition currently. Considering bicycle as another vehicle type or vehicle group would increase the effort of data collection and the complexity of the calculation process. Therefore, in this study, it is acceptable that bicycles are classified into the motorcycle group.

3.3 Volume Characteristics

Typical traffic composition in mixed flow during peak-hours at surveyed approaches is presented in Table 3-2 and Figure 3-1. The motorcycle share is higher than 85% while the shares of all other vehicle types include cars, middle vehicles and heavy vehicles are less than 15% of the traffic composition.

Table 3-2: Traffic Composition in Mixed Flow through Observed Approaches

Approach	MC	C	MV	HV
A14	94.65%	4.50%	0.51%	0.34%
A15	95.42%	1.96%	1.31%	1.31%
A16	96.34%	3.66%	0.00%	0.00%
A17	97.11%	2.18%	0.64%	0.06%
A18	97.50%	2.50%	0.00%	0.00%
A19	89.60%	9.60%	0.44%	0.36%

Approach	MC	C	MV	HV
A20	85.10%	14.21%	0.54%	0.15%
A21	88.34%	9.95%	0.63%	1.08%
A22	90.50%	8.97%	0.19%	0.33%
A23	86.24%	13.68%	0.09%	0.00%
A24	91.79%	7.86%	0.08%	0.27%
A25	84.95%	14.85%	0.00%	0.20%
A26	94.28%	5.65%	0.04%	0.04%
A27	94.39%	5.12%	0.30%	0.20%
A28	94.93%	4.97%	0.09%	0.00%
A29	95.63%	4.11%	0.04%	0.22%

Note. Own Table

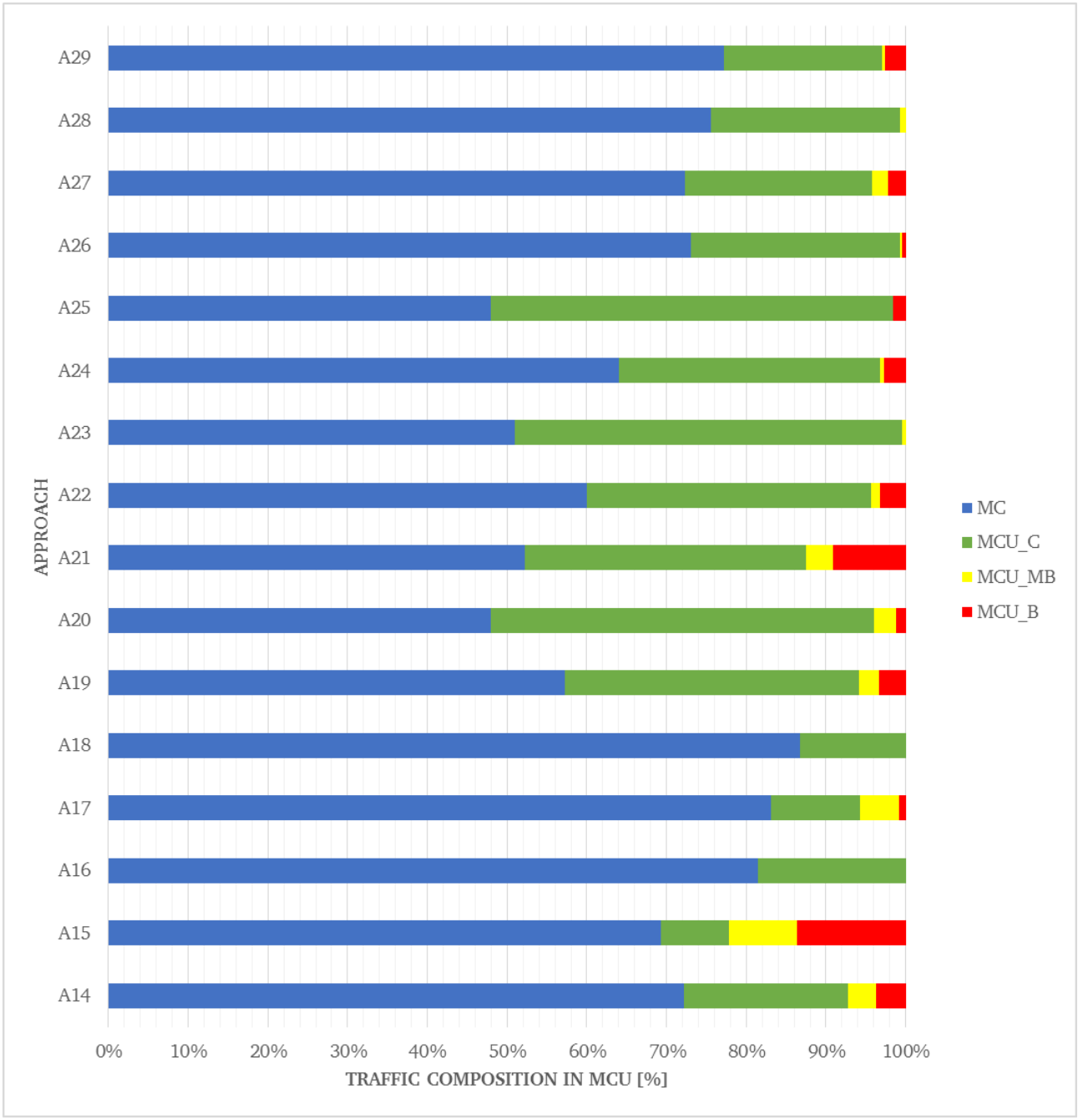

Figure 3-1: Traffic Composition of Mixed Flow in Terms of MCU at Signalised Intersections in MDCs

Note. Own Graph

The percentage of motorcycles is very high as compared to other western countries. However, all of the existing highway capacity manuals from western countries do not take into consideration the effect of motorcycles. On the other hand, the high percentage of motorcycles in the flow interferes with the performance of other vehicles. The average speed of other vehicles is drastically reduced. This proves that the high percentage of motorcycles in MDCs can greatly influence the capacity analysis of signalised intersections.

3.4 Speed Characteristics

Speed characteristics are essential factors in traffic engineering. It shows the quality of the traffic stream operating on the segment or in the intersection. Obviously, speed is an essential part of traffic engineering projects, such as road geometric design, regulation and control of traffic operations, accident analysis, congestions and correlation between capacity and speed.

At signalised intersections, any change in the flow speed may affect the saturation flow rate and the approach capacity. In this study, the average flow speeds during the entering time and the clearing time are analysed. The clearing speed is the average speed of the last motorcycle which is passing a clearing distance during a clearing time. The entering speed is the average speed of the first motorcycle which is passing an entering distance during an entering time. Observed results are illustrated in Appendix B.

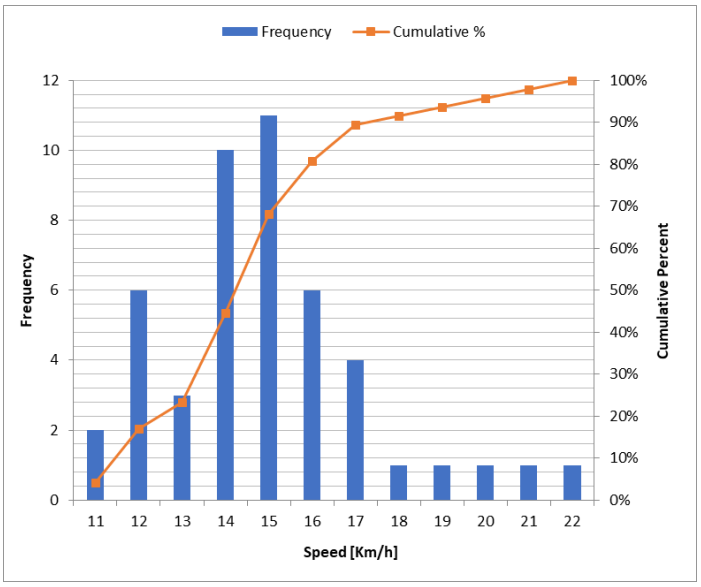

Figure 3-2: Distribution of Entering Speed at Approach A32

Note. Own Graph

Figure 3-2 give a distribution of entering speed at one approach. Every data of entering speed was estimated in each cycle. During the entering time, vehicles change from the standstill state to the discharging state. The flow speed starts from the standstill speed (zero) to the operating speed. From the cumulative frequency distribution curve, the median speed (the 50th-percentile) is obtained as 16 km/h or 4.4 m/s while the 85th-percentile speed is obtained as 19 km/h or 5.3 m/s. Clearly, the high traffic volume under the saturated condition makes the flow slower than expected. Besides, the non-lane-based behaviour makes the lateral and longitudinal distances smaller, and vehicles would run at a slow speed to adapt narrow safety spaces around them.

.

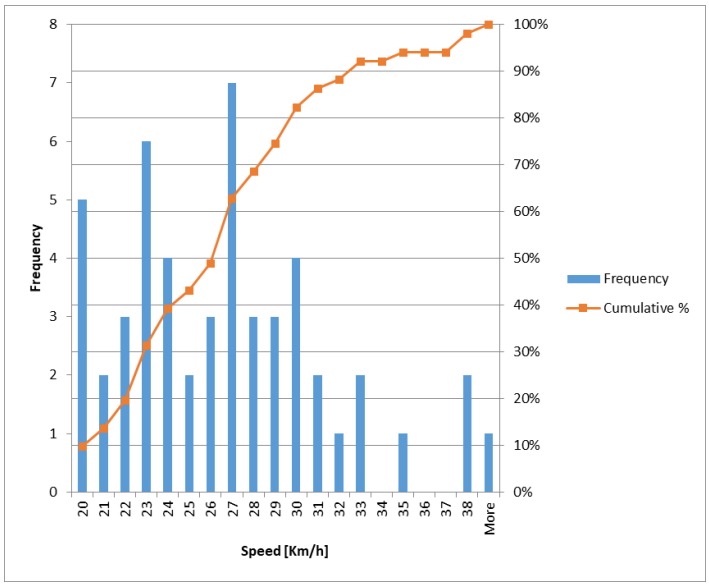

Figure 3-3: Distribution of Clearing Speed at Approach A32

Note. Own Graph

Figure 3-3 presents a distribution of measured clearing speeds at one approach. Every data of clearing speed was estimated in each cycle. During the clearing time, vehicles may reach the designed speed since the discharge flow rate is lower than the one in the saturated traffic conditions. In Figure 3-3, the median clearing speed (the 50th-percentile) is obtained as 26 km/h or 7.2 m/s while the 85th-percentile clearing speed is obtained as 33 km/h or 9.2 m/s.

In conclusion, the entering speed and the clearing speed in MDCs are assumed to be 5 m/s and 8 m/s. These outputs will be used for measuring the entering time and the clearing time.

3.5 Lane Allocation

Although the approaches are organised by separated lanes drivers do not use assigned lanes properly. Vehicle streams are mixed up for every approach of signalised intersections. Distributions of mixing levels are different regarding shared space areas (or lanes). Figure 3-4 gives information about a typical lane allocation for vehicles before entering a signalised intersection. The kerbside lane is assigned for two-wheeled and three-wheeled vehicles. The middle lane is assigned to all kinds of vehicles types. The median lane is assigned for four-wheeled vehicles.

Figure 3-4: A Typical Post Sign of Lane Allocation

Note. Own Picture

The varieties of lane distribution are based on traffic regulations, traffic composition, speed and volume number and location of access points, the origin-destination patterns of drivers, development environment, and local habits (TRB, 1985). In case of traffic pattern in MDCs, general forms of lane distributions are also introduced.

For width of approaches less than 5 m, only one-lane approaches are set up for mixed condition. In the flow, two-wheeled motor vehicles (motorcycles and bicycles) run on the right side while four-wheeled vehicles run on the left side of the road. Heavy vehicles may not be allowed to use such narrow approaches.

For approaches of 5 m to 9 m width, two-lane approaches are designed. Four-wheeled vehicles are assigned to run on the median side for all movement. Two-wheeled motor vehicles can run on both lanes. They use the kerbside lane to go straight or turn right and use the median lane to turn left.

For approaches with 9 m and over width, 3 or more lanes would be set up. Four-wheeled vehicles are assigned to run on the left-side lanes (median lane and middle lanes), and motorcycles can run on all lanes but in different allocation levels. Motorcycles use the median lane to turn left, the middle lanes to go through and, the shoulder lane to go through or turn right.

3.6 Signal Programs in MDCs

Most of the intersections of MDCs are operated under two-phase fixed-time signal programs. The traffic-actuated signal programs are used at some new roads where four-wheeled vehicles are separated from motorcycles because the detection technology hardly applies for motorcycles. Two-phase fixed-time signal programs in MDCs also have some benefits and drawbacks. The advantages are the number of phases in one hour can be optimised, and the total intergreen time is low so that the phase transition time can be reduced. The disadvantages are the occurrence of many conflicts between intersecting flows, especially conflicts between through-flows and opposing left-turning flows, conflicts among right-turning flow, left-turning flows, and through-flows in the same direction. Thus, bothered flows may decrease the saturation flow rate. Besides, conflicts between pedestrians and right-turning or opposing left-turning movements also affect the capacity at high pedestrian demand areas. Despite the existing of conflicts between streams, somehow traffic flows still move slowly depending on the interaction degree of intersecting streams. In the next chapters, this interesting phenomenon will be analysed.

Besides the two-phase signal program, the traffic signal countdown systems are installed for most of the signalised intersection in MDCs (Figure 3-5). It is a digital clock synchronised with a signal-timing controller. It counts down from the start to the end of the phase. The system informs motorists in a queue during any red time on when the green starts and to warn clearing vehicles in the amber time when the red comes. Theoretically, the total start-up lost time of automobiles is decreased and the effective green time of each phase is increased by using signal countdown systems, resulting in an increase of capacities of signalised intersections. Nevertheless, the signal countdown system brings more disadvantages than advantages in practice. The signal countdown system would make the driver even more active than expected. Drivers tend to depart before the start of green and try to accelerate to pass the stop line during the amber time. Consequently, the more frequent the behaviour ‘red-light running’ happens, the steeper the increase in accident risk.

.

Figure 3-5: Traffic Signal Countdown System

Note. Own Picture

On the other hand, intergreen time in MDCs is set up in a minimum value to increase the effective green time and reduce the lost time. The observed data showed that the intergreen time of 5 seconds is set for most of the cases. That amount seems not enough for large intersections, especially under the slow speed flow. A short intergreen time would lead to a high risk of conflict between clearing and entering vehicles and affects the intersection capacities. Figure 3-6 shows an example that entering vehicles are blocked by clearing vehicles because of inadequate intergreen time.

Figure 3-6: Entering Vehicles were Blocked by Clearing Vehicles due to Inadequate Intergreen Time

Note. Own picture

3.7 Driver Behaviour

3.7.1 Grouping Behaviour

During the peak hours, an interesting traffic phenomenon occurs within the signalised intersection that vehicle groups form before crossing the intersection (Figure 3-7). This may be a reflection of drivers' psychology. Making groups to cross the intersection makes drivers feel safer and more confident (Huynh, Boltze, Vu, 2013). In the group, the role of the leading vehicle is very important because it will decide how the group reacts with the surrounding environment (stop or go). If the leading driver feels more powerful and aggressive thanks to the support of the following drivers, he (or she) can cross the conflicting area with a small gap whereas the one who feels passive and less powerful (such as crossing alone or being supported by a smaller number of followers) would not do. As a result, when two or more groups of vehicles interact together at conflict areas, the stronger or bigger group can pass through while the weaker group has to wait until it can find an acceptable gap. Such behaviour is the so-called 'grouping behaviour' (Tuan, Shimizu, 2010).

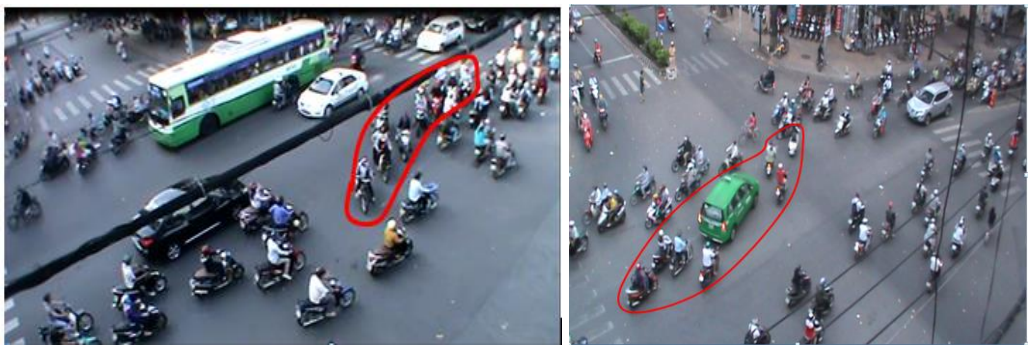

Figure 3-7: Grouping Behaviour at the Shared Space

Note. Own Picture

Grouping behaviour may affect the capacity of signalised intersections. Left-turning movements grouping together have opportunities to find suitable gaps among opposing through-movements. When a left-turning group is bigger, it could accept small gaps. As a result, the capacity of left-turning traffic would increase. In the other hand, through-vehicles must stop when the opposing left-turning group is big enough and it starts to pass the conflict area. Consequently, the capacity of through-traffic would decline.

3.7.2 Non-lane-based Movements at Signalised Intersections

Non-lane-based movement is an essential characteristic of the mixed traffic flow in MDCs and differs from lane-based movement (Figure 3-8). In this situation, vehicles do not run on the assigned lanes even though the lane mark is already drawn. There are several reasons for the non-lane-based behaviour of motorcycles or cars. First, motorcycles can change their positions to more convenient areas to move forward or turn right/left because of their small size and high manoeuvrability. Second, the complex turning movements and the lack of separate turning lanes force vehicles to make a lot of lane changes from their assigned lane before reaching the desired directions. Third, there are not enough spaces for vehicles in the desired areas. When a car in a middle lane wants to turn right, it will try to change to the kerbside lane. However, the high density of motorcycles running in the kerbside lane prevents that car to get its purpose and forces that car to make a non-lane-based movement.

Figure 3-8: Lane-based Movements in Car Traffic-based Cities and Non-lane-based Movements in Mixed Traffic

Note. Own Picture

Non-lane-based movements affect the intersection capacity. In this case, the capacity for mixed traffic flow is measured not based on the lane width but a standard approach width instead. Therefore, the term '**the approach capacity**' and '**the normalised capacity**' is introduced in Chapter 4.

3.7.3 Maneuvers of Motorcycles in the Queue

In fact, during the red interval, queuing cars always stop while some motorcycles are still moving. Motorcycles in the queue tend to move ahead during the queue formation or the queue discharge (Chu et al., 2010). Motorcycles far from the stop line can move by zigzag movements to the front of the queue to get closer to the stop line. Another reason is that motorcycles stopping behind four-wheeled vehicles may try to move away to avoid exhaust smoke or heating air.

The manoeuvres of motorcycles during the queuing state may change the density distribution in the queue. The density at locations closer to the stop line is higher than the other locations. This characteristic contributes to creating a 'capacity reduction phenomenon' which is described in later chapters.

3.7.4 Maneuvers of Motorcycles during the Red Time

In MDCs, drivers may violate red-light regulations. During the red time, a proportion of motorcycle drivers want to turn right. Vehicles try to depart before the end of the red time (when the green light still not turns on) and cross the stop line after the red light turns on. Furthermore, while the signal countdown system is installed, right-turning motorcycles have more aggressive to make a right-turn-on-red decision. Figure 3-9 shows a right-turning motorcycle runs during the red interval. The red-light running behaviour may lead to increase the capacity but reduce the safety level. Thus, it should be considered jointly with the balance between capacity and safety aspects.

Figure 3-9: Right Turn on Red of a Motorcyclist

Note. Own Picture

There are also some motorcycles standing over the stop line during the red time as shown in Figure 3-10. Though this kind of behaviour is not allowed in the traffic rule, it appears because of the high willingness to passing the stop line as soon as possible. In fact, those vehicles may affect not only pedestrians but also the discharge flow rate of the queue after the stop line. Thus, considering the effect of such illegal activities in capacity analyses is still controversial at the present time.

Figure 3-10: Motorcycles standing over the Stop line during the Red Time

Note. Own Picture

3.8 Conclusions

The specific characteristics of traffic streams at signalised intersections in MDCs have been described. These can be summarised:

- There are different vehicle types with different physical dimensions and engine powers operating in the MDCs road network. These are two-wheeled vehicles (bicycles, motorcycles, scooters) and four-wheeled vehicles (cars, middle buses, middle trucks, heavy buses, and heavy trucks). Thus, it is necessary to group them into four main types: motorcycles, cars, middle vehicles, heavy vehicles.

- The significant difference among dimensions of vehicle types in the mixed flow requires a conversion from the heterogeneous flows to homogeneous flows. It is suggested applying motorcycles as the standard unit in this case because its share is much higher than the ones of other vehicle types in the flow.

- The flow speed may vary depending on the time intervals. In the saturated state, the entering speed is assumed at 5 m/s, and the clearing speed is assumed at 8 m/s.

- Lane allocation affects the discharge flows by changing the turning behaviour of vehicles. Motorcycles are assigned on the right side, and cars are assigned on the left side of the traffic stream. Thus, right-turning motorcycles may not affect the discharge flow, but right-turning cars could. Besides, both left-turning motorcycles and left-turning cars could affect the discharge flows.

- Traffic signal control has a significant effect on flows and capacities at intersections. The two-phase fixed-time signal programs applied in most of the intersections would reduce the number of phase transition. However, they contribute to increasing the conflict frequency of flows running in the same phase. The traffic signal countdown system could help to reduce the lost time but could increase the risk level of red-light running behaviour.

- Traffic behaviours such as the grouping, the non-lane-based movement and the red-light running behaviour contribute to the change of intersection capacity in the sense of increasing. In contrast, the safety level decreases, and if an accident or a blockage event occurs within the intersection, the capacity will go down sharply by then. So, it is necessary to consider the effect of traffic behaviour on the intersection operation while balancing traffic capacity and traffic safety.

The mentioned traffic characteristics are used to create the capacity model conducted in Chapter 4 and Chapter 5.

4 Capacity Model Structure and Calculation Method

4.1 Introduction

This chapter mentions the overall capacity model for MDCs as illustrated in Figure 4-1. The capacity model comprises four distinct modules:

1. Input module
2. Saturation flow rate module
3. Traffic signal module
4. Capacity calculation module

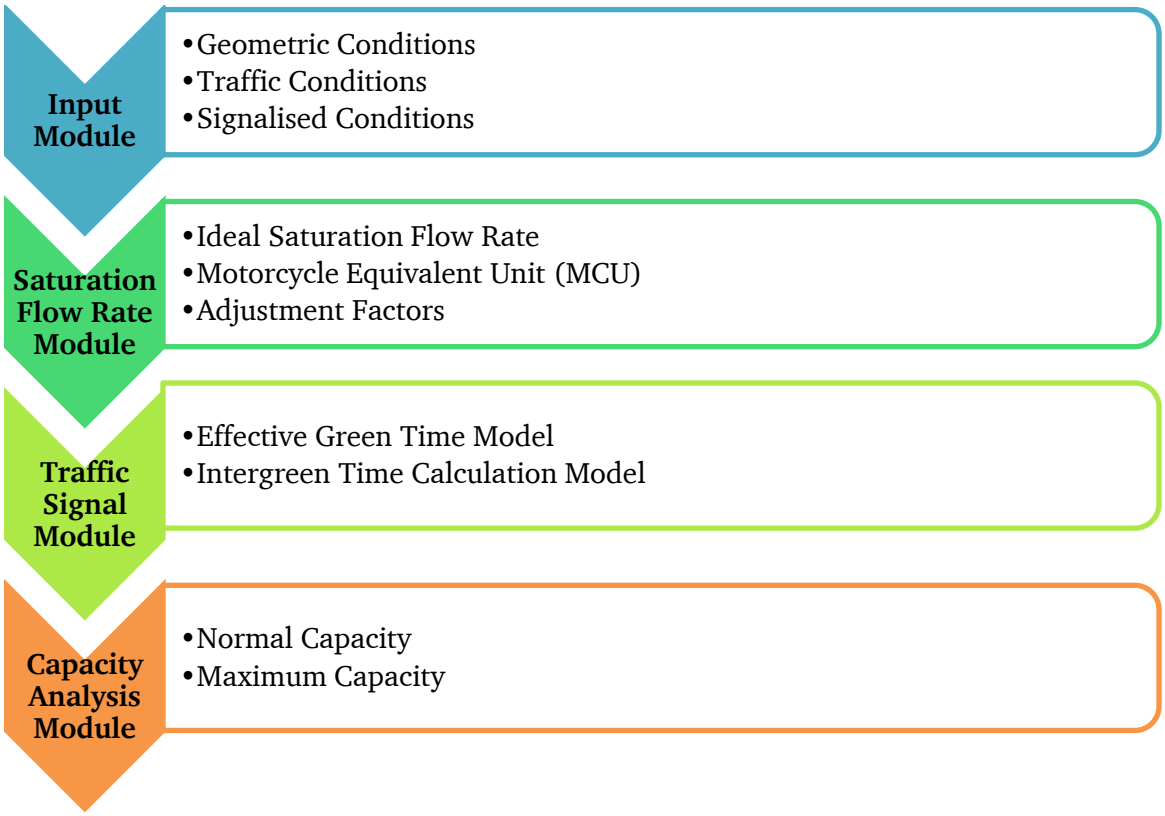

Figure 4-1: The Capacity Model Structure for MDCs

Note. Own Graph

The input module refers to data considered as input parameters for the capacity calculation model. All data in this module will be presented in Section 4.2.

The saturation flow rate module is used to compute the saturation flow rate for each approach of the intersection. It is based on the adjustment of an 'ideal' saturation flow rate to reflect a variety of prevailing conditions. In this module, the motorcycle equivalent unit (MCU) is introduced and applied to convert the heterogeneous traffic flow to homogeneous motorcycle flow that serves the saturation flow rate and the capacity calculation. This content will be written in Section 4.3

The traffic signal module mentions the signal data that serve the capacity calculation. In this module, calculation methods for the effective green time and the intergreen time under MDCs condition are

depicted. The effective green time model and the intergreen time model are presented in Section 4.4 and Section 4.5

The capacity analysis module which will be illustrated in Section 4.6 refers to the final step of the whole capacity calculation process for signalised intersections within MDCs.

4.2 Input Module

Table 4-1 gives the required input information to conduct a capacity analysis. The input data are categorised into four main parts: geometric conditions, traffic conditions, signalisation conditions, and default conditions.

Table 4-1: Input Data

Conditions	Parameter	Symbol	Unit
Geometric Conditions	Approach Width	w	[m]
	Entering Distance	l_e;$l_{e,op}$; l_{e1};$l_{e,op1}$	[m]
	Clearing Distance	l_{cl}	[m]
Traffic Conditions	Homogeneous Motorcycle Saturation Flow Rate	S_{0w}	[veh/h]
	Left-turning Volume	$q_{MC,LT}$;$q_{C,LT}$;$q_{MV,LT}$;$q_{HV,LT}$;$q_{PC,LT}$	[veh/h]
	Through Volume	$q_{MC,TH}$;$q_{C,TH}$;$q_{MV,TH}$;$q_{HV,TH}$;$q_{PC,TH}$	[veh/h]
	Right-turning Volume	$q_{MC,RT}$;$q_{C,RT}$;$q_{MV,RT}$;$q_{HV,RT}$;$q_{PC,RT}$	[veh/h]
	Proportion of Left-turning Motorcycles, Left-turning passenger cars in the flow that excludes Right-turning Motorcycles[1]	$p'_{MC,LT}$;$p'_{PC,LT}$	[-]
	Proportion of Right-turning Motorcycles, Right-turning passenger cars in the flow that excludes Right-turning Motorcycles	$p'_{MC,RT}$;$p'_{PC,RT}$	[-]
Signalised Conditions	Cycle Length	t_C	[s]
	Green Time	t_G	[s]
	Amber Time	t_A	[s]
	Intergreen Time	t_{ig}	[s]
Default Conditions	Grade Adjustment Factor	$f_G = 1$	[-]
	Parking Adjustment Factor	$f_P = 1$	[-]
	Bus Blockage Adjustment Factor	$f_B = 1$	[-]
	Pedestrians Adjustment Factor	$f_{Ped} = 1$	[-]

Note. Own Table

4.2.1 Geometric Conditions

Different intersection geometries would lead to different capacity results. The intersection geometry information includes approach width and some other information related to the conflict between traffic streams, such as entering distance and clearing distance.

Approach width is the sum of each single lane width in the approach. The term '**approach width**' instead of lane width is applied throughout this study because of the non-lane base behaviour of the traffic flow. All movements in a stream including through, right-turning and left-turning movements

[1] Right-turning motorcycles are considered having no effect on the performance of the approaching flow due to their turning positions.

run in the same phase in two-phase signal programs. That makes the traffic flow of the whole approach runs at the same time and likely does not strictly follow the lanes.

Entering distance l_e and clearing distance l_{cl} are used to estimate entering and clearing times. Distances are measured from the middle point of the stop line to the conflict point between the entering route and the clearing route as shown in Figure 4-2.

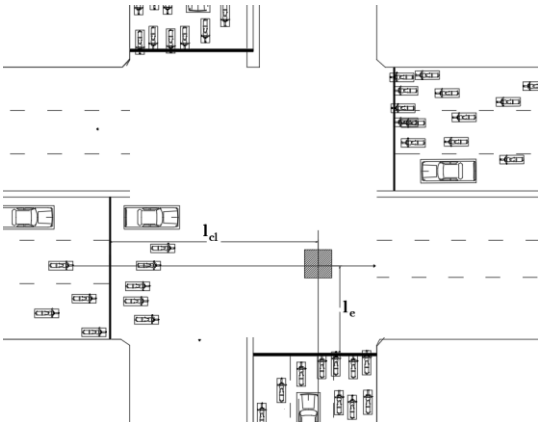

Figure 4-2. Entering and Clearing Distances

Note. Own Drawing

4.2.2 Traffic Conditions

Traffic conditions in this study include the motorcycle saturation flow rate of each approach, the traffic volumes for each movement according to each vehicle type on each approach, and the proportion of each type of turning vehicles in the approaching flow that excludes right-turning motorcycles.

4.2.3 Signalised Conditions

Signalised conditions are based on the fixed two-phase signal program. Complete information regarding signalisation is needed. A phase diagram illustrating phase plan, cycle length, green times, red times and change intervals should be drawn.

Besides, the impact of signal countdown system would be considered by estimating the amber time and the start-up lost time for MDCs.

4.2.4 Default Conditions

There are some conditions neglected in the capacity model even though they are proven to be affecting factors. The following assumptions in this study are explained below:

- **Approach grade:** All field surveys were conducted in an urban area (Ho Chi Minh City), and approach grade are almost the same for all observed intersections. Thus, the grade is not considered in this study. The default value of grade remains a range of 2% to 4%.
- **Parking activity**: Parking activities would also not be included in the capacity estimation because of the sample size limitation.
- **Bus blockage**: The effect of bus blockage at intersections would be ignored in the capacity procedure.
- **Pedestrian activities**: Pedestrian activities would not be mentioned because the pedestrian flow rate is quite low.
- **Exclusive left-turning or right-turning lanes:** The approach capacity requires the same width along the approach in this study. Therefore, exclusive turning lane would not be considered.

4.3 Saturation Flow Rate Model

The following formula determines an appropriate saturation flow rate on an approach:

$$S = S_0 \cdot f_w \cdot f_{veh} \cdot f_{turn} = S_{0w} \cdot f_{veh} \cdot f_{turn} \quad (4\text{-}1)$$

Where	S	=	Saturation flow rate of the whole approach	[veh/h]
	S_0	=	Normalised motorcycle saturation flow rate per 1 m wide approach	[mcu/h]
	S_{0w}	=	Approach motorcycle saturation flow rate, $S_{0w} = S_0 \cdot f_w$	[mcu/h]
	f_w	=	Adjustment factor for approach width in the traffic stream	[-]
	f_{veh}	=	Adjustment factor for vehicle types in the traffic stream	[-]
	f_{turn}	=	Adjustment factor for turning movements in the traffic stream	[-]

In Equation 4-1, the saturation flow rate is estimated based on the motorcycle saturation flow rate and influencing factors. Influencing factors are applied when one or several prevailing conditions differ from the ideal conditions. As mentioned in Chapter 2, the influencing elements include only the main factors, such as approach width, vehicle type, traffic composition, and turning movements. Other factors, such as area type, grade, parking activities, bus blockage, and pedestrian activities are because of the lack of data collection and the thesis scope limitation.

4.3.1 Normalised Motorcycle Saturation Flow Rate and Approach Motorcycle Saturation Flow Rate

The saturation flow rate reflects the departure rate of straight-through vehicular traffic flow passing the stop line of an approach at a signalised intersection during the green interval under ideal geometric, pavement surface, traffic, and weather conditions in a given community (Teply et al., 2008). In MDCs, this term should be modified because of the non-lane-based characteristic. The ideal saturation flow rate of an approach lane is not suitable in this case. Thus, the terms 'approach motorcycle saturation flow rate' and 'normalised motorcycle saturation flow rate' are introduced.

'Approach motorcycle saturation flow rate' is defined as the maximum rate of through-motorcycle flow that can pass through the whole approach width for one-hour effective green time. The approach motorcycle saturation flow rate is determined as:

$$S_{0w} = \frac{Q_{MC}}{T} \cdot 3600 \quad (4\text{-}2)$$

Where	S_{0w}	=	Approach motorcycle saturation flow rate	[mcu/h]
	Q_{MC}	=	Number of vehicles passing the stop line during saturated green time	[veh]
	T	=	Saturated green time	[s]

To estimate S_{0w}, the field survey method would be applied by counting a number of motorcycles passing the stop line during the saturated green time. The results are described in Chapter 5.

'Normalised homogeneous motorcycle saturation flow rate' is defined as the maximum rate of motorcycle flow that can pass through a one-meter approach width for one-hour effective green time. One-meter approach width is not real and even does not cover the width of the car or other four-wheeled vehicle types. However, it is selected as a standard unit for a capacity comparison between different approach dimensions of different intersections. The normalised saturation flow rate of homogeneous motorcycle flow S_0 in an approach should be calculated as:

$$S_0 = \frac{S_{0w}}{f_w}; \quad f_w = f(w) \tag{4-3}$$

Where	S_0	=	Normalised motorcycle saturation flow rate per 1 m wide approach	[mcu/(h*m)]
	S_{0w}	=	Approach motorcycle saturation flow rate	[mcu/h]
	f_w	=	Adjustment factor for approach width in the traffic stream	[-]

4.3.2 Motorcycle Equivalent Unit

There is a fact that the heterogeneous traffic flow is more common than the homogeneous motorcycle traffic flow in urban areas. Different traffic compositions in the flow would make different traffic performance and influence the saturation flow rate. To solve this problem, a technique of converting heterogeneous stream to homogeneous stream is applied by using basic a vehicle equivalent unit. In dominant car traffic-based flow, the passenger car is selected as the basic vehicle because it is the main transport mode. The vehicle equivalent unit in that traffic situation is termed as the passenger car units (PCU). However, in motorcycle dominant traffic, apparently, the motorcycle becomes the main transport mode. Thus, the vehicle equivalent units should be the motorcycle unit (MCU).

In this study, MCU values are estimated by using regression methods. First, all vehicle types are grouped into four categories: motorcycles, cars, middle vehicles and heavy vehicles. Then, the saturated green time T is assumed to be correlated with the number of vehicle types crossing the stop line. The general form of a regression model is given below:

$$T = n_1 \cdot N_{MC} + n_2 \cdot N_C + n_3 \cdot N_{MV} + n_4 \cdot N_{HV} \tag{4-4}$$

Where	T	=	Saturated green time	[s]
	$n_1; n_2; n_3; n_4$	=	Coefficient of motorcycles, cars, middle vehicles and heavy vehicles	[s/veh]
	$N_{MC}; N_C; N_{MV}; N_{HV}$	=	Number of motorcycles, cars, middle vehicles and heavy vehicles passing the stop line	[veh]

Motorcycle unit of vehicle type i:

$$MCU_i = \frac{n_i}{n_1} \tag{4-5}$$

Regression results of the MCU model would be presented in Chapter 5.

4.3.3 Adjustment Factor for Vehicle Types

The adjustment factor for vehicle types represents the occupied space by these vehicles in proportion to motorcycle within the mixed traffic flow. In developed countries, the effect of vehicle type on passenger car is applied for heavy vehicles. In MDCs, all four-wheeled vehicles are considered as influencing factors to the motorcycle flow.

The adjustment factor for vehicle types could be expressed by:

$$f_{veh} = \frac{q_{MC} + q_C + q_{MV} + q_{HV}}{q_{MC} + q_C \times MCU_{\mathrm{C}} + q_{MV} \times MCU_{\mathrm{MV}} + q_{HV} \times MCU_{\mathrm{HV}}} \tag{4-6}$$

Where	f_{veh}	=	Adjustment factor for vehicle types	[-]
	$q_{MC}; q_C; q_{MV}; q_{HV}$	=	Flow rate of motorcycles, cars, middle vehicles, and heavy vehicles	[veh/h]
	$MCU_C; MCU_{MV}; MCU_{HV}$	=	MCU values for cars, middle vehicles, and heavy vehicles	[-]

4.3.4 Adjustment Factor for Turning Movements

The adjustment factor for turning movements accounts for the effect of turning activities on the approach discharge flow rate. Turning activities in the intersection depend on several variables:

- Turning vehicle types
- Type of signal phasing (protected, permitted…)
- Pedestrian activities
- The proportion of turning movements in the traffic stream
- The opposing flow which conflicts with the targeted flow (opposing through-flow conflicts with the left-turning flow and the opposing left-turning flow conflict with the through-flow)

In this thesis, the pedestrian activities are not considered because the number of pedestrians walking across the intersection is insignificant. Besides, because the two-phase signal program is applied for most of the case, there is only permitted phase for turning movements.

Several vehicle types in mixed flows can be classified into two types: passenger cars (include cars, middle vehicles, and heavy vehicles) and motorcycles because of the difference in traffic behaviours. More specifically, bicycles and other two-wheelers are converted to motorcycles while middle vehicles, heavy vehicles, and other four-wheelers are converted to passenger cars.

The effects of turning activities on the saturation flow rate can be explained in two different cases:
- Case 1: Turning effect without the interference of opposing flows
- Case 2: Turning effect with the interference of opposing flows

4.3.4.1 Adjustment factor for Turning Movements without the Interference of Opposing Flows

In this case, the saturation flow rate is only affected by turning movements in the same direction. There is no effect from opposing flows. This case occurs when the targeted flow runs in a one-way street, or in a two-way street in which left turns are not permitted for both directions. Turning adjustment factors include two main parts: The adjustment factor for right-turning movements and the adjustment factor for left-turning movements.

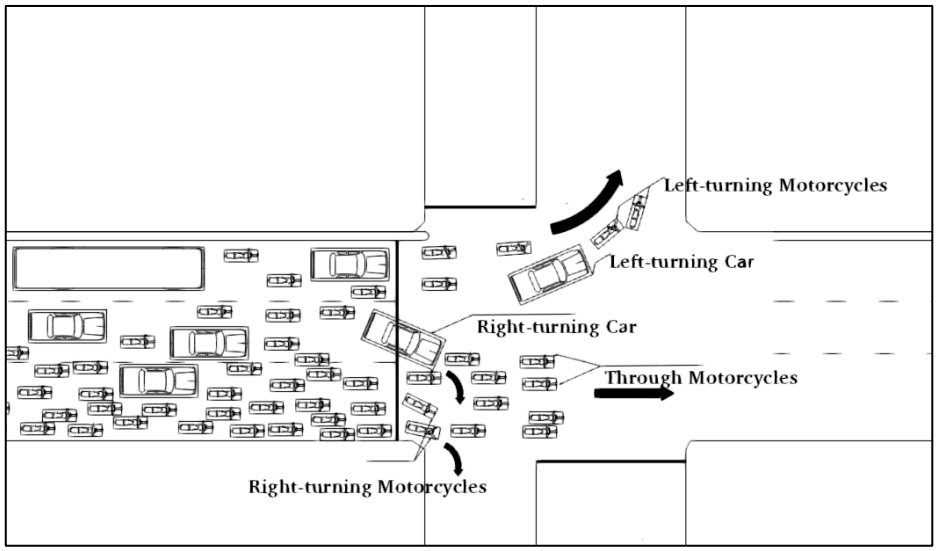

Figure 4-3: Traffic Operation at a one-way Street

Note. Own Drawing

Right-turning motorcycles do not affect the saturation flow rate because of their turning positions and high flexibility behaviour. However, right-turning four-wheeled vehicles from the middle area of the approach would block the motorcycle flows running on the right side of the flow and influence the approach saturation flow rate. Moreover, right-turning passenger cars (include cars, middle vehicles and heavy vehicles) would try to avoid the conflict with through-motorcycles, so their trajectories would not be smooth curves. In conclusion, the right-turning adjustment factor depends on the percentage of four-wheeled vehicles in the total traffic and that turning radius has no effect.

Left-turning motorcycles would try to reach to the left side of the queue during the red interval. Sometimes, however, because there are not enough spaces for left turners on the left side, and the queued through-cars will impede, not all left-turning motorcycles wait on the left side of the flow. Some left-turning motorcycles would stop on the right side and then try to turn left when the green starts. This activity would affect the saturation flow rate. Besides, left-turning passenger cars were proven to influence the saturation flow rate, as well (TRB, 2010).

In conclusion, the influence factors include three parts: right-turning passenger cars, left-turning motorcycles and left-turning passenger cars. The adjustment factor for turning movements can be estimated using multiple regression models between the observed and the estimated data and it is computed as:

$$f_{turn,1} = \frac{S}{S_{ow} \cdot f_{veh}} \tag{4-7}$$

Where	$f_{turn,1}$	=	Adjustment factor for turning movements	[-]
	S	=	Approach saturation flow rate	[veh/h]
	S_{0w}	=	Approach motorcycle saturation flow rate	[mcu/h]
	f_{veh}	=	Adjustment factor for vehicle types	[-]

Equation (4-7) can be rewritten as:

$$f_{turn,1} = \frac{(S - q_{MC,RT})}{S_{ow} \cdot f_{veh}} + \frac{q_{MC,RT}}{S_{ow} \cdot f_{veh}} = \frac{(S - q_{MC,RT})}{S_{ow} \cdot f_{veh} - q_{MC,RT}} \cdot \frac{S_{ow} \cdot f_{veh} - q_{MC,RT}}{S_{ow} \cdot f_{veh}} + \frac{q_{MC,RT}}{S_{ow} \cdot f_{veh}} \quad (4\text{-}8)$$

Set:

$$f_1 = \frac{S - q_{MC,RT}}{S_{ow} \cdot f_{veh} - q_{MC,RT}} \quad (4\text{-}9)$$

By combining Equation (4-8) and (4-9), the adjustment factor for turning movements can be written below:

$$f_{turn,1} = \frac{q_{MC,RT}}{S_{ow} \cdot f_{veh}} + f_1 \cdot \left(1 - \frac{q_{MC,RT}}{S_{ow} \cdot f_{veh}}\right) \quad (4\text{-}10)$$

The adjustment factor f_1 in Equation (4-9) is a function of the proportion of right-turning cars, the proportion of left-turning motorcycles and the proportion of left-turning cars in the flow excluding right-turning motorcycles.

$$\begin{aligned} f_1 &= f_{RT,1} \cdot f_{LT,1} = f\left(p'_{PC,RT}\right) \cdot f\left(p'_{MC,LT}, p'_{PC,LT}\right) \\ p'_{PC,RT} &= \frac{q_{PC,RT}}{S - q_{MC,RT}}; p'_{MC,LT} = \frac{q_{MC,LT}}{S - q_{MC,RT}}; p'_{PC,LT} = \frac{q_{PC,LT}}{S - q_{MC,RT}} \end{aligned} \quad (4\text{-}11)$$

Where	$f_{RT,1}; f(p'_{PC,RT})$	=	Adjustment factor for right-turning movements	[-]
	$f_{LT,1}; f(p'_{MC,LT}, p'_{PC,LT})$	=	Adjustment factor for left-turning movements	[-]
	$p'_{PC,RT}; p'_{MC,LT}; p'_{PC,LT}$	=	Proportion of right-turning passenger cars, left-turning motorcycles, and left-turning passenger cars in the flow excluding right-turning motorcycles	[-]

There are some boundary conditions for f_1 in Equation (4-11)

$$\begin{cases} p'_{PC,RT} = 0 \rightarrow f_{RT,1} = \mathrm{f}\left(p'_{PC,RT}\right) = 1 \\ p'_{PC,LT} = 0, p'_{MC,LT} = 0 \rightarrow f_{LT,1} = \mathrm{f}\left(p'_{MC,LT}, p'_{C,LT}\right) = 1 \end{cases} \quad (4\text{-}12)$$

It is noted that the condition of 100% of right-turning passenger cars or 100% of left-turning passenger cars are not considered because of the MDC concept. A nonlinear function in which a dependent variable is f_1 and independent variables are $p'_{PC,RT}$, $p'_{MC,LT}$, and $p'_{PC,LT}$ is applied. The adjustment factor for turning movements f_1 in this case can be expressed by:

$$f_1 = f_{RT,1} \cdot f_{LT,1} = \frac{1}{1 + a_1 \cdot p'_{PC,RT}} \times \frac{1}{1 + b_1 \cdot p'_{MC,LT} + c_1 \cdot p'_{PC,LT}} \quad (4\text{-}13)$$

where	$q_{MC,RT}$	=	Flow rate of right-turning motorcycles	[veh/h]
	S_{ow}	=	Approach motorcycle saturation flow rate	[veh/h]
	f_{veh}	=	Adjustment factor for vehicle types	[-]
	$p_{C,RT}^{'}; p_{MC,LT}^{'}; p_{C,LT}^{'}$	=	Proportion of right-turning passenger cars, left-turning motorcycles, and left-turning passenger cars in the flow excluding right-turning motorcycles	[-]
	$a_1; b_1; c_1$	=	Coefficients	[-]

The calibration process of turning adjustment factors will be presented in Chapter 5.

4.3.4.2 Adjustment Factor for Turning Movements with the Interference of Opposing Flows

At intersections of two-way roads controlled by fixed-time two-phase signal programs, there are many conflicts between left-turning movements and opposing through-movements, and between opposing left-turning movements and through-vehicles. All these conflicts would affect the targeted saturation flow rate and make calculation procedures more complicated.

The special procedure for estimating the left-turning adjustment factor in permitted phasing was first established in the 1985 Highway Capacity Manual (TRB, 1985), and some similar methods were also applied by Akçelik (1981). In such methods, a fundamental assumption is that left turners must give priority to opposing through-movements. Left turners by then could not across the intersection when opposing through-movements is still operating under saturated condition. In MDCs conditions, there is no priority rule applied entirely. Left-turning movements even can pass the intersection during the saturated state if they could find appropriate gaps. Thus, the implemented method to estimate the adjustment for left-turning movements in MDCs is quite different when compared to the one being applied in car traffic-based cities.

The effective green time should be divided to two periods, which have different traffic operations: the first period is from the start of the start-up lost time l_1 to the end of the entering time t_{e1} (the time needed by vehicles run from the stop line to the conflict point between the clearing through flow and the opposing clearing left-turning flow); the second period is from the end of the entering time to the end of the effective green time.

- During the time $(t_{e1} - l_1)$ (from the end of the start-up lost time l_1 to the end of the entering time t_{e1}), left-turning movements are not impeded by opposing through-movements and through-vehicles are not also influenced by opposing left turners (Figure 4-4). The turning effect in this period is similar to the effect of turning movements without the interference of opposing stream mentioned in section 4.3.5.

- During the rest of effective green time $t_g - (t_{e1} - l_1)$, the situation is more complicated. Assume the departure flow remains a saturated state during this interval. Left turners are impeded by opposing through-movements. They need time to stop at the intersection and find suitable gaps between opposing through-movements. The stopping activities of left turners affect the saturation flow rate of the targeted stream. On the other hand, opposing left turners may block through-vehicles and the saturation flow rate of this stream changes subsequently.

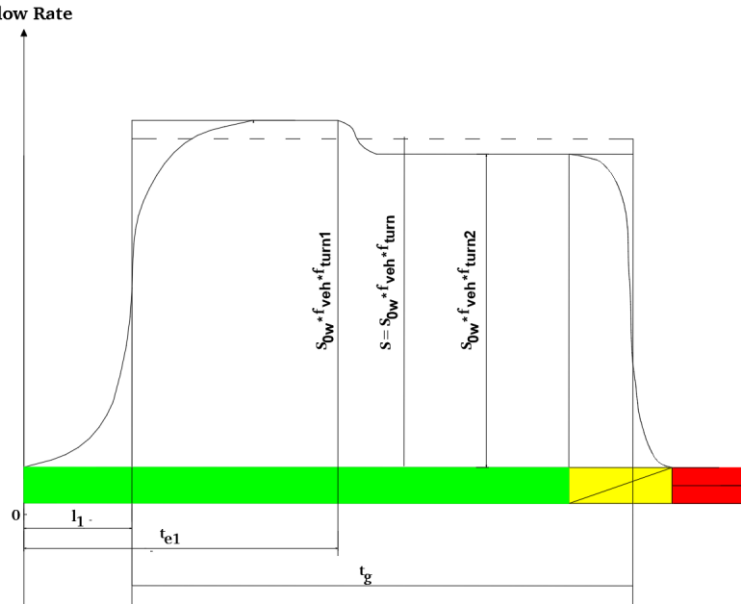

Figure 4-4: Changes of Flow Rate over Time Periods

In Figure 4-4, the total turning adjustment factor in this case could be identified as:

$$f_{turn} = \frac{t_{e1}-l_1}{t_g} \cdot f_{turn,1} + \frac{t_g-(t_{e1}-l_1)}{t_g} \cdot f_{turn,2} \quad (4\text{-}14)$$

where f_{turn} = Adjustment factor for turning movements with the interference of opposing flows during the effective green time t_g [-]

$f_{turn,1}$ = Adjustment factor for turning movements without the interference of opposing flows during the time $t_{e1} - l_1$ [-]

$f_{turn,2}$ = Adjustment factor for turning movements with the interference of opposing flows during the rest of effective green time $t_g - (t_{e1} - l_1)$ [-]

Equation 4-14 is applied when $t_{e1} \geq l_1$. In case $t_{e1} < l_1$, the flow is still accelerating to the saturation state. The turning adjustment factor in this case could be modified as:

$$f_{turn} = f_{turn,2} \quad (4\text{-}15)$$

The adjustment factor for turning movements $f_{turn,1}$ is similar to the case in Chapter 4.3.4.1 because right-turning movements do not make conflicts with the opposing flows.

The adjustment factor for turning movements $f_{turn,2}$ is a combination of the adjustment factor for right-turning movements $f_{RT,2}$, the adjustment factor for left-turning movements $f_{LT,2}$ and the adjustment factor for opposing left-turning movements. Muiltple all above factors, we have:

$$f_2 = f_{RT,2} \cdot f_{LT,2} \cdot f_{OPL,2} \quad (4\text{-}16)$$

The effect of right-turning movement remains the same in any green time duration. Thus, the adjustment factor of right-turning movements in this case is predicted the same as the one in Section 4.3.4.1:

$$f_{RT,2} = f_{RT,1} = \frac{1}{1+a_1 \cdot p'_{PC,RT}} \quad (4\text{-}17)$$

The effect of left-turning movements in this case is more complex than the case in Section 4.3.4.1. Left turners would be impeded by opposing through-movements while they are interacting at the conflict area. Normally, left-turning movements would stop, give way to opposing through traffic and wait for suitable gaps to across the conflict area. There are some reasons explaining how left turners somehow could find gaps:

- The grouping behaviour could help left turners to accept a smaller gap depending on the group size. Thus, there could be some opportunities for left turn vehicles to pass the intersection.

- The opposing through flow rate does not always run in the saturated state. Figure 4-5 shows the change in performance of opposing flow depending on the section's position (let see Section A-A at the stop line position and Section B-B at the location before the conflict area with left-tuning vehicles). If there is no turning vehicle at section A-A, the saturation flow rate at Section A-A ($S_{OP,A-A}$) is equal to the saturation flow rate at Section B-B ($S_{OP,B-B}$). The flow running from Section A-A to Section B-B remains a saturated state and the gaps between vehicles are so small that targeted left-turning vehicles cannot pass through. However, if there are some turning vehicles at Section A-A, $S_{OP,B-B}$ is higher than $S_{OP,A-A}$ because the saturation flow rate at Section A-A is affected by turning movements, while the saturation flow rate at Section B-B is not (assume that the approach width from Section A-A to Section B-B remains the same and the proportions of vehicle type are the same for all flows). The saturation degrees at both Section A-A and Section B-B are calculated as:

$$\begin{cases} g_{A-A} = \dfrac{q_{OP,LT} + q_{OP,TH} + q_{OP,RT}}{S_{A-A}} \\ g_{B-B} = \dfrac{q_{OP,TH}}{S_{B-B}} \end{cases} \quad (4\text{-}18)$$

In Equation 4-18, we can conclude that $g_{B-B} \leq g_{A-A}$. Consequently, the gaps between vehicles of flow crossing Section B-B is higher than the gaps between vehicles of flow crossing Section A-A and this will make more opportunities for targeted left-turning vehicles to pass through the opposing flow.

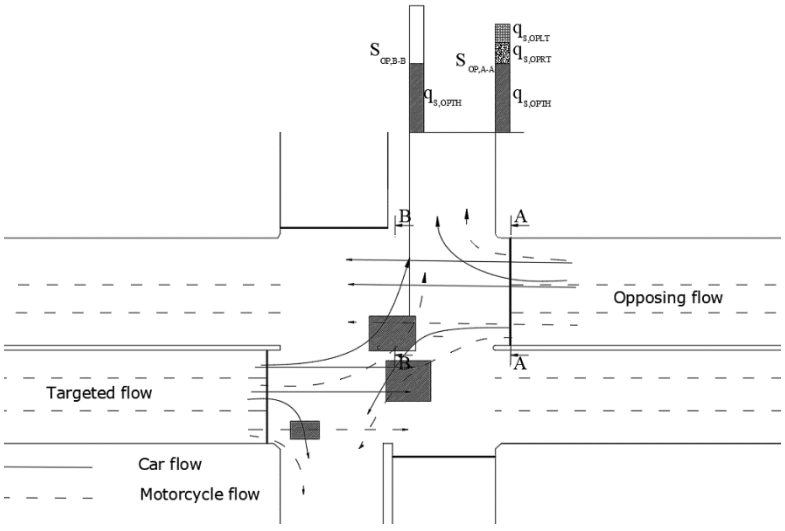

Figure 4-5: The change of Saturation Degree on Opposing Flow

In general, the adjustment factor for left-turning movements is a function of proportion of left-turning movements (passenger cars and motorcycles) in the flow excluding right-turning motorcycles $p_{LT}^{'}$ and interaction degree between left-turning movements and opposing through-movements $g_{int,TH-OPL}$: The adjustment factor for left-turning movements could be suggested as:

$$f_{LT,2} = 1 - P(p_{LT}^{'}; g_{int,TH-OPL}) \tag{4-19}$$

Moreover, interaction degree between left-turning movements and opposing through-movements $g_{int,TH-OPL}$ is a function of proportion of left-turning movements in the flow rate excluding right-turning motorcycles $p_{LT}^{'}$ and the saturation degree of opposing through-movements at the section before the conflict area $g_{OPT}^{'}$.

$$g_{\text{int},TH-OPL} = Q(p_{LT}^{'}; g_{OPT}^{'}) \tag{4-20}$$

There are some conditions for f_{LT2} and other variables in Equation 4-19:

Condition 1: If there is no opposing flow ($g_{OPT}^{'}=0$) or no left-turning movement, the interaction between left-turning movements and opposing through-movements will not happen. in this case:

$$g_{\text{int},TH-OPL} = \text{Q}(p_{LT}^{'} = 0 \vee g_{OPT}^{'} = 0) = 0 \tag{4-21}$$

Thus, the form of the interaction degree $g_{int,TH-OPL}$could be expressed as:

$$g_{\text{int},TH-OPL} = m_1 \cdot p_{LT}^{'} \cdot g_{OPT}^{'} \tag{4-22}$$

Where m_1 is a coefficient.

Condition 2: If there is no opposing flow ($g_{OPT}^{'}=0$), the adjustment factor for left-turning movements f_{LT2} now depends on the proportion of left-turning movements and has the form as:

$$f_{LT,2} = 1 - f(p_{LT}^{'}; g_{\text{int},TH-OPL} = 0) = \frac{1}{1 + k_1 \cdot p_{LT}^{'}} = 1 - \frac{k_1 \cdot p_{LT}^{'}}{1 + k_1 \cdot p_{LT}^{'}} \tag{4-23}$$

Where k_1 is a coefficient.

Based on the Equation 4-19, 4-22 and 4-23, the form of f_{LT2} could be set up as:

$$f_{LT,2} = 1 - \frac{k_1 \cdot p_{LT}^{'}}{1 + k_1 \cdot p_{LT}^{'} + m_1 \cdot p_{LT}^{'} \cdot g_{OPT}^{'}} = 1 - \frac{k_1 \cdot p_{LT}^{'}}{1 + k_1 \cdot p_{LT}^{'} \cdot (1 + m_2 \cdot g_{OPT}^{'})} \tag{4-24}$$

Where $m_2 = \frac{m_1}{k_1}$ is a coefficient.

The Equation 4-24 reflects the effect of left-turning movements and the interaction between left-turning flow and opposing through-flow. However, the effect of motorcycles and the effect of cars in the left-turning flow and the opposing through-flow are different. Therefore, the proportion of left-turning movements and the saturation degree of opposing through-flow in Equation 4-24 should be adjusted as follows:

$$k_1 \cdot p'_{LT} = a_2 \cdot p'_{MC,LT} + b_2 \cdot p'_{PC,LT} \quad (4\text{-}25)$$

$$m_2 \cdot g'_{OPT} = \frac{d_2 \cdot q_{MC,OPT} + e_2 \cdot q_{PC,OPT}}{S_{OPT}} \quad (4\text{-}26)$$

Where	$p'_{MC,LT}$; $p'_{PC,LT}$	=	Proportion of left-turning motorcycles and passenger cars in the targeted flow excluding right-turning motorcycles	[-]
	$q_{MC,OPT}$; $q_{PC,OPT}$	=	Opposing through flow rate of motorcycles and passenger cars	[veh/h]
	S_{OPT}	=	Saturation flow rate of opposing through-movements at the section before the conflict area	[veh/h]
	a_2; b_2; c_2; d_2; e_2	=	Coefficients	[-]

Finally, the adjustment factor for left-turning movements could be justified as:

$$f_{LT,2} = 1 - \frac{a_2 \cdot p'_{MC,LT} + b_2 \cdot p'_{PC,LT}}{1 + (a_2 \cdot p'_{MC,LT} + b_2 \cdot p'_{PC,LT}) \cdot (c_2 + \frac{d_2 \cdot q_{MC,OPT} + e_2 \cdot q_{PC,OPT}}{S_{OPT}})} \quad (4\text{-}27)$$

Where	f_{LT2}	=	Adjustment factor for left-turning movements	[-]
	$p'_{MC,LT}$; $p'_{PC,LT}$	=	Proportion of left-turning motorcycles and passenger cars in the targeted flow excluding right-turning motorcycles	[-]
	$q_{MC,OPT}$; $q_{PC,OPT}$	=	Opposing through flow rate of motorcycles and passenger cars	[veh/h]
	S_{OPT}	=	Saturation flow rate of opposing through-movements at the section before the conflict area	[veh/h]
	a_2; b_2; c_2; d_2; e_2	=	Coefficients	[-]

The effect of opposing left-turning movements on the saturation flow rate is similar to the effect of left turners. Opposing left turners passing the intersection would make conflicts with through-vehicles. Normally, opposing left turners would stop, give way to through traffic and then try to find suitable gaps from the through-flow. After opposing left turners find a gap and start to move, through-vehicles must stop before the conflict area and by then affect the targeted saturation flow rate. Similar with the creating process of $f_{LT,2}$, the adjustment factor for opposing left-turning movements is estimated as:

$$f_{OPL,2} = 1 - \frac{(a_3 \cdot q_{MC,OPL} + b_3 \cdot q_{PC,OPL}) \cdot (c_3 + \frac{d_3 \cdot q_{MC,TH} + e_3 \cdot q_{PC,TH}}{S_{TH}})}{1 + (a_3 \cdot q_{MC,OPL} + b_3 \cdot q_{PC,OPL})} \quad (4\text{-}28)$$

Where	$f_{OPL,2}$	=	Adjustment factor for opposing left-turning movements	[-]
	$q_{MC,OPL}$; $q_{PC,OPL}$	=	Proportion of left-turning motorcycles and passenger cars in the targeted flow	[-]
	$q_{MC,TH}$; $q_{PC,TH}$;	=	Through flow rate of motorcycles and passenger cars	[veh/h]
	S_{TH}	=	Saturation flow rate of through-vehicles at the section before the conflict area	[veh/h]
	a_3; b_3; c_3; d_3; e_3	=	Intercepts	[-]

The adjustment factor for turning movements with the interference of opposing flows $f_{turn,2}$ can be written below:

$$f_2 = f_{RT,2} \cdot f_{LT,2} \cdot f_{OPL,2} \tag{4-29}$$

$$f_{turn,2} = \frac{q_{MC,RT}}{S} + f_2 \cdot \left(1 - \frac{q_{MC,RT}}{S}\right) \tag{4-30}$$

The calibration results of turning effect are presented in Chapter 5.

4.4 Effective Green Time Model

Effective green time is one of the essential inputs to calculate the capacity of signalised intersections. The effective green time t_g is determined by the displayed green time t_G minus the start-up lost time l_1 at the beginning green period when vehicles are speeding up, plus the time gained by vehicles making use of the amber period λ_2 (green end-lag time).

$$t_g = t_G - l_1 + (t_A - l_2) = t_G - l_1 + \lambda_2 \tag{4-31}$$

Where	t_g	=	Effective green time	[s]
	t_G	=	Displayed green time	[s]
	l_1	=	Start-up lost time	[s]
	t_A	=	Amber time	[s]
	l_2	=	Clearance lost time	[s]
	λ_2	=	Green end-lag time, $\lambda_2 = t_A - l_2$	[s]

In MDCs conditions, there are some differences between theoretical models and real situations. In the queuing state, there are several illegal traffic situations, such as vehicles stopping over the stop line, vehicles standing in the wrong direction (standing in the opposing flow's road), vehicles running on the sidewalk and vehicles turning right during the red time (Figure 4-5 and Figure 4-6). In the departure state, vehicles do not always depart right after the green light turns on. They would depart earlier or later depending on some specific situations (the effect of signal countdown system would make vehicles leave sooner and the impact of short intergreen time would make vehicles depart later). In the clearing state, there are some cases where vehicles try to cross the stop line even when the red light is on. Although those behaviours are illegal and should not be encouraged, these phenomena occur almost in every cycle, especially during peak hours. Therefore, it is needed to consider the effect of illegal stopping vehicles on the capacity. The impact of illegal stopping vehicles will be converted to the change of the effective green time.

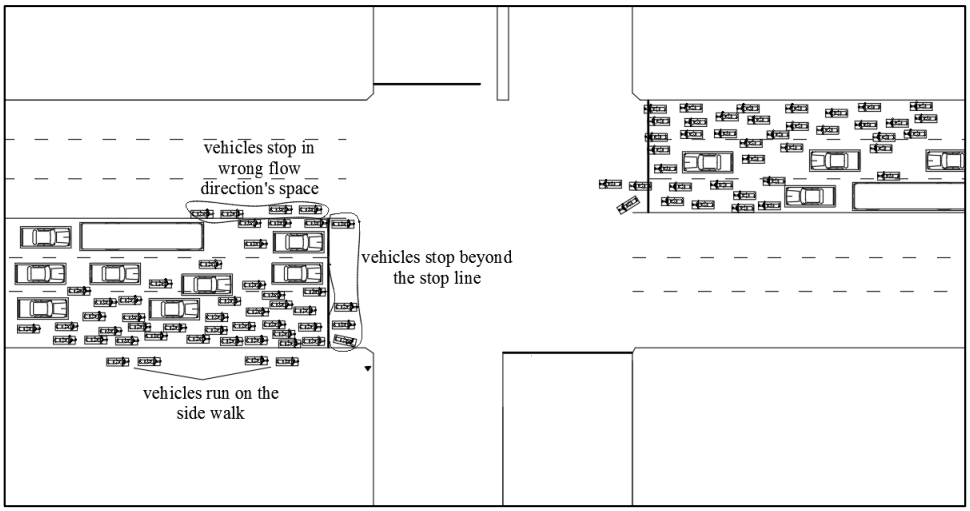

Figure 4-6: Illegal Activities During the Queued State

Note. Own Drawing

Figure 4-7: Vehicles Stop beyond the Stop line During the Red Time

Note. Own Picture

Start-up lost times and clearance lost time are estimated by a method as shown in Figure 4-8. The start-up lost time is defined by determining the number of vehicles cross the stop line from the start of green to the time that the flow reaches the saturation state. The clearance lost time is estimated by the number of vehicles crossing the stop line from the end of saturation flow state to the end of amber.

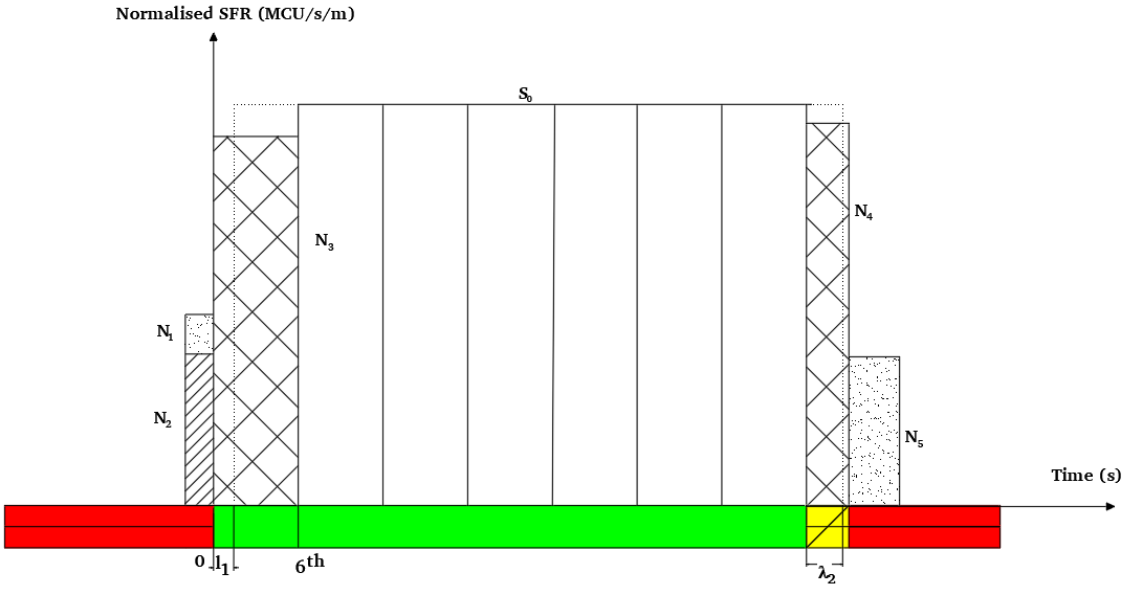

Figure 4-8: Effective Green Time Calculation Model

Note. Own Graph

To eliminate the effect of mixed traffic condition on the effective green time, assume the traffic flows are homogeneous motorcycle flows. In Figure 4-8, the number of motorcycles passing the stop line in different timing state would be separated, as follows:

- N_1: The number of motorcycles per 1 m wide approach stopping over the stop line during the red time [mcu/m]
- N_2: The number of motorcycles per 1 m wide approach departing over the stop line during the red time [mcu/m]
- N_3: The number of motorcycles per 1 m wide approach departing over the stop line during the first 6-second green period [mcu/m]
- N_4: The number of motorcycles per 1 m wide approach clearing over the stop line during the amber time [mcu/m]
- N_5: The number of motorcycles per 1 m wide approach clearing over the stop line during the red time [mcu/m]
- s_0: The normalised saturation flow rate per 1 m wide approach [veh/(h*m)] (the saturation flow starts after the first six seconds of the displayed green interval)

Two models of effective green time calculation are introduced depending on different assumptions:

Model 1: The assumption is that motorcycles must follow the traffic rule strictly. The red-light running behaviour is not considered.

Model 2: The calculation adapts to the actual traffic situation and the actual traffic behaviour. The red-light running behaviour is considered in this case.

In model 1, effective green time is considered as the normal effective green time. All motorcycles operating in the illegal state are eliminated (N_1,N_2,N_5 are ignored). Components of the model 1 are described:

$$l_{1,nor} = 6 - \frac{N_3}{S_0} \cdot 3,600$$
$$\lambda_{2,nor} = \frac{N_4}{S_0} \cdot 3,600 \quad (4\text{-}32)$$
$$t_{g,nor} = t_G - l_{1,nor} + \lambda_{2,nor}$$

Where	$t_{g,nor}$	=	Normal effective green time	[s]
	t_G	=	Displayed green time	[s]
	$l_{1,nor}$	=	Normal start-up lost time	[s]
	$\lambda_{2,nor}$	=	Normal green end-lag time	[s]

In model 2, the effective green time is considered as the maximum effective green time. The components of the model 2 are given:

$$l_{1,\max} = 6 - \frac{N_1 + N_2 + N_3}{S_0} \cdot 3,600$$
$$\lambda_{2,\max} = \frac{N_4 + N_5}{S_0} \cdot 3,600 \quad (4\text{-}33)$$
$$t_{g,\max} = t_G - l_{1,\max} + \lambda_{2,\max}$$

Where	$t_{g,max}$	=	Maximum effective green time	[s]
	$l_{1,max}$	=	Maximum start-up lost time	[s]
	$\lambda_{2,max}$	=	Maximum green end-lag time	[s]

Results of effective green time estimation are included in Chapter 5.

4.5 Intergreen Time Model

Chapter 2 introduced the intergreen time calculation methods. The German method seems to be suitable for MDCs conditions because of similar traffic behaviour and the high demand situation. Vehicles especially motorcycles are very flexible, having wide visions and can accelerate and decelerate quickly. Entering motorcycles tend to start right after clearing vehicles passing the conflict point instead of passing completely the intersection. Thus, the intergreen time calculation method in this study will follow the German method, but in some different cases, it would be modified to be appropriate for MDCs conditions. The intergreen time in MDCs could be determined below:

$$t_{ig} = t_{cr} + t_{cl} - t_e \quad (4\text{-}34)$$

Where	t_{ig}	=	Intergreen time	[s]
	t_{cr}	=	Crossing time	[s]
	t_{cl}	=	Clearing time	[s]
	t_e	=	Entering time	[s]

The crossing time is the time taken by the last vehicle in the approaching stream that crosses the intersection to reach the stop line, after the onset of the amber signal (Arasan, Boltze, 2006). The crossing time t_{cr} is regularly estimated based on the dilemma zone theory and lower than or equal to the amber time t_A.

$$t_{cr} \leq t_A \tag{4-35}$$

The clearing time t_{cl} is the time needed to cover the clearing distance l_{cl} (see Section 2.5.2) at a clearing speed v_{cl} (RiLSA, 2015). In MDCs, the fixed-time two-phase signal program assigned creates conflicts between clearing streams, especially between clearing through-vehicles and clearing opposing left-turning movements within the same phase. Figure 4-9 shows how clearing vehicles interact with each other before they pass the conflict area of entering vehicles. Therefore, the interaction time between clearing streams should be added to the clearing time calculation. The clearing time for MDCs is given as:

$$t_{cl} = \frac{l_{cl}}{v_{cl}} + t_{\text{int}} = \frac{l_0 + l_{veh}}{v_{cl}} + t_{\text{int}} \tag{4-36}$$

where t_{cl} = Clearing time [s]
l_{cl} = Clearing distance [m]
l_0 = Basic clearing distance [m]
l_{veh} = Vehicle length [m]
t_{int} = Interaction time between though-clearing vehicles and clearing left-turning movements [s]

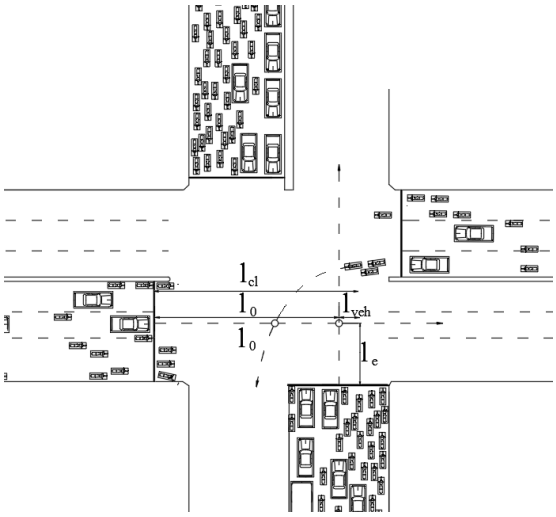

Figure 4-9: Clearing and Entering Distances

Note. Own Drawing

Besides the fundamental components of clearing time, it should be increased by the interaction time t_{int} to take into consideration the effect of the conflict between clearing through-vehicles and opposing-clearing left-turning movements during the intergreen time. The clearing through-vehicles would continue to move or stop to give way to the opposing-clearing left-turning movements depending on the number and the type of left-turners. Usually, the clearing through-vehicles may decelerate and then make a stop/go decision.

The interaction time can be measured by observing two clearing states:

State 1: The free flow clearing time, $t_{cl,free}$: The time that clearing through-vehicles are running without the interference of opposing clearing left-turning movements.

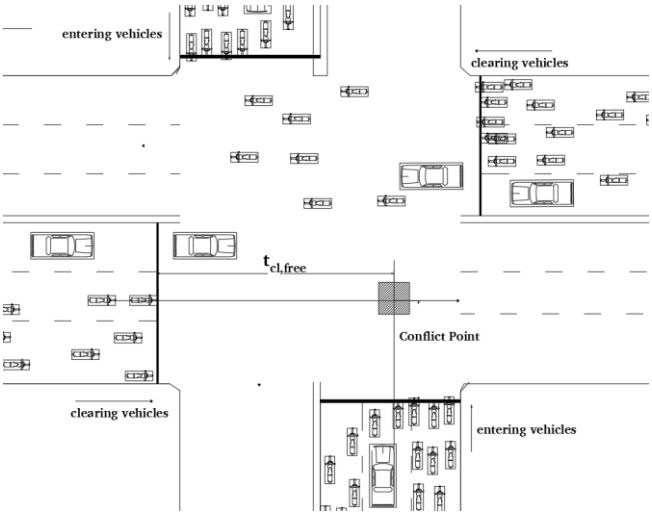

Figure 4-10: Clearing through-vehicles are running in free flow state

By selecting several cycles in which the opposing clearing left-turning vehicles would not impede the movement of the clearing through vehicles at the end of the green time, then $t_{cl,free}$ can be measured by observing the time that vehicles in clearing direction at the end of the green time can move from the stop line to the conflict point.

State 2: The normal clearing time, $t_{cl,int}$: The time that clearing through-vehicles are running with the interference of opposing clearing left-turning movements.

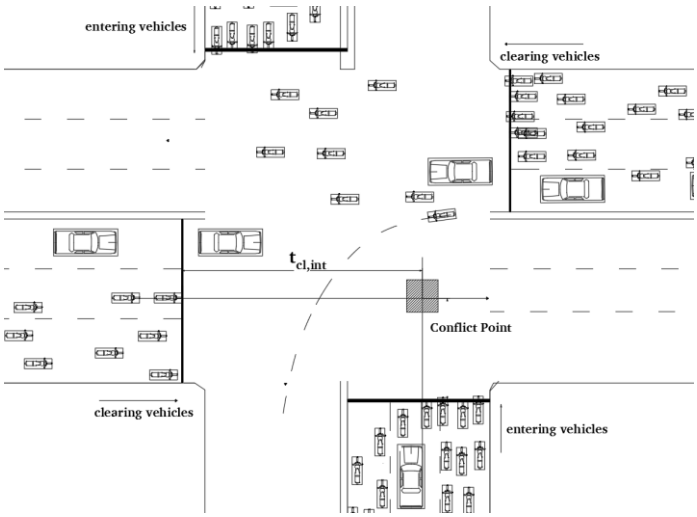

Figure 4-11: Clearing through-vehicles are running with the interference of opposing clearing left-turning movements

By selecting several cycles in which the opposing clearing left-turning vehicles impede the movement of the clearing through vehicles at the end of the green time, then $t_{cl,int}$ can be measured by observing the time that vehicles in clearing direction at the end of the green time can move from the stop line to the conflict point. The clearing time of through vehicle in this case is obviously higher are than the one in the case of they are running in free flow state (case 1) because they need more time to react with the interference of opposing clearing left-turning movements.

Finally, the interaction time could be suggested as:

$$t_{int} = t_{cl,free} - t_{cl,int} \quad (4\text{-}37)$$

The entering time t_e is calculated from the time when the first motorised vehicle (usually motorcycle) departs to cross the stop line from the start of green to the time it gets the conflict point of the clearing vehicle. The entering time is calculated by:

$$t_e = \frac{l_e}{V_e} \tag{4-38}$$

where t_e = Entering time [s]
l_e = Entering distance [m]
V_e = Entering speed [m/s]

4.6 Capacity Calculation Model

The approach capacity is computed based on several elements including saturation flow rate, effective green time, cycle time. The value of approach capacity may vary depending on whether or not illegal activities are taken into consideration. Thus, two kinds of capacity are estimated: normal capacity and maximum capacity.

4.6.1 Normal Capacity

The normal capacity $C_{nor,i}$ is computed from the normal effective green time t_g under the assumption that all vehicles must follow the traffic rule and no illegal activities are accepted. The normal capacity is usually smaller than the real capacity because the amount of capacity retrieved from illegal activities is not considered.

$$C_{nor,i} = \frac{t_{g-nor}}{t_C} \times S_i \tag{4-39}$$

where $C_{nor,i}$ = Normal capacity of approach i [veh/h]
S_i = Saturation flow rate of approach i [veh/h]
t_{g-nor} = Normal effective green time [s]
t_C = Cycle time [s]
i = Index indicating approach [-]

4.6.2 Maximum Capacity

The maximum capacity $C_{max,i}$ is calculated with the effect of illegal traffic activities including red-light running. The maximum effective green time would lead to the maximum capacity. Thus, the maximum capacity at approach i could be calculated as:

$$C_{\max,i} = \frac{t_{g-\max}}{t_C} \times S_i \tag{4-40}$$

where $C_{max,i}$ = Maximum capacity of approach i [veh/h]
S_i = Saturation flow rate of approach i [veh/h]
t_{g-max} = Maximum effective green time [s]
t_C = Cycle time [s]
i = Index indicating approach [-]

4.7 Conclusions

The theoretical capacity model is built up as the combination of the saturation flow rate model, the effective green time model and the intergreen time model. The normal capacity and the maximum capacity are estimated depending on the different effective green times.

The homogeneous motorcycle flow condition is updated by adjustment factors to calculate the saturation flow rate for different traffic situations. The mentioned adjustment factors are the effect of approach width, the effect of vehicle type in the flow, and the effect of turning activities. In the model, the term 'normalised saturation flow rate' is introduced as the saturation flow rate passing over one-meter approach width because the saturation flow rate per lane is not proper to use in the calculation.

The effective green time model is determined based on the change of the start-up lost time and the green end-lag time. Two calculation models are set up. The first model is suggested while the norm "no red-light running' is strictly obeyed. Right-turning motorcycles, vehicles departing before the green time, and vehicles clearing after the amber time during the red time are eliminated. Therefore, the effective green time is lower than the real value. In the second model, the operations of vehicles during the red time (red-light running time) are considered within the calculation. The effective green time could reach the maximum value because all the discharged vehicles are considered.

The intergreen time model applies the German method with some modifications to adapt to the MDC's conditions. Besides, crossing time, clearing time, entering time, and interaction time between through and opposing left-turning movements during the clearing time must be added to the model because of the fixed-time two-phase signal program make those flows running in the same phase.

Above models are developed based on the theoretical formulation of vehicle traffic in MDCs and they need to be validated in practice which will be presented in Chapter 5.

5 Capacity Model Calibration

5.1 Introduction

Chapter 4 described the proposed capacity model theoretically. In this chapter, the calibration process including field surveys and data collection at signalised intersections in Ho Chi Minh City are presented. The empirical study in section 5.2 explains how data were collected in such specific traffic patterns. Then the calibration process in section 5.3 shows calibrated results which contribute to creating a complete capacity analysis model for MDCs. Finally, summaries and conclusions are depicted in Section 5.4.

5.2 Empirical Studies

This part describes the required data for the capacity model. Through field observations, data from the real traffic situation would be collected and clarified for different purposes.

5.2.1 Survey Requirements

Input data needed for the capacity model are retrieved from the vehicle characteristics, the traffic flow, the signal program, and the intersection geometry. All types of required data for this study are as follows:

Traffic volume: Traffic volume is the primary data for the capacity model. Traffic volume includes homogeneous motorcycle flow rate, homogenous car flow rate, and mixed traffic flow rate. Each volume data would be used for determining the ideal saturation flow calculation, the adjustment factor for the vehicle type, and the effect of turning activities. Traffic volumes are counted as the number of vehicles passing the stop line during different time intervals and they are classified as follows:

- Volumes are collected during the red time to determine the number of vehicles red-light running
- Volumes are counted during the first 6 seconds of the green interval to estimate the start-up lost time
- Volumes are observed from the start of green to the end of the saturated green time: only homogeneous motorcycle flows are applied in this case. Data are collected at each 2-second slice during the observation interval.
- Volumes are gathered from the first 6 seconds of the green interval to the end of saturated green time.
- Volumes are collected during the amber time to measure the green end-lag time

Timing intervals: Timing intervals in each cycle could be classified into several parts such as the entering time, the effective green time, the amber time, the red time, and the interaction time between the clearing through-vehicles and the clearing opposing left-turning movements

Traffic composition: Traffic composition is the secondary data extracted from volume data. This data includes the proportion among flows according to each vehicle type and each movement direction. It is assumed that traffic composition is stable over time intervals.

Headway: This data is used for estimating the homogeneous car saturation flow rate on separate car lanes.

Speed: Entering speed and clearing speed of each vehicle type at intersections would estimate the intergreen time.

Signal program: Signal program including cycle time, green time, amber time, intergreen time and red time would be used for the traffic flow evaluation.

Vehicle dimension: Vehicle dimensions are collected to calculate the intergreen time between different vehicle streams.

Intersection characteristics: Road geometries, approach width, entering distances, clearing distances are critical factors affecting the speed, the driver's behaviour and the intersection capacity. So, such characteristics must be collected for capacity analysis.

5.2.2 Requirements of Data Collection

Data collection should meet the following requirements:

- Traffic volume of each surveyed sample should be significant to ensure the saturation state occurs through a saturated green time.
- Vehicle type crossing the stop line must be well observed.
- Good weather condition is required for data collection: dry weather, dry pavement, normal windy condition.
- Bus stop stations must not locate near surveyed approaches to avoid the effect of bus blockage on the capacity.
- No on-street parking along the surveyed path to prevent the impact of parking activities on the capacity.
- The surveyed approach must not be selected near petrol stations or other attractive places (restaurants, shopping mall) to avoid abnormal driver behaviours.

5.2.3 Selection of Surveyed Intersections

Data were gathered from 36 approaches of 25 signalised intersections in Ho Chi Minh City, Vietnam. The surveys were conducted during the afternoon peak hour (16:30-18:30). Besides, only two cameras are used, they cannot cover all traffic flows and approaches. Thus, we selected appropriate approaches on which we can observe the needed traffic flows for the video recording.

Table 5-1 shows 36 surveyed approaches at selected intersections. The studied approaches are classified into five groups as presented in Figure 5-1 depending on different analysis purposes:

- **Group 1:** Eight approaches for only through-motorcycles are observed to analyse the homogeneous motorcycle saturation flow rate. There is no interference from the opposing flows to the targeted flows.
- **Group 2:** Four approaches for only through-cars are selected to analyse the homogeneous car saturation flow rate. There is no interference from the opposing flows to the targeted flows.
- **Group 3:** Eight approaches for through mixed vehicles are chosen to analyse the MCU value for vehicle types, and the effect of vehicle types on the saturation flow rate. There is no impedance from the opposing flows to the flow on the targeted approaches.
- **Group 4:** Five approaches on which the targeted flows are not impeded by the opposing flows are collected to analyse the effect of turning movements on the saturation flow rate without the interference of opposing flows. This case happens at intersections on which one-way streets or protected left-turning movements are applied.
- **Group 5:** Eleven approaches on which the targeted flows are impeded by the opposing flows are recorded to analyse the effect of turning movements on the saturation flow rate with the interference of opposing flows. This case happens at normal intersections on which all turning movements are allowed.

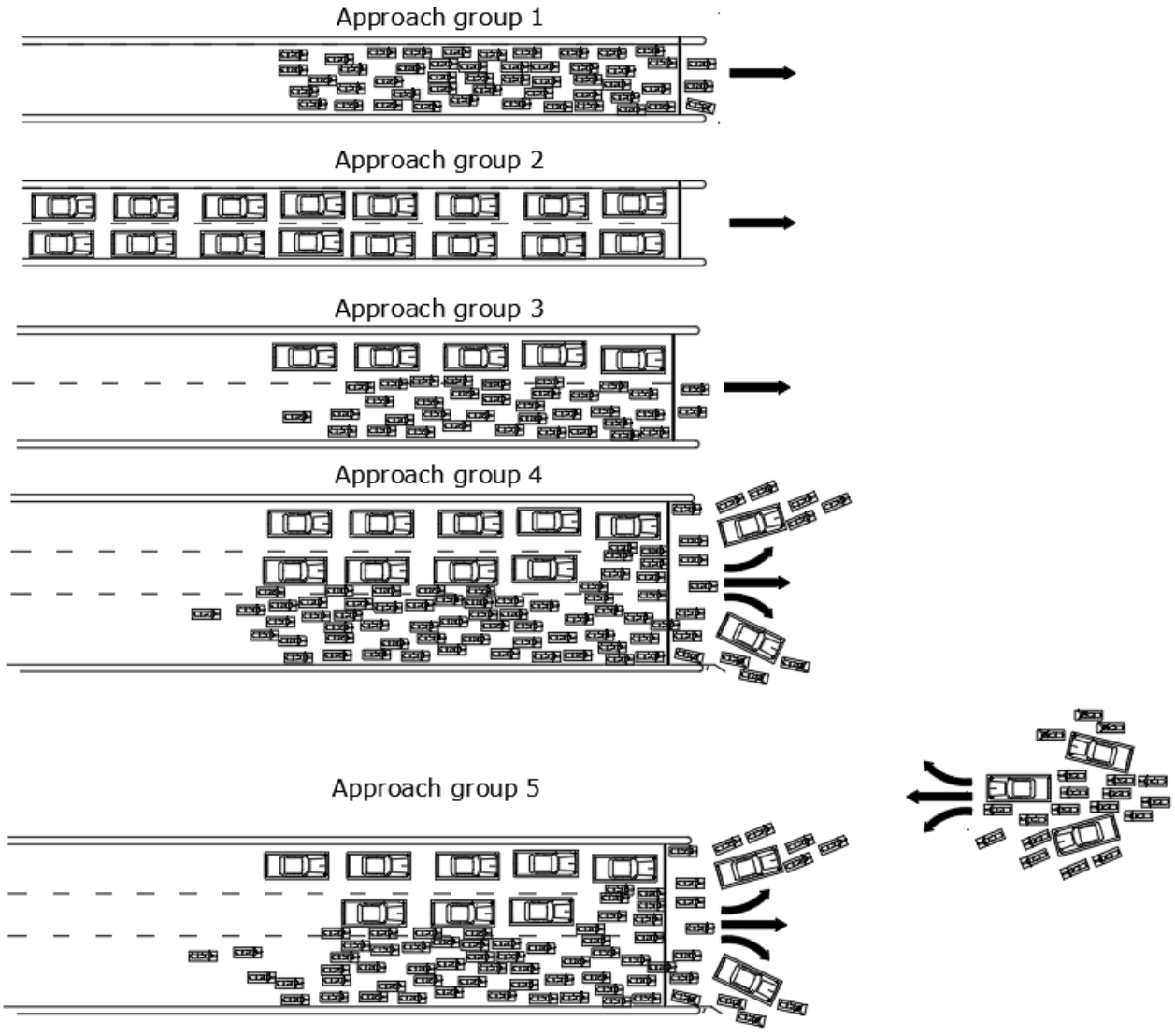

Figure 5-1: Classification of Approach Groups

Table 5-1: List of Surveyed Approaches

ID	Node	Observed Approach	W (m)	Mixed Flow	MC Flow	Car Flow	TH	LT	RT	OPT	OPL	Purpose	No. of sample
A01	Nam Ky Khoi Nghia - Tran Quoc Toan	Nam Ky Khoi Nghia	2.7	✓	✓		✓						28
A02	Tôn Đức Thắng-Nguyễn Hữu Cảnh	Ton Duc Thang	4		✓		✓						34
A03	Cong Hoa - Tan Ky Tan Quy	Cong Hoa	4.2		✓		✓					To analyse the homogenous motorcycle saturation flow rate	33
A04	Tay Hoa - Xa Lo Ha Noi	Xa Lo Ha Noi	5.5		✓		✓						41
A05	Truong Chinh - Pham Van Bach	Truong Chinh	9		✓		✓						43
A06	Vo Van Kiet - Nguyen Thai Hoc	Vo Van Kiet	4.5		✓		✓						44
A07	Mai Chi Tho-Dong Van Cong	Dong Van Cong	8		✓		✓						11
A08	Mai Chi Tho-Nguyen Thi Dinh	Nguyen Thi Dinh	3.8		✓		✓						17
A09	Cong Hoa - Tan Ky Tan Quy	Cong Hoa	3.5			✓	✓						26
A10	Vo Van Kiet - Nguyen Thai Hoc	Vo Van Kiet	3.5			✓	✓					To analyse the homogenous car saturation flow rate	21
A11	Mai Chi Tho-Dong Van Cong	Mai Chi Tho	3.5			✓	✓						18
A12	Mai Chi Tho-Nguyen Thi Dinh	Mai Chi Tho	3.5	✓	✓	✓	✓						10
A14	Cong Hoa - Tan Ky Tan Quy	Cong Hoa	7.9	✓			✓						31
A15	Truong Chinh - Pham Van Bach	Truong Chinh	3.5	✓			✓						16
A16	Su Van Hanh - To Hien Thanh	Su Van Hanh	3.8	✓			✓					To determine the MCU values and the effect of vehicle types on the saturation flow rate	9
A17	Truong Chinh - Phan Huy Ich	Phan Huy Ich	6.5	✓			✓						33
A18	Mai Chi Tho-Dong Van Cong	Tran Hung Dao	8	✓			✓						25
A19	Cong Hoa - Tan Ky Tan Quy	Cong Hoa	12	✓			✓						27
A24	Nguyen Thi Minh Khai - Mac Dinh Chi	Nguyen Thi Minh Khai	7	✓			✓		✓				29
A20	Nam Ky Khoi Nghia - Tran Quoc Toan	Nam Ky Khoi Nghia	9.8	✓			✓						30
A21	Dinh Bo Linh - Nguyen Xi	Dinh Bo Linh	11	✓			✓		✓			To determine the effect of turning movements without the interference of opposing flows on the saturation flow rate	35
A22	Nguyen Thi Minh Khai - Dinh Tien Hoang	Dinh Tien Hoang	11	✓			✓		✓				48
A23	Nguyen Dinh Chieu - Truong DInh	Nguyen Dinh Chieu	10	✓			✓		✓				22
A25	Dinh Bo Linh - Bach Dang	Dinh Bo Linh	11	✓			✓	✓	✓				46
A26	Nguyen Thong-Ly Chinh Thang	Ly Chinh Thang	7	✓			✓	✓	✓	✓	✓		29
A27	Dien Bien Phu - Hai Ba Trung	Hai Ba Trung	6.6	✓			✓	✓		✓			46

ID	Node	Observed Approach	W (m)	Mixed Flow	MC Flow	Car Flow	TH	LT	RT	OPT	OPL	Purpose	No. of sample
A28	Cach Mang Thang 8 - Vo Van Tan	Cach Mang Thang 8	7.2	✓			✓		✓	✓			30
A29	Tran Hung Dao - Nguyen Thai Hoc	Nguyen Thai Hoc	12	✓			✓	✓	✓	✓	✓		50
A30	Tran Hung Dao - Nguyen Thai Hoc	Tran Hung Dao	11	✓			✓	✓	✓	✓	✓	To determine the effect of turning movements with the interference of opposing flows on the saturation flow rate	43
A31	Hoang Dieu - Khanh Hoi	Khanh Hoi	5	✓			✓	✓	✓	✓	✓		21
A32	3/2 - Cao Thang	3 thang 2	11	✓			✓	✓	✓	✓	✓		24
A33	Nguyen Chi Thanh - Ly Thuong Kiet	Nguyen Chi Thanh	6	✓			✓	✓	✓	✓	✓		15
A34	An Duong Vuong-Nguyen Tri Phuong	Nguyen Tri Phuong	6.5	✓			✓	✓	✓	✓	✓		40
A35	3/2 - Le Hong Phong	3 thang 2	11	✓			✓	✓	✓	✓	✓		40
A36	Dinh Tien Hoang-Tran Quang Khai	Dinh Tien Hoang	7.2	✓			✓	✓	✓	✓	✓		35

Note. Own Table

Mixed flow: The observed flow was mixed by several vehicle groups

MC flow: The observed flow was homogeneous motorcycle flow

Car flow: The observed flow was homogeneous car flow

TH, LT, RT, OPT, OPL: Through, left-turning, right-turning, opposing through and opposing left-turning flow

5.2.4 Data Collection Methods

Traffic flow data recording method: Although there are many data collection methods to observe the traffic flow and its characteristics (IPTS, 2008), not all of them are suitable for motorcycle dominated flow. Among these methods, the video image processing (VIP) technology is the most suitable and reliable way to collect required data related to motorcycle flow. In this study, the traffic flows were recorded by cameras installed at elevated positions near the intersections. The view angle of cameras would be adjusted until it covers the targeted flows and the shared spaces where the conflicts among streams occur. The videos were recorded in MP4, AVI, and MTS formats. The camera resolution was set from 640x480 pixels to 1920x1080 pixels. The frame rate fluctuated from 25 to 30 frames per second. The video recording data was stored on a hard disc for the in-house data extraction.

Figure 5-2: An Example of Traffic Flow Recording Using Cameras

Note. Own Picture

Traffic volume data collection method: Unlike car flow, there is no available counting software which could help to extract the data in case of dominated motorcycle traffic flow. Thus, all 26 surveyed intersections were processed by counters manually based on the recorded videos. Two video processing software, KMP player and Camtasia 8, were used depending on the video format. The processing software slowed down the playing speed of the input videos by maximum 10 times. This technique would help to count accurately the traffic volume because there are too many motorcycles in the videos. Then, the extracted data were saved as Excel files for further analysis. Slowing down the input video, however, will increase the effort of traffic count. The time for this task was estimated as 1,000 counting hours.

Geometry data collection method: The geometry data were collected in the field using some metric devices. One surveyor uses a distance wheel meter or a laser distance meter (Figure 5-3) to measure the lane width, the approach width, and other intersection geometry dimensions to sketch the complete intersection layout. The secondary geometry data such as the crossing distance, the clearing distance, and other additional distances would be defined by using this layout.

Figure 5-3: Metric Devices Using for Geometry Data Collection

Note. Own Picture

Speed data collection method: The average speed of each vehicle type could be collected by observing the movement of vehicles passing pre-defined reference points during a time interval. The required speed data include entering speed, crossing speed, discharging speed.

Time data collection method: Required time intervals were collected from the videos recorded in the field. The time values were extracted in milliseconds since motorcycles with their small dimensions and high mobility could pass a section in less than 1 second.

5.3 Calibration Results

5.3.1 Motorcycle Saturation Flow Rate and the Capacity Reduction Phenomenon

In this part, approaches in group 1 were selected. The number of motorcycles passing the stop line during a saturated green time was counted. The saturated green time was divided into 2-second periods to detect fluctuations of discharge flow rates. It is assumed that vehicles passing the stop line when the light turns green would be counted for the discharge flow rate. Observed data are presented in Appendix C.1.

The graphs depicted from Figure 5-4 to Figure 5-8 show the discharge flow rates of motorcycle traffic. In all graphs, the discharge flow rates increase sharply at the first green interval and then remain stable to the peak value before declining in the later parts of the green interval. This phenomenon is called '**Capacity reduction phenomenon**".

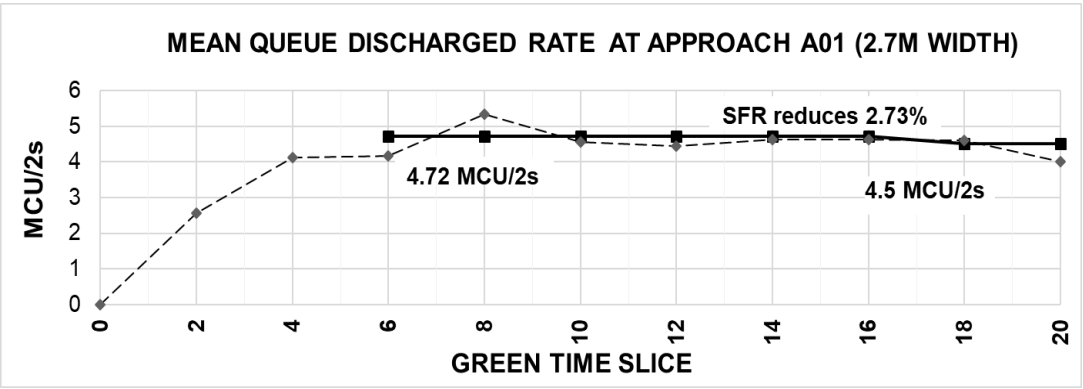

Figure 5-4: Mean Motorcycle Queue Discharge Flow Rate at Approach A01 (w=2.7 m)

Note. Own Graph

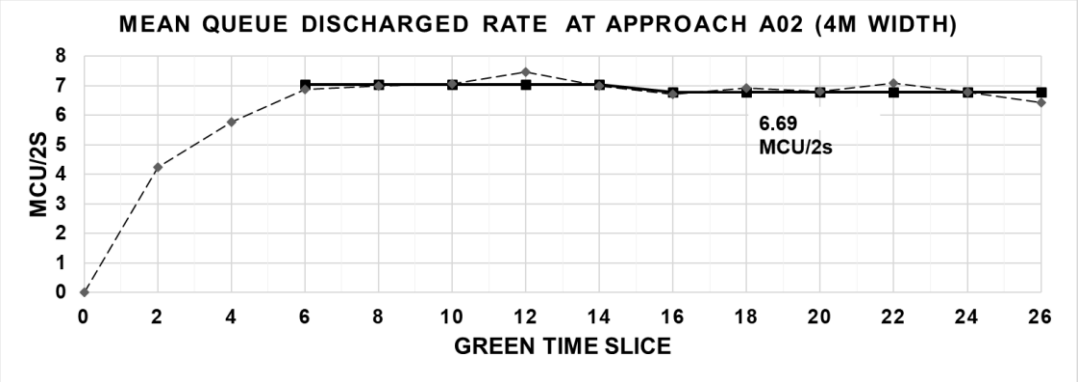

Figure 5-5: Mean Motorcycle Queue Discharge Flow Rate at Approach A02 (w=4 m)

Note. Own Graph

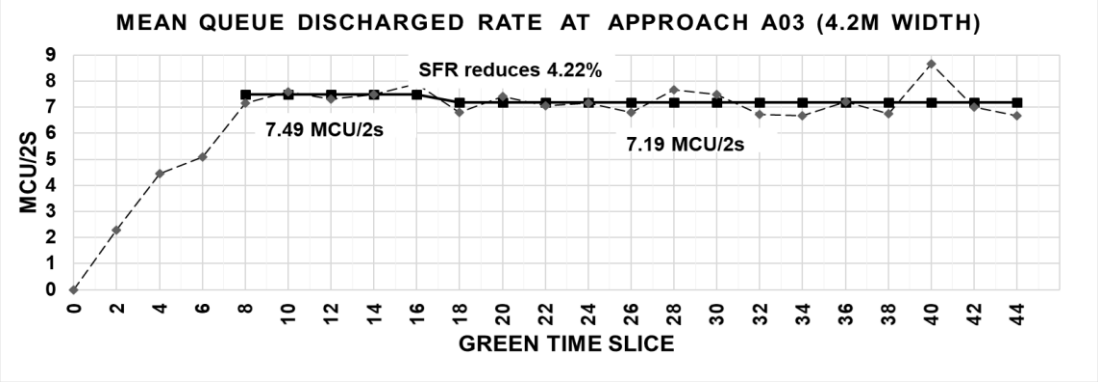

Figure 5-6: Mean Motorcycle Queue Discharge Flow Rate at Approach A03 (w=4.2 m)

Note. Own Graph

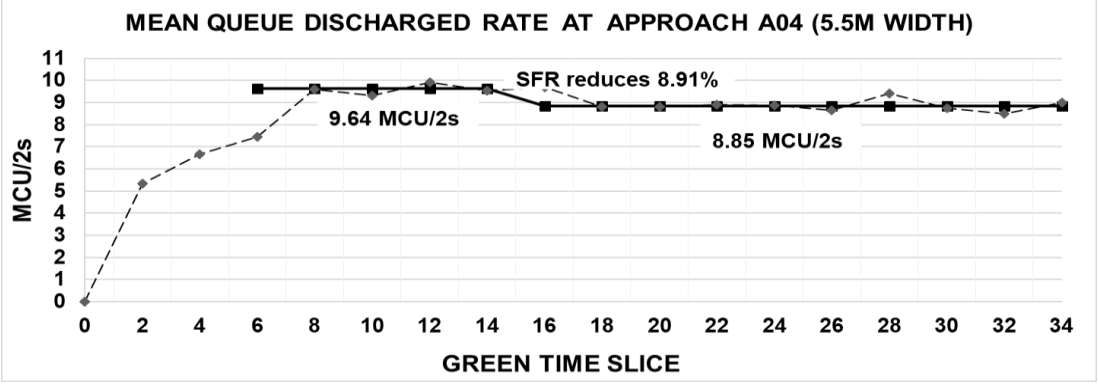

Figure 5-7: Mean Motorcycle Queue Discharge Flow Rate at Approach A04 (W=5.5m)

Note. Own Graph

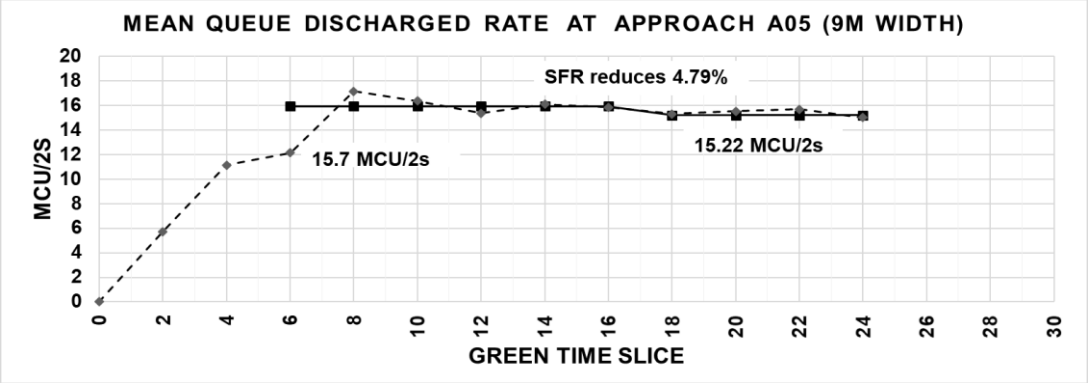

Figure 5-8: Mean Motorcycle Queue Discharge Flow Rate at Approach A04 (w=9.0 m)

Note. Own Graph

The saturation flow rate model of car dependent flow is based on the hypothesis that queue discharge increases rapidly to a steady maximum when the traffic signal turns to green, resulting in the number of vehicles remaining constant with the highest value during the saturated green time (Akçelik, 1981), (Teply et al., 2008). This assumption is not correct for motorcycle traffic. The observed results show that the green time could be separated into three durations. The first duration is from the 0^{th} second to 6^{th} second, the second one is from the 6^{th} to the 16^{th} second, and the third one is from 16^{th} second to the rest of observed green time.

In the first period, the lost time would occur because vehicles need time to start and move. The situation, in this case, is complex. In some studied areas where all the traffic signals are installed with the signal countdown systems, drivers are active and know precisely when the green time comes; they can start up even before the green begins. On the other hand, there are cases that motorcycles standing beyond the stop line during the red time do not realise exactly when the green begins until they see some vehicles are moving (Figure 5-9). This situation would reduce the discharge flow rate and affect the saturation flow rate. Thus, it is recommended that the first part of the green interval should be eliminated to avoid the effect of lost time and driving behaviour errors on the saturation flow rate.

Figure 5-9: The Impedance of Vehicles stopping over the Stop line to the Discharge Flow

Note. Own Picture

In the second part, the discharge flow rate of motorcycles reaches a peak value and then reduces to a smaller value in the third period. The reduction rate is not significant with small approaches where vehicles must stop in narrow road sections. However, the reduction rate becomes more significant when observing wider approaches where motorcycles can stop in a larger horizontal distance. This result could be explained by unequal distribution of density in the queued area. Instead, the density in the area close to the stop line is higher than the one in the back. Moreover, vehicles in the further area have more time to pass the stop line and the dispersion effect on motorcycle flow would then happen. The dispersion effect makes the discharge flow rate fluctuating up and down between successive time slices.

The saturation flow rate can be classified into two cases depending on the green time t_G. If t_G is lower than 16 s, the saturation flow rate would have the highest value. If t_G is equal or higher than 16 s, the saturation flow rate would be lower because of the capacity reduction phenomenon. Eight approaches which have only motorcycles were selected for the data collection and data analysis. A simple linear regression model reflecting the relationship between the saturation flow rate and the approach width was implemented and was drawn in Figure 5-10. Raw data, calculated parameters, and the regression results are described in Appendix C.2.

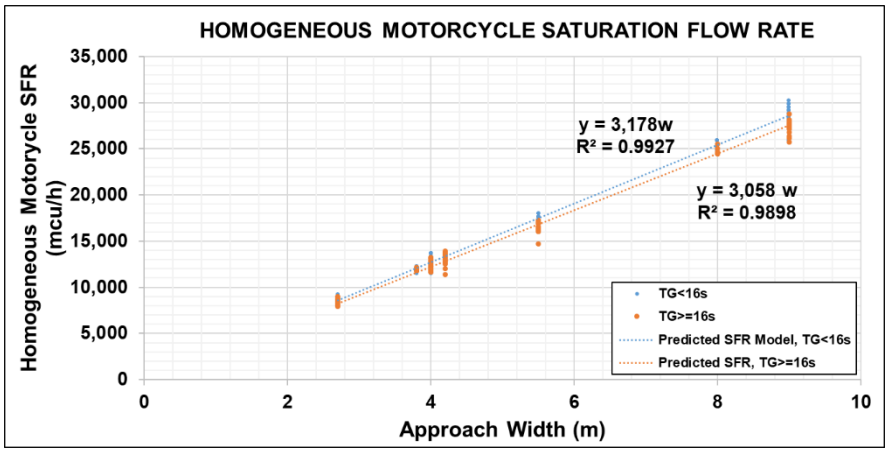

Figure 5-10: Motorcycle Saturation Flow Rate

Note. Own Graph

The equation of homogeneous motorcycle saturation flow rate is computed as follows:

$$\begin{cases} S_{0w} = 3{,}178 \times w \;\; if \; t_G < 16\; s \\ S_{0w} = 3058 \times w \;\; if \; t_G \geq 16\; s \end{cases} \tag{5-1}$$

In Equation 5-1, the constant is zero because the saturation flow rate is zero if the approach width is set as zero.

Figure 5-10 and Equation 5-1 show a high linear correlation between the saturation flow rate S_{0w} and the approach width W. The results depicted that the normalised homogeneous motorcycle flow rate is estimated at 3,058 mcu/(h*m) when the green time is equal or higher than 16 s and at 3,178 mcu/(h*m) when the green time is lower than 16 s. Accordingly, the saturation flow rate in the 3.5 m approach width could reach to around 11,000 mcu/h. this is equal to 5.5 times as many as the car saturation flow rate (2,000 pcu/h). This result is similar to the study of (Nguyen et al., 2007) when he pointed out that the saturation flow rate of 3.5 m approach width should be 11,241 mcu/h. Moreover, if the rate of motorcycle occupancy is assumed at 1.2, then homogeneous motorcycle flow could carry around 13,000 passengers to pass through a 3.5 m wide approach. Thus,

motorcycles are much more efficient than cars and even buses in terms of the passenger capacity aspect.

Note: If there is no information about the displayed green time. The case of $t_G \geq 16$ s is applied for further calculation.

5.3.2 Homogeneous Car Saturation Flow Rate

In MDCs, there are intersections that cars are separated from motorcycles as shown in Figure 5-11. In such cases, saturation flow rate values for cars traffic are determined by using the headway method which has been applied in developed countries.

Figure 5-11: Separate Car Traffic Flows at Signalised Intersection

Note. Own Picture

Four approaches with separated car lanes were chosen to observe the headway from the first car to the last car in the queue. Raw data and other calculated parameters are presented in Appendix C.3. The headway characteristics of car flow at each approach are depicted in Figure 5-12. Results show that the headway of car flow in MDCs differs from the one in car traffic-based cities. The headway remains stable after the fourth car's position, which is higher than the values found by other studies. It could be explained by the difference in the traffic environment. In MDCs, car drivers usually run under the pressure of crowded surrounding motorcycle traffic, they have to pay much attention to keep their own vehicles safe. As a result, the reaction time of car drivers in MDCs would be longer than the one in developed countries even if they are running on separated roads. Besides, operational speeds of cars in MDCs are also lower than those in developed countries.

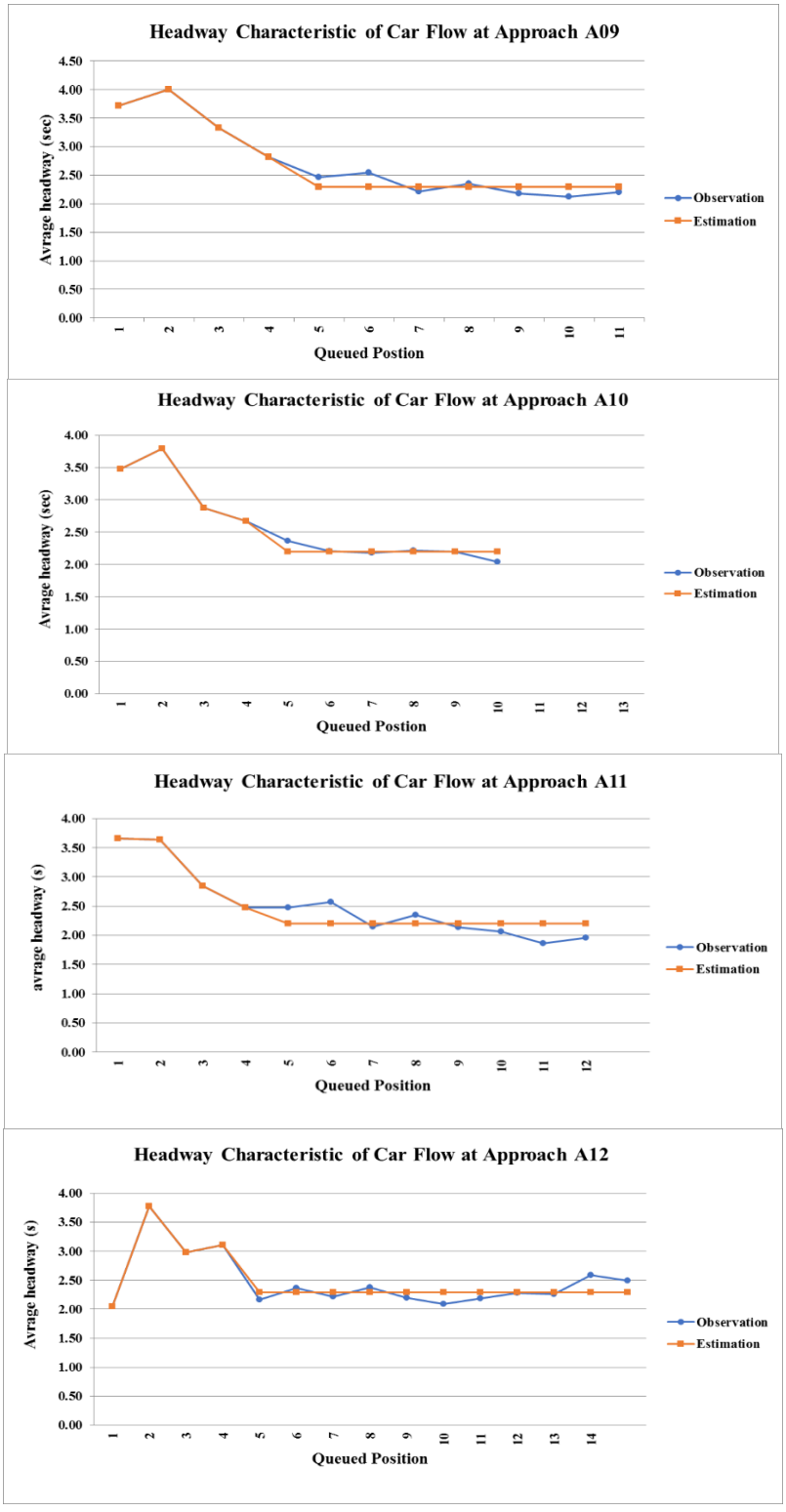

Figure 5-12: Headway Characteristics of Car Flows in MDCs

Note. Own Graph

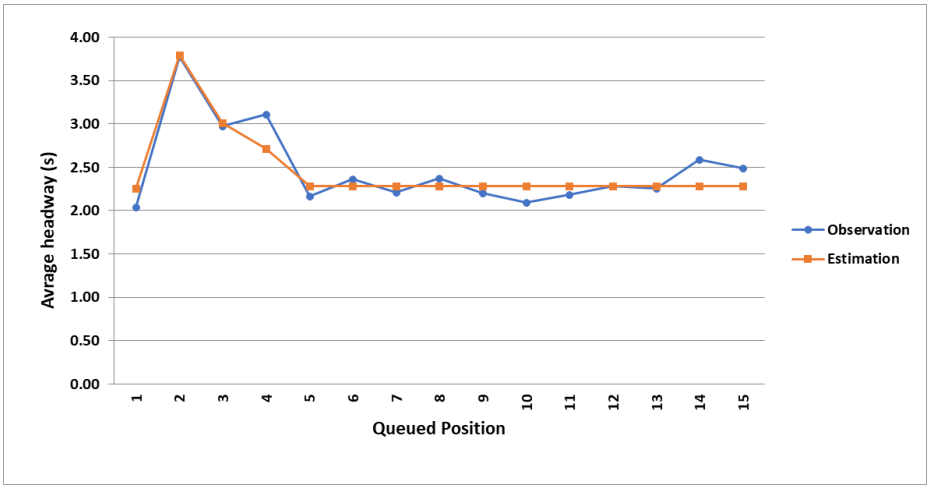

Figure 5-13: Average Headway Characteristics of Car Flows in MDCs

Note. Own Graph

Figure 5-13 shows the average headway h_s in MDCs. h_s is estimated as 2.3 s. In conclusion, the homogenous car saturation flow rate could be defined below:

$$S_{0C} = \frac{3,600}{h_s} = \frac{3,600}{2.3} = 1,565 \qquad [\text{pcu/(h*ln)}] \qquad (5\text{-}2)$$

The estimated saturation flow rate result of 1,565 pcu/h is much lower than the amount of 2,000 pcu/h in car traffic-based cities. There may be some reasons for this difference. The first one is the difference in driving behaviour of drivers throughout countries. Cars follow strictly the 'lane-based behaviour' in car dependent cities while they follow the 'non-lane-based behaviour' in MDCs particularly at signalised intersections. In that condition, cars take more time to react and they try to remain in safe spaces with surrounding motorcycles. Thus, even running in a separated lane, cars in MDCs could not respond as fast as cars in developed countries. The second reason could be unsuitable layout designs of signalised intersections including intersection geometries and applied signal programs.

5.3.3 Motorcycle Equivalent Unit

The MCU values for vehicles are estimated by using regression techniques. In this study, eight approaches are selected to collect the traffic volume and the traffic composition during the saturated green time. There are no turning activities and no interference from opposing flows to eliminate the effect of turning movements. Raw data, calculated parameters, and the regression results are illustrated in Appendix C.4.

As mentioned in Chapter 4, a regression model reflecting the relationship between the saturated green time T and the number of vehicles by vehicle types passing the stop line during that time is established. The numerical analysis is given:

$$T = 1.16 \cdot N_{MC} + 7.46 \cdot N_C + 11.05 \cdot N_{MV} + 17.95 \cdot N_{HV} \qquad (5\text{-}3)$$

where	T	=	Saturated green time	[s]
	$N_{MC}, N_C; N_{MV}; N_{HV}$	=	Number of motorcycles, cars, middle vehicles and heavy vehicles passing the stop line	[veh]

Table 5-2: The Results of Statistically Significant Test of MCU values

	Coefficient	MCU Value	PCU Value	Std.Error	t	Sig.
N_{MC}	1.16	1	0.16	0.006	179.556	0.000
N_C	7.46	6.4	1	0.112	66.718	
N_{MV}	11.05	9.5	1.5	0.472	23.398	
N_{HV}	17.95	15.5	2.4	0.544	33.019	

Note. Own Table

Table 5-2 shows the MCU values for different vehicles. The figures are 6.4, 1.5, and 2.4 for cars, middle vehicles, and heavy vehicles, respectively. When converting to PCU values from Table 5-2, the PCU values for motorcycles, middle vehicles and heavy vehicles are 0.16, 1.5, and 2.4, respectively. The results come close to values given in Lan et al. (2005)

The observed data shows that the percentage of four-wheeled vehicles in the traffic flow is fewer than 2% in which the share of middle vehicles and heavy vehicles is much lower than the car share. Thus, the real mixed flow should be converted to the virtual mixed flow with two vehicle types: motorcycle and passenger car. The passenger car values of middle vehicles and heavy vehicles are suggested as 1.5 and 2.4. By then, the proportion of passenger cars in the traffic flow is as:

$$P_{PC} = \frac{q_C + q_{MV} \times 1.5 + q_{HV} \times 2.4}{q_{MC} + q_C + q_{MV} \times 1.5 + q_{HV} \times 2.4} \quad (5\text{-}4)$$

where P_{PC} = Proportion of passenger cars in the traffic flow [-]
$q_{MC}; q_C; q_{MV}; q_{HV}$ = Volume of motorcycles, cars, middle vehicles and heavy vehicles passing the stop line [veh/h]

It is the fact that the MCU values for cars are different depending on the car share in the flow. When the car share is so low that they run individually, motorcycles will run surrounding and the required safety space for that car is small (Figure 5-14). In the mixed flow, when the car share increases until cars could run in the platoon, motorcycles can hardly run between longitudinal gaps of successive cars (Figure 5-15). Consequently, the required safety spaces for cars, in this case, are wider than the one in the former case.

Figure 5-14: Small Safety Space of Individual Car

Note. Own Picture

Figure 5-15: Motorcycles hardly run between Longitudinal Gaps of Successive Cars

Note. Own Picture

The recommended MCU values for different vehicle types are depicted in Table 5-3. The higher passenger car share, the higher MCU values are determined. When the passenger car share is lower than 2%, the MCU value for cars is 5.5, and when the flow is the homogeneous car flow, the MCU value for cars is 6.8.

Table 5-3: Recommended MCU Values for Different Vehicles

P_{PC}	≤ 2%	4%	6%	8%	10%	12%	14%	16%	18%	20%	100%
MCU_C	5.5	5.8	5.9	6.0	6.1	6.2	6.2	6.3	6.3	6.3	6.8
MCU_{MV}	8.25	8.7	8.85	9.0	9.15	9.3	9.3	9.45	9.45	9.45	10.2
MCU_{HV}	13.2	13.92	14.16	14.4	14.64	14.88	14.88	15.12	15.12	15.12	16.32

Note. Own Table

Note:

- The result of MCU values for passenger cars is determined for all movements of that passenger car at the intersection.
- For the normal calculation, in case of the percentage of cars is lower than 2%, the default MCU values for cars, middle vehicles, and heavy vehicles are 5.5, 8.25, and 13.2, respectively.
- For the normal calculation, in case of cars could run in the platoon in the mixed flow (the percentage of cars is higher than 8%), the default MCU values for cars, middle vehicles, and heavy vehicles are 6, 9, and 14.4, respectively.
- The PCU values of middle vehicles and heavy vehicles are 1.5 and 2.4, respectively.

5.3.4 Adjustment Factor for Vehicle Types

As mentioned in Chapter 4, the adjustment factor for vehicle types on the saturation flow rate is calculated as:

$$f_{veh} = \frac{q_{MC} + q_C + q_{MV} + q_{HV}}{q_{MC} + q_C \times MCU_{\mathrm{C}} + q_{MV} \times MCU_{\mathrm{MV}} + q_{HV} \times MCU_{\mathrm{HV}}} \quad (5\text{-}5)$$

where f_{veh} = Adjustment factor for vehicle types [-]
$q_{MC}; q_C; q_{MV}; q_{HV}$ = Flow rate of motorcycles, cars, middle vehicles, and heavy vehicles [veh/h]
$MCU_C; MCU_{MV}; MCU_{HV}$ = MCU values for cars, middle vehicles, and heavy vehicles [-]

The MCU value for cars, middle vehicles, and heavy vehicles are determined from Table 5-3 or could be set as the default values as mentioned in the note box. The detailed calculations to measure the effect of vehicle type are shown in Appendix C.5.

Figure 5-16 illustrates the calibration results about the adjustment factor for vehicle types to the saturation flow rate. This figure shows a high correlation between the estimated normalised saturation flow rate using the results of adjustment factors of vehicle type and the observed normalised saturation flow rate.

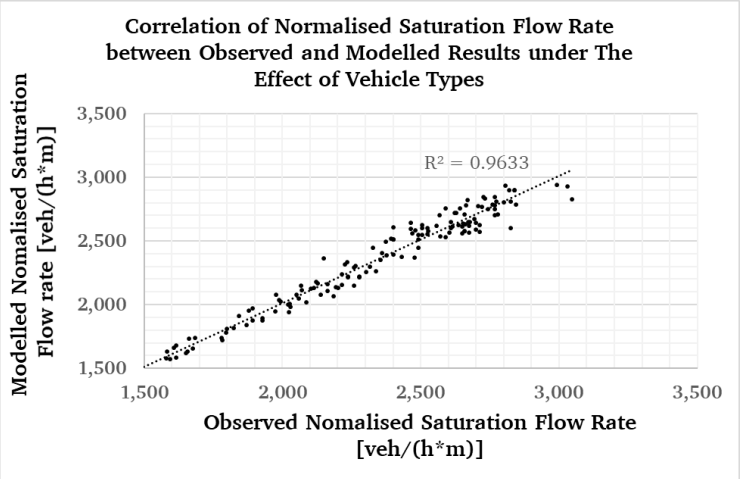

Figure 5-16: Correlation of Normalised Saturation Flow Rate between Observed and Modelled Results under the Effect of Vehicle Type

Note. Own Graph

5.3.5 Adjustment Factor for Turning Movements

5.3.5.1 Adjustment factor for Turning Movements without the Interference of Opposing Flows

In the theoretical model, the adjustment factor for turning movements without the interference of opposing flows $f_{turn,1}$ includes the proportion of right-turning cars, the proportion of left-turning motorcycles and the proportion of left-turning cars in the traffic flow and excludes right-turning motorcycles. Five approaches in Group 4 were selected to analyse the impact of those factors on the saturation flow rate. Raw data and other calculated parameters are presented in Appendix C.6. The estimation process is shown below:

$$f_1 = \frac{1}{1+7.07\cdot p'_{PC-RT}} \cdot \frac{1}{1+0.03\cdot p'_{MC-LT}+0.72\cdot p'_{PC-LT}}$$
$$f_{turn,1} = \frac{q_{MC,RT}}{S_{ow}\cdot f_{veh}} + f_1 \cdot \left(1-\frac{q_{MC,RT}}{S_{ow}\cdot f_{veh}}\right) \quad (5\text{-}6)$$

Where	$q_{MC,RT}$	=	Flow rate of right-turning motorcycles	[veh/h]
	S_{ow}	=	Base saturation flow rate	[veh/h]
	f_{veh}	=	Adjustment factor for vehicle types	[-]
	$p'_{PC-RT}; p'_{MC-LT}; p'_{PC-LT}$	=	Proportion of right-turning passenger cars, left-turning motorcycles, and left-turning passenger cars in the flow excluding right-turning motorcycles	[-]

From Equation 5-6, right-turning cars have the highest effect because turning positions of vehicles play an important role in the discharge flow rate. Regards the targeted flow, right-turning cars from the left side would block through-motorcycles running on the right side, while left-turning cars from the left side do not block other flows. Moreover, left-turning motorcycles have less impact than left-turning cars because of their higher flexible manoeuvrability.

The calibration results about the adjustment factor for turning movements without the interference of opposing flows to the saturation flow rate is given in Figure 5-16. This figure shows a high correlation between the observed normalised saturation flow rate and the estimated normalised saturation flow rate.

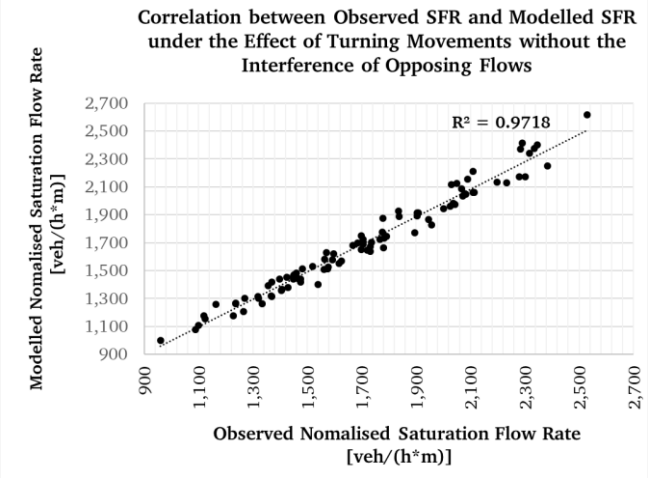

Figure 5-17: Correlation between Observed and Modelled Saturation Flow Rate under the Effect of Turning Movements without the Interference of Opposing Flows

Note. Own Graph

5.3.5.2 Adjustment Factor for Turning Movements with the Interference of Opposing Flows

As mention in Chapter 4, the turning effect is separated into two cases:

Turning effect during the entering time:

The adjustment factor for turning movements could be applied in the same way as in Section 5.3.5.1. During this time, there are neither conflicts between left-turning movements and opposing through-movements nor conflicts between through-flows and opposing left-turning flows exists. The adjustment factor for the turning effect during this period is the same as the adjustment factor presented in Equation 5-6.

Turning effect during the rest of green time:

Six approaches comprising turning activities were selected for the analysis. Raw data and calculated parameters used for the model are presented in Appendix C.7.

The adjustment factor for right-turning passenger cars is computed as:

$$f_{RT,2} = f\left(p'_{PC,RT}\right) = \frac{1}{1 + 4.46 \cdot p'_{PC,RT}} \tag{5-7}$$

where $f_{RT,2}$ = Adjustment factor for right-turning passenger cars [-]
$p'_{PC,RT}$ = Proportion of right-turning passenger cars in the flow excluding right-turning motorcycles [-]

The adjustment factor for left-turning movements could be suggested in the follows:

$$f_{LT,2} = 1 - \frac{2.02\, p'_{MC,LT} + 133.19 \cdot p'_{PC,LT}}{1 + (2.02 \cdot p'_{MC,LT} + 133.19 \cdot p'_{PC,LT}) \cdot (4.89 - \frac{1.43 \cdot q_{MC,OPT} + 15.18 \cdot q_{PC,OPT}}{S_{OPT}})} \quad (5\text{-}8)$$

where	f_{LT2}	=	Adjustment factor for left-turning movements	[-]
	$p'_{MC,LT}$; $p'_{PC,LT}$	=	Proportion of left-turning motorcycles and passenger cars in the targeted flow excluding right-turning motorcycles	[-]
	$q_{MC,OPT}$; $q_{PC,OPT}$	=	Opposing through flow rate of motorcycles and passenger cars	[veh/h]
	S_{OPT}	=	Saturation flow rate of opposing through-movements at the section before the conflict area	[veh/h]

Opposing left-turners passing the intersection would make conflicts with through-vehicles. Usually, opposing left-turners would try to find suitable gaps from the through movement. When opposing left-turners accept proper gaps and move, through-vehicles must stop before the conflict area and by then affect the targeted saturation flow rate.

$$f_{OPL,2} = 1 - \frac{(\frac{0.73 \cdot q_{MC,OPL} + 9.35 \cdot q_{PC,OPL}}{3600}) \cdot (0.79 - \frac{0.65 \cdot q_{MC,TH} + 0.36 \cdot q_{PC,TH}}{S_{TH}})}{1 + \frac{0.73 \cdot q_{MC,OPL} + 9.35 \cdot q_{PC,OPL}}{3600}} \quad (5\text{-}9)$$

The adjustment factor for turning movements with the interference of opposing flows in the second part of green interval $f_{turn,2}$ can be written below:

$$f_{turn,2} = \frac{q_{MC,RT}}{S_{ow} \cdot f_{veh}} + f_2 \cdot \left(1 - \frac{q_{MC,RT}}{S_{ow} \cdot f_{veh}}\right) \quad (5\text{-}10)$$

$$f_2 = f_{RT,2} \cdot f_{LT,2} \cdot f_{OPL,2}$$

In this case, the total turning adjustment factor is identified as:

$$f_{turn} = \frac{t_{e1} - l_1}{t_g} \cdot f_{turn,1} + \frac{t_g - (t_{e1} - l_1)}{t_g} \cdot f_{turn,2} \quad (5\text{-}11)$$

where	f_{turn}	=	Adjustment factor for turning movements with the interference of opposing flows during the effective green time t_g	[-]
	$f_{turn,1}$	=	Adjustment factor for turning movements without the interference of opposing flows during the time $t_{e1} - l_1$	[-]
	$f_{turn,2}$	=	Adjustment factor for turning movements with the interference of opposing flows during the rest of effective green time $t_g - (t_{e1} - l_1)$	[-]

The calibration results about the adjustment factor for turning movements to the saturation flow rate is given in Figure 5-18. This figure shows a high correlation between observed normalised saturation flow rate and estimated normalised saturation flow rate using the results of vehicle type adjustment factor and turning adjustment factor.

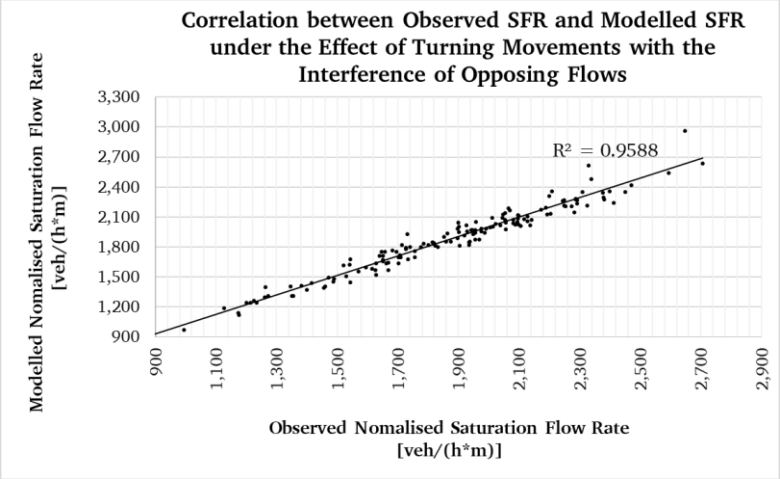

Figure 5-18: Correlation between Observed and Modelled Normalised Saturation Flow Rate under the Effect of Turning Movements with the Interference of Opposing Flows

Note. Own Graph

5.3.6 Amber Time Calculation

In terms of vehicle dynamics, motorised traffic changes from green to red by the transition signal AMBER before RED (FGSV, 1992).

In car traffic-based cities, when the signal light turns from green to amber, drivers need time to recognise and respond to the signal change before slowing down the speed. Thus, the reaction time is added to the amber time estimation. The amber time is measured as:

$$t_A \geq \frac{v_{cl}}{2 \cdot b_v} + t_{re} \tag{5-12}$$

Where t_A = Amber time [s]
v_{cl} = Clearing speed [m/s]
b_v = Deceleration [m/s^2]
t_{re} = Reaction time [s]

In MDCs, the signal countdown systems are installed at signal signposts (Figure 3-5) to help drivers in recognising the current signal state. The device allows drivers to anticipate and identify the exact point of the signal change. In this case, the drivers have reacted to the signal change before the green time end. Thus, the reaction time needs not to be added to the amber time estimation in MDCs. The amber time by then is modified depending on the speed and the deceleration of vehicles. In this study, passenger car and motorcycle are selected for the amber time estimation:

$$t_A \geq \frac{v_{cl}}{2 \cdot b_v} \tag{5-13}$$

In the saturated state, parameters are assumed:

Car: v_{cl}= 7 m/s; b_v= 3.5 m/s^2 ; Motorcycle: v_{cl}= 10 m/s; b_v=5 m/s^2 $\rightarrow$ $\boldsymbol{t_A \geq 1\ s}$ $\rightarrow$ the minimum amber time is 1 s.

In the free flow state, parameters are assumed:

Car: v_{cl}= 14 m/s; b_v= 3.5 m/s^2 ; Motorcycle: v_{cl}= 14 m/s; b_v=5 m/s^2 $\rightarrow$ $\boldsymbol{t_A \geq 1.4\ s}$ $\rightarrow$ the minimum amber time is 2 s.

In general, the minimum amber time for MDCs can be set up from 1 s to 2 depending on the traffic state (saturated state or free flow state). However, 3-second amber time is suggested to be set up as the default value at most of the intersections. The higher amber time could keep the flows run safely. So, it is suggested to apply 3-second amber time for all cases.

Note: In the normal case, the amber time t_A should be set up as 3 s because of the safety reason.

5.3.7 Effective Green Time Model Calibration

The theoretical model in Chapter 4 introduced two effective green time models:
- Model 1: Red-light running is ignored,
- Model 2: Red-light running is considered.

Two approaches on which only motorcycles are running, were selected to observe the number of motorcycles passing the stop line during the first 6-second green period, the amber time, and the red time to estimate the value of components to the effective green time. The detail data and the calculation expression of components to the effective green time are given in Appendix D.

Start-up lost time calculation: It is assumed that late depart would be ignored when the intergreen time is designed correctly. Thus, the data which were not affected by short intergreen time would be selected for analysis.

By counting the number of motorcycles passing the stop line during different time intervals as mentioned in Section 4.4, the start-up lost time for two models can be estimated as:

$$l_{1,nor} = 6 - \frac{N_3}{S_0} \cdot 3,600$$
$$l_{1,\max} = 6 - \frac{N_1 + N_2 + N_3}{S_0} \cdot 3,600 \quad (5\text{-}14)$$

Where
- $l_{1,nor}$ = Normal start-up lost time [s]
- $l_{1,max}$ = Maximum start-up lost time [s]
- N_1 = The number of motorcycles per 1 m wide approach stopping over the stop line during the red time [mcu/m]
- N_2 = The number of motorcycles per 1 m wide approach departing over the stop line during the red time [mcu/m]
- N_3 = The number of motorcycles per 1 m wide approach departing over the stop line during the first 6-second green period [mcu/m]
- S_0 = Normalised saturation flow rate over 1 m wide approach [mcu/(s*m)]

Distributions of start-up lost time are illustrated in Figure 5-19 and Figure 5-20 for both models. The 50th-85th percentile range of start-up lost time in model 1 is around 2 s to 2.5 s and the same range of start-up lost time in model 2 is from 0.5 s to 1.5 s.

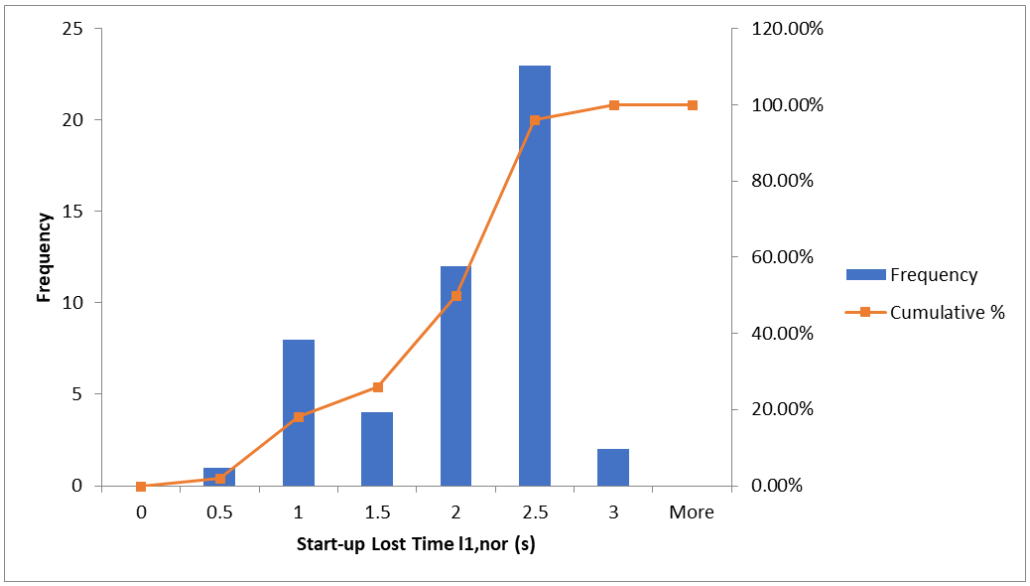

Figure 5-19: Distribution of Start-up lost Time $l_{1,nor}$ (Model 1)

Note. Own Graph

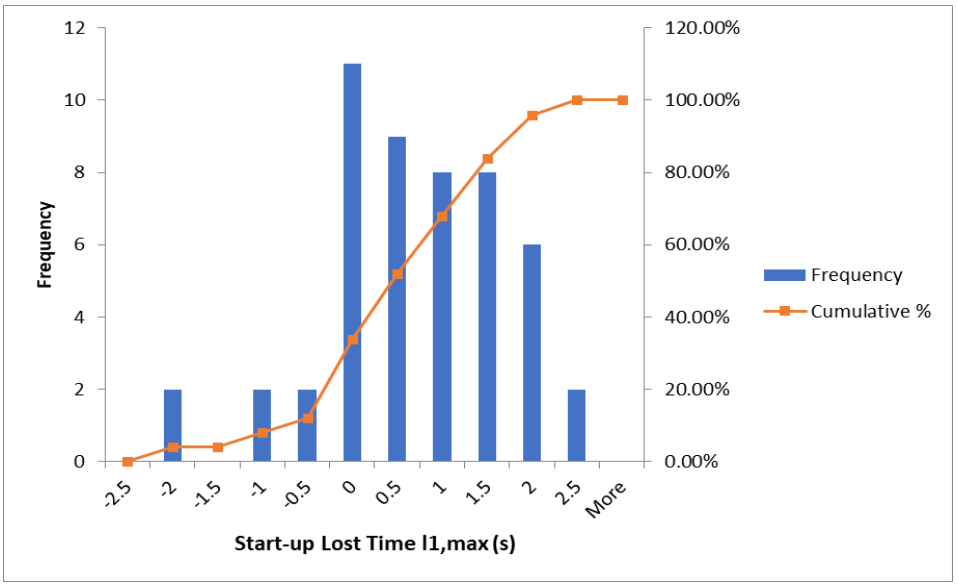

Figure 5-20: Distribution of Start-up Lost Time $l_{1,max}$ (Model 2)

Note. Own Graph

Green end-lag time calculation: The green end-lag time is the time during which traffic still flows after the displayed green time is over.

By counting the number of motorcycles passing the stop line during different interval after the displayed green time is over (Section 4.4). The green end-lag time for two models can be estimated as:

$$\lambda_{2,nor} = \frac{N_4}{S_0} \cdot 3,600$$
$$\lambda_{2,\max} = \frac{N_4 + N_5}{S_0} \cdot 3600 \quad (5\text{-}15)$$

Where	$\lambda_{2,nor}$	=	Normal green end-lag time	[s]
	$\lambda_{2,max}$	=	Normal green end-lag time	[s]
	N_4	=	The number of motorcycles per 1 m wide approach clearing over the stop line during the amber time	[mcu/m]
	N_5	=	The number of motorcycles per 1 m wide approach clearing over the stop line during the red time	[mcu/m]
	S_0	=	Normalised saturation flow rate over 1 m wide approach	[mcu/(s*m)]

The observation shows that the saturated state does not always remain through the displayed green time, Flows run under unsaturated state during the last green period and during the amber time. So, it is assumed that during the amber time, the discharged rate could reach 80% of the saturation flow rate. The number of motorcycles per 1 m wide approach clearing over the stop line during the amber time N_4 is calculated:

$$N_4 = 0.8 \cdot S_0 = 0.8 \cdot 3,058 \cdot \frac{t_A}{3,600} = 0.8 \cdot 3,058 \cdot \frac{3}{3,600} = 2.04 \ \text{[mcu/m]} \quad (5\text{-}16)$$

In model 1, the normal green end-lag time in model 1 is computed as:

$$\lambda_{2,nor} = \frac{N_4}{S_0} \cdot 3,600 = \frac{2.04}{3,058} \cdot 3,600 = 2.4 \ \text{[s]} \quad (5\text{-}17)$$

In model 2, the maximum green end-lag time distribution is illustrated in Figure 5-21. The 50th-85th percentile range of green end-lag time is around 3 to 3.5 seconds.

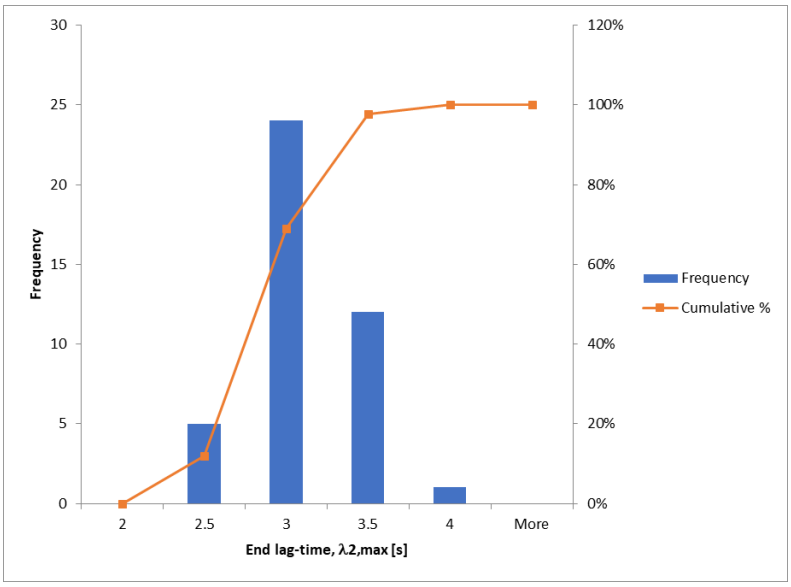

Figure 5-21: Distribution of Green End-lag Time $\lambda_{2,max}$ in model 2 (Illegal Activities are accepted)

Note. Own Graph

The normal effective green time is estimated as:

$$t_{g,nor} = t_G - l_{1,nor} + \lambda_{2,nor} = t_G - (2\ s\ to\ 2.5\ s) + 2.4 \simeq t_G \quad (5\text{-}18)$$

The maximum effective green time is computed below:

$$t_{g,max} = t_G - l_{1,mas} + \lambda_{2,max} = t_G - (0.5\ s\ to\ 1.5\ s) + (3\ s\ to\ 3.5\ s) \simeq t_G + 2 \quad (5\text{-}19)$$

Where t_G is the displayed green time.

In conclusion, the effective green time in model 1 equals the displayed green time. The effective green time in model 2 equals the displayed green time plus 2 seconds.

Note:
- Model 1: $t_{g,nor} = t_G$
- Model 2: $t_{g,nor} = t_G + 2$

5.3.8 Intergreen Time Model Calibration

The intergreen time in MDCs can be determined as:

$$t_{ig} = t_{cr} + t_{cl} - t_e \quad (5\text{-}20)$$

where t_{ig} = Intergreen time [s]
t_{cr} = Crossing time [s]
t_{cl} = Clearing time [s]

In MDCs, all movements in one direction are assigned to run in the same phase. So, the crossing time for all movements should be selected for the intergreen time calculation. In fact, there are many cases where vehicles try to cross the stop line when the amber is on. Thus, the crossing time is suggested to be equal to the amber time to increase the intergreen time and increase the safety level.

$$t_{\text{cr}} = t_A = 3\ [s] \quad (5\text{-}21)$$

The clearing time t_{cl} in MDCs is defined as the time need to cover the clearing distance l_{cl} at a clearing speed v_{cl} in plus with the interaction time $t_{int,TH-OPL}$ between clearing through-vehicles and opposing clearing left-turning movements. The clearing time is computed by:

$$t_{cl} = \frac{l_{cl}}{v_{cl}} + t_{int,TH-OPL} \quad (5\text{-}22)$$

Note: Assume the observed clearing speed v_{cl} is 8 m/s for motorcycles.

The interaction time could be recommended depending on the interaction type. It is as follows:

$t_{int,TH-OPL} = 0\ to\ 2\ s$ when a through-motorcycle interacts with an opposing left-turning clearing motorcycle
$t_{int,TH-OPL} = 1\ to\ 2\ s$ when a through-motorcycle interacts with an opposing left-turning clearing car
$t_{int,TH-OPL} = 2\ to\ 3\ s$ when a through-car interacts with an opposing left-turning clearing motorcycle
$t_{int,TH-OPL} = 3\ to\ 4\ s$ when a through-car interacts with an opposing left-turning clearing car

Note: In the normal case, the probability of clearing through-motorcycle interacting with an opposing left-turning motorcycle is the highest. Thus, $t_{int,TH-OPL}$ should be set to 2 s to avoid a long intergreen time.

When determining intergreen times, clearing and entering distances must be identified. The centre lines of the approach or the footway allocated to involved traffic streams are used to measure their length.

The entering time depends on the entering distance l_e and the entering speed v_e. The entering distance can be obtained from real geometric information of intersection. The entering speed is estimated at 5 m/s (see Section 3.4). Thus, the entering time is computed as:

$$t_{\mathrm{e}} = \frac{l_e}{v_e} = \frac{l_e}{5} \tag{5-23}$$

5.4 Complete Capacity Model

In case all the signal information is pre-defined, the complete capacity model would use Equation 4-37 to calculate the normal capacity or Equation 4-38 to calculate the maximum capacity in section 4.6, chapter 4. The normal capacity $C_{nor,i}$ and the maximum capacity are illustrated as:

$$\begin{cases} C_{nor,i} = \dfrac{t_{g,nor}}{t_C} \times \mathrm{S}_i \\ C_{\max,i} = \dfrac{t_{g,\max}}{t_C} \times \mathrm{S}_i \end{cases} \tag{5-24}$$

where

$C_{nor,i}$	=	Normal capacity of approach i	[veh/h]
$C_{max,i}$	=	Maximum capacity of approach i	[veh/h]
S_i	=	Saturation flow rate of approach i	[veh/h]
$t_{g,nor}$	=	Normal effective green time	[s]
$t_{g,max}$	=	Maximum effective green time	[s]
t_C	=	Cycle time	[s]
i	=	Index indicating approach	[-]

The minimum cycle time is required:

$$\mathrm{t}_{\mathrm{C\_min}} = \frac{\sum t_{ig}}{1 - \sum \frac{q_i}{S_i}} \tag{5-25}$$

where

t_{C_min}	=	Minimum cycle time	[s]
t_{ig}	=	Intergreen time	[s]
q	=	Flow rate of the approach i	[veh/h]
S	=	Saturation flow rate of the approach i	[veh/h]

5.5 Conclusions

In this chapter, a calibrated capacity model is expressed as the combination of the saturation flow rate model, the effective green time model and the intergreen time model. Based on data collection and data analysis procedures, some interesting results are attained and can be summarised as follows:

- There is an exciting phenomenon named as '**capacity reduction phenomenon**' is related to the discharge flow rate. This phenomenon occurs when the saturation flow rate is observed, the rate reaches to the highest value from the 6th second to the 16th second of green time, and thereafter it slightly reduces to a smaller saturation flow rate which remains the same until the end of the saturated green time. Observation results showed that the normalised homogeneous motorcycle flow rate is calculated at 3,058 mcu/(h*m) when the green time is higher or equal to 16s. That rate is estimated at 3,178 mcu/(h*m) when the green time is lower than 16 s.

- The ideal saturation flow rate of cars was also observed and measured at 1,565 pcu/(h*ln). Motorcycle equivalent unit (MCU) is chosen as a basic unit to convert heterogeneous streams to homogeneous motorcycle streams in this study. The MCU values may vary depending on the share of cars in the flow. The MCU value changes from 5.5 to 6.8 corresponding with the car share value of 5% to 100%. The recommended MCU values for cars, middle vehicles, and heavy vehicles for normal calculation are 6, 9 and 14.4, respectively. Besides, the PCU value for middle vehicles and heavy vehicles are 1.5 and 2.4, respectively, and these are used for converting all four-wheeled vehicles to only passenger cars.

- The effect of vehicle type on the capacity was calculated by converting all other vehicle types in the mixed flow to the motorcycle flow. The numerical results indicated that the impact of vehicle type was the primary factor and contributed to reducing the approach capacity significantly.

- The effect of turning movements on the capacity in MDCs differs greatly from that one in car traffic-based cities. In MDCs, the effect of turning movements depends on their turning positions in the flow. Different turning types have different effects on the approach capacity. Right-turning motorcycles do not influence the discharge flow rate because they are assigned to run on the right side of the flow. Right-turning cars, however, affect the through-flow significantly because of its left-side position. Left-turning motorcycles interfere through discharge cars and left-turning cars would reduce the discharging speed of through-vehicles.

- The effective green time model applies a method to count the number of motorcycles passing the stop line during certain time periods. The curves are replaced by equal area rectangles Two models were classified: model 1, which the rule of red-light running is strictly obeyed, and model 2, which the rule of red-light running is ignored. In the first model, the effective green time was proven to be equal to the displayed green time. In the second model, the effective green time was estimated to be equal to the displayed green time plus two seconds.

- The method of intergreen time calculation for MDCs is similar to the German method with some modifications. The crossing time was recommended to be equal to the amber time which is set up at 3 s for most cases. The clearing time is equal to the clearing time in German method plus with the interaction time between clearing through-vehicles and clearing opposing left-turning movements. The interaction time depends on vehicle types at each flow and was suggested at 1 s. The entering time was calculated by the entering distance which was defined from the middle point of the stop line to the centre of the conflict area between the entering route and the clearing route, and the entering speed was observed at 5 m/s.

6 Procedure for Application

This chapter presents a step-by-step guide for capacity calculation at signalised intersections in MDCs. The format of this chapter would be organised similarly to the one presented in FGSV (2015), TRB (2010), or other highway capacity manuals for the sake of simplicity.

The procedure in this thesis is only applied for the case that the approach width remains the same or the length of separate left-turn/right-turn lane is longer than the queue length of the arrival flow. Based on the calibration results in Chapter 5, the calculation procedure is presented in the following steps.

6.1 Input Module

The input module includes the characteristics of geometric, traffic flow and signalisation conditions. For the existing intersections, most of these data will be recorded from field surveys. For the planning intersections, traffic data will be forecasted while geometric and signal designs will also be proposed. Table 6-1 shows the worksheet for the input module.

Step 1 -Record traffic volumes

Hourly volumes are inserted for each approach into boxes shown in each corner of the intersection diagram. Besides, left-turning, go through, and right-turning volumes are shown below these table's cells, at the head of the appropriate directional arrow. The volume of left-turning, go-through, and right-turning vehicles on each approach should equal the value shown in the approach volume box.

The passenger car volume will be calculated by converting all other four-wheeled vehicles to passenger car by this equation:

$$q_{PC} = q_C + 1.5 \cdot q_{MV} + 2.4 \cdot q_{HV} \quad (6\text{-}1)$$

Table 6-1: Worksheet for Input Module

	INPUT WORKSHEET						
	Intersection: …….. Date:…….. Analyst: ……. Time period: …….						
	GEOMETRIC CONDITIONS  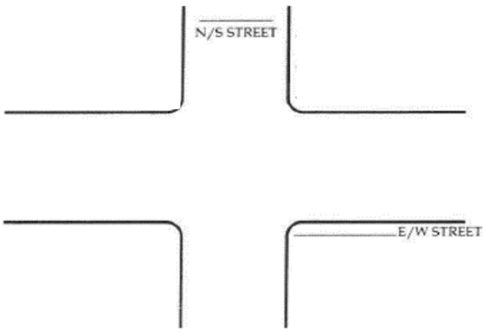 Unit: m						
	TRAFFIC CONDITIONS						
Approach	Movement	Volume [veh/h]					Approach Width [m]
		q_{MC}	q_C	q_{MV}	q_{HV}	q_{PC}	
EB	LT						
	TH						
	RT						
WB	LT						
	TH						
	RT						
NB	LT						
	TH						
	RT						
SB	LT						
	TH						
	RT						
	SIGNALISATION CONDITIONS						
Timing Plan					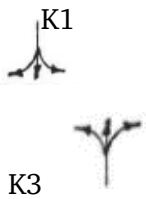		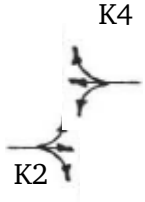

Note. Own Worksheet

Step 2- Enter geometries and traffic conditions

Details of traffic conditions and signal program should be shown in the worksheet. Features should include:

1. Approach direction
2. Type of movement
3. Detail traffic volume of each direction corresponding to each vehicle type
4. Approach width
5. Phasing type
6. Signal timing plan

6.2 Saturation Flow Rate Module

In this module, the approach saturation flow rate under prevailing conditions is computed. A worksheet for this module is shown in Table 6-2.

Table 6-2: Worksheet for Saturation Flow Rate Calculation

SATURATION FLOW RATE ADJUSTMENT WORKSHEET					
Approach	Approach Width	Motorcycle Saturation Flow Rate	Adjustment Factor for Vehicle Types	Adjustment Factor for Turning Movements	Adjusted Saturation Flow Rate
	w	S_{ow}	f_{veh}	f_{turn}	S
	[m]	[mcu/h]	[-]	[-]	[veh/h]
(1)	(2)	(3)	(4)	(5)	(6)
EB					
WB					
NB					
SB					

Note. Own Worksheet

Step 1: Enter approach width

The approach width is the first data needed to be identified to calculate the motorcycle saturation flow rate of each approach. The approach width is included in column (2).

Step 2: Calculate the motorcycle saturation flow rate

The motorcycle saturation flow rate S_{0w} is a function of approach width w as follows:

$$\begin{cases} S_{0w} = 3178 \times w \; if \; t_G < 16s \\ S_{0w} = 3058 \times w \; if \; t_G \geq 16s \end{cases}$$

If there is no information for designed green time, the case of $t_G \geq 16\ s$ should be applied for further calculation.

Step 3: Calculate the adjustment factor for vehicle types

The adjustment factor for vehicle types is a function of vehicle type's proportion and the MCU values for vehicle types.

$$f_{veh} = \frac{q_{MC} + q_C + q_{MV} + q_{HV}}{q_{MC} + q_C \times MCU_{\mathrm{C}} + q_{MV} \times MCU_{\mathrm{MV}} + q_{HV} \times MCU_{\mathrm{HV}}}$$

In normal calculation, the MCU values for cars, middle vehicles, and heavy vehicles could be selected as 6, 9, and 14.4 respectively.

Step 4: Calculate the adjustment factor for turning movements

As mentioned above, turning adjustment factor is separated into two cases: turning movements without the interference of opposing flows and turning movements with the impedance of opposing flows. Two separate worksheets for computational processes are provided in Table 6-3 and Table 6-4 for two cases.

In the case of the adjustment factor for turning movements without the interference of opposing flows, the calculation procedure is conducted step-by-step below:

1. Calculate the motorcycle saturation flow rate S_{0w}.
2. Calculate the proportion of converted right-turning passenger cars p'_{PC-RT} in the total converted flow rate excluding right-turning motorcycles.
3. Calculate the proportion of left-turning motorcycles p'_{MC-LT} in the total converted flow rate excluding right-turning motorcycles.
4. Calculate the proportion of left-turning passenger cars p'_{PC-LT} in the total flow rate excluding right-turning motorcycles.
5. Calculate the adjustment factor for turning effect f_1.
6. Calculate the adjustment factor for turning movements without the interference of opposing flows f_{turn1}.

Table 6-3: Worksheet of Adjustment Factor for Turning Movements without the Interference of Opposing Flows

SUPLEMENTAL WORKSHEET FOR TURNING ADJUSTMENT FACTOR f_{turn1} WITHOUT THE INTERFERENCE OF OPPOSSING FLOWS				
INPUT VARIABLES	EB	WB	NB	SB
Effective Green Time, t_g [s]				
Approach Width, w [m]				
Left-turning Motorcycle Flow Rate, $q_{MC,LT}$ [veh/h]				
Left-turning Passenger Car Flow Rate, $q_{PC,LT}$ [veh/h]				
Through-motorcycle Flow Rate, $q_{MC,TH}$ [veh/h]				
Through Passenger Car Flow Rate, $q_{PC,TH}$ [veh/h]				
Right-turning Motorcycle Flow Rate, $q_{MC,RT}$ [veh/h]				
Right-turning Passenger Car Flow Rate, $q_{PC,RT}$ [veh/h]				
INPUT VARIABLES	EB	WB	NB	SB
$S_{0w} = 3058 \cdot w$				
$\sum q = \sum q_{MC} + \sum q_{PC}$				
$p'_{PC,RT} = \frac{q_{PC,RT}}{\sum q - q_{MC,RT}}$				
$p'_{MC,LT} = \frac{q_{MC,LT}}{\sum q - q_{MC,RT}}$				
$p'_{PC,LT} = \frac{q_{PC,LT}}{\sum q - q_{MC,RT}}$				
$f_{RT,1} = f_{RT,2} = \frac{1}{1 + 7.07 \cdot p'_{PC,RT}}$				
$f_{LT1} = \frac{1}{1 + 0.03 \cdot p'_{MC,LT} + 0.72 \cdot p'_{PC,LT}}$				
$f_1 = f_{RT,1} \cdot f_{LT,1}$				
$f_{turn,1} = \frac{q_{MC,RT}}{S_{ow} \cdot f_{veh}} + f_1 \cdot (1 - \frac{q_{MC,RT}}{S_{ow} \cdot f_{veh}})$				

Note. Own Worksheet

In the case of the adjustment factor for turning movements with the interference of opposing flow, the calculation procedure is much more complicated and is presented step-by-step as follows:

1. Calculate the effective green time t_g.
2. Calculate the proportion of right-turning passenger cars $p'_{PC,RT}$ in the total flow rate excluding right-turning motorcycles.
3. Calculate the proportion of left-turning motorcycles $p'_{MC,LT}$ in the total flow rate excluding right-turning motorcycles.
4. Calculate the proportion of left-turning passenger cars $p'_{PC,LT}$ in the total flow rate excluding right-turning motorcycles.
5. Calculate f_1.
6. Calculate the adjustment factor for turning movements without the interference of opposing flows $f_{turn,1}$ during the entering time.
7. Calculate the entering time t_{e1}.
8. Calculate f_2.
9. Calculate the adjustment factor for turning movements with the interference of opposing flow, $f_{turn,2}$ during the rest of effective green time.
10. Calculate the adjustment factor for turning movements f_{turn}.

Table 6-4: Worksheet of Adjustment Factor for Turning Movements with the Interference of Opposing Flows

SUPLEMENTAL WORKSHEET FOR TURNING ADJUSTMENT FACTOR f_{turn} WITH THE INTERFERENCE OF OPPOSSING MOVEMENT				
INPUT VARIABLES	EB	WB	NB	SB
Effective green time, t_g [s]				
Approach Width, w [m]				
Opposing Approach Width, w_{op} [m]				
Entering distance, l_{e1}; $l_{e,op1}$ [m]				
Entering speed, v_{e1} ;$v_{e,op1}$ [m/s] *(default value: 5 m/s)*				
Left-turning Motorcycle Flow Rate, $q_{MC,LT}$ [veh/h]				
Left-turning Passenger Car Flow Rate, $q_{PC,LT}$ [veh/h]				
Through-motorcycle Flow Rate, $q_{MC,TH}$ [veh/h]				
Through Passenger Car Flow Rate, $q_{PC,TH}$ [veh/h]				
Right-turning Motorcycle Flow Rate, $q_{MC,RT}$ [veh/h]				
Right-turning Passenger Car Flow Rate,$q_{PC,RT}$ [veh/h]				
Opposing Left-turning Motorcycle Flow Rate, $q_{MC,OPL}$ [veh/h]				
Opposing Left-turning Passenger Car Flow Rate, $q_{PC,OPL}$ [veh/h]				
Opposing Through-motorcycle Flow Rate, $q_{MC,OPT}$ [veh/h]				
Opposing Through Passenger Car Flow Rate, $q_{PC,OPT}$ [veh/h]				
COMPUTATIONS	EB	WB	NB	SB
$S_{0w} = 3,058 \cdot \mathrm{w}$				

$\sum q = \sum q_{MC} + \sum q_{PC}$				
$p'_{PC,RT} = \frac{q_{PC,RT}}{\sum q - q_{MC,RT}}$				
$p'_{MC,LT} = \frac{q_{MC,LT}}{\sum q - q_{MC,RT}}$				
$p'_{PC,LT} = \frac{q_{PC,LT}}{\sum q - q_{MC,RT}}$				
$f_{RT,1} = \frac{1}{1 + 7.07 \times p'_{PC,RT}}$				
$f_{LT,1} = \frac{1}{1 + 0.03 \cdot p'_{MC,LT} + 0.72 \cdot p'_{PC,LT}}$				
$f_1 = f_{RT,1} \cdot f_{LT,1}$				
$f_{turn1} = \frac{q_{MC,RT}}{S_{ow} \cdot f_{veh}} + f_1 \cdot (1 - \frac{q_{MC,RT}}{S_{ow} \cdot f_{veh}})$				
$t_{e1} = \min(\frac{l_{e1}}{v_{e1}}; \frac{l_{e,op1}}{v_{e,op1}})$				
$f_{RT,2} = 1 - \frac{1}{1 + 4.46 \cdot p'_{PC,RT}}$				
$f_{LT,2} = 1 - \frac{2.02 \cdot p'_{MC,LT} + 133.19 \cdot p'_{PC,LT}}{1 + (2.02 \cdot p'_{MC,LT} + 133.19 \cdot p'_{PC,LT}) \times (4.89 - \frac{1.43 \cdot q_{MC,OPT} + 15.18 \cdot q_{PC,OPT}}{S_{OPT}})}$				
$f_{OPL,2} = 1 - \frac{(\frac{0.73 \cdot p'_{MC,OPL} + 9.35 \cdot p'_{PC,OPL}}{3,600}) \cdot (0.79 - \frac{0.65 \cdot q_{MC,TH} + 0.36 \cdot q_{PC,TH}}{S_{TH}})}{1 + (\frac{0.73 \cdot p'_{MC,OPL} + 9.35 \cdot p'_{PC,OPL}}{3,600})}$				
$f_2 = f_{RT,2} \cdot f_{LT,2} \cdot f_{OPL,2}$				
$f_{turn2} = \frac{q_{MC,RT}}{S_{ow} \cdot f_{veh}} + f_2 \cdot (1 - \frac{q_{MC,RT}}{S_{ow} \cdot f_{veh}})$				
$f_{turn} = \frac{t_{e1} - l_1}{t_g} \cdot f_{turn,1} + \frac{t_g - (t_{e1} - l_1)}{t_g} \cdot f_{turn,2}$ when $t_{e1} > l_1 = 2s$ $f_{turn} = f_{turn,2}$ when $t_{e1} \le l_1 = 2s$				

Note. Own Worksheet

Step 6: Calculate the adjusted saturation flow rate

The adjusted saturation flow rate for an approach is computed by multiplying the basic saturation flow rate by each of adjustment factors determined in Table 6-2 and Table 6-3.

$$S = S_0 \cdot f_w \cdot f_{veh} \cdot f_{turn} = S_{0w} \cdot f_{veh} \cdot f_{turn}$$

6.3 Capacity Analysis Module

In this module, information and computational results from the previous modules are combined to compute the approach capacity. Table 6-5 gives a worksheet for these computations.

Table 6-5: Worksheet for Capacity Analysis

CAPACITY WORKSHEET						
Approach	Arrival Flow Rate	Adjusted Saturation Flow Rate	Normal Effective Green Time	Maximum Effective Green Time	Normal Approach Capacity	Maximum Approach Capacity
	$\sum q$	S	$t_{g,\text{nor}}$	$t_{g,max}$	C_{nor}	C_{max}
	[m]	[veh/h]	[s]	[s]	[veh/h]	[veh/h]
(1)	(2)	(3)	(4)	(5)	(6)	(7)
EB						
WB						
NB						
SB						
Cycle length: t_C.....s Total Intergreen time: T_Z .....s						

Note. Own Worksheet

Step 1: Enter the arrival flow rate for each approach

The arrival flow rate for each approach obtained from Table 6-1 is entered in column (3) of the worksheet.

Step 2: Enter the adjusted saturation flow rate for each approach

The adjusted saturation flow rate for each approach obtained from Table 6-2 is entered in column (4) of the worksheet.

Step 3: Calculate the intergreen time.

Calculate the intergreen time between signal groups. Depending on the interaction type of the through clearing-vehicles and the clearing opposing left-turning movements, the intergreen time calculation would be different.

$$t_{ig} = t_{cr} + t_{cl} - t_e$$

$$t_{\text{cr}} = t_A = 3\ [s]$$

$$t_{cl} = \frac{l_{cl}}{v_{cl}} + t_{\text{int},TH-OPL}$$

$t_{int,TH-OPL} = 0\ to\ 2\ s$ when a through-motorcycle interacts with a clearing opposing left-turning motorcycle
$t_{int,TH-OPL} = 1\ to\ 2\ s$ when a through-motorcycle interacts with a clearing opposing left-turning car
$t_{int,TH-OPL} = 2\ to\ 3\ s$ when a through-car interacts with a clearing opposing left-turning motorcycle
$t_{int,TH-OPL} = 3\ to\ 4\ s$ when a through-car interacts with a clearing opposing left-turning car

The default value of $t_{int,TH-OPL}$; v_{cl} could be set up as 2 s, and 8 m/s respectively

$$t_e = \frac{l_e}{v_e} = \frac{l_e}{5}$$

Step 4: Calculate the minimum cycle time (In case no information about the signal program is given).

The minimum cycle time is computed below:

$$\mathrm{t}_{\mathrm{C\_min}} = \frac{\sum t_{ig}}{1 - \sum \frac{q_i}{S_i}}$$

If there is no designed cycle time information, the minimum cycle time could be used for capacity calculation.

Step 5 – Calculate the minimum green time for approach i (in case no information about the signal program is given).

$$\mathrm{t}_{\mathrm{G,min,i}} = \frac{q_i}{S_i} \cdot \mathrm{t}_{\mathrm{C,min}}$$

If there is no designed green time information, the minimum green time could be used for capacity calculation.

Step 6: Calculate the effective green time.

The normal effective green time is computed when the illegal traffic activities are not considered:

$$t_{\mathrm{g,nor}} = t_G$$

The maximum effective green time is computed when the illegal traffic activities are considered;

$$t_{\mathrm{g,max}} = t_G + 2$$

Step 7: Calculate the approach capacity.

The normal approach capacity: $C_{nor} = \frac{t_{g,nor}}{t_C} \cdot S$

The maximum approach capacity: $C_{\max} = \frac{t_{g,\max}}{t_C} \cdot S$

7 Sample Calculation

7.1 Description

This chapter presents one example that illustrates the real traffic operation at a typical signalised intersection in Ho Chi Minh City. The layout of the selected intersection, named as Dinh Tien Hoang-Tran Quang Khai, is illustrated in Figure 7-1. It is a simple four-leg intersection with a two-phase pre-timed signal program. The cycle length is set up as 70 s. The traffic volume at each approach was observed during the peak hour (17:00-18:00).

The objective is to calculate the capacity of the whole intersection. Then the traffic signal program is re-designed to conclude with the suitability of the current traffic performance at the analysed intersection.

The approach capacity and the intersection capacity would also be calculated and followed by the guideline in Chapter 6.

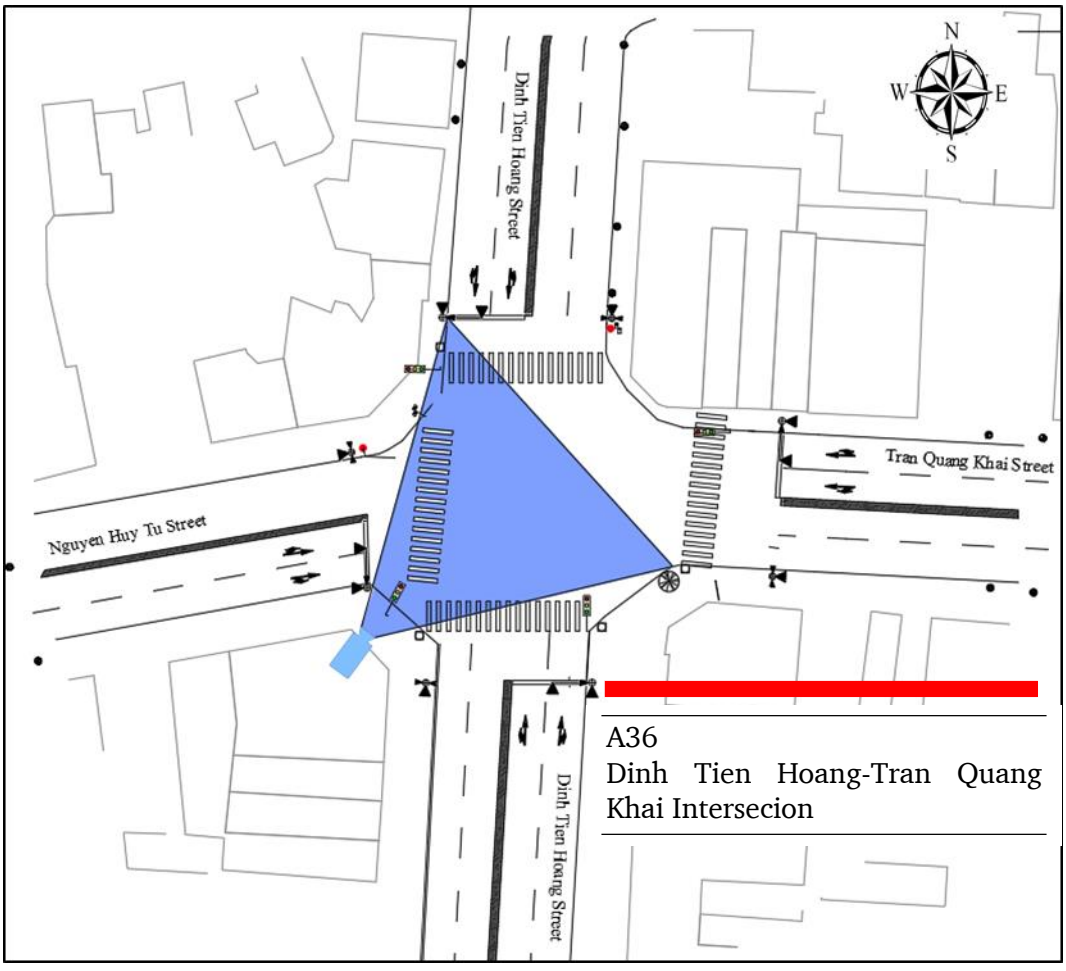

Figure 7-1: Intersection and Surveyed Layout at Dinh Tien Hoang-Tran Quang Khai Intersection

Note. Own Drawing

7.2 Solution

7.2.1 Input Model

Table 7-1 shows the input module worksheet for this calculation. All relative geometric conditions are illustrated in the diagram on the upper half of the sheet. Other relevant characteristics are shown in the centre of the worksheet. The two-phase signal timing plan is drawn at the bottom of the spreadsheet.

Table 7-1: Input Module Worksheet for Sample Calculation

	INPUT WORKSHEET						
	Intersection: Dinh Tien Hoang-Tran Quang Khai				Date: 20.12.2017		
	Analyst: Huynh Duc Nguyen				Time period: 17:00-18:00		
	GEOMETRIC CONDITIONS NORTH Unit: m				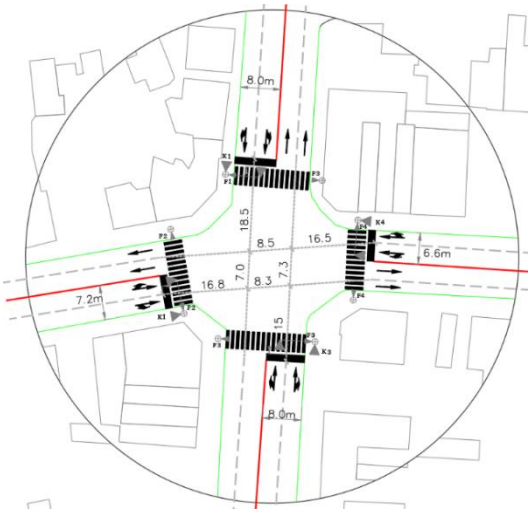		
	TRAFFIC CONDITIONS						
Approach	Movement	Volume [veh/h]					Approach Width [m]
		q_{MC}	q_C	q_{MV}	q_{HV}	q_{PC}	
EB	LT	1,764	55	0	14	89	6.6
	TH	2,400	73	0	9	95	
	RT	818	95	0	5	107	
WB	LT	477	0	0	0	0	7.2
	TH	1,941	82	0	0	82	
	RT	1,505	14	0	0	14	
NB	LT	859	0	0	0	0	8.0
	TH	6,873	430	0	41	528	
	RT	82	0	0	0	0	
SB	LT	716	31	0	0	31	8.0
	TH	4,996	230	10	10	269	
	RT	506	26	5	10	58	
	SIGNALISATION CONDITIONS						
Timing Plan	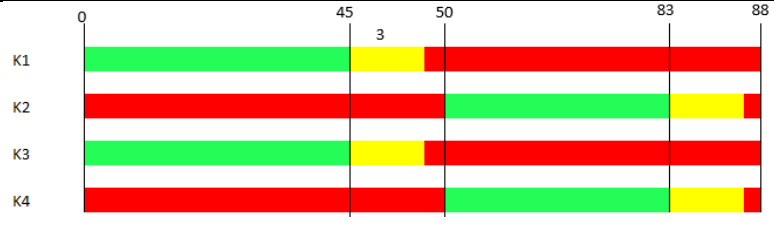				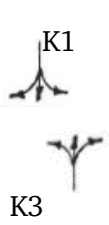		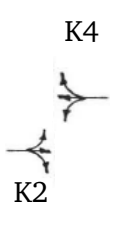

Note. Own Worksheet

7.2.2 Saturation Flow Rate Calculation

Table 7-2 illustrates the worksheet for the saturation flow rate module. The normalised homogeneous motorcycle saturation flow rate is 3,058 mcu/(h*m) because the green interval is longer than 16 s. The columns contain all adjustment factors to estimate the adjusted saturation flow rate, as follows:

- The approach width is estimated in Table 7-1
- The motorcycle saturation flow rate is calculated by using Equation 5-1.
- The adjustment factor for vehicle types is computed by using Equation 5-5.
- The adjustment of turning movements is computed throughout supplemental worksheet which shown in Table 7-3.
- The adjusted saturation flow rate is calculated by using Equation 4-1.

Table 7-2: Saturation Flow Rate Worksheet for Sample Calculation

SATURATION FLOW RATE ADJUSTMENT WORKSHEET					
Appr	Approach Width	Motorcycle Saturation Flow Rate	Adjustment Factor for Vehicle Types	Adjustment Factor for Turning Movements	Adjusted Saturation Flow Rate
	w	S_{ow}	f_{veh}	f_{turn}	S
	[m]	[mcu/h]	[-]	[-]	[veh/h]
(1)	(2)	(3)	(4)	(5)	(6)
EB	6.6	20,183	0.778	0.762	11,975
WB	7.2	22,018	0.893	0.780	15,337
NB	8	24,464	0.754	0.817	15,068
SB	8	24,464	0.782	0.726	13,880

Note. Own Worksheet

In Table 7-3, the columns contain all components to the adjustment value of turning movements (case 2), as follows:

Table 7-3: Adjustment Factor for Turning Movements with the Interference of Opposing Flows Worksheet for Sample Calculation

WORKSHEET FOR TURNING ADJUSTMENT FACTOR f_{turn} WITH THE INTERFERENCE OF OPPOSSING MOVEMENT				
INPUT VARIABLES	EB	WB	NB	SB
Effective Green Time, t_g [s]	33	33	45	45
Approach Width, w [m]	6.6	7.2	8	8
Opposing Approach Width, w_{op} [m]	7.2	6.6	8	8
Entering Distance, l_{e1}; $l_{e,op1}$ [m]	25	26	24	23
Entering Speed, v_{e1}; $v_{e,op1}$ [m/s] *(default value: 5 m/s)*	5	5	5	5
Left-turning Motorcycle Flow Rate, $q_{MC,LT}$ [veh/h]	1764	477	859	716
Left-turning Passenger Car Flow Rate, $q_{PC,LT}$ [veh/h]	89	0	0	31

Through-motorcycle Flow Rate, $q_{MC,TH}$ [veh/h]	2400	1941	6873	4996
Through Passenger Car Flow Rate, $q_{PC,TH}$ [veh/h]	77	82	578	281
Right-turning Motorcycle Flow Rate, $q_{MC,RT}$ [veh/h]	818	1505	82	506
Right-turning Passenger Car Flow Rate, $q_{PC,RT}$ [veh/h]	67	14	0	70
Opposing Left-turning Motorcycle Flow Rate, $q_{MC,OPL}$ [veh/h]	477	1764	716	859
Opposing Left-turning Passenger Car Flow Rate, $q_{PC,OPL}$ [veh/h]	0	89	31	0
Opposing Through-motorcycle Flow Rate, $q_{MC,OPT}$ [veh/h]	1941	2400	4996	6873
Opposing Through Passenger Car Flow Rate, $q_{PC,OPT}$ [veh/h]	82	77	281	578
COMPUTATIONS	EB	WB	NB	SB
$S_{0w} = 3,058 \cdot \mathrm{w}$	20,183	22,018	24,464	24,464
$f_{veh,TH} = \frac{q_{MC,TH} + q_{PC,TH}}{q_{MC,TH} + q_{PC,TH} \cdot MCU_C}$	0.866	0.831	0.721	0.790
$f_{veh,OPT} = \frac{q_{MC,OPT} + q_{PC,OPT}}{q_{MC,OPT} + q_{PC,OPT} \cdot MCU_C}$	0.831	0.866	0.790	0.721
$S_{TH} = S_0 \cdot \mathrm{w} \cdot f_{veh,TH}$	17,480	18,307	17,630	19,320
$S_{OPT} = S_0 \cdot \mathrm{w}_{OPT} \cdot f_{veh,OPT}$	18,307	17,480	19,320	17,630
$\sum q = \sum q_{MC} + \sum q_{PC}$	5214	4019	8392	6600
$p'_{PC,RT} = \frac{q_{PC,RT}}{\sum q - q_{MC,RT}}$	0.015	0.006	0.000	0.011
$p'_{MC,LT} = \frac{q_{MC,LT}}{\sum q - q_{MC,RT}}$	0.401	0.190	0.103	0.118
$p'_{PC,LT} = \frac{q_{PC,LT}}{\sum q - q_{MC,RT}}$	0.020	0.000	0.000	0.005
$f_{RT,1} = \frac{1}{1 + 5.39 \times p'_{PC,RT}}$	0.903	0.962	1.000	0.925
$f_{LT,1} = \frac{1}{1 + 0.34 \cdot p'_{MC,LT} + 0.64 \cdot p'_{PC,LT}}$	0.974	0.994	0.997	0.993
$f_1 = f_{RT,1} \cdot f_{LT,1}$	0.879	0.957	0.997	0.919

$f_{turn1} = \frac{q_{MC,RT}}{\sum q} + f_1 \cdot (1 - \frac{q_{MC,RT}}{\sum q})$	0.898	0.973	0.997	0.925
$t_{e1} = \min(\frac{l_{e1}}{v_{e1}}; \frac{l_{e,op1}}{v_{e,op1}})$	5	5	4.6	4.6
$f_{RT,2} = \frac{1}{1 + 4.37 \cdot p'_{PC,RT}}$	0.937	0.976	1.000	0.952
$f_{LT,2} = 1 - \frac{5.09 \cdot p'_{MC,LT} + 30.9 \cdot p'_{PC,LT}}{1 + (5.09 \cdot p'_{MC,LT} + 30.9 \cdot p'_{PC,LT}) \times (9.66 - \frac{5.03 \cdot q_{MC,OPT} + 22.56 \cdot q_{PC,OPT}}{S_{OPT}})}$	0.798	0.862	0.890	0.797
$f_{OPL,2} = 1 - \frac{(\frac{0.75 \cdot p'_{MC,OPL} + 6.28 \cdot p'_{PC,OPL}}{3,600}) \cdot (0.8 - \frac{0.75 \cdot q_{MC,OPL} + 6.28 \cdot q_{PC,OPL}}{S_{OPT}})}{1 + (\frac{0.75 \cdot p'_{MC,OPL} + 6.28 \cdot p'_{PC,OPL}}{3,600})}$	0.938	0.734	0.903	0.908
$f_2 = f_{RT,2} \cdot f_{LT,2} \cdot f_{OPL,2}$	0.702	0.617	0.804	0.689
$f_{turn2} = \frac{q_{MC,RT}}{\sum q} + f_2 \cdot (1 - \frac{q_{MC,RT}}{\sum q})$	0.749	0.760	0.806	0.713
$f_{turn} = \frac{t_{e1} - l_1}{t_g} \cdot f_{turn,1} + \frac{t_g - (t_{e1} - l_1)}{t_g} \cdot f_{turn,2}$ when $t_{e1} > l_1 = 2s$	0.762	0.780	0.817	0.726

Note. Own Worksheet

7.2.3 Capacity Calculation

Table 7-4 presents the worksheet for the capacity analysis module. Columns contain all adjustments to the adjusted saturation flow rate, as follows:

- The arrival flow rate is retrieved in Table 7-3.
- The adjustment saturation flow rate is retrieved in Table 7-2.
- The normal effective green time is computed by using Equation 5-18.
- The maximum effective green time is computed by using Equation 5-19.
- The normal approach capacity is calculated by using Equation 5-23
- The maximum approach capacity is calculated by using Equation 5-23.

Table 7-4: Worksheet for Capacity Analysis

CAPACITY WORKSHEET						
Appr	Arrival Flow Rate	Adjusted Saturation Flow Rate	Normal Effective Green time	Maximum Effective Green Time	Normal Approach Capacity	Maximum Approach Capacity
	$\sum q$	S	$t_{g,\mathrm{nor}}$	$t_{g,max}$	C_{nor}	C_{max}
	[m]	[veh/h]	[s]	[s]	[veh/h]	[veh/h]
(1)	(2)	(3)	(4)	(5)	(6)	(7)
EB	5,214	11,975	33	35	4,491	4,763
WB	4,019	15,337	33	35	5,751	6,100
NB	8,392	15,068	45	47	7,705	8,048
SB	6,600	13,880	45	47	7,098	7,413
				Total	**25,045**	**26,324**
Cycle length: $t_C = 88$ [s] Total intergreen time: $t_{ig} = 10$ [s]						

Note. Own Worksheet

In conclusion, the normal intersection capacity is calculated at 25,045 veh/h, and the maximum intersection capacity is computed at 26,324 veh/h. However, the results have been achieved by the assumption that the intergreen time does not affect the intersection capacity. In fact, through the real observations, there were some cycles that the intergreen time was not long enough, and so that conflicts occurred between clearing flows and the entering flows. Consequently, the intersection capacity of those cycles reduced sharply. So, it is necessary to re-design an effective signal program for such an intersection.

7.2.4 Re-design the Traffic Signal Program

The saturation flow rate of each approach utilised the results shown in Table 7-3. Table 7-5 presents the intergreen time calculation between signal groups. The intergreen time model proposed in Section 5.3.8 is applied for the below calculations.

Table 7-5: Intergreen Time Between Signal Groups

Ending	**Beginning**	**Clearing**						**Entering**				**Rounded**
SG	**SG**	**$t_{ü}$ [s]**	**l_o [m]**	**l_{veh} [m]**	**v_r [m/s]**	**t_{int} [s]**	**t_{cl} [s]**	**l_e [m]**	**v_e [m/s]**	**t_e [s]**	**t_{ig} s]**	**t_{ig} [s]** **$t_{cr} + t_{cl} - t_e$**
K1	K2	3	25.5	2	8	2	5.44	16.8	5	3	5.08	6
K1	K4	3	18.5	2	8	2	4.56	25.0	5	5	2.56	3
K2	K3	3	25.1	2	8	2	5.39	15.0	5	3	5.39	6
K2	K1	3	16.8	2	8	2	4.35	25.5	5	5	2.25	3
K3	K2	3	15.0	2	8	2	4.13	25.1	5	5	2.11	3
K3	K4	3	22.3	2	8	2	5.04	16.5	5	3	4.74	5
K4	K1	3	25.0	2	8	2	5.38	18.5	5	4	4.68	5
K4	K3	3	16.5	2	8	2	4.31	22.3	5	4	2.85	3

Note. Own Table

Table 7-6: Intergreen Time Calculation Between Phases

Phase		Signal group		t_{ig}	relevant t_{ig}
Ending	**Beginning**	**Ending**	**Beginning**	**[s]**	**[s]**
I	II	K1	K2	6	6
			K4	3	
		K3	K2	3	
			K4	5	
II	I	K2	K1	3	6
			K3	6	
		K4	K1	5	
			K3	3	
Intergreen time sum					12

Note. Own Worksheet

The cycle time is 88 s. The green time for each phase is estimated as:

$$t_{G,I} = \frac{\max(\frac{q_{NB}}{S_{NB}};\frac{q_{SB}}{S_{SB}})}{\max(\frac{q_{NB}}{S_{NB}};\frac{q_{SB}}{S_{SB}})+\max(\frac{q_{EB}}{S_{EB}};\frac{q_{WB}}{S_{WB}})}\cdot(t_u - t_{ig}) = \frac{\max(\frac{8,392}{15,225};\frac{6,600}{14,060})}{\max(\frac{8,392}{15,225};\frac{6,600}{14,060})+\max(\frac{5,214}{12,118};\frac{4,019}{15,590})}\cdot(88-12) = 42.7 = 43s$$

$$t_{G,II} = t_C - \sum t_{ig} - t_{G,II} = 88 - 12 - 43 = 33s$$

The new signal timing plan is drawn as:

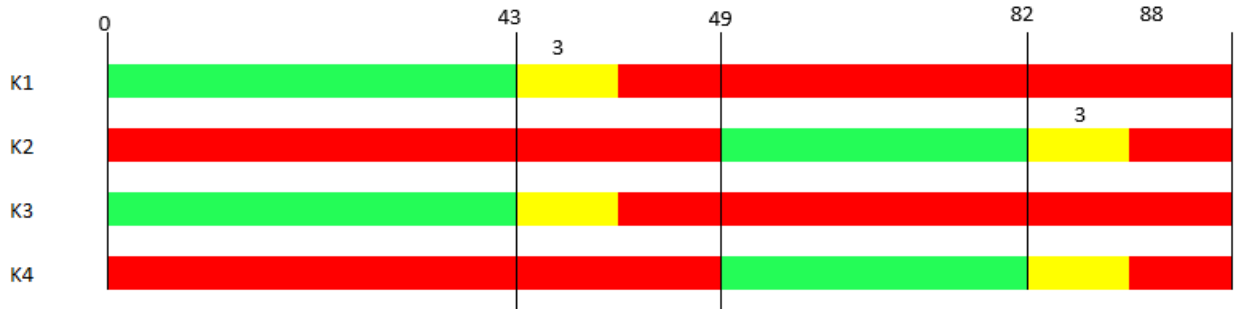

The intersection capacity is calculated and given in Table 7-7

Table 7-7: Worksheet for Capacity Analysis

CAPACITY WORKSHEET						
Appr	Arrival Flow Rate	Adjusted Saturation Flow Rate	Normal Effective green time	Maximum Effective green time	Normal Approach Capacity	Maximum Approach Capacity
	$\sum q$	S	$t_{g,\mathrm{nor}}$	$t_{g,max}$	C_{nor}	C_{max}
	[m]	[veh/h]	[s]	[s]	[veh/h]	[veh/h]
(1)	(2)	(3)	(4)	(5)	(6)	(7)
EB	5,214	11,975	33	35	4,491	4,763
WB	4,019	15,337	33	35	5,751	6,100
NB	8,392	15,068	43	45	7,363	7,705
SB	6,600	13,880	43	45	6,782	7,098
				Total	**24,387**	**25,666**
Cycle length: $t_C = 88$ [s] Total Intergreen time: $t_{ig} = 12$ [s]						

Note. Own Worksheet

In conclusion, the normal intersection capacity and the maximum intersection capacity per the new signal timing plan are 24,387veh/s and 25,666 veh/s, respectively.

8 Conclusions and Recommendations

8.1 Introduction

The presented study has accomplished the goal of analysing the capacity of signalised intersection in MDCs. This chapter summarises all outcomes which were conducted through previous chapters. Section 8.2 starts with the specific characteristics of traffic flows which may affect the intersection capacity. Then, Section 8.3 describes main achievements of the capacity models. After that, Section 8.4 gives some limitations of the thesis to point out that which issues have been introduced and solved, which problems have not been mentioned. Finally, Section 8.5 concludes with some recommendations for further studies.

8.2 Conclusions from Traffic Characteristics in MDCs

Traffic characteristics in MDCs have been proven as the unique characteristics which affect the intersection capacity. Those features are summarised:

- Several vehicle types are operating in the road network in MDCs, from two-wheeled vehicles, such as bicycles, motorcycles, and scooters to four-wheeled vehicles, such as cars, middle buses, middle trucks, heavy buses, and heavy trucks. These vary from the dimension to the engine power. Thus, it is necessary to group all vehicle types into four main categories: Motorcycles, cars, middle vehicles, and heavy vehicles.

- In the mixed flow, motorcycles have an extreme proportion compared with the proportion of four-wheeled vehicles. The observations pointed out that the motorcycle share is always higher than 85% while the four-wheeled vehicles share is lower than 15%. Thus, motorcycles are suggested to be chosen as standard vehicles for capacity analysis.

- Flow speed may vary depending on the time interval. In the saturated state, the entering speed is assumed at 5 m/s, and the clearing speed is recommended at 8 m/s.

- Lane allocation affects turning activities and impacts on the discharge flow Motorcycles are assigned on the right side, and cars are assigned on the left side of the stream. Thus, right-turning motorcycles may not affect the discharge flow, but right-turning cars could. Both left-turning motorcycles and left-turning cars may affect the discharge flows.

- The traffic signal programs have high impacts on the flows and the intersection capacity. Indeed, the two-phase fixed-time signal program reduces the number of phase transitions but contribute to increasing the conflicts of flows running in the same phase. Additionally, the traffic signal countdown system reduces the lost time but increase the risk level of red-light running behaviour.

- Specific traffic behaviours, such as grouping behaviour, non-lane-based behaviour and red-light running behaviour contribute to increasing the intersection capacity. By contrast, the safety level decreases, and if an accident or a blockage event occurs inside the intersection, the capacity will go down by then. So, it is necessary to consider the effect of traffic behaviour on traffic flows at signalised intersections in the trend of balance between capacity and safety.

8.3 Conclusions from Capacity Model

8.3.1 Conditions of Capacity Model

The presented capacity model only works well and can be applied appropriately under the MDCs conditions:

- A two-phase signal program is applied (optional state).
- Non-lane-based behaviour is admitted.
- The share of motorcycles in the traffic composition is dominant.
- Motorcycles are assigned on the right side of the flow, and four-wheeled vehicles are assigned on the left side of the flow.
- The grouping behaviour inside the intersection is considered.

Without these conditions, some scenarios may happen:

- Conversion of vehicles to motorcycles may not provide an appropriate estimation.
- Four-wheeled vehicles may not block the through-motorcycles when they turn right.
- Left-turning motorcycles may not interfere through four-wheeled vehicles.
- The interaction between left-turning flows and the opposing through-flows, between through-flows and opposing left-turning flows, would not occur.

Consequently, the recommended capacity model cannot be applied. So, the user should consider the similarity of the traffic conditions before using the introduced capacity model.

8.3.2 Conclusions from Capacity Reduction Phenomenon

There is an interesting phenomenon named as '**capacity reduction phenomenon**'. This phenomenon occurs while observing the saturation flow rate. The saturation flow rate reaches the highest value from the 6^{th} second to the 16^{th} second of the green interval. Thereafter, it slightly reduces to a smaller value which remains the same until the end of the saturated green time. The main reason for this case is that the vehicles tend to stop as close to the stop line as possible. However, vehicles which stop far from stop line have no willing to follow that intention. The queued motorists stopping at the closed area with the stop line is higher than the queued motorists standing in the rear. As a result of this, the phenomenon would happen while vehicles are discharging.

The effect of '**capacity reduction phenomenon**' on the saturation flow rate and the capacity depends on the green interval. If the green interval is lower than 16 s, the saturation flow rate reach to the highest. If the green interval is equal to or higher than 16 s, the saturation flow rate decreases to a lower value.

8.3.3 Conclusions from Normalised Motorcycle Saturation Flow Rate

The term '**normalised homogeneous motorcycle flow rate**' is introduced as the maximum rate of motorcycle flow that can pass through a 1 m wide approach for one-hour effective green time. This term is used widely, and it contributes to establishing the capacity model and comparing the capacity of different approach widths.

The normalised motorcycle saturation flow rate is calculated at 3,058 mcu/(h*m) when the green interval is higher or equal to 16 s. That rate is estimated as 3,178 mcu/(h*m) when the green interval is lower than 16 s. The motorcycle saturation flow rate of a 3.5 m wide approach could reach

to around 11,000 mcu/h. This value is even equal to 5.5 times as many as the homogeneous car saturation flow rate (2,000 pcu/h). Moreover, if the rate of motorcycle occupancy is assumed at 1.2, homogeneous motorcycle flow can carry around 13,000 passengers to pass through a 3.5 m wide approach. Thus, in terms of passenger capacity aspect, motorcycles are much more efficient than cars and even buses.

8.3.4 Conclusions from Ideal Passenger Car Saturation Flow Rate

The ideal saturation flow rate of passenger cars is also observed in some separated approaches. The result is measured as 1,565 pcu/(h*ln) per the headway of 2.3 s, much lower than the studied value in car traffic-based cities (2,000 pcu/(h*ln)). There are reasons to explain this result. First, driving behaviour varies across countries. In car traffic-based cities, the 'lane-based behaviour' is followed at every intersection. In MDCs, however, cars mainly run in mixed conditions and follow the 'non-lane-based behaviour' at most of the intersections. Cars take more time to react and remain a safe space with surrounding motorcycles in such conditions. Thus, even running in separated lanes, cars could not respond as fast as cars in developed countries. Second, the layout design of signalised intersection which includes the intersection geometry and the applied signal program is unsuitable with the traffic flow performance.

The ideal saturation flow rate of passenger cars affects the capacity model through the MCU value calculation. The MCU value for cars is equal to 6.8 according to 100% of passenger car share in the traffic flow.

8.3.5 Conclusions from Motorcycle Equivalent Unit under Saturated State

Conversion of vehicles to motorcycles is implemented by applying the motorcycle equivalent unit (MCU). The simple reason is that the motorcycle share is dominant in the traffic composition for MDCs. MCU values were determined by using the regression method. The results show that the MCU values may vary depending on the proportion of cars in the traffic flow. The MCU values change from 5.5 to 6.8 corresponding to the passenger car share varies from 5% to 100%.

In field survey, the passenger car share was observed from 0% to 20% (under the mixed flow condition) and 100% (in separated car lanes). The MCU results that match with 20% to 99% of passenger car share was not verified.

The recommended MCU values for cars, middle vehicles, and heavy vehicles are 6, 9 and 14.4, respectively. They are used for determining the effect of vehicle type on the capacity. Besides, the PCU values for middle vehicles and heavy vehicles are 1.5 and 2.4. They are used for converting all four-wheeled vehicles to passenger cars only.

8.3.6 Conclusions from the Effect of Vehicle Types on the Capacity

In this study, motorcycles are considered as the smallest vehicle types and the basic vehicle units. So, the effect of vehicle types on the capacity is calculated by converting all other vehicle types in the mixed flow to motorcycles. The analysed results figured out that the impact of vehicle types is the primary factor and contribute to reducing the approach capacity.

8.3.7 Conclusions from the Effect of Turning Movements on the Capacity

The effect of turning movements on the capacity in MDCs differs from that one in car traffic-based cities. Turning movements in MDCs affect the capacity on different levels depending on their turning

position in the flow. Different turning types have different effects on the approach capacity. Right-turning motorcycles do not influence the discharge flow rate because they are assigned to run on the right side of the flow. Right-turning cars, however, affect the through movements because of its left-side position of the discharge flow. Left-turning motorcycles interfere through discharge cars and left-turning cars would reduce the discharging speed of the through-vehicles.

The effect of turning movements was categorised into 2 cases:

- Case 1: The targeted flow operates without the interference of opposing flows.
- Case 2: The targeted flow operates with the interference of opposing flows including the opposing through-flow and the opposing left-turning flow.

In case 1, the turning effect includes right-turning and left-turning effects. The right-turning effect accounts for the blocking effect of right-turning cars and the left-turning effect accounts for the interfering effect on the targeted discharge flow rate. Calculated results showed that right-turning cars give a higher impact than left-turning movements and left-turning cars give a higher influence than left-turning motorcycles.

In case 2, the situation is much more complicated. The turning effect comes not only from right-turning and left-turning movements but also from opposing left-turning movements. The turning effect would change depending on periods of green interval. During the entering interval, turning movements run without the interference of opposing flows, and the turning effect could be considered as the same in case 1. After the entering interval, the targeted flows make conflicts with opposing flows. The turning effect in this situation would include the blocking effect of right-turning cars; the interaction among left-turning movements (motorcycles and cars) and opposing through-movements, the interaction between targeted through-vehicles and opposing left-turning movements.

8.3.8 Conclusions from Effective Green Time Model

The effective green time model applies a method by counting the number of motorcycles can pass the stop line via time periods. The curves are replaced by equal area rectangles. Two models are introduced: model 1 referees that the rule 'no red-light running' must be obeyed; model 2 stipulates that the rule 'no red-light running' should be ignored.

In model 1, the start-up lost time was measured between 2 s and 2.5 s, and the green end-lag time was assumed at 2.4 s. Thus, the effective green time t_g was equal to the displayed green time t_G.

In model 2, the start-up lost time was measured from 0.5 s to 1.5 s (the early depart before green time was considered), and the green end-lad time was estimated as 3 s to 3.5 s (overrun on red was considered). Therefore, the effective green time t_g was equal to the displayed green time t_G plus two seconds.

8.3.9 Conclusions from the Intergreen Time Model

The intergreen time model for MDCs applies the German method with some modifications. The crossing time is recommended to be equal to the amber time which is set up as 3 s for most cases. The clearing time in MDCs is equal to the clearing time in German method plus with the interaction time between clearing through-vehicles and opposing clearing left-turning movements. The interaction time depends on the vehicle types at each flow and it is suggested as 2 s (the case of clearing through-motorcycles interact with clearing opposing left-turning motorcycles) to avoid a

long intergreen time. The entering time is calculated by the entering distance, which is defined from the middle-point stop line to the centre of the conflict area.

8.3.10 Conclusions from the Complete Capacity Model

The complete capacity model is introduced as the combination of the saturation flow rate model, the intergreen time model and the effective green time model. The normal capacity is presented to the assumption of the rule 'no red-light running' must be obeyed. Besides, the maximum capacity is also given to the assumption of the rule 'no run red-light running' could be ignored.

In this thesis, the normal capacity is recommended for the capacity analysis. The maximum capacity is considered as an adaption to the current traffic situation while the illegal activities could not be controlled.

8.4 Limitations of the Thesis

Data collection was conducted in only one city. The area type factor which reflects the driver behaviour in different areas was ignored. Thus, the application of this study was narrowed down to only intersections which had similar traffic conditions of the studied city (see section 8.3.1).

Some traffic conditions, such as approach grade, parking activities, and bus blockage, were also neglected in this thesis even though they had been proven to be affecting factors. So, the suggested capacity model should only be applied for signalised intersections which do not have those activities. The effect of pedestrians on the intersection capacity was also eliminated in this study because the pedestrian flow rate was insignificant by the field surveys.

The capacity model aims to measure the approach capacity. The approach width is required to remain the same through the queue length. Therefore, the suggested capacity model is not applied for some intersections which have short separate turning lanes.

The share of four-wheeled vehicles in the surveyed data was lower than 15%, and even the share of middle vehicles and heavy vehicles in most of the data samples were smaller than 1% and could not reflect their effect on the performance of traffic flows. Thus, the conversion of all four-wheeled vehicle types to passenger cars is also a limitation of this thesis.

8.5 Recommendations for Further Studies

Further studies should focus on completing a comprehensive capacity model which could be applied for all potential traffic conditions in MDCs. Larger-scale data collection should be conducted through different cities. Other possible influencing factors to the capacity should be considered, such as approach grades, bus-stop activities, parking activities, pedestrian flows. Some methods and solutions to optimise the intersection capacity should be studied. The question is whether the performance of the traffic flows in a two-phase signal system is better than the one in multiple-phase signal system or not is still a controversial one. In a two-phase signal system, the transition time is optimised, but conflicts among flows running in the same phase may affect the intersection capacity. In a multiple-phase signal system, traffic flows are separated, and conflicts among streams are eliminated. However, the lost time because of the increase in the number of phases would contribute to reducing the capacity.

Future studies should utilise the capacity model for MDCs to analyse the quality of the intersection via evaluated parameters, such as the level of service (LOS) and the total delay.

Abbreviations

General terms

Abbreviation	Description
CBD	Centre Busniess District
FGSV	Forschungsgesellschaft für Strassen- und Verkehrswesen (Road and Transportation Research Association)
GPA	Grade Point Average
HBS	Handbuch für die Bemessung von Straßenverkehrsanlagen (German Highway Capacity Manual)
HCM	Highway Capacity Manual
IHCM	Indonesian Highway Capacity Manual
ITE	Institute of Transportation Engineers
IPTS	Institute for Prospective Technological Studies
JSTE	Japan Society of Traffic Engineers
MDCs	Motorcycle Dependent Cities
MCU	Motorcycle Equivalent Unit
PCU	Passenger Car Equivalent Unit
RiLSA	Richtlinien für Lichtsignalanlagen (Guidelines for Traffic Signals)
SFR	Saturation Flow Rate
VIP	Video Image Processing

Calculation Paramaters

Symbol		Description	Unit
C	=	Lane capacity	[veh/h]
$C_{nor,i}$	=	Normal capacity of approach i	[veh/h]
$C_{max,i}$	=	Maximum capacity of approach i	[veh/h]
f_B	=	Bus blockage adjustment factor	[-]
f_G	=	Grade adjustment factor	[-]
f_P	=	Parking adjustment factor	[-]
f_{Ped}	=	Pedestrians adjustment factor	[-]
$f(p'_{MC,LT})$	=	Adjustment factor for left-turning motorcycles excluding right-turning motorcycles	[-]
$f(p'_{PC,LT})$	=	Adjustment factor for left-turning passenger cars excluding right-turning motorcycles	[-]
$f(p'_{PC,RT})$;	=	Adjustment factor for right-turning passenger cars excluding right-turning motorcycles	[-]
f_{RT}	=	Adjustment factor for right-turning movements	[-]
f_{LT}	=	Adjustment factor for left-turning movements	[-]
f_{OPL}	=	Adjustment factor for opposing left-turning movements	[-]
f_{turn}	=	Adjustment factor for turning movements	[-]
$f_{turn,1}$	=	Adjustment factor for turning movements in case of no interference of opposing flows	[-]
$f_{turn,2}$	=	Adjustment factor for turning movements in case of interference of opposing flows	[-]
f_{veh}	=	Adjustment factor for vehicle types in the traffic stream	[-]
g	=	Saturation degree	[-]
$g_{int,TH-OPL}$	=	Interaction degree between left-turning movements and opposing through-movements	[-]

Abbreviations

$g_{OPT}^{'}$	=	Saturation degree of opposing through-movements at the section before the conflict area	[-]
l_0	=	Basic clearing distance	[m]
l_1	=	Start-up lost time	[s]
$l_{1,nor}$	=	Normal start-up lost time	[s]
$l_{1,max}$	=	Maximum start-up lost time	[s]
l_2	=	Clearance lost time	[s]
l_e	=	Entering distance from the stop line of the entering flow to the conflict point between the entering flow and the clearing flow	[m]
l_{e1}	=	Entering distance from the stop line of the entering through flow to the conflict point between the entering through flow and the opposing entering left-turning flow	[m]
$l_{e,op1}$	=	Entering distance from the stop line of the opposing entering left-turning flow to the conflict point between the entering through flow and the opposing entering left-turning flow	[m]
l_{cl}	=	Clearing distance from the stop line of the clearing flow to the conflict point between the entering flow and the clearing flow	[m]
l_{veh}	=	Vehicle length	[m]
MCU_C	=	Motorcycle equivalent unit of cars	[-]
MCU_{MV}	=	Motorcycle equivalent unit of middle vehicles	[-]
MCU_{HV}	=	Motorcycle equivalent unit of heavy vehicles	[-]
N_1	=	Number of vehicles stopped over a 1 m wide stop line during the red time	[mcu/m]
N_2	=	The number of motorcycles per 1 m wide approach departing over the stop line during the red time	[mcu/m]
N_3	=	The number of motorcycles per 1 m wide approach departing over the stop line during the first 6-second green period	[mcu/m]
N_4	=	The number of motorcycles per 1 m wide approach clearing over the stop line during the amber time	[mcu/m]
N_5	=	The number of motorcycles per 1 m wide approach clearing over the stop line during the red time	[mcu/m]
$p_{MC,LT}^{'}; p_{PC,LT}^{'}$	=	Proportion of left-turning motorcycles, left-turning passenger cars, in the flow excluding right-turning motorcycles	[-]
$p_{PC,RT}^{'}$	=	Proportion of right-turning passenger cars in the flow excluding right-turning motorcycles	[-]
P_{PC}	=	Proportion of passenger cars in the traffic flow	[-]
$q_{i,LT}$	=	Flow rate of left-turning of vehicle type i during the saturated green time *T*	[veh/h]
$q_{i,TH}$	=	Flow rate of through-vehicles type i during the saturated green time *T*	[veh/h]
$q_{i,RT}$	=	Flow rate of right-turning vehicles type i during the saturated green time *T*	[veh/h]
S	=	Saturation flow rate	[veh/h]
S_0	=	Normalised saturation flow rate	[veh/(h*m)]
S_{0C}	=	Passenger car saturation flow rate	[pcu/(h*ln)]
S_{0w}	=	Motorcycle saturation flow rate per the approach width w	[mcu/h]
t_A	=	Amber time	[s]
t_C	=	Cycle length	[s]
t_{cl}	=	Clearing time	[s]
$t_{cl,free}$	=	Free flow clearing time	[s]
$t_{cl,int}$	=	Normal clearing time	[s]
t_{cr}	=	Crossing time	[s]

Abbreviations

t_e	=	Entering time from the stop line of the entering flow to the conflict point between the entering flow and the clearing flow	[s]
t_{e1}	=	Entering time from the stop line of the entering flow to the conflict point between the entering through flow and the opposing entering left-turning flow	[s]
t_{ig}	=	Intergreen time	[s]
$t_{int,TH-OPL}$	=	Interaction time between clearing through-vehicles and opposing clearing left-turning movements	[s]
t_g	=	Effective green time	[s]
$t_{g,nor}$	=	Normal effective green time	[s]
$t_{g,max}$	=	Maximum effective green time	[s]
t_G	=	Displayed green time	[s]
t_R	=	Displayed red time	[s]
t_{re}	=	Reaction time	[s]
T	=	Saturated green time	[s]
v_e	=	Entering speed	[m/s]
v_{cl}	=	Clearing speed	[m/s]
w	=	Approach width	[m]
w_{op}	=	Opposing approach width	[m]
λ_2	=	Green end-lag time	[s]
$\lambda_{2,nor}$	=	Normal green end-lag time	[s]
$\lambda_{2,max}$	=	Maximum green end-lag time	[s]

List of Figures

List of Figures

List of Tables

References

Akcelik, R., Australian Road Research Board. (1981). *Traffic signals: capacity and timing analysis.* Vermont South, Vic.: Australian Road Research Board, Australia.

Abidin, N.I.B.Z. (2007). *Evaluating signalized intersection capacity based on Malaysian road conditions.* Master Thesis, Universiti Sains Malaysia, Malaysia.

Arasan, T., Boltze M. (2004). Design of Intergreen Intervals in Signal-Time Settings: The State of the Art. *Highway Research Bulletin, 70. Indian Roads Congress Highway Research Board.* New Delhi, India.

Arasan, T., Boltze M., Subramanyam, S. (2006). Determination of Intergreen Intervals in Signal-Time Settings for Heterogeneous Traffic. *Indian Highways, Volume 34*.

Ben-Akiva, M. E., Lerman, S. R. (2006). *Discrete choice analysis: theory and application to travel demand*. Cambridge, Mass: The MIT Press.

Boltze M. (1988). *Optimierung von Umlaufzeiten in der Lichtsignalsteuerung für Straßennetze (Optimisation of Cycle Times in Traffic Signal Control of Road Networks)*. Doctoral Dissertation, Technische Hochschule Darmstadt, Germany.

Chandra, S. (2004). Capacity estimation procedure for two lane roads under mixed traffic conditions. *Indian Institute of Technology*, 139-170.

Chaudhry, M.S., Ranjitkar, P. (2009). Capacity analysis of signalized intersection: A comparative study of micro simulation and analytical approaches. *The Eastern Asia Society for Transportation Studies, Vol 7*.

Chu, C.M., Sano, K. (2003). Analysis of motorcycle effects to saturation flow rate at signalized intersection in developing countries. *Journal of Eastern Asia Society for Transportation Studies, Vol 8*, 1211-1222.

Chu, C.M., Sano, K., Tran, M. T., Matsumoto, S. (2010). Development of Motorcycle Unit (MCU) for Motorcycle-Dominated Traffic. *Journal of the Eastern Asia Society for Transportation, 8*, 1596-1608.

Chu, C.M., Sano, K., Matsumoto, S. (2010). Maneuvers of motorcycles in queues at signalized intersections. *Journal of Advanced Transportation.* doi: 10.1002/atr.144

Do, Q.C. (2009). *Traffic signals in motorcycle dependent cities*. Doctoral Thesis, Technische Universität Darmstadt, Germany.

Easa, S. M. (1993). Reliability Based Design of Intergreen Interval at Traffic Signals. *Journal of Transportation Engineering,* 119(2), 255-271. doi:10.1061/(asce)0733-947x(1993)119:2(255)

FGSV–Forschungsgesellschaft *für* Strassen- und Verkehrswesen. (1992). *Richtlinien für Lichtsignalanlagen (Guidelines for Traffic Signals)*. FGSV 321, FGSV-Verlag, Cologne, Germany.

FGSV–Forschungsgesellschaft *für* Strassen- und Verkehrswesen. (2015). *Richtlinien für Lichtsignalanlagen (Guidelines for Traffic Signals)*. FGSV 321, FGSV-Verlag, Cologne, Germany.

FGSV–Forschungsgesellschaft *für* Strassen- und Verkehrswesen. (2010). *Handbuch fuẗr die Bemessung von Straßenverkehrsanlagen (Germam Highway Capacity Manual)*. FGSV-Verl, Cologne, Germany.

FGSV–Forschungsgesellschaft *für* Strassen- und Verkehrswesen. (2015). *Handbuch fuẗr die Bemessung von Straßenverkehrsanlagen (Germam Highway Capacity Manual)*. FGSV-Verl, Cologne, Germany.

Gazis, D., Herman, R., Maradudin, A. (1960). The Problem of the Amber Signal Light in Traffic Flow. *Operations Research,8(1)*, 112-132. doi:10.1287/opre.8.1.112

Gray-Calhoun, Associates. (2003). *Traffic Signal Design Guidelines*. Georgia Department of Transportation, United States of America.

Guberiníc, S., Senborn, G., Lazíc, B. (2008). *Optimal traffic control: urban intersections*. Boca Raton, FL: CRC Press.

Hsu, Tien-Pen, Nguyen, X.D., Sadullah, A.F.M. (2003). A comparative study on motorcycle traffic development of Taiwan, Malaysia and Vietnam. *Journal of the Eastern Asia Society for Transportation Studies*, *Vol.5*, 179-193.

Huynh, D.N., Boltze., M., Vu, A.T. (2013). Modelling Mixed Traffic Flow at Signalised Intersection Using Social Force Model. *Proceedings of the Eastern Asia Society for Transportation Studies*, Vol.9, 1734-1749.

ITE- Institute of Transportation Engineers. (1999). *Traffic Engineering Handbook, 5th edition*. Washington, D.C.: Institute of Transportation Engineers.

ITE- Institute of Transportation Engineers. (2009). *Traffic Engineering Handbook, 6th edition*. Washington, D.C.: Institute of Transportation Engineers.

IPTS- Institute for Prospective Technological Studies. (2008). *Road Traffic Data: Collection Methods and Applications*. Retrieved from ftp://ftp.jrc.es/pub/EURdoc/JRC47967.TN.pdf

James, H.K., Iris, J.F. (1993). *Manual of Traffic Signal Design*. Prentice-Hall, Inc., Englewood Cliffs.

JSTE- Japan Society of Traffic Engineers. (1988). *The planning and design of at-grade intersections*. Tokyo, Japan.

JSTE- Japan Society of Traffic Engineers. (1990). *The planning and design of at-grade intersections: applications*. Tokyo, Japan.

JSTE- Japan Society of Traffic Engineers. (2006). *Manual on traffic signal control*. Tokyo, Japan.

Khuat, V.H. (2006). *Traffic management in motorcycle dependent cities*. Doctoral Thesis, Technische Universität Darmstadt, Germany.

Kockelman, K.M., Shabih, R.A (2000). Effect of vehicle type on the capacity of signalized intersections: the case of light-duty trucks. *Journal of Transportation Engineering*. 126, no. 6:506–12.

Lan, L.W., Chang, C.W. (2005). Inhomogeneous cellular automata modeling for mixed traffic with cars and motorcycles. *Journal of Advanced Transportation 39*, 323-349

Lee, Tzu-Chang, Polak, John, W., Bell, Michael, G.H., Wigan, Marcus, R. (2010). The Passenger Car Unit values of motorcycles at the beginning of a green period and in a saturation flow. *12th WCTR*, Lisbon, Portugal.

Li, S., Zhu, K., Gelder, B. V., Nagle, J., Tuttle, C. (2002). Reconsideration of Sample Size Requirements for Field Traffic Data Collection with Global Positioning System Devices. *Transportation Research Record: Journal of the Transportation Research Board*, *1804*, 17-22. doi:10.3141/1804-03.

Limanond, T., Chookerd, S., Routonglang, N. (2009). Effects of countdown timers on queue discharge characteristics of through movement at signalized intersection," *Transp. Res. C, Emerg. Technol.*, vol. 17, no. 6, pp. 662_671.

Maini, P. (1997). Study of lost time at signalized intersections. "*Traffic Congestion and Traffic Safety in the 21st Century: Challenges, Innovations, and Opportunities; Proceedings of the conference in Chicago, Illinois*", pp. 180–186. American Society of Civil Engineers, New York

Malaysia: Ministry of Works (2011). *Malaysian Highway Capacity Manual*. Malaysia

MKJI- Manual Kapasitas Jalan Indonesia (Indonesian Highway Capacity Manual). (1997). Jakarta, Indonesia.

Miller, A.J. (1968). The capacity of signalized intersections in Australia. *Australian Road Research 393 Board*. Bulletin No.3.

Montgomery, D.C., Runger, G.C. (2003). *Applied statistics and probability for engineers*. Hoboken, NJ: Wiley.

Nguyen, Q.H., Montgomery, H., Timms, P. (2007). Should Motorcycle be blame for traffic congestion in Vietnamese cities? *Codatu XIII Conference*, Ho Chi Minh City, Vietnam.

Nguyen, Q.H. (2007). *Saturation flow and vehicle equivalence factors in traffic dominated by motorcycle*. Doctoral Thesis, The University of Leeds, UK.

Patil, G.R., Patare, P., Sangole, J.P., Tech, M. (2010). Gap acceptance behaviour of two-wheelers at limited priority uncontrolled intersections. *TRB 90th Annual Meeting.*

Pelechano, N., Obrien, K., Silverman, B., Badler, N. (2005). Crowd Simulation Incorporating Agent Psychological Models, Roles and Communication. doi:10.21236/ada522128

Powell, Mark (2000). A model to represent motorcycle behaviour at signalised intersections incorporating an amended first order macroscopic approach. *Transportation Research Part A: Policy and Practice*, *34*, 497-514.

Rahman, M.M, Ahmed, S.N. Hassan, T. (2005). Comparison of saturation flow rate at signalized intersections in Yokohama and Dhaka. *The Eastern Asia Society for Transportation Studies*, *Vol. 5*, 959 – 966.

Retzko, H.G., Boltze, M. (1987). Timing of Intergreen Periods at Signalized Intersections: The German method. *ITE Journal*, 23-26.

Rodegerdts, L. A. (2004). *Signalised intersections: informational guide*. McLean, VA: Federal Highway Administration.

Roess, R.P., Prassas, E. S., McShane, W. R. (2011). *Traffic engineering*. Upper Saddle River, NJ: Pearson Prentice Hall.

Shikata S, Katakura M, Oguchi T, Murai N. An analysis on lost time with the change of right-turn phases. *Proceeding of Traffic Engineering Meeting 2003*; 23:57–60.

Tang, K. (2008). A Study on the Evaluation of Group-Based Signal Control Policy for Signalized Intersections. *Doctoral dissertation*, Department of Civil Engineering, Nagoya University, Japan

Teply, S., Allingham, D.I., Richardson, D.B., Stephenson, B.W. (2008). *Canadian Capacity Guide for Traffic Signal Intersections*. Institute of Transportation Engineers District 7, Canada.

TRB- Transportation Research Board, National Research Council. (1985). *Highway Capacity Manual*. Washington D.C, United States of America.

TRB- Transportation Research Board, National Research Council. (1994). *Highway Capacity Manual*. Washington D.C, United States of America.

TRB- Transportation Research Board, National Research Council. (2000). *Highway Capacity Manual*. Washington D.C, United States of America.

TRB- Transportation Research Board, National Research Council. (2010). *Highway Capacity Manual*. Washington D.C, United States of America.

Vien, L.L., Ibrahim, W.H.W., Mohd, A.F. (2008). Effect of Motorcycles Travel Behaviour on Saturation Flow Rates at Signalized Intersections in Malaysia. *23rd ARRB Conference –Research Partnering with Practitioners*, Adelaide, Australia.

Vu, T.A. (2007). *Interactions between Motorcycles and Automobiles in Mixed Traffic- The case of Ha Noi City*. Doctoral Thesis, The University of Tokyo, Japan.

Vu, A.T., N., Shimizu, T. (2010). An analysis of the interactions between vehicle groups at intersections under mixed traffic flow conditions. *Journal of Eastern Asia Society for Transportation Studies*, *Vol 8*, 1999-2017.

Webster, F.V. and Cobbe, B. (1966). *Traffic signals*. Road Research Technical Paper, No. 56, Road Research Laboratory, HMSO (Her Majesty's Stationery Office), London., UK.

Webster, F.V. (1963), *A method of measuring saturation flow at traffic signals*. Road research Laboratory Road Note 34, Crowthorne, UK.

Washington, S.P., Karlaftis, M.G., Mannering, F.L. (2003). *Statistical and econometric methods for transportation data analysis*. Boca Raton: Chapman and Hall/CRC Press.

Wolfermann, A. (2009). *Influence of Intergreen Time on the Capacity of Signalised Intersections*. Doctoral Thesis, Technische Universität Darmstadt, Germany.

Xuan, X., Daganzo, C.F., Cassidy, M.J. (2011). Increasing the Capacity of Signalized Intersections with Separate Left Turn Phases. *Transportation Research Part B*, 769-781.

Appendices

A Survey Locations

Surveys were conducted at 25 intersections (36 approaches). Depending on the intersection layout, the camera positions and the analysed target, the stop line observations, or the whole intersection observations were implemented. Approaches with different measurements were listed in Table 5-1. Layouts of the intersections are given on the following pages. The camera positions are also marked.

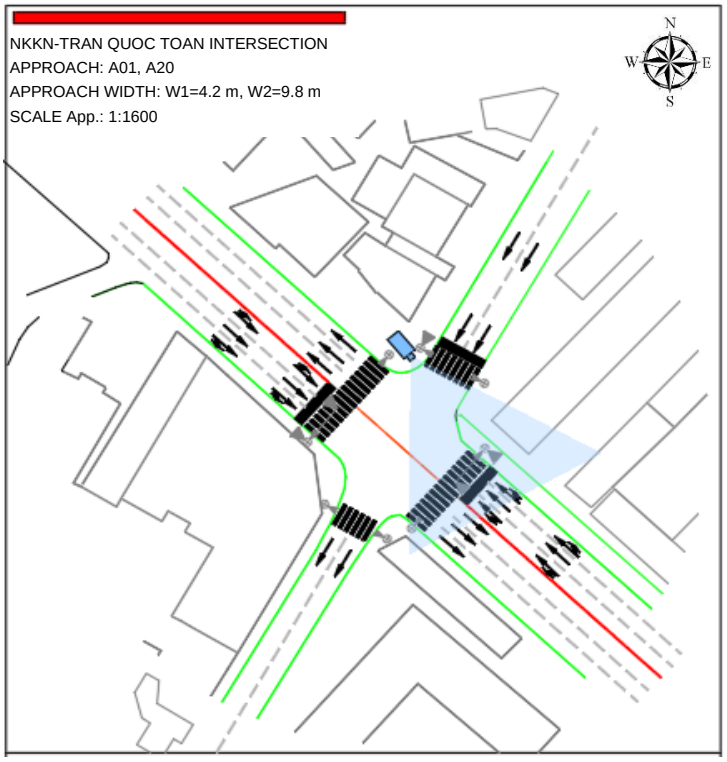

Figure A-1: Layout of Nam Ky Khoi Nghia-Tran Quoc Toan intersection

Note. Own Drawing

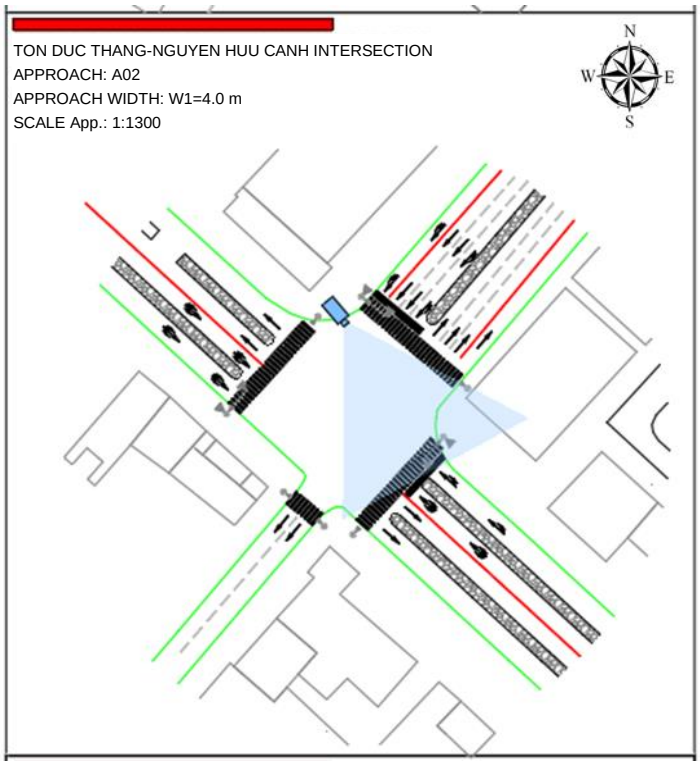

Figure A-2: Layout of Ton Duc Thang- Nguyen Huu Canh Intersection

Note. Own Drawing

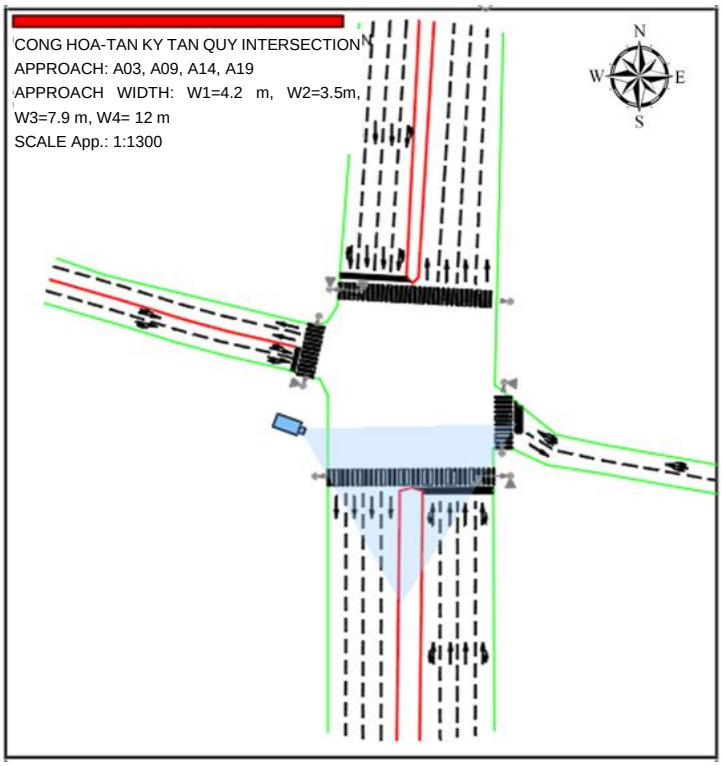

Figure A-3: Layout of Cong Hoa-Tan Ky Tan Quy Intersection

Note. Own Drawing

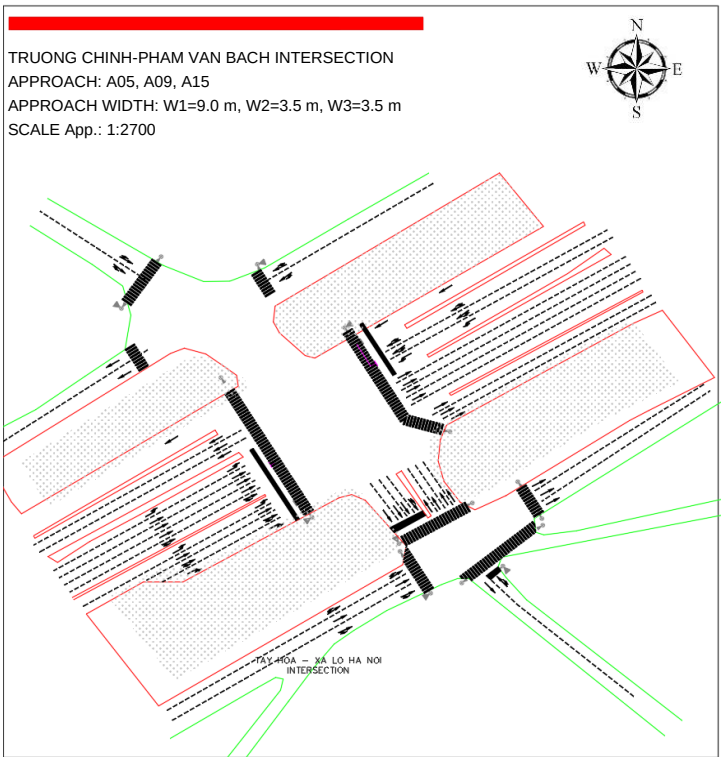

Figure A-4: Layout of Tay Hoa-Xa Lo Ha Noi Intersection

Note. Own Drawing

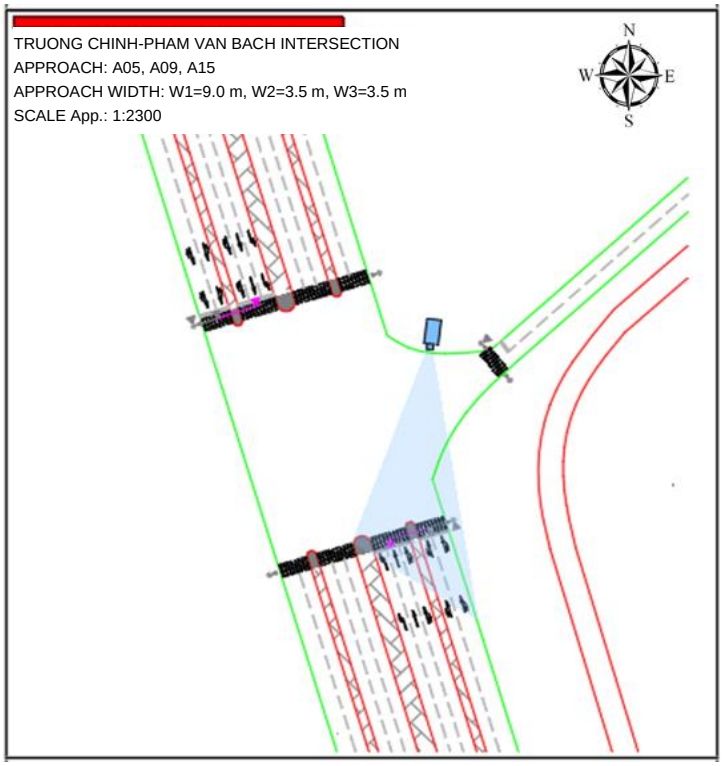

Figure A-5: Layout of Truong Chinh-Pham Van Bach Intersection

Note. Own Drawing

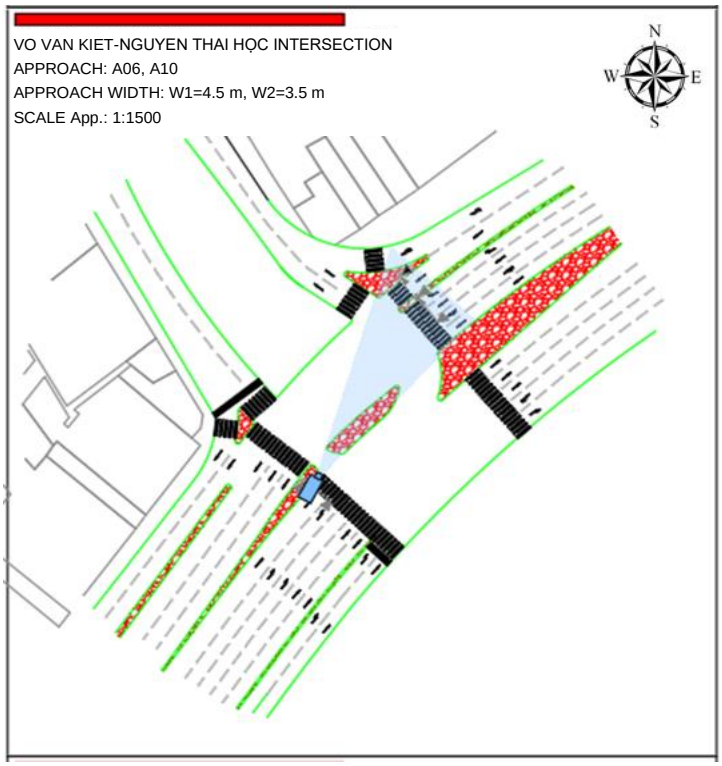

Figure A-6: Layout of Vo Van Kiet-Nguyen Thai Hoc Intersection

Note. Own Drawing

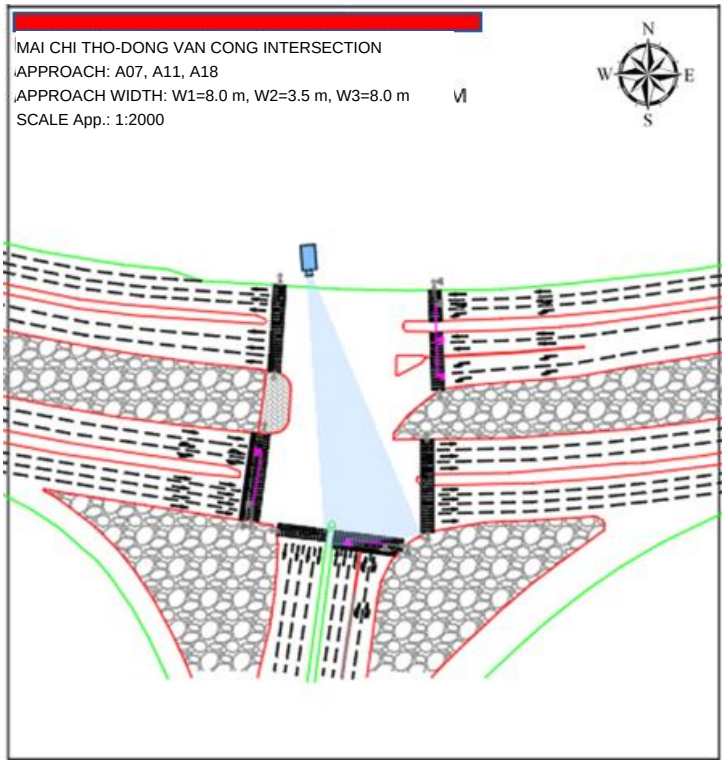

Figure A-7: Layout of Mai Chi Tho-Dong Van Cong Intersection

Note. Own Drawing

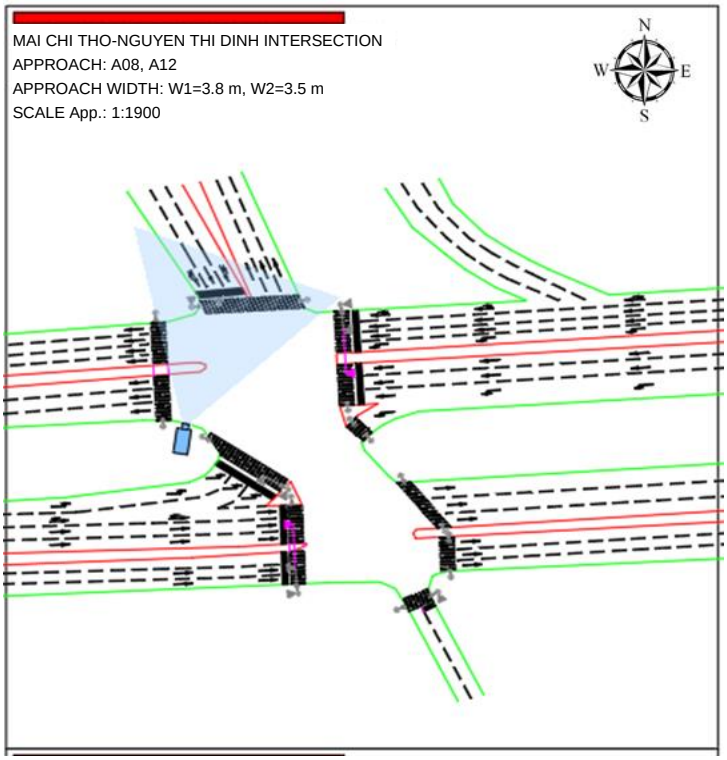

Figure A-8: Layout of Mai Chi Tho-Nguyen Thi Dinh Intersection

Note. Own Drawing

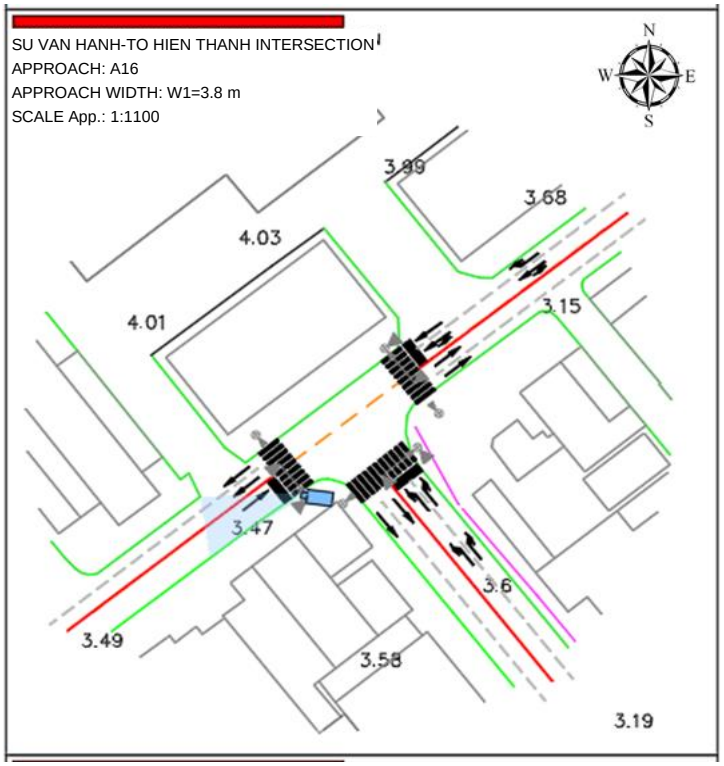

Figure A-9: Layout of Su Van Hanh-To Hien Thanh Intersection

Note. Own Drawing

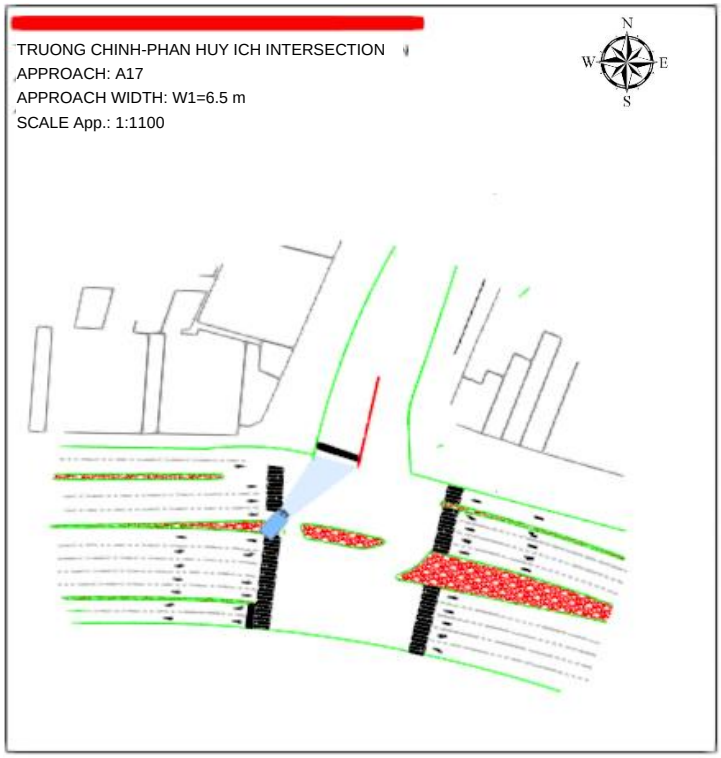

Figure A-10: Layout of Truong Chinh-Phan Huy Ich Intersection

Note. Own Drawing

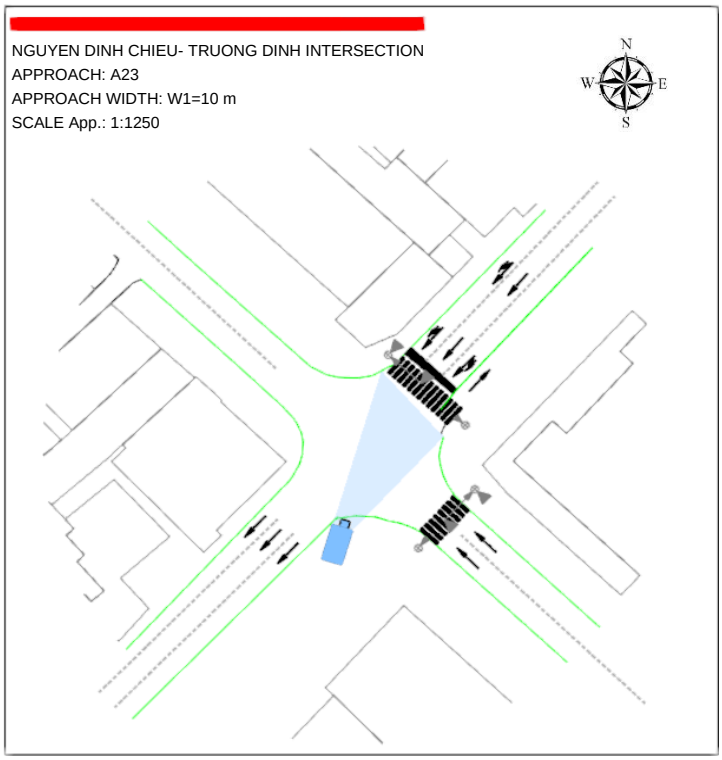

Figure A-11: Layout of Nguyen Dinh Chieu-Truong Dinh Intersection

Note. Own Drawing

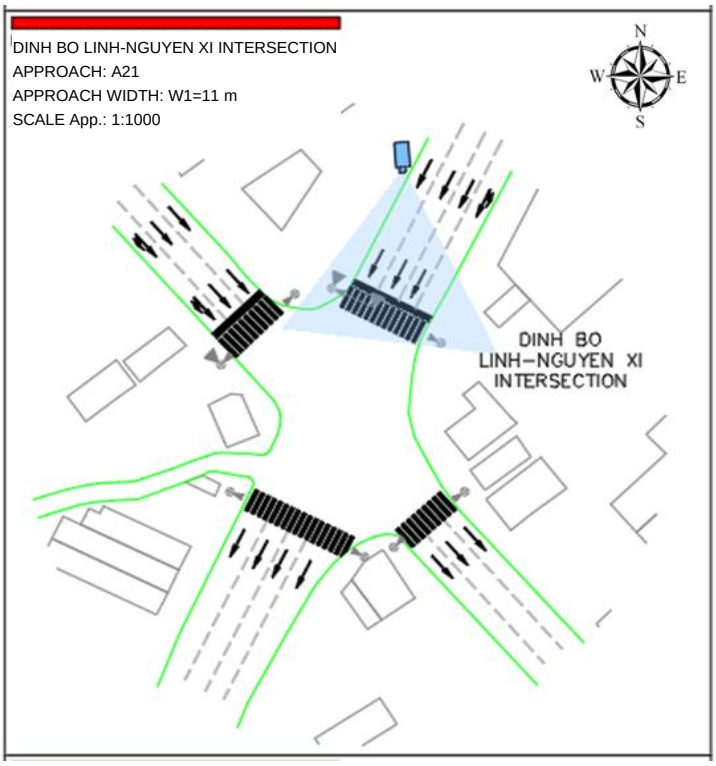

Figure A-12: Layout of Dinh Bo Linh-Nguyen Xi Intersection

Note. Own Drawing

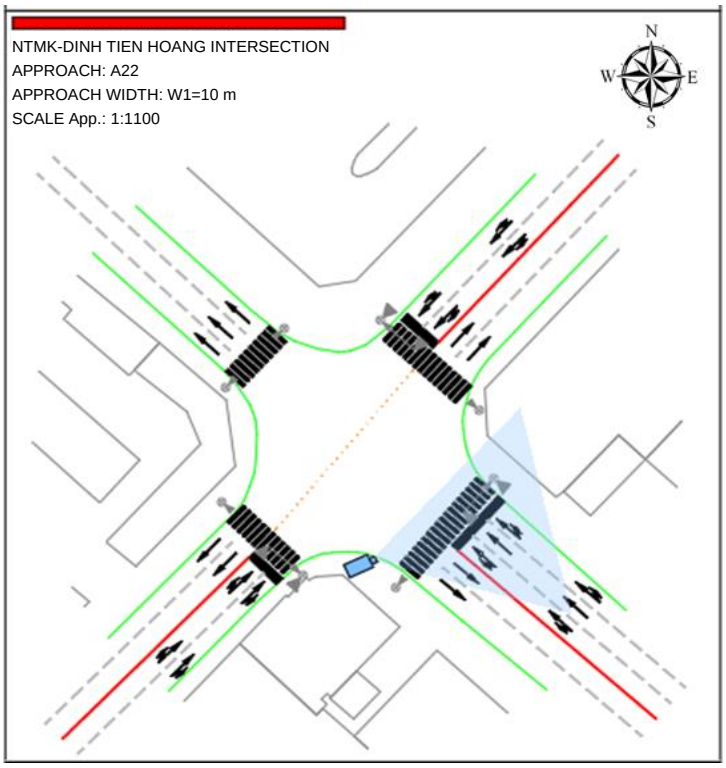

Figure A-13: Layout of Nguyen Thi Minh Khai-Dinh Tien Hoang Intersection

Note. Own Drawing

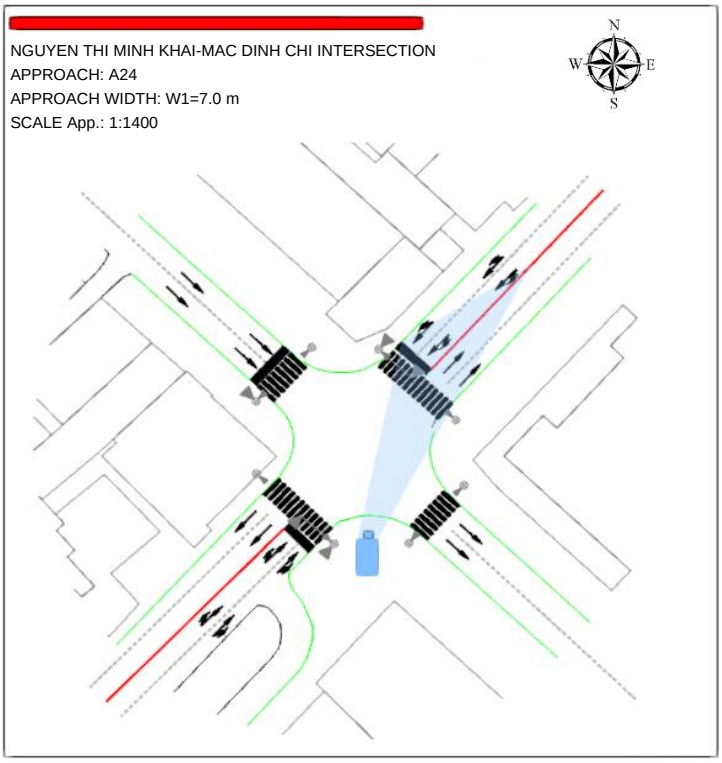

Figure A-14: Layout of Nguyen Thi Minh Khai-Dinh Tien Hoang Intersection

Note. Own Drawing

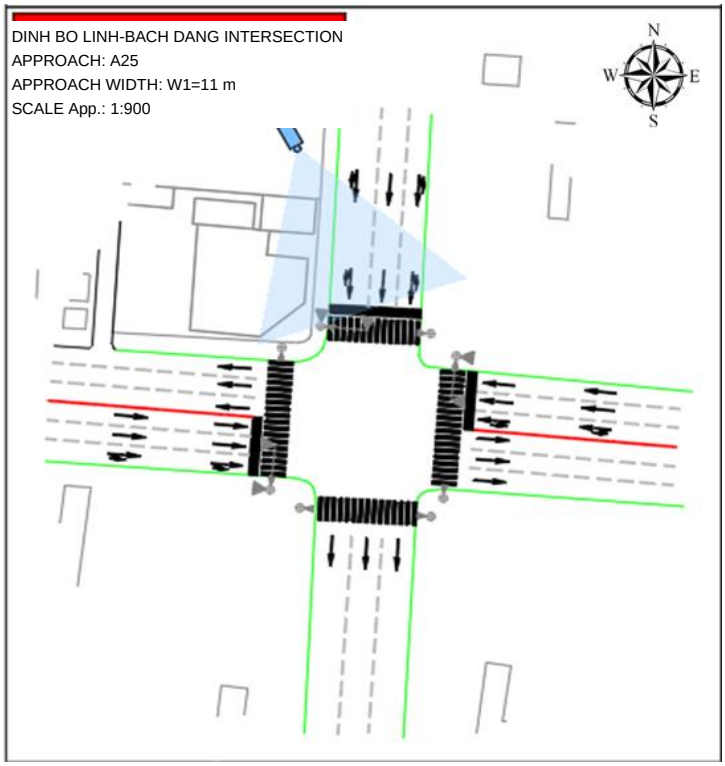

Figure A-15: Layout of Dinh Bo Linh-Bach Dang Intersection

Note. Own Drawing

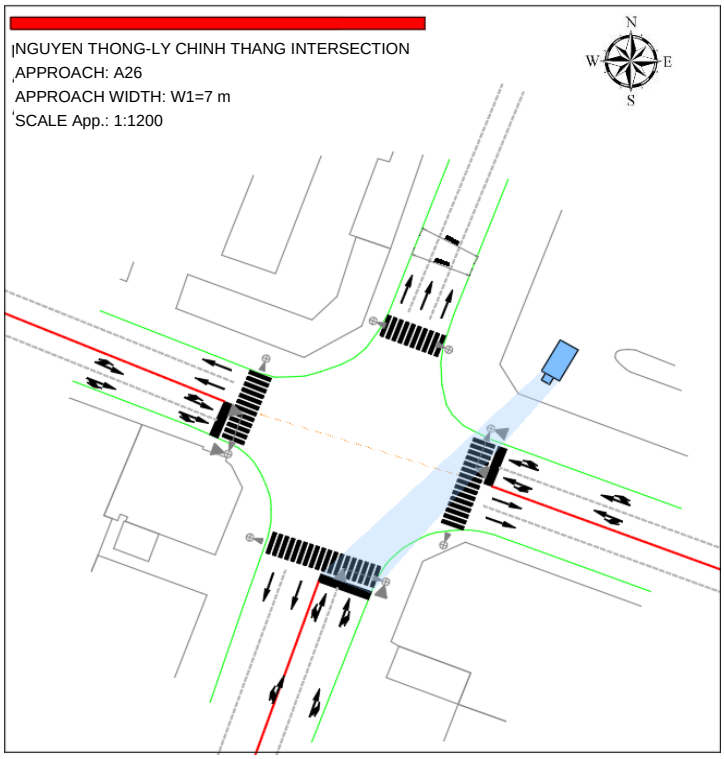

Figure A-16: Layout of Nguyen Thong-Ly Chinh Thang Intersection

Note. Own Drawing

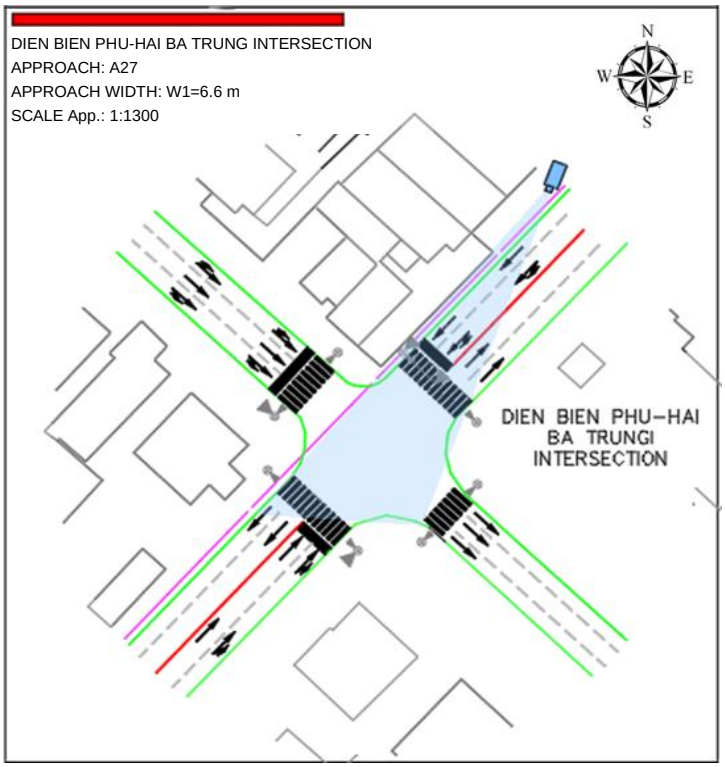

Figure A-17: Layout of Dien Bien Phu-Hai Ba Trung Intersection

Note. Own Drawing

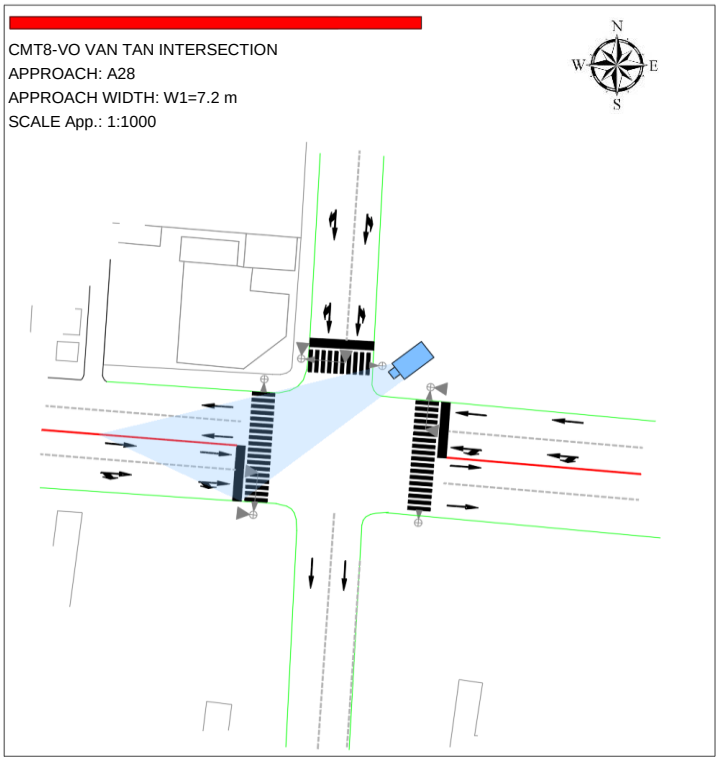

Figure A-18: Layout of CMT8-Vo Van tan Intersection

Note. Own Drawing

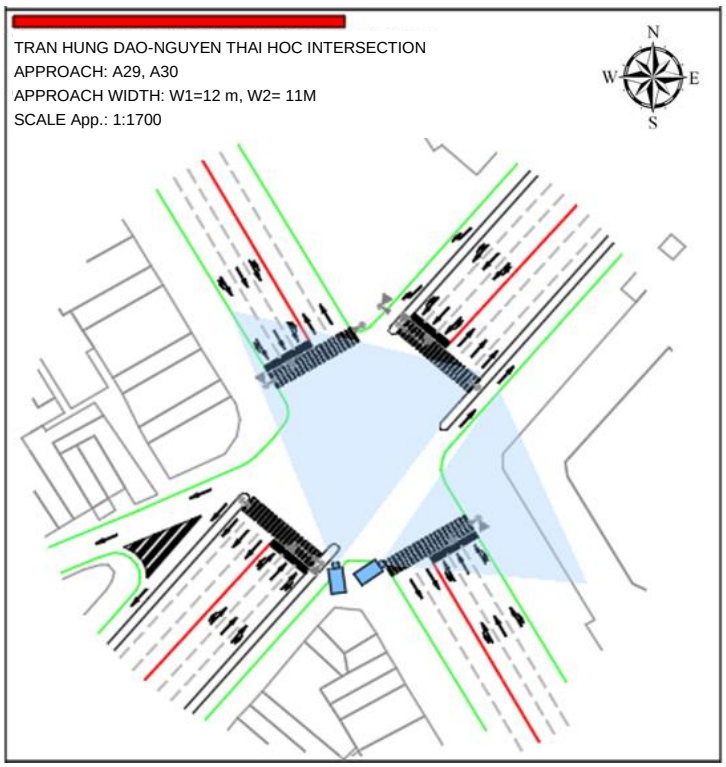

Figure A-19: Layout of Tran Hung Dao-Nguyen Thai Hoc Intersection

Note. Own Drawing

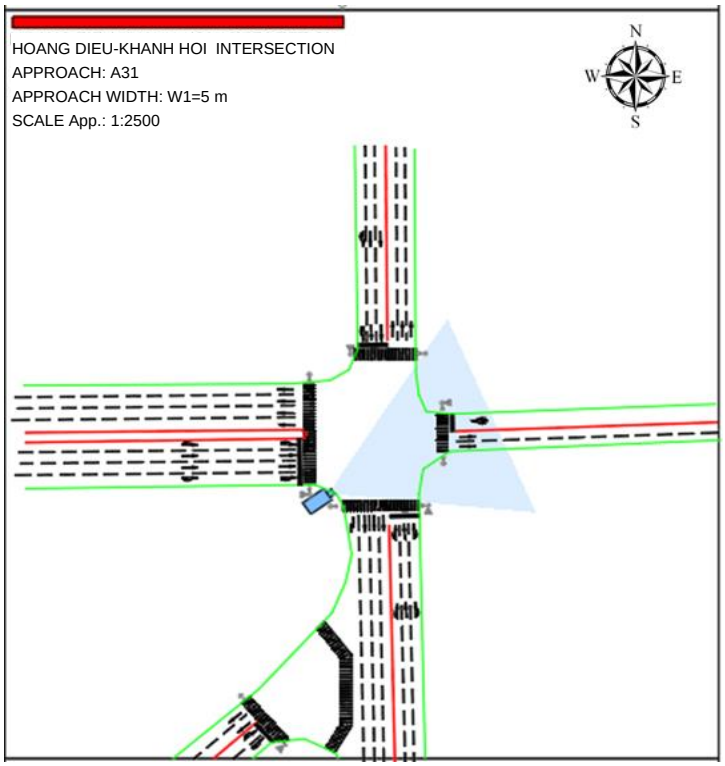

Figure A-20: Layout of Hoang Dieu-Khanh Hoi Intersection

Note. Own Drawing

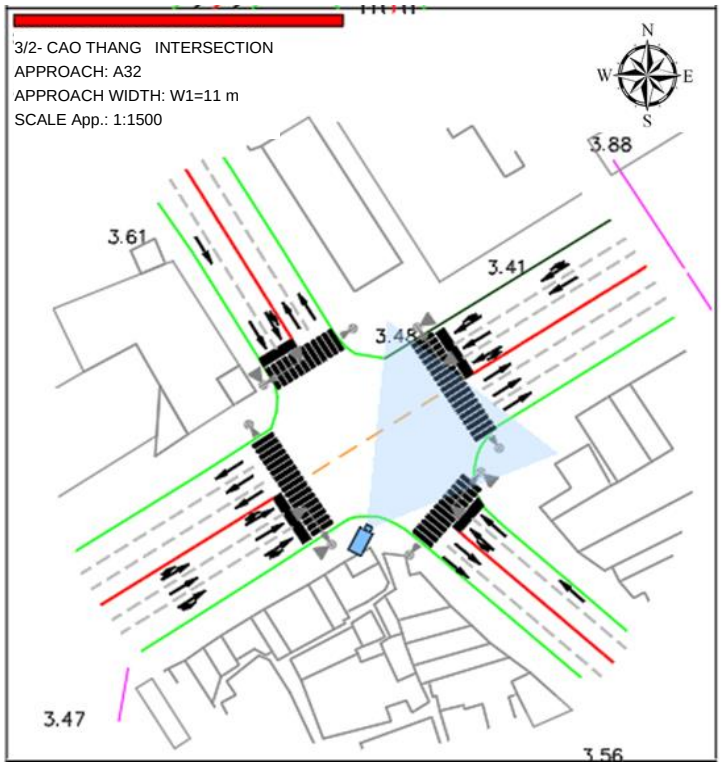

Figure A-21: Layout of 3/2-Cao Thang Intersection

Note. Own Drawing

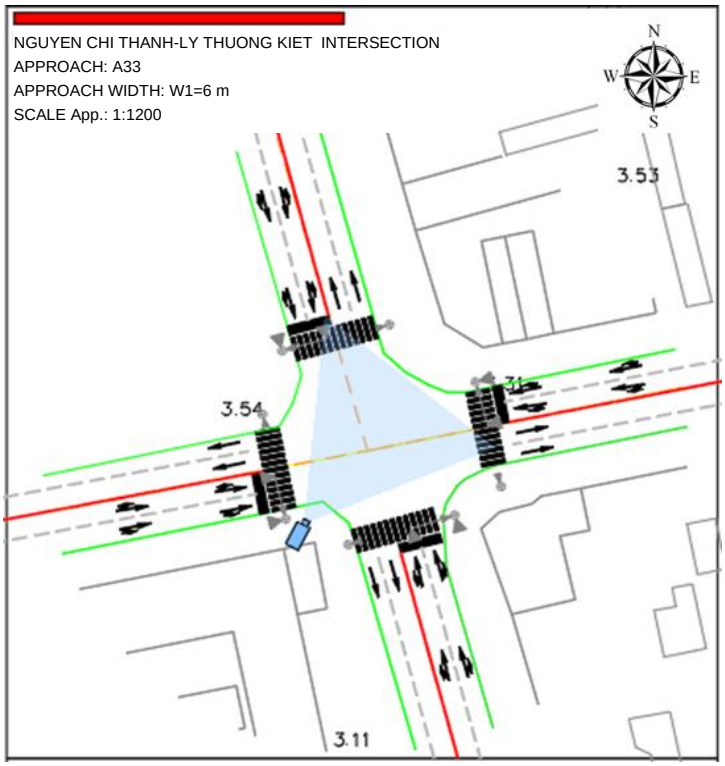

Figure A-22: Layout of Nguyen Chi Thanh-Ly Thuong Kiet Intersection

Note. Own Drawing

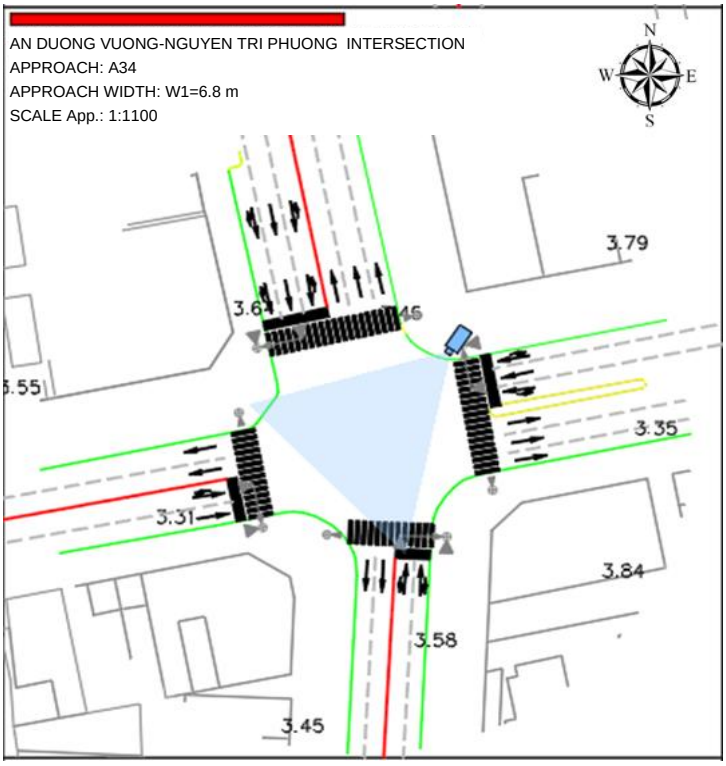

Figure A-23: Layout of An Duong Vuong-Nguyen Tri Phuong Intersection

Note. Own Drawing

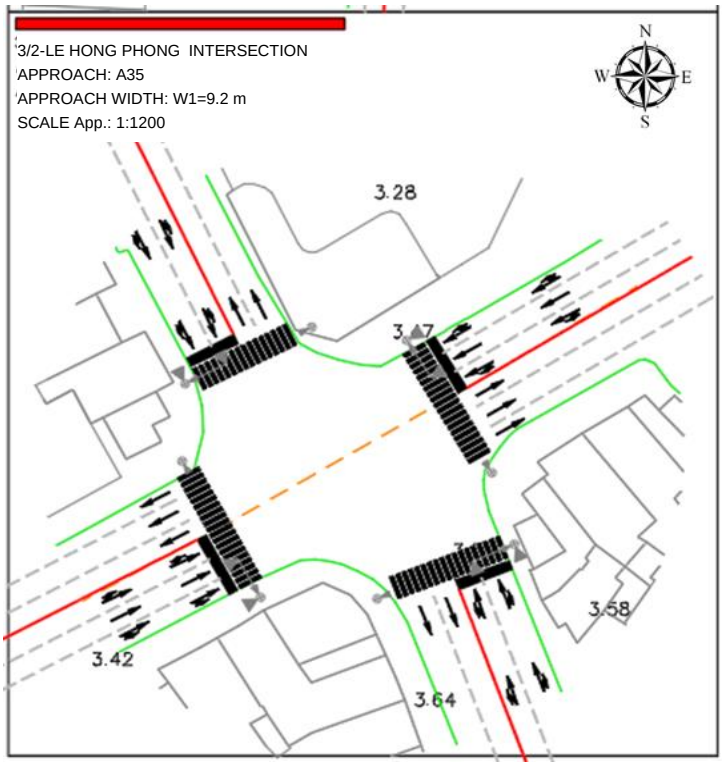

Figure A-24: Layout of 3/2-Le Hong Phong Intersection

Note. Own Drawing

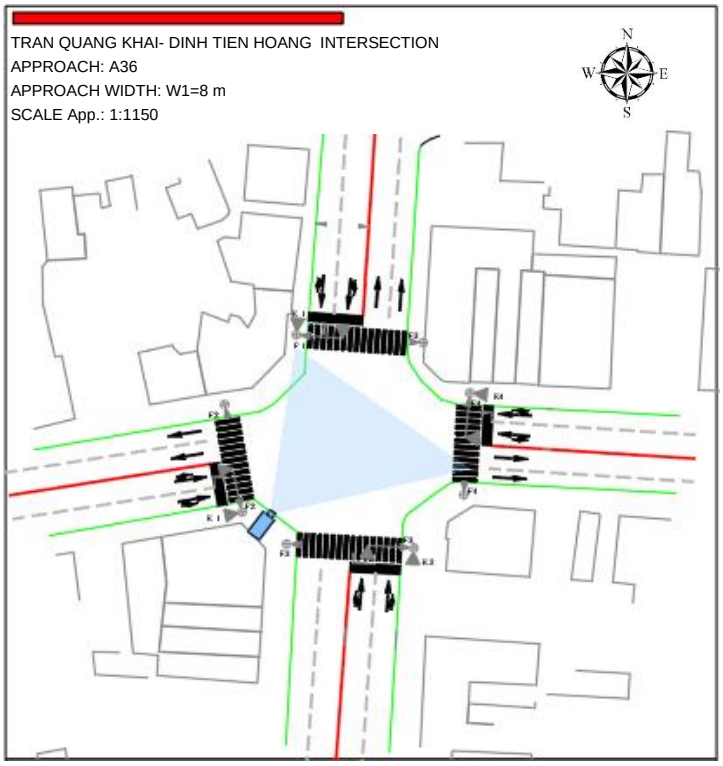

Figure A-25: Layout of Dinh Tien Hoang- Tran Quang Khai Intersection

Note. Own Drawing

B Speed Data

Speed data include entering speed data from the entering stream and clearing speed data from the clearing stream (Figure B-1).

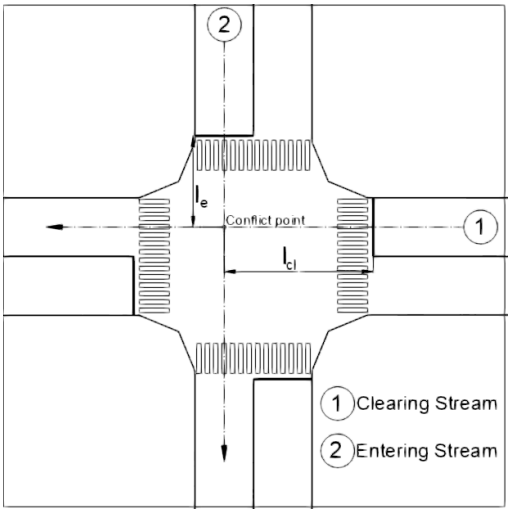

Figure B-1: Example of the interaction between straight clearing stream and straight entering stream

The Entering speed is estimated by observing the entering distance, and the time that motorcycle can complete that distance. Every data sample was estimated for each cycle length (Table B-1). Firstly, the entering distance was measured as the distance from the stop line (measured from the centre of the approach) to the conflict point. Then the entering time was collected by the time the first motorcycle start moving to the time it reaches the central point of the conflict area. Finally, the entering speed was calculated by:

$$v_e = \frac{l_e \times 3.6}{t_e} \quad \text{(B-1)}$$

where v_e = Entering speed [km/h]
l_e = Entering distance [m]
t_e = Entering time [s]

Speed [km/h]	Frequency [km/h]	Cumulative Percent [%]	Percentile [%]
11	2	4.26%	
12	6	17.02%	
13	3	23.40%	
14	10	44.68%	50th
15	11	68.09%	
16	6	80.85%	85th
17	4	89.36%	
18	1	91.49%	
19	1	93.62%	
20	1	95.74%	
21	1	97.87%	
22	1	100.00%	
More	0	100.00%	

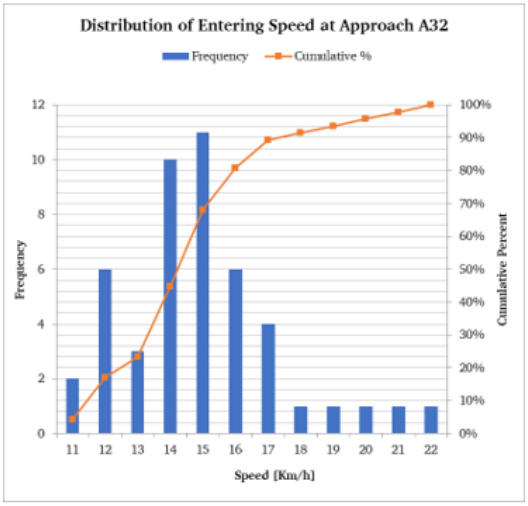

Figure B-2: Frequency Distribution of Entering Speed at Approach A32

Note. Own Table and Graph

Table B-1: Data of Entering Speed Estimation

Entering Speed Study
Data Collection Form

Location: 3/2-Cao Thang Intersection

Vehicle Number	**Speed**	**Vehicle Number**	**Speed**	**Vehicle Number**	**Speed**
[-]	[km/h]	[-]	[km/h]	[-]	[km/h]
1	11	17	15	33	15
2	14	18	11	34	11
3	13	19	13	35	16
4	15	20	14	36	15
5	15	21	13	37	16
6	15	22	13	38	20
7	13	23	15	39	12
8	14	24	15	40	19
9	15	25	14	41	15
10	10	26	13	42	12
11	13	27	14	43	15
12	12	28	11	44	15
13	17	29	15	45	14
14	12	30	22	46	16
15	13	31	11	47	21
16	16	32	16	48	16

Note. Own Table

The clearing speed is estimated by observing the clearing distance, and the time that motorcycle can complete that distance. Every data sample was estimated for each cycle length (Table B-2). Firtlsy, the clearing distance was measured as the distance from the stop line to the central point of the conflict area. Then the clearing time was collected by the time the last motorcycle passing the stopline to the time it reaches the central point of the conflict area. Finally, the clearing speed was calculated by:

$$v_{cl} = \frac{l_{cl} \times 3.6}{t_{cl}} \tag{B-2}$$

where v_e = Clearing speed [km/h]
l_e = Clearing distance [m]
t_e = Clearing time [s]

Table B-2: Data of Clearing Speed Estimation

Clearing Speed Study					
Data collection Form					
Location: 3/2-Cao Thang Intersection					
Vehicle number	Speed	Vehicle number	Speed	Vehicle number	Speed
[-]	[km/h]	[-]	[km/h]	[-]	[km/h]
1	25	18	26	35	20
2	27	19	27	36	33
3	20	20	31	37	24
4	23	21	24	38	25
5	30	22	38	39	29
6	20	23	27	40	27
7	26	24	30	41	23
8	26	25	20	42	23
9	32	26	28	43	28
10	27	27	24	44	35
11	31	28	30	45	23
12	28	29	20	46	21
13	26	30	21	47	37
14	24	31	21	48	23
15	27	32	30	49	23
16	37	33	20	50	23
17	25	34	20	51	28

Note. Own Table

Speed [km/h]	*Frequency* [km/h]	*Cumulative Percent* [%]	*Percentile* [%]
20	5	9.80%	
21	2	13.73%	
22	3	19.61%	
23	6	31.37%	
24	4	39.22%	
25	2	43.14%	
26	3	49.02%	50th
27	7	62.75%	
28	3	68.63%	
29	3	74.51%	
30	4	82.35%	85th
31	2	86.27%	
32	1	88.24%	
33	2	92.16%	
34	0	92.16%	
35	1	94.12%	
36	0	94.12%	
37	0	94.12%	
38	2	98.04%	
More	1	100.00%	

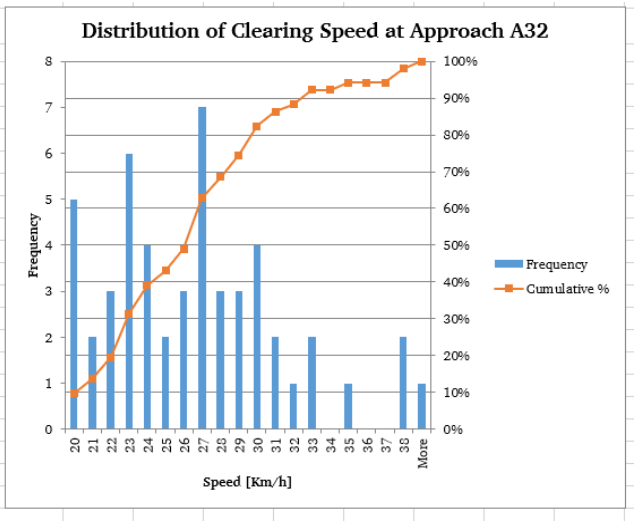

Figure B-3: Frequency Distribution of Clearing Speed at Approach A32

Note. Own Table and Graph

C Data for Saturation Flow Rate Model

This section presents raw data and calculated parameters of all elements for calculating the saturation flow rate model, includes:

- Discharge flow rate data of motorcycle flow at 2-second slices
- Motorcycle flow rate data
- Headway data of car flow
- Data of MCU model
- Data of vehicle type effect model
- Data of turning effect model in case 1
- Data of turning effect model in case 2

C.1 Discharge Flow Rate Data

The queued discharge flow rate of motorcycle flows in five distinct approaches is shown from Table C-1 to Table C-5. Data were only recorded from the start of green to the end of the saturated green time. All other flows passing the stop line before the start of green or after the end of the saturated green time were neglected.

Table C-1: Queue Discharged Rate at Approach A01

	Sample	Green Time Slices										
		0	2	4	6	8	10	12	14	16	18	20
Number of Motorcycles passing the Stop line in 2-second Slices	1	0	3	3	4	5	4	4	6	5		
	2	0	2	4	3	5	5	4	4	5		
	3	0	3	4	3	5	3	5	4	4	5	
	4	0	3	4	4	5	5	4	5	6	5	
	5	0	2	5	4	5	4	4	4	5	5	
	6	0	3	4	5	5	3	4	4			
	7	0	3	4	5	5	4	4	4			
	8	0	3	3	4	5	6	5	4	4	4	4
	9	0	3	5	3	5	4	4				
	10	0	3	5	4	6	4	5				
	11	0	3	3	6	6	6	5	4	4		
	12	0	2	5	4	7	6	4	5	5	5	
	13	0	2	3	4	5	5	5	7			
	14	0	1	4	5	5	4	5	4	4	4	4
	15	0	2	4	4	5	4	5	4	4	4	4
	16	0	3	4	4	6	6	5	4	5	5	
	17	0	2	5	5	5	5	4	5	4	4	
	18	0	3	5	4	6	4	4	6	5	5	4

Note. Own Table

Table C-2: Queue Discharged Rate at Approach A02

	Sample	Green Time Slices													
		0	2	4	6	8	10	12	14	16	18	20	22	24	26
Number of Motorcycles passing the Stop line in 2-second Slices	1	0	3	4	6	6	8	8	7	7	6				
	2	0	5	6	7	8	8	7	6	7	7	7	6		
	3	0	5	8	8	7	7	7	6	7	7	6			
	4	0	5	6	7	7	7	8	7	7	8	7	7	7	6
	5	0	5	6	7	8	7	9	7	7	7	7	8	8	7
	6	0	4	7	8	8	7	8	8	7	8	7	7	6	
	7	0	4	6	7	6	7	7	7	6	7				
	8	0	3	5	6	6	7	8	8	7	8	7	7	6	
	9	0	4	6	7	8	7	7	7	6	7				
	10	0	5	6	7	6	6	8	7	6					
	11	0	5	6	7	6	7	7	6	7	6	6	7	7	6
	12	0	4	5	6	7	7	7	6	6					
	13	0	4	5	7	7	7	8	8	6	8	7	7	6	7
	14	0	4	6	8	7	7	6	7	6	6	7	7	8	7
	15	0	4	5	7	8	7	7	6	7	6	7	7	6	6
	16	0	4	5	6	7	6	8	8	8	6				
	17	0	4	6	6	7	8	7	8	7	7	7	8	7	6

Note. Own Table

Table C-3: Queue Discharged Rate at Approach A03

	Sample	Green Time Slices																						
		0	2	4	6	8	10	12	14	16	18	20	22	24	26	28	30	32	34	36	38	40	42	44
Number of Motorcycles passing the Stop line in 2-second Slices	1	0	1	6	6	8	8	6	8	7														
	2	0	3	4	5	7	8	8	7	8	7	8	6											
	3	0	1	4	3	7	7	6	8	9	7	9												
	4	0	2	4	6	6	7	7	7	9	8	7	6	8										
	5	0	2	3	4	9	9	6	7	9	7	7												
	6	0	2	3	4	6	8	7	7	8	8	9												
	7	0	2	3	3	9	7	6	6	8	7	7	8											
	8	0	3	3	7	7	9	9	7	9	7	11	7	7	9	8								
	9	0	2	5	5	9	9	8	8	9	7	10	7	7	7									
	10	0	2	5	6	6	8	8	8	6	6	6	6											
	11	0	2	4	7	8	9	8	7	7	8	8	8											
	12	0	3	5	5	8	7	9	7	7	6	7	7	7	6	6	7	7	4	7	6	9	7	7
	13	0	3	5	5	7	7	6	8	6	6	6	9	6	7	8	7	7	7					
	14	0	4	6	6	7	5	6	8	8	7	7	8	9	8	8	6	7	8	6				
	15	0	3	6	4	7	7	8	7	6	6	6	6	7	6	8	9	6	8	7	7	8	8	6
	16	0	3	6	5	6	7	8	8	9	6	6	6	10	5	7	8	6	8	8	7	9	6	7
	17	0	2	4	5	6	8	7	7	9	6	5	7	6	6	9	8	8	5	8	7			
	18	0	3	5	6	7	9	7	9	9	7	6	7	6	7	8	8							
	19	0	1	4	5	6	5	8	8	8	6	7	7	7										
	20	0	2	4	5	7	8	8	8	7	7	9	8	6	7	7	7	6						

Note. Own Table

Table C—4: Queue Discharged rate at approach A04

	Sample	Green time slices																		
		0	**2**	**4**	**6**	**8**	**10**	**12**	**14**	**16**	**18**	**20**	**22**	**24**	**26**	**28**	**30**	**32**	**34**	**36**
Number of Motorcycles passing the Stop line in 2-second Slices	1	0	7	9	7	10	8	11	10	10	8	10	10	9	10					
	2	0	6	5	10	9	9	9	8	12	8									
	3	0	7	8	7	11	9	8	11	11	7	8	8	8	8	10				
	4	0	3	6	5	9	10	11	9	9	9	9	8	10	8					
	5	0	7	10	9	9	9	12	9	11	10	10	9	10	8	11	10	8	8	10
	6	0	4	6	7	9	10	9	10											
	7	0	6	6	8	10	10	10	9	8	9	8	8	9	12	9	9	8	9	
	8	0	6	4	8	9	11	11	10	7										
	9	0	5	5	8	10	9	9	10	10	10	8	10							
	10	0	6	10	7	10	10	9	9	10	9	8	9	10	8	9	7	8		
	11	0	4	4	6	9	10	10	10	8										
	12	0	6	7	7	9	9	10	11	10	8	9	9	9	8	10	9	10	10	8
	13	0	4	6	8	10	8	10	9	10										
	14	0	4	6	7	11	9	9	10	10	9	8	9	8	8	9				
	15	0	5	8	8	9	9	11	8	10	10	10	9	7	8	8				

Note. Own Table

Table C-5. Queue Discharged rate at approach A05

	Sample	Green time slices												
		0	**2**	**4**	**6**	**8**	**10**	**12**	**14**	**16**	**18**	**20**	**22**	**24**
Number of Motorcycles passing the Stop line in 2-second Slices	1	0	2	9	13	17	15	15	17	15	17	14	15	15
	2	0	5	9	11	17	15	17	14	14	14	14		
	3	0	6	15	11	15	16	15	14	15	14			
	4	0	3	12	12	16	17	15	18	15				
	5	0	7	7	13	19	21	11	19	14	15	17	14	14
	6	0	7	10	12	18	15	17	16	19				
	7	0	8	10	15	19	15	16	17	14				
	8	0	9	15	11	18	16	16	18	17	17	15	16	
	9	0	3	16	8	15	16	15	15					
	10	0	8	12	15	18	19	16	17	16	15	17	16	
	11	0	5	13	11	17	19	17	14	17	15			
	12	0	5	10	14	15	14	15	15	17	18	16	17	16
	13	0	7	15	11	18	14	15	16	16	14	16		
	14	0	5	3	13	18	17	15	15	17	14	15	16	

Note. Own Table

C.2 Motorcycle Saturation Flow Rate Data

Raw data and saturation flow rate calculation are depicted in section C.2.1, and regression results are presented ins section C.2.2.

C.2.1 Raw Data and Saturation Flow Rate Calculation

Raw data include the name of observed approach in column [1], the saturated green time, T in column [2]; the approach width, w in column [3]; and the number of motorcycles passing the stop line during the saturated green time, q_{MC} in column [4]. Then the saturation flow rate, S_{0w} in column [5] is calculated as:

$$[5] = \frac{[4]}{[2]} \cdot 3600 \tag{C-1}$$

Table C-6: Survey Results of Motorcycle Saturation Flow Rate

No	Approach	T [s]	w [m]	q_{MC} [m]	S_{0w} [mcu/h]	No	Approach	T [s]	w [m]	q_{MC} [m]	S_{0w} [mcu/h]
	[1]	[2]	[3]	[4]	[5]		[1]	[2]	[3]	[4]	[5]
1	A01	10	3	24	8,640	36	A02	10	4	36	12,960
2		10	3	24	8,640	37		10	4	37	13,320
3		8	3	19	8,550	38		10	4	38	13,680
4		8	3	19	8,550	39		10	4	33	11,880
5		6	3	14	8,400	40		10	4	36	12,960
6		10	3	24	8,640	41		10	4	32	11,520
7		5	3	12	8,640	42		10	4	33	11,880
8		9	3	23	9,200	43		10	4	33	11,880
9		9	3	22	8,800	44		10	4	33	11,880
10		8	3	20	9,000	45		10	4	35	12,600
11		6	3	14	8,400	46		10	4	33	11,880
12		9	3	21	8,400	47		10	4	35	12,600
13		8	3	20	9,000	48		10	4	37	13,320
14		10	3	25	9,000	49		10	4	37	13,320
15		12	3	29	8,700	50		12	4	42	12,600
16		12	3	29	8,700	51		16	4	54	12,150
17		11	3	26	8,509	52		14	4	47	12,086
18		16	3	36	8,100	53		20	4	71	12,780
19		11	3	26	8,509	54	A03	10	4	38	13,680
20		13	3	31	8,585	55		10	4	36	12,960
21		11	3	25	8,182	56		9	4	34	13,600
22		15	3	33	7,920	57		10	4	38	13,680
23		12	3	30	9,000	58		10	4	38	13,680
24		12	3	27	8,100	59		10	4	37	13,320
25		11	3	25	8,182	60		8	4	30	13,500
26		17	3	41	8,682	61		7	4	26	13,371
27		13	3	30	8,308	62		7	4	25	12,857
28		15	3	33	7,920	63		10	4	38	13,680
29		12	3	30	9,000	64		10	4	36	12,960
30		12	3	27	8,100	65		18	4	67	13,400
31		11	3	25	8,182	66		11	4	42	13,745
32		17	3	41	8,682	67		18	4	60	12,000
33	A02	10	4	35	12,600	68		16	4	60	13,500
34		10	4	35	12,600	69		24	4	85	12,750
35		10	4	34	12,240	70		18	4	65	13,000

No	Approach	T [s]	w [m]	q_{MC} [m]	S_{0w} [mcu/h]
	[1]	[2]	[3]	[4]	[5]
71	A03	23	4	88	13,774
72		14	4	50	12,857
73		14	4	53	13,629
74		13	4	48	13,292
75		18	4	57	11,400
76		17	4	64	13,553
77		13	4	48	13,292
78		18	4	66	13,200
79		10	4	38	13,680
80		8	4	31	13,950
81		25	4	88	12,672
82		15	4	55	13,200
83		18	4	68	13,600
84		19	4	66	12,505
85		12	4	45	13,500
86		14	4	51	13,114
87	A04	7	6	34	17,486
88		10	6	50	18,000
89		9	6	43	17,200
90		10	6	49	17,640
91		10	6	49	17,640
92		10	6	47	16,920
93		10	6	48	17,280
94		10	6	48	17,280
95		10	6	49	17,640
96		10	6	49	17,640
97		10	6	50	18,000
98		10	6	45	16,200
99		10	6	49	17,640
100		10	6	47	16,920
101		10	6	49	17,640
102		20	6	108	19,440
103		13	6	62	17,169
104		22	6	99	16,200
105		15	6	71	17,040

No	Approach	T [s]	w [m]	q_{MC} [m]	S_{0w} [mcu/h]
	[1]	[2]	[3]	[4]	[5]
106	A04	19	6	84	15,916
107		25	6	114	16,416
108		29	6	144	17,876
109		16	6	80	18,000
110		30	6	141	16,920
111		20	6	96	17,280
112		20	6	88	15,840
113		41	6	184	16,156
114		39	6	173	15,969
115		11	6	53	17,345
116		15	6	66	15,840
117		22	6	98	16,036
118	A05	10	9	78	28,080
119		10	9	79	28,440
120		10	9	81	29,160
121		10	9	80	28,800
122		10	9	78	28,080
123		10	9	81	29,160
124		10	9	84	30,240
125		10	9	78	28,080
126		10	9	72	25,920
127		10	9	78	28,080
128		10	9	79	28,440
129		10	9	80	28,800
130		10	9	81	29,160
131		10	9	82	29,520
132		10	9	83	29,880
133		10	9	83	29,880
134		10	9	81	29,160
135		10	9	78	28,080
136		10	9	79	28,440
137		10	9	77	27,720
138		10	9	82	29,520
139		10	9	81	29,160
140		7	9	55	28,286

No	Approach	T [s]	w [m]	q_{MC} [m]	S_{0w} [mcu/h]
	[1]	[2]	[3]	[4]	[5]
141		9	9	72	28,800
142		13	9	99	27,415
143		16	9	121	27,225
144		16	9	124	27,900
145		15	9	110	26,400
146		11	9	80	26,182
147		11	9	88	28,800
148		15	9	114	27,360
149		11	9	85	27,818
150		14	9	107	27,514
151		15	9	115	27,600
152		14	9	107	27,514
153		12	9	92	27,600
154		13	9	93	25,754
155		19	9	145	27,474
156	**A05**	16	9	122	27,450
157		14	9	108	27,771
158		16	9	123	27,675
159		15	9	113	27,120
160		16	9	121	27,225
161		16	9	119	26,775
162		16	9	122	27,450
163		11	9	86	28,145
164		13	9	100	27,692
165		15	9	115	27,600
166		13	9	99	27,415
167		10	9	76	27,360
168		16	9	121	27,225
169		12	9	92	27,600
170		11	9	84	27,491
171		10	4	35	12,600
172		10	4	35	12,600
173	**A06**	10	4	34	12,240
174		10	4	37	13,320
175		10	4	34	12,240

No	Approach	T [s]	w [m]	q_{MC} [m]	S_{0w} [mcu/h]
	[1]	[2]	[3]	[4]	[5]
176		10	4	37	13,320
177		10	4	33	11,880
178		10	4	36	12,960
179		10	4	33	11,880
180		10	4	35	12,600
181		10	4	35	12,600
182		10	4	38	13,680
183		10	4	36	12,960
184		10	4	38	13,680
185		10	4	36	12,960
186		10	4	36	12,960
187		10	4	34	12,240
188		10	4	35	12,600
189		10	4	33	11,880
190		10	4	35	12,600
191		10	4	37	13,320
192		10	4	35	12,600
193	**A06**	16	4	55	12,375
194		12	4	42	12,600
195		23	4	80	12,522
196		15	4	52	12,480
197		26	4	88	12,185
198		12	4	41	12,300
199		16	4	56	12,600
200		17	4	59	12,494
201		15	4	55	13,200
202		30	4	103	12,360
203		31	4	109	12,658
204		24	4	80	12,000
205		17	4	60	12,706
206		23	4	80	12,522
207		38	4	125	11,842
208		20	4	65	11,700
209		35	4	115	11,829
210		31	4	103	11,961

No	Approach	T [s]	w [m]	q_{MC} [m]	S_{0w} [mcu/h]
	[1]	[2]	[3]	[4]	[5]
221		14	8	96	24,686
222		15	8	102	24,480
223	**A07**	11	8	78	25,527
224		23	8	160	25,043
225		19	8	129	24,442
226		10	3.8	33	11,880
227		10	3.8	34	12,240
228		10	3.8	32	11,520
229		10	3.8	33	11,880
230		10	3.8	34	12,240
231		7	3.8	23	11,829
232		7	3.8	24	12,343
233		10	3.8	35	12,600
234	**A08**	18	3.8	61	12,200
235		22	3.8	73	11,945
236		32	3.8	105	11,813
237		24	3.8	79	11,850
238		14	3.8	46	11,829
239		18	3.8	55	11,000
240		15	3.8	50	12,000
241		16	3.8	53	11,925
242		15	3.8	48	11,520

Note. Own Table

C.2.2 Regression Results

The regression model shows the relationship between the homogeneous saturation flow rate and the approach width, retrieved from Table C-1.

$$\begin{cases} S_{0w} = 3179 \times w \; if \; t_G < 16 \; s \\ S_{0w} = 3058 \times w \; if \; t_G \geq 16 \; s \end{cases} \quad \text{(C-2)}$$

Regression results in case of $t_G < 16\ s$

Regression Statistics	
Multiple R	0.999498
R Square	0.998995
Adjusted R Square	0.990067
Standard Error	584.6067
Observations	113

ANOVA					
	df	SS	MS	F	Significance F
Regression	1	3.81E+10	3.81E+10	111379.8	1.9E-168
Residual	112	38277684	341765		
Total	113	3.81E+10			

	Coefficients	Standard Error	t Stat	P-value	Lower 95%	Upper 95%	Lower 95.0%	Upper 95.0%
Intercept	-	-	-	-	-	-	-	-
X	3178.945	9.525326	333.7361	9.7E-170	3160.072	3197.818	3160.072	3197.818

Note. Own Tables

Regression results in case of $t_G \geq 16\ s$

Regression Statistics	
Multiple R	0.999
R Square	0.999
Adjusted R Square	0.992
Standard Error	644.705
Observations	144.000

ANOVA					
	df	SS	MS	F	Significance F
Regression	1	4.474E+10	4.47E+10	107642.3	0.000
Residual	143	59437244	415645.1		
Total	144	4.48E+10			

	Coefficients	Standard Error	t Stat	P-value	Lower 95%	Upper 95%	Lower 95.0%	Upper 95.0%
Intercept	-	-	-	-	-	-	-	-
X	3057.56	9.32	328.09	0.00	3039.14	3075.99	3039.14	3075.99

Note. Own Tables

C.3 Headway Data of Car Flow

The headway of car flow at four distinct approaches is illustrated from Table C-7 to Table C-10. The headway is recorded from consecutive cars in the queue. The average headway of 2.3 s is also retrieved from those tables. The headway characteristics of car flows were also described in Figure 5- 11 and Figure 5-12, Section 5.3.3.

Table C-7: Survey Results of Motorcycle Saturation Flow Rate at Approach A09

Approach A09	Vehicle Position / Samples	1	2	3	4	5	6	7	8	9	10	11	12	13	14	15
Headway (s)	1	2.04	3.86	3.94	3.11	2.13	2.88									
	2	2.72	4.00	2.12	2.95	2.65										
	3	2.23	5.52	3.82	3.31	2.23	1.95									
	4	5.66	3.32	2.55	2.42	2.50	2.46	1.91								
	5	2.48	4.14	2.49	3.36	2.76	2.65	0.00								
	6	0.08	4.05	6.29	1.66	2.45	2.90	1.64								
	7	1.16	4.34	3.83	2.58	3.09	2.25	0.00								
	8	3.89	6.89	2.94	3.36	2.10	2.61	0.00								
	9	1.86	2.65	3.33	1.84	2.35	2.76	1.92								
	10	1.88	3.32	3.59	2.47	2.68	1.70	1.72	2.53	1.72	2.26					
	11	0.73	5.33	2.69	2.74	2.00	2.72	2.16								
	12	1.56	2.88	2.82	2.26	2.61	2.71	2.80	2.22							
	13	2.40	3.82	3.30	3.17	2.64	2.95	3.13	2.20	2.47	2.21					
	14	3.40	2.85	2.22	2.35	2.43	2.59	2.41	2.46	2.36	1.91	2.20				
	15	1.25	4.01	3.68	3.12	2.30										
	16	2.08	3.12	3.77	4.38	2.61	2.43									
	Average Headways	3.71	4.01	3.34	2.82	2.47	2.54	2.21	2.35	2.18	2.13	2.20				

Note. Own Table

Table C-8: Survey Results of Motorcycle Saturation Flow rate at Approach A10

Approach A10	Vehicle Position / Samples	1	2	3	4	5	6	7	8	9	10	11	12	13	14	15
Headway (s)	1	1.92	5.40	1.88	2.51	3.65	2.34	2.19	1.89	2.06	2.30					
	2	3.13	4.78	2.82	2.88	1.71										
	3	1.60	3.13	2.58	2.48	2.44	1.50	2.02								
	4	1.07	5.32	3.66	2.22	1.86										
	5	1.91	2.83	3.41	2.27	1.89	2.56	2.33	3.53							
	6	3.09	3.96	1.94	3.01	2.25	1.88	1.70	1.90							
	7	2.20	3.39	2.73	2.32	2.46	3.64	1.74	2.20							
	8	2.13	3.27	2.32	3.76	2.09	1.82	2.36	2.38	2.77	1.78					
	9	3.25	3.88	3.35	3.05	2.30	2.79	2.02	2.32							
	10	1.96	4.30	2.71	1.98	2.51	2.01	3.33	1.82	1.26						
	11	1.80	2.48	2.02	2.82	2.47	1.83	3.87	1.84							
	12	2.08	4.05	2.25	3.86	2.14	2.14									
	13	2.26	4.36	3.90	2.51	2.09	3.04	2.18								
	14	2.28	2.86	3.92	3.54	2.15	1.77	1.96	1.89	2.70						
	15	4.45	2.41	2.43	1.73	2.18	1.95									
	16	1.58	5.49	3.11	2.81	2.64	1.89	1.79	2.61							
	17	2.95	3.21	3.84	2.17	2.05										
	18	4.94	3.69	3.78	2.86	3.15	1.63	1.61								
	19	2.19	2.48	3.30	2.61	2.52	2.27	1.70								
	20	1.76	5.53	2.42	2.67	2.25	2.54	1.89	2.00							
	21	3.50	2.92	1.90	2.12	2.91	2.20									
	Average Headway	2.48	3.80	2.87	2.67	2.37	2.21	2.18	2.22	2.20	2.04					

Note. Own Table

Table C-9: Survey Results of Motorcycle Saturation Flow Rate at Approach A11

Approach A11	Vehicle Position / Samples	1	2	3	4	5	6	7	8	9	10	11	12	13	14	15
Headway (s)	1	1.82	3.62	3.54	2.57	2.12	3.00	1.97	1.94	1.67						
	2	2.15	2.74	2.53	3.15	1.83	3.32	2.02								
	3	1.87	5.50	2.52	2.30	2.56	3.01	1.79								
	4	3.81	5.28	2.05	2.18	2.64	2.56	2.46	2.04	1.95						
	5	2.79	3.30	4.47	1.84	2.77	2.68	2.21	2.47	0.00						
	6	2.69	1.83	2.36	2.22	2.51	1.91	2.13	3.47	0.00						
	7	2.58	3.22	2.31	2.80	2.76	2.93	1.63	2.12	1.86	1.93					
	8	2.64	5.36	2.96	2.17	3.37	1.99	2.12	1.48							
	9	4.46	3.56	3.32	2.06	2.60	2.70									
	10	2.15	3.50	2.33	2.56	1.65	1.65	3.42	2.35	2.47	1.92					
	11	2.41	2.56	3.66	2.66	1.95	3.28									
	12	1.86	4.01	2.89	3.07	2.83	1.65									
	13	1.47	2.93	2.13	3.74	1.97	1.90	2.13	2.99	2.00	2.28	1.64				
	14	1.76	3.33	2.71	2.33	2.65	2.85	2.12	1.76	1.91						
	15	1.06	5.18	3.73	3.08	2.52	2.02	2.08	2.14	2.68	2.15	2.09	1.96			
	16	0.89	3.16	2.19	2.28	2.79	2.42	1.98	1.96							
	17	1.00	2.92	3.03	1.97	2.42	2.51	2.21	3.17							
	18	1.05	3.46	3.13	1.75	2.34	4.32	1.73	2.23							
	Average Headway	2.14	3.64	2.88	2.48	2.46	2.59	2.13	2.32	1.61	2.07					

Note. Own Table

Table C-10. Survey Results of Motorcycle Saturation Flow Rate at Approach A12

Approach A12	Vehicle Position / Samples	1	2	3	4	5	6	7	8	9	10	11	12	13	14	15
Headway (s)	1	2.48	4.27	3.38	2.92	2.00	2.22	2.28	1.53	2.25	2.05	2.18	2.13	1.83	2.59	2.49
	2	2.50	2.95	2.74	3.40	2.13	2.22	2.28	2.52							
	3	1.36	2.31	2.56	2.65	2.52	2.11	2.03	2.40							
	4	1.64	4.80	2.97	3.00	2.27	2.00	2.18	2.52	2.15	2.14	2.18	2.43	2.69		
	5	1.10	6.00	3.82	2.22	2.79	2.73	2.06	2.92							
	6	2.16	3.78	3.08	4.00	2.06	2.86									
	7	4.02	3.16	2.84	2.96	1.85	2.04	2.78								
	8	1.92	3.82	2.04	3.20	1.94	2.52	2.12								
	9	1.14	2.88	3.12	2.78	2.00	2.08	2.14								
	10	2.12	3.78	3.22	3.94	2.08	2.84	2.06								
	Average Headway	2.04	3.78	2.98	3.11	2.16	2.36	2.21	2.38	2.20	2.09	2.18	2.28	2.26	2.59	2.49

Note. Own Table

C.4 Data of Motorcycle Equivalent Unit Model

Motorcycle equivalent unit model and the vehicle type effect model use the same data set which is collected from six different approaches and is presented Table C-11 to Table C-13 per share of four-wheeled vehicles in the traffic flow. Section C.4.1 shows raw data and the calculated parameters, then Section C.4.2 gives the regression results of MCU model.

C.4.1 Raw Data and Calculation Parameters

Raw data include approach name, saturated green time, the number of vehicles passing the stop line during the observed time (motorcycles, cars, middle vehicles and heavy vehicles) are illustrated from column [1] to column [7].

The calculated parameters include the number of vehicles passing 1-meter width of the stop line during the observed green time are given from column [8] to column [11].

$$[8]=\frac{[4]}{[2]};[9]=\frac{[5]}{[2]};[10]=\frac{[6]}{[2]};[11]=\frac{[7]}{[2]} \quad \text{(C-3)}$$

Table C-11: Through Discharge Flow Rate of Mixed Flow during Saturated Green Time (% Four-wheeled Vehicle Share: 0%-5%)

% four-wheeled vehicle share: 0%-5%											
No.	**Approach**	**Width**	**Saturated Green Time**	**Number of Vehicles passing the Stop line**				**Number of Vehicles passing a 1 m wide Stop line**			
		w	**T**	**MC**	**C**	**MV**	**HV**	**MC**	**C**	**MV**	**HV**
	[-]	**[m]**	**[s]**	**[veh]**	**[veh]**	**[veh]**	**[veh]**	**[veh/m]**	**[veh/m]**	**[veh/m]**	**[veh/m]**
	[1]	**[2]**	**[3]**	**[4]**	**[5]**	**[6]**	**[7]**	**[8]**	**[9]**	**[10]**	**[11]**
1	A14	7.9	13	82	1	0	0	10.35	0.13	0.00	0.00
2		7.9	18	108	1	1	0	13.63	0.13	0.13	0.00
3		7.9	14	81	1	1	0	10.23	0.13	0.13	0.00
4		7.9	18	104	3	0	0	13.21	0.38	0.00	0.00
5		7.9	17	98	3	0	0	12.36	0.38	0.00	0.00
6		7.9	15	84	3	0	0	10.66	0.38	0.00	0.00
7		7.9	19	106	4	0	0	13.37	0.51	0.00	0.00
8		7.9	10	56	2	0	0	7.11	0.25	0.00	0.00
9		7.9	15	75	1	1	1	9.44	0.13	0.13	0.13
10		7.9	23	127	5	0	0	16.07	0.63	0.00	0.00
11		7.9	9	49	2	0	0	6.26	0.25	0.00	0.00
12		7.9	17	90	3	1	0	11.39	0.38	0.13	0.00
13		7.9	19	100	5	0	0	12.67	0.63	0.00	0.00
14	A15	3.5	25	61	0	0	1	17.56	0.00	0.00	0.29
15		3.5	18	48	1	0	0	13.73	0.29	0.00	0.00
16		3.5	16	40	0	1	0	11.40	0.00	0.29	0.00
17		3.5	15	39	1	0	0	11.18	0.29	0.00	0.00
18		3.5	14	29	0	0	1	8.21	0.00	0.00	0.29
19		3.5	22	52	1	1	0	14.93	0.29	0.29	0.00
20		3.5	13	26	0	0	1	7.36	0.00	0.00	0.29
21		3.5	11	25	0	1	0	7.15	0.00	0.29	0.00
22	A16	3.8	16	46	1	0	0	12.15	0.26	0.00	0.00
23		3.8	15	43	1	0	0	11.30	0.26	0.00	0.00
24		3.8	13	36	1	0	0	9.60	0.26	0.00	0.00
25		3.8	11	30	1	0	0	7.90	0.26	0.00	0.00
26		3.8	10	27	1	0	0	7.05	0.26	0.00	0.00

27		3.8	20	54	2	0	0	14.11	0.53	0.00	0.00
28		3.8	9	24	1	0	0	6.20	0.26	0.00	0.00
29		3.8	25	64	3	0	0	16.91	0.79	0.00	0.00
30		6.5	16	83	1	0	0	12.75	0.15	0.00	0.00
31		6.5	13	64	0	1	0	9.87	0.00	0.15	0.00
32		6.5	12	61	1	0	0	9.35	0.15	0.00	0.00
33		6.5	10	50	1	0	0	7.65	0.15	0.00	0.00
34		6.5	11	55	1	0	0	8.50	0.15	0.00	0.00
35		6.5	11	53	0	1	0	8.17	0.00	0.15	0.00
36		6.5	10	50	1	0	0	7.65	0.15	0.00	0.00
37		6.5	9	44	1	0	0	6.80	0.15	0.00	0.00
38		6.5	9	44	1	0	0	6.80	0.15	0.00	0.00
39		6.5	8	31	0	0	1	4.81	0.00	0.00	0.15
40	A17	6.5	7	31	0	1	0	4.77	0.00	0.15	0.00
41		6.5	6	28	1	0	0	4.25	0.15	0.00	0.00
42		6.5	6	25	0	1	0	3.92	0.00	0.15	0.00
43		6.5	12	55	2	0	0	8.51	0.31	0.00	0.00
44		6.5	12	53	1	1	0	8.17	0.15	0.15	0.00
45		6.5	12	53	1	1	0	8.17	0.15	0.15	0.00
46		6.5	10	44	2	0	0	6.81	0.31	0.00	0.00
47		6.5	10	44	2	0	0	6.81	0.31	0.00	0.00
48		6.5	10	44	2	0	0	6.81	0.31	0.00	0.00
49		6.5	10	44	2	0	0	6.81	0.31	0.00	0.00
50		6.5	10	44	2	0	0	6.81	0.31	0.00	0.00
51		6.5	15	64	2	1	0	9.87	0.31	0.15	0.00
52		8	17	110	1	0	0	13.76	0.13	0.00	0.00
53		8	17	110	1	0	0	13.76	0.13	0.00	0.00
54		8	15	97	1	0	0	12.06	0.13	0.00	0.00
55		8	26	166	2	0	0	20.73	0.25	0.00	0.00
56		8	20	125	2	0	0	15.63	0.25	0.00	0.00
57		8	28	174	3	0	0	21.74	0.38	0.00	0.00
58		8	25	154	3	0	0	19.19	0.38	0.00	0.00
59		8	22	133	3	0	0	16.64	0.38	0.00	0.00
60		8	15	91	2	0	0	11.38	0.25	0.00	0.00
61	A18	8	13	77	2	0	0	9.68	0.25	0.00	0.00
62		8	25	148	4	0	0	18.50	0.50	0.00	0.00
63		8	25	143	5	0	0	17.81	0.63	0.00	0.00
64		8	23	129	5	0	0	16.11	0.63	0.00	0.00
65		8	21	121	4	0	0	15.10	0.50	0.00	0.00
66		8	19	107	4	0	0	13.40	0.50	0.00	0.00
67		8	18	100	4	0	0	12.55	0.50	0.00	0.00
68		8	18	100	4	0	0	12.55	0.50	0.00	0.00
69		8	23	129	5	0	0	16.11	0.63	0.00	0.00
70		8	9	50	2	0	0	6.28	0.25	0.00	0.00

Note. Own Table

Table C-12: Through Discharge Flow Rate of Mixed Flow during Saturated Green Time (Four-wheeled Vehicle Share: 5%-10%)

% four-wheeled vehicle share: 5%-10%											
No.	**Approach**	**Width**	**Saturated Green Time**	**Number of Vehicles passing the Stop line**				**Number of Vehicles passing a 1 m wide Stop line**			
		w	**T**	**MC**	**C**	**MV**	**HV**	**MC**	**C**	**MV**	**HV**
	[-]	**[m]**	**[s]**	**[veh]**	**[veh]**	**[veh]**	**[veh]**	**[veh/m]**	**[veh/m]**	**[veh/m]**	**[veh/m]**
	[1]	**[2]**	**[3]**	**[4]**	**[5]**	**[6]**	**[7]**	**[8]**	**[9]**	**[10]**	**[11]**
1		7.9	11	54	3	0	0	6.84	0.38	0.00	0.00
2		7.9	14	69	4	0	0	8.73	0.51	0.00	0.00
3		7.9	11	47	2	0	1	5.95	0.25	0.00	0.13
4		7.9	11	48	2	0	1	6.08	0.25	0.00	0.13
5		7.9	18	81	5	0	1	10.25	0.63	0.00	0.13
6		7.9	11	50	4	0	0	6.33	0.51	0.00	0.00
7		7.9	12	53	3	1	0	6.71	0.38	0.13	0.00
8		7.9	15	65	4	1	0	8.23	0.51	0.13	0.00
9	A14	7.9	20	94	7	0	0	11.90	0.89	0.00	0.00
10		7.9	19	88	7	0	0	11.14	0.89	0.00	0.00
11		7.9	9	36	2	0	1	4.56	0.25	0.00	0.13
12		7.9	13	56	4	1	0	7.09	0.51	0.13	0.00
13		7.9	12	52	5	0	0	6.58	0.63	0.00	0.00
14		7.9	16	66	5	1	0	8.35	0.63	0.13	0.00
15		7.9	16	65	5	0	1	8.23	0.63	0.00	0.13
16		7.9	18	73	5	2	0	9.24	0.63	0.25	0.00
17		7.9	13	47	3	1	1	5.95	0.38	0.13	0.13
18		3.5	11	25	2	0	0	7.14	0.43	0.00	0.00
19		3.5	8	16	0	1	0	4.57	0.00	0.29	0.00
20	A15	3.5	16	31	1	1	0	8.86	0.29	0.29	0.00
21		3.5	16	27	2	1	0	7.71	0.57	0.29	0.00
22		3.5	14	29	2	0	0	8.16	0.53	0.00	0.00
23		6.5	9	36	1	1	0	5.54	0.15	0.15	0.00
24		6.5	8	32	2	0	0	4.92	0.31	0.00	0.00
25	A17	6.5	11	41	2	1	0	6.31	0.31	0.15	0.00
26		6.5	15	52	3	1	0	8.00	0.46	0.15	0.00
27		6.5	6	22	2	0	0	3.35	0.31	0.00	0.00
28		8	25	140	5	0	0	17.50	0.63	0.00	0.00
29		8	23	123	5	0	0	15.38	0.63	0.00	0.00
30		8	21	111	4	0	0	13.88	0.50	0.00	0.00
31	A18	8	19	110	4	0	0	13.75	0.50	0.00	0.00
32		8	18	103	4	0	0	12.88	0.50	0.00	0.00
33		8	18	102	4	0	0	12.75	0.50	0.00	0.00
34		8	23	124	5	0	0	15.50	0.63	0.00	0.00
35		8	9	52	2	0	0	6.53	0.25	0.00	0.00
36		11.5	12	87	5	0	0	7.57	0.43	0.00	0.00
37		11.5	14	95	5	1	0	8.26	0.43	0.09	0.00
38		11.5	18	120	8	0	0	10.43	0.70	0.00	0.00
39		11.5	13	88	6	0	0	7.65	0.52	0.00	0.00
40		11.5	18	125	7	1	0	10.89	0.61	0.09	0.00
41		11.5	21	139	11	0	0	12.09	0.96	0.00	0.00
42	A19	11.5	14	86	8	0	0	7.48	0.70	0.00	0.00
43		11.5	15	82	6	1	1	7.13	0.52	0.09	0.09
44		11.5	17	98	9	1	0	8.52	0.78	0.09	0.00
45		11.5	19	113	12	0	0	9.83	1.04	0.00	0.00
46		11.5	19	109	12	0	0	9.48	1.04	0.00	0.00
47		11.5	9	54	6	0	0	4.70	0.52	0.00	0.00
48		11.5	13	87	6	1	0	7.55	0.51	0.10	0.00

Note. Own Table

Table C-13: Through Discharge Flow Rate of Mixed Flow during Saturated Green Time (Four-wheeled Vehicle Share: 10%-15%)

% four-wheeled vehicle share: 10%-15%											
No.	**Approach**	**Width**	**Saturated Green Time**	**Number of Vehicles passing the Stop line**				**Number of Vehicles passing a 1 m wide Stop line**			
		W	**T**	**MC**	**C**	**MV**	**HV**	**MC**	**C**	**MV**	**HV**
	[-]	**[m]**	**[s]**	**[veh]**	**[veh]**	**[veh]**	**[veh]**	**[veh/m]**	**[veh/m]**	**[veh/m]**	**[veh/m]**
	[1]	**[2]**	**[3]**	**[4]**	**[5]**	**[6]**	**[7]**	**[8]**	**[9]**	**[10]**	**[11]**
1	A14	7.9	9	26	2	1	1	3.25	0.25	0.13	0.13
2	A15	3.5	11	15	1	1	0	4.26	0.29	0.29	0.00
3		3.5	20	19	1	0	2	5.49	0.29	0.00	0.57
4	A19	11.5	19	98	9	0	2	8.52	0.78	0.00	0.17
5		11.5	18	94	12	0	0	8.17	1.04	0.00	0.00
6		11.5	12	70	8	0	0	6.07	0.70	0.00	0.00
7		11.5	16	80	12	0	0	6.96	1.04	0.00	0.00
8		11.5	11	47	9	0	0	4.13	0.78	0.00	0.00
9		11.5	15	68	8	2	0	5.87	0.70	0.17	0.00
10		11.5	18	81	13	0	1	7.04	1.13	0.00	0.09
11		11.5	13	60	10	0	0	5.22	0.87	0.00	0.00
12		11.5	11	48	6	2	0	4.17	0.52	0.17	0.00
13		11.5	17	77	12	0	1	6.70	1.04	0.00	0.09
14		11.5	13	59	10	0	0	5.13	0.87	0.00	0.00
15		11.5	12	53	8	0	1	4.61	0.70	0.00	0.09
16		11.5	14	64	10	1	0	5.57	0.87	0.09	0.00
17		11.5	13	51	7	1	1	4.43	0.61	0.09	0.09
18		11.5	17	65	9	1	2	5.65	0.78	0.09	0.17
19	A20	9.8	10	49	6	0	0	5.01	0.61	0.00	0.00
20		9.8	13	60	7	0	0	6.12	0.71	0.00	0.00
21		9.8	7	30	3	1	0	3.06	0.31	0.10	0.00
22		9.8	8	37	5	0	0	3.78	0.51	0.00	0.00
23		9.8	13	59	8	0	0	6.02	0.82	0.00	0.00
24		9.8	11	49	7	0	0	5.00	0.71	0.00	0.00
25		9.8	13	54	9	0	0	5.51	0.92	0.00	0.00
26		9.8	9	32	5	0	1	3.27	0.51	0.00	0.10
27		9.8	14	50	10	0	0	5.14	1.02	0.00	0.00

Note. Own Table

C.4.2 Regression Results

The Case: % four-wheeled vehicle share: 0%-5%

The MCU of cars, middle vehicles, and heavy vehicles are calculated at 5.5, 7.77, 12.75 respectively.

Regression Statistics	
Multiple R	0.996
R Square	0.992
Adjusted R Square	0.992
Standard Error	0.414
Observations	70

ANOVA

	df	SS	MS	F	Significance F
Regression	4	1431.984	357.996	2085.044	0.000
Residual	65	11.160	0.172		
Total	69	1443.145			

	Coefficients	Standard Error	t Stat	P-value	Lower 95%	Upper 95%	Lower 95.0%	Upper 95.0%
Intercept	0.209	0.156	1.341	0.185	-0.102	0.519	-0.102	0.519
MC	1.003	0.015	67.067	0.000	0.974	1.033	0.974	1.033
C	5.499	0.386	14.259	0.000	4.729	6.269	4.729	6.269
MV	7.794	0.753	10.352	0.000	6.290	9.297	6.290	9.297
HV	12.788	0.909	14.072	0.000	10.973	14.602	10.973	14.602

Note. Own Tables

The Case: % four-wheeled vehicle share: 5%-10%

The MCU of cars, middle vehicles, and heavy vehicles are calculated at 6.13, 9.18, 13 respectively.

Regression Statistics	
Multiple R	0.996
R Square	0.992
Adjusted R Square	0.991
Standard Error	0.352
Observations	48

ANOVA

	df	SS	MS	F	Significance F
Regression	4	634.574	158.643	1281.527	0.000
Residual	43	5.323	0.124		
Total	47	639.897			

	Coefficients	Standard Error	t Stat	P-value	Lower 95%	Upper 95%	Lower 95.0%	Upper 95.0%
Intercept	0.111	0.202	0.548	0.586	-0.296	0.517	-0.296	0.517
MC	0.992	0.020	50.520	0.000	0.952	1.031	0.952	1.031
C	6.077	0.288	21.075	0.000	5.496	6.659	5.496	6.659
MV	9.101	0.645	14.114	0.000	7.801	10.401	7.801	10.401
HV	12.887	1.257	10.250	0.000	10.352	15.423	10.352	15.423

Note. Own Tables

The Case: % four-wheeled vehicle share: 10%-15%

The MCU values for cars, middle vehicles, and heavy vehicles are calculated at 6.29, 11.51, 16.17 respectively.

Regression Statistics	
Multiple R	0.995
R Square	0.990
Adjusted R Square	0.988
Standard Error	0.304
Observations	27

ANOVA

	df	*SS*	*MS*	*F*	*Significance F*
Regression	4	204.289	51.072	551.259	0.000
Residual	22	2.038	0.093		
Total	26	206.327			

	Coefficients	*Standard Error*	*t Stat*	*P-value*	*Lower 95%*	*Upper 95%*	*Lower 95.0%*	*Upper 95.0%*
Intercept	-0.134	0.291	-0.459	0.650	-0.736	0.469	-0.736	0.469
MC	1.017	0.068	14.900	0.000	0.875	1.158	0.875	1.158
C	6.397	0.464	13.799	0.000	5.436	7.358	5.436	7.358
MV	11.702	1.019	11.482	0.000	9.588	13.816	9.588	13.816
HV	16.440	0.652	25.205	0.000	15.088	17.793	15.088	17.793

Note. Own Tables

C.5 Data of Vehicle Type Effect Model

The vehicle type effect model used the results from motorcycle equivalent unit model. The correlation of normalised saturation flow rate between observed and modelled results are illustrated in Table C-14 to Table C-16. Data from columns are explained below:

Data from [1] to [6] are retrieved from column [1], [8], [9], [10], [11] (Table C-11 to table C-13 respectively).

$$[7] = \frac{[3]+[4]+[5]+[6]}{[3]+MCU_{C}\cdot[4]+MCU_{MV}\cdot[5]+MCU_{HV}\cdot[6]}$$

$$[8] = \frac{[3]+[4]+[5]+[6]}{[2]}\cdot 3600$$

$$[9] = S_0 \cdot [7] = 3,058 \cdot [7]$$

Table C-14: Correlation between Observed and Modelled Normalised Saturation Flow Rate (% Four-wheeled Vehicle Share: 0%-5%)

% Four-wheeled Vehicle Share: 0%-5%									
No.	Appr.	ΔT	MC	C	MV	HV	f_{veh}	Normalised SFR	
								Observation	Model
		[s]	[veh]	[veh]	[veh]	[veh]	[veh/h]	[veh/(h*m)]	[veh/(h*m)]
	[1]	[2]	[3]	[4]	[5]	[6]	[7]	[8]	[9]
1	A14	13	10.35	0.13	0.00	0.00	0.95	2,902	2,900
2		18	13.63	0.13	0.13	0.00	0.91	2,776	2,773
3		14	10.23	0.13	0.13	0.00	0.88	2,695	2,692
4		18	13.21	0.38	0.00	0.00	0.89	2,718	2,716
5		17	12.36	0.38	0.00	0.00	0.88	2,698	2,696
6		15	10.66	0.38	0.00	0.00	0.87	2,650	2,648
7		19	13.37	0.51	0.00	0.00	0.86	2,628	2,627
8		10	7.11	0.25	0.00	0.00	0.87	2,650	2,648
9		15	9.44	0.13	0.13	0.13	0.77	2,357	2,358
10		23	16.07	0.63	0.00	0.00	0.85	2,614	2,613
11		9	6.26	0.25	0.00	0.00	0.85	2,604	2,603
12		17	11.39	0.38	0.13	0.00	0.82	2,519	2,515
13		19	12.67	0.63	0.00	0.00	0.82	2,520	2,519
14	A15	25	17.56	0.00	0.00	0.29	0.84	2,569	2,574
15		18	13.73	0.29	0.00	0.00	0.92	2,803	2,801
16		16	11.40	0.00	0.29	0.00	0.86	2,629	2,624
17		15	11.18	0.29	0.00	0.00	0.90	2,751	2,750
18		14	8.21	0.00	0.00	0.29	0.72	2,184	2,192
19		22	14.93	0.29	0.29	0.00	0.83	2,536	2,532
20		13	7.36	0.00	0.00	0.29	0.69	2,116	2,125
21		11	7.15	0.00	0.29	0.00	0.79	2,434	2,427
22	A16	16	12.15	0.26	0.00	0.00	0.91	2,794	2,792
23		15	11.30	0.26	0.00	0.00	0.91	2,776	2,774
24		13	9.60	0.26	0.00	0.00	0.89	2,732	2,730
25		11	7.90	0.26	0.00	0.00	0.87	2,672	2,671
26		10	7.05	0.26	0.00	0.00	0.86	2,634	2,632
27		20	14.11	0.53	0.00	0.00	0.86	2,634	2,632
28		9	6.20	0.26	0.00	0.00	0.85	2,586	2,585

29		25	16.91	0.79	0.00	0.00	0.83	2,548	2,547
30		16	12.75	0.15	0.00	0.00	0.95	2,904	2,902
31		13	9.87	0.00	0.15	0.00	0.91	2,775	2,770
32		12	9.35	0.15	0.00	0.00	0.93	2,852	2,850
33		10	7.65	0.15	0.00	0.00	0.92	2,811	2,809
34		11	8.50	0.15	0.00	0.00	0.93	2,833	2,832
35		11	8.17	0.00	0.15	0.00	0.89	2,723	2,718
36		10	7.65	0.15	0.00	0.00	0.92	2,811	2,809
37		9	6.80	0.15	0.00	0.00	0.91	2,783	2,781
38		9	6.80	0.15	0.00	0.00	0.91	2,783	2,781
39		8	4.81	0.00	0.00	0.15	0.73	2,234	2,242
40	A17	7	4.77	0.00	0.15	0.00	0.83	2,530	2,524
41		6	4.25	0.15	0.00	0.00	0.86	2,645	2,643
42		6	3.92	0.00	0.15	0.00	0.80	2,442	2,435
43		12	8.51	0.31	0.00	0.00	0.86	2,645	2,643
44		12	8.17	0.15	0.15	0.00	0.83	2,543	2,539
45		12	8.17	0.15	0.15	0.00	0.83	2,543	2,539
46		10	6.81	0.31	0.00	0.00	0.84	2,562	2,560
47		10	6.81	0.31	0.00	0.00	0.84	2,562	2,560
48		10	6.81	0.31	0.00	0.00	0.84	2,562	2,560
49		10	6.81	0.31	0.00	0.00	0.84	2,562	2,560
50		10	6.81	0.31	0.00	0.00	0.84	2,562	2,560
51		15	9.87	0.31	0.15	0.00	0.81	2,480	2,477
52		17	13.76	0.13	0.00	0.00	0.96	2,941	2,939
53		17	13.76	0.13	0.00	0.00	0.96	2,941	2,939
54		15	12.06	0.13	0.00	0.00	0.96	2,925	2,923
55		26	20.73	0.25	0.00	0.00	0.95	2,904	2,902
56		20	15.63	0.25	0.00	0.00	0.93	2,858	2,856
57		28	21.74	0.38	0.00	0.00	0.93	2,843	2,841
58		25	19.19	0.38	0.00	0.00	0.92	2,817	2,815
59		22	16.64	0.38	0.00	0.00	0.91	2,784	2,782
60		15	11.38	0.25	0.00	0.00	0.91	2,790	2,788
61	A18	13	9.68	0.25	0.00	0.00	0.90	2,748	2,747
62		25	18.50	0.50	0.00	0.00	0.89	2,736	2,734
63		25	17.81	0.63	0.00	0.00	0.87	2,655	2,653
64		23	16.11	0.63	0.00	0.00	0.86	2,620	2,618
65		21	15.10	0.50	0.00	0.00	0.87	2,674	2,673
66		19	13.40	0.50	0.00	0.00	0.86	2,634	2,632
67		18	12.55	0.50	0.00	0.00	0.85	2,610	2,608
68		18	12.55	0.50	0.00	0.00	0.85	2,610	2,608
69		23	16.11	0.63	0.00	0.00	0.86	2,620	2,618
70		9	6.28	0.25	0.00	0.00	0.85	2,610	2,608

Note. Own Table

Table C-15. Correlation between Observed and Modelled Normalised Saturation Flow Rate (% Four-wheeled Vehicle Share: 5%-10%)

% Four-Wheeled Vehicle Share: 5%-10%									
No.	Appr.	ΔT	MC	C	MV	HV	f_{veh}	Normalised SFR	
								Observation	Model
		[s]	[veh]	[veh]	[veh]	[veh]	[veh/h]	[veh/(h*m)]	[veh/(h*m)]
	[1]	[2]	[3]	[4]	[5]	[6]	[7]	[8]	[9]
1	A14	11	6.84	0.38	0.00	0.00	0.79	2,361	2,408
2		14	8.73	0.51	0.00	0.00	0.78	2,376	2,387
3		11	5.95	0.25	0.00	0.13	0.69	2,071	2,116
4		11	6.08	0.25	0.00	0.13	0.70	2,113	2,129
5		18	10.25	0.63	0.00	0.13	0.70	2,203	2,134
6		11	6.33	0.51	0.00	0.00	0.72	2,237	2,216
7		12	6.71	0.38	0.13	0.00	0.71	2,165	2,163
8		15	8.23	0.51	0.13	0.00	0.71	2,127	2,169
9		20	11.90	0.89	0.00	0.00	0.74	2,301	2,256
10		19	11.14	0.89	0.00	0.00	0.73	2,278	2,219
11		9	4.56	0.25	0.00	0.13	0.64	1,975	1,947
12		13	7.09	0.51	0.13	0.00	0.68	2,138	2,080
13		12	6.58	0.63	0.00	0.00	0.69	2,165	2,109
14		16	8.35	0.63	0.13	0.00	0.68	2,051	2,080
15		16	8.23	0.63	0.00	0.13	0.65	2,022	1,998
16		18	9.24	0.63	0.25	0.00	0.66	2,025	2,005
17		13	5.95	0.38	0.13	0.13	0.59	1,823	1,816
18	A15	11	7.14	0.43	0.00	0.00	0.77	2,478	2,370
19		8	4.57	0.00	0.29	0.00	0.68	2,186	2,065
20		16	8.86	0.29	0.29	0.00	0.71	2,121	2,179
21		16	7.71	0.57	0.29	0.00	0.62	1,929	1,894
22	A16	14	8.16	0.53	0.00	0.00	0.76	2,233	2,333
23	A17	9	5.54	0.15	0.15	0.00	0.74	2,338	2,265
24		8	4.92	0.31	0.00	0.00	0.77	2,354	2,349
25		11	6.31	0.31	0.15	0.00	0.70	2,215	2,155
26		15	8.00	0.46	0.15	0.00	0.70	2,068	2,152
27		6	3.35	0.31	0.00	0.00	0.70	2,195	2,136
28	A18	25	17.50	0.63	0.00	0.00	0.85	2,610	2,598
29		23	15.38	0.63	0.00	0.00	0.83	2,505	2,548
30		21	13.88	0.50	0.00	0.00	0.85	2,464	2,595
31		19	13.75	0.50	0.00	0.00	0.85	2,700	2,592
32		18	12.88	0.50	0.00	0.00	0.84	2,675	2,566
33		18	12.75	0.50	0.00	0.00	0.84	2,650	2,562
34		23	15.50	0.63	0.00	0.00	0.83	2,524	2,551
35		9	6.53	0.25	0.00	0.00	0.84	2,712	2,572
36	A19	12	7.57	0.43	0.00	0.00	0.78	2,401	2,392
37		14	8.26	0.43	0.09	0.00	0.75	2,258	2,291
38		18	10.43	0.70	0.00	0.00	0.76	2,226	2,316
39		13	7.65	0.52	0.00	0.00	0.75	2,264	2,304
40		18	10.89	0.61	0.09	0.00	0.75	2,317	2,298
41		21	12.09	0.96	0.00	0.00	0.73	2,236	2,222
42		14	7.48	0.70	0.00	0.00	0.70	2,102	2,129
43		15	7.13	0.52	0.09	0.09	0.64	1,878	1,952
44		17	8.52	0.78	0.09	0.00	0.67	1,989	2,034
45		19	9.83	1.04	0.00	0.00	0.67	2,059	2,049
46		19	9.48	1.04	0.00	0.00	0.66	1,994	2,027
47		9	4.70	0.52	0.00	0.00	0.66	2,087	2,021
48	A20	13	7.55	0.51	0.10	0.00	0.70	2,260	2,149

Note. Own Table

Table C-16. Correlation between Observed and Modelled Normalised Saturation Flow Rate (% Four-wheeled Vehicle Share: 10%-15%)

% Four-wheeled Vehicle Share: 10%-15%									
No.	Appr.	ΔT	MC	C	MV	HV	f_{veh}	Normalised SFR	
								Observations	Model
		[s]	[veh]	[veh]	[veh]	[veh]	[veh/h]	[veh/(h*m)]	[veh/(h*m)]
	[1]	[2]	[3]	[4]	[5]	[6]	[7]	[8]	[9]
1	A14	9.00	3.25	0.25	0.13	0.13	0.45	1,503	1,376
2	A15	11.00	4.26	0.29	0.29	0.00	0.52	1,581	1,581
3		20.00	5.49	0.29	0.00	0.57	0.38	1,142	1,174
4	A19	19.00	8.52	0.78	0.00	0.17	0.58	1,796	1,783
5		18.00	8.17	1.04	0.00	0.00	0.63	1,843	1,913
6		12.00	6.07	0.70	0.00	0.00	0.65	2,030	1,981
7		16.00	6.96	1.04	0.00	0.00	0.59	1,800	1,809
8		11.00	4.13	0.78	0.00	0.00	0.54	1,608	1,659
9		15.00	5.87	0.70	0.17	0.00	0.55	1,617	1,683
10		18.00	7.04	1.13	0.00	0.09	0.53	1,651	1,623
11		13.00	5.22	0.87	0.00	0.00	0.57	1,686	1,742
12		11.00	4.17	0.52	0.17	0.00	0.51	1,594	1,575
13		17.00	6.70	1.04	0.00	0.09	0.53	1,657	1,632
14		13.00	5.13	0.87	0.00	0.00	0.57	1,662	1,731
15		12.00	4.61	0.70	0.00	0.09	0.52	1,617	1,587
16		14.00	5.57	0.87	0.09	0.00	0.54	1,677	1,657
17		13.00	4.43	0.61	0.09	0.09	0.49	1,445	1,495
18		17.00	5.65	0.78	0.09	0.17	0.47	1,418	1,423
19	A20	10.00	5.01	0.61	0.00	0.00	0.63	2,024	1,940
20		13.00	6.12	0.71	0.00	0.00	0.64	1,893	1,969
21		7.00	3.06	0.31	0.10	0.00	0.56	1,784	1,722
22		8.00	3.78	0.51	0.00	0.00	0.61	1,929	1,876
23		13.00	6.02	0.82	0.00	0.00	0.61	1,893	1,874
24		11.00	5.00	0.71	0.00	0.00	0.60	1,870	1,841
25		13.00	5.51	0.92	0.00	0.00	0.57	1,780	1,742
26		9.00	3.27	0.51	0.00	0.10	0.48	1,553	1,460
27		14.00	5.14	1.02	0.00	0.00	0.53	1,584	1,630

Note. Own Table

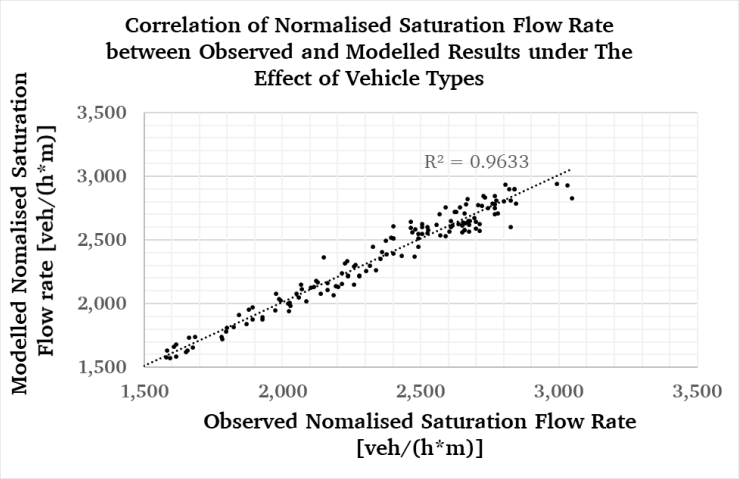

Figure C-1: Correlation between Observed and Modelled Normalised Saturation Flow Rate under the Effect of Vehicle Type

Note. Own Graph

C.6 Data of Turning Effect Without the Interference of Opposing Flows

C.6.1 Raw Data

Table C-17 gives information about raw data for defining the effect turning effect without the interference of opposing flow. Raw data include approach name, saturated green time, approach width, the number of through, left-turning and right-turning vehicles passing the stop line during the observed time by vehicle types in each direction are illustrated from column [1] to column [14].

Table C-17: Raw data for Turning Effect Model (without the Interference of Opposing Flows)

No	Appr	Saturated Green Time	Approach Width	Number of Through-vehicles				Number of Left-turning Vehicles				Number of Right-turning Vehicles			
		T	w	MC	C	MV	HV	MC	C	MV	HV	MC	C	MV	HV
		[s]	[m]	[veh]	[veh]	[veh]	[veh]	[veh]	[veh]	[veh]	[veh]	[veh]	[veh]	[veh]	[veh]
		[1]	[2]	[3]	[4]	[5]	[6]	[7]	[8]	[9]	[10]	[11]	[12]	[13]	[14]
1	A21	15	11	34	8	0	0	0	0	0	0	4	0	0	1
2		18	11	50	5	0	1	0	0	0	0	3	3	0	0
3		10	11	27	7	0	0	0	0	0	0	2	1	0	0
4		11	11	49	2	0	1	0	0	0	0	7	1	0	0
5		21	11	62	8	1	0	0	0	0	0	6	3	0	0
6		10	11	28	4	0	1	0	0	0	0	3	1	0	0
7		13	11	30	6	0	2	0	0	0	0	2	1	0	0
8		9	11	27	4	0	2	0	0	0	0	2	0	0	0
9		15	11	59	8	1	0	0	0	0	0	9	0	0	0
10		20	11	67	6	0	2	0	0	0	0	3	2	0	0
11		15	11	49	7	0	0	0	0	0	0	9	2	0	0
12		16	11	38	5	1	1	0	0	0	0	6	2	0	0
13		24	11	91	10	0	0	0	0	0	0	15	3	0	0
14		24	11	64	9	1	2	0	0	0	0	7	2	0	0
15		18	11	70	4	1	2	0	0	0	0	8	1	0	0
16		19	11	57	8	0	1	0	0	0	0	7	2	0	0
17		13	11	44	5	1	0	0	0	0	0	11	1	0	0
19		7	11	42	2	1	0	0	0	0	0	3	0	0	0
20		16	11	72	6	0	0	0	0	0	0	10	2	0	0
21		12	11	61	4	1	0	0	0	0	0	8	0	0	0
22		35	11	133	9	2	1	0	0	0	0	17	4	0	0
23		19	11	90	3	0	2	0	0	0	0	14	1	0	0
24		23	11	87	11	0	1	0	0	0	0	15	1	0	0
25		25	11	84	9	3	0	0	0	0	0	15	2	0	0
26		25	11	88	4	2	1	0	0	0	0	14	4	0	0
27		26	11	81	8	1	1	0	0	0	0	19	3	0	0
28		9	11	39	6	0	0	0	0	0	0	3	0	0	0
29		31	11	107	10	0	1	0	0	0	0	28	3	0	0
30		21	11	71	7	2	1	0	0	0	0	18	1	0	0
31		16	11	47	7	0	1	0	0	0	0	8	1	0	0

No	Appr	Saturated Green Time	Approach Width	Number of Through-vehicles				Number of Left-turning Vehicles				Number of Right-turning Vehicles			
		T	w	MC	C	MV	HV	MC	C	MV	HV	MC	C	MV	HV
		[s]	[m]	[veh]	[veh]	[veh]	[veh]	[veh]	[veh]	[veh]	[veh]	[veh]	[veh]	[veh]	[veh]
		[1]	[2]	[3]	[4]	[5]	[6]	[7]	[8]	[9]	[10]	[11]	[12]	[13]	[14]
32		33	11	114	15	0	0	0	0	0	0	19	4	0	0
33		23	11	105	10	0	1	0	0	0	0	10	1	0	0
34		19	11	71	5	0	2	0	0	0	0	7	2	0	0
35		28	11	74	8	0	2	0	0	0	0	15	2	0	1
36		8	10	29	5	0	0	0	1	0	0	1	0	0	0
37		26	10	104	6	0	0	0	3	0	0	7	1	0	1
38		19	10	55	7	0	0	4	2	0	0	9	2	0	0
39		16	10	54	7	0	0	0	2	0	0	13	1	0	0
40		23	10	73	5	0	0	10	3	0	0	13	0	0	1
41		28	10	103	10	1	0	1	4	0	0	14	1	0	0
42		15	10	65	4	0	0	3	3	0	0	10	0	0	0
43		14	10	65	4	0	0	2	3	0	0	5	0	0	0
44		18	10	55	3	1	0	3	3	0	0	4	0	0	1
45		18	10	56	8	0	0	0	0	0	0	7	0	0	1
46		7	10	31	4	0	0	1	0	0	0	2	0	0	0
47		15	10	48	6	0	0	0	0	0	0	3	0	0	1
48		12	10	56	3	0	0	4	0	0	0	9	1	0	0
49		17	10	59	12	0	0	0	0	0	0	12	0	0	0
50		36	10	170	11	0	1	7	0	0	0	18	2	0	0
51		29	10	154	10	0	0	0	0	0	0	24	1	0	0
52		10	10	64	3	0	0	0	0	0	0	5	0	0	0
53	A22	33	10	129	14	0	0	5	0	0	0	19	3	0	0
54		22	10	125	3	0	0	2	1	0	0	13	2	0	0
55		38	10	128	17	0	1	4	1	0	0	22	2	0	0
56		31	10	129	11	0	0	1	1	0	0	16	3	0	0
57		28	10	128	11	0	0	2	1	0	0	23	1	0	0
58		25	10	111	6	0	1	7	1	0	0	15	1	0	0
59		32	10	76	14	0	0	4	0	0	0	11	1	0	2
60		21	10	63	10	0	0	3	1	0	0	6	2	0	0
61		25	10	101	6	2	0	3	0	1	0	14	0	1	0
62		11	10	50	5	0	0	0	1	0	0	4	0	0	0
63		11	10	53	2	0	0	3	1	0	0	4	1	0	0
64		10	10	54	3	0	0	0	1	0	0	8	0	0	0
65		28	10	94	7	0	0	4	2	0	0	14	2	0	1
66		10	10	28	6	0	0	0	0	0	0	4	1	0	0
67		18	10	44	8	0	0	1	1	0	0	6	1	1	0
68		21	10	88	8	0	0	3	2	0	0	18	0	0	0
69		16	10	83	4	0	0	3	2	0	0	11	0	0	0
70		23	10	70	7	0	0	1	2	0	0	9	1	0	1

No	Appr	Saturated Green Time	Approach Width	Number of Through-vehicles				Number of Left-turning Vehicles				Number of Right-turning Vehicles			
		T	w	MC	C	MV	HV	MC	C	MV	HV	MC	C	MV	HV
		[s]	[m]	[veh]	[veh]	[veh]	[veh]	[veh]	[veh]	[veh]	[veh]	[veh]	[veh]	[veh]	[veh]
		[1]	[2]	[3]	[4]	[5]	[6]	[7]	[8]	[9]	[10]	[11]	[12]	[13]	[14]
71	A23	12	9	23	5	0	0	0	0	0	0	0	2	0	0
72		12	9	33	4	0	0	0	0	0	0	0	2	0	0
73		19	9	45	8	0	0	0	0	0	0	0	3	0	0
74		15	9	43	8	0	0	0	0	0	0	2	1	0	0
75		10	9	27	8	0	0	0	0	0	0	1	0	0	0
76		12	9	34	6	0	0	0	0	0	0	0	1	0	0
77		7	9	33	3	0	0	0	0	0	0	2	0	0	0
78		16	9	52	8	0	0	0	0	0	0	0	1	0	0
79		13	9	39	6	0	0	0	0	0	0	3	1	0	0
80		21	9	58	11	0	0	0	0	0	0	2	2	0	0
81		15	9	38	7	1	0	0	0	0	0	2	1	0	0
82		25	9	113	12	0	0	0	0	0	0	3	0	0	0
83		8	9	23	6	0	0	0	0	0	0	2	0	0	0
84		10	9	26	8	0	0	0	0	0	0	0	0	0	0
85		13	9	50	5	0	0	0	0	0	0	0	1	0	0
86		7	9	30	4	0	0	0	0	0	0	0	0	0	0
87		10	9	44	5	0	0	0	0	0	0	0	0	0	0
88		15	9	62	8	0	0	0	0	0	0	0	0	0	0
89		13	9	28	5	0	0	0	0	0	0	0	2	0	0
90		8	9	42	3	0	0	0	0	0	0	0	0	0	0
91		14	9	70	5	0	0	0	0	0	0	1	0	0	0
92		12	9	59	5	0	0	0	0	0	0	0	0	0	0

Note. Own Table

C.6.2 Calculation Parameters

Calculated parameters are computed from raw data in Table C-17 and are given from column [15] to column [28] in Table C-18.

$[15] = [3]$ $\quad$ $[16] = [4] + 1.5 \cdot [5] + 2.4 \cdot [6];$

$[17] = [7]$ $\quad$ $[18] = [8] + 1.5 \cdot [9] + 2.4 \cdot [10];$

$[19] = [11]$ $\quad$ $[20] = [12] + 1.5 \cdot [13] + 2.4 \cdot [14]$

$$[21] = \frac{[20]}{[15]+[16]+[17]+[18]+[20]}$$

$$[22] = \frac{[18]}{[15]+[16]+[17]+[18]+[20]}$$

$$[23] = \frac{[17]}{[15]+[16]+[17]+[18]+[20]}$$

$$[24] = \frac{[15]+[16]+[17]+[18]+[19]+[20]}{1 \cdot ([15]++[17]+[19]) + 6 \cdot ([16]+[18]+[20])}$$

$$[25] = \frac{[15]+[16]+[17]+[18]+[19]+[20]}{[1]} \cdot 3600$$

$$[26] = 3058 \cdot [2]$$

$$[27] = \frac{[25] - \frac{[25] \cdot 3600}{[1]}}{[26] \cdot [24] - \frac{[25] \cdot 3600}{[1]}}$$

$$[28] = \frac{[19] \cdot 3600}{[1].[25]} + [27] \cdot (1 - \frac{[19] \cdot 3600}{[1].[25]})$$

Table C-18: Calculated Parameters for Turning Effect Model (without the Interference of Opposing Flows)

No	Appr	Time	Approach Width	Through-vehicles		Left-turning Vehicles		Right-turning Vehicles		Proportion of Turning Vehicles			Vehicle Type Effect	Observed SFR	Estimated Based SFR	Turning Effect	
		T	w	MC	PC	MC	PC	MC	PC	$p'_{PC,RT}$	$p'_{MC,LT}$	$p'_{PC,LT}$	f_{veh}	S	S_{0w}	f_1	f_{turn}
		[s]	**[m]**	[veh]	[veh]	[veh]	[veh]	[veh]	[veh]	**[-]**	**[-]**	**[-]**	**[veh/h]**	**[veh/h]**	**[-]**	**[-]**	**[-]**
		[1]	**[2]**	[15]	[16]	[17]	[18]	[19]	[20]	**[21]**	**[22]**	**[23]**	**[24]**	**[25]**	**[26]**	**[27]**	**[28]**
1		15	11	34	8	0	0	4	2.4	0.054	0.000	0.000	0.482	11616	32109	0.734	0.756
2		18	11	50	7.4	0	0	3	3	0.050	0.000	0.000	0.549	12680	32109	0.709	0.723
3		10	11	27	7	0	0	2	1	0.029	0.000	0.000	0.481	13320	32109	0.857	0.864
4		11	11	49	4.4	0	0	7	1	0.018	0.000	0.000	0.695	20095	32109	0.890	0.902
5		21	11	62	9.5	0	0	6	3	0.040	0.000	0.000	0.563	13800	32109	0.749	0.768
6		10	11	28	6.4	0	0	3	1	0.028	0.000	0.000	0.509	13824	32109	0.834	0.847
7		13	11	30	10.8	0	0	2	1	0.024	0.000	0.000	0.426	12129	32109	0.882	0.887
8		9	11	27	8.8	0	0	2	0	0.000	0.000	0.000	0.462	15120	33380	0.979	0.980
9		15	11	59	9.5	0	0	9	0	0.000	0.000	0.000	0.620	18600	32109	0.926	0.935
10		20	11	67	10.8	0	0	3	2	0.025	0.000	0.000	0.564	14904	32109	0.818	0.824
11		15	11	49	7	0	0	9	2	0.034	0.000	0.000	0.598	16080	32109	0.817	0.841
12	A21	16	11	38	8.9	0	0	6	2	0.041	0.000	0.000	0.502	12353	32109	0.745	0.773
13		24	11	91	10	0	0	15	3	0.029	0.000	0.000	0.647	17850	32109	0.843	0.862
14		24	11	64	15.3	0	0	7	2	0.025	0.000	0.000	0.505	13245	32109	0.804	0.819
15		18	11	70	10.3	0	0	8	1	0.012	0.000	0.000	0.612	17860	32109	0.900	0.909
16		19	11	57	10.4	0	0	7	2	0.029	0.000	0.000	0.552	14476	32109	0.802	0.820
17		13	11	44	6.5	0	0	11	1	0.019	0.000	0.000	0.625	17308	32109	0.838	0.866
19		7	11	42	3.5	0	0	3	0	0.000	0.000	0.000	0.735	24943	33380	1.018	1.017
20		16	11	72	6	0	0	10	2	0.025	0.000	0.000	0.692	20250	32109	0.901	0.912
21		12	11	61	5.5	0	0	8	0	0.000	0.000	0.000	0.730	22350	32109	0.948	0.953
22		35	11	133	14.4	0	0	17	4	0.026	0.000	0.000	0.647	17321	32109	0.819	0.837
23		19	11	90	7.8	0	0	14	1	0.010	0.000	0.000	0.719	21373	32109	0.916	0.926
24		23	11	87	13.4	0	0	15	1	0.010	0.000	0.000	0.618	18219	32109	0.907	0.919

No	Appr	Time	Approach Width	Through-vehicles		Left-turning Vehicles		Right-turning Vehicles		Proportion of Turning Vehicles			Vehicle Type Effect	Observed SFR	Estimated Based SFR	Turning Effect	
		T	w	MC	PC	MC	PC	MC	PC	$p'_{PC,RT}$	$p'_{MC,LT}$	$p'_{PC,LT}$	f_{veh}	S	S_{0w}	f_1	f_{turn}
		[s]	[m]	[veh]	[veh]	[veh]	[veh]	[veh]	[veh]	[-]	[-]	[-]	[veh/h]	[veh/h]	[-]	[-]	[-]
		[1]	[2]	[15]	[16]	[17]	[18]	[19]	[20]	[21]	[22]	[23]	[24]	[25]	[26]	[27]	[28]
25		25	11	84	13.5	0	0	15	2	0.020	0.000	0.000	0.596	16488	32109	0.843	0.864
26		25	11	88	9.4	0	0	14	4	0.039	0.000	0.000	0.633	16618	32109	0.798	0.822
27		26	11	81	11.9	0	0	19	3	0.031	0.000	0.000	0.607	15909	32109	0.788	0.823
28		9	11	39	6	0	0	3	0	0.000	0.000	0.000	0.615	19200	33380	0.931	0.935
29		31	11	107	12.4	0	0	28	3	0.025	0.000	0.000	0.661	17466	32109	0.790	0.829
30		21	11	71	12.4	0	0	18	1	0.012	0.000	0.000	0.604	17554	32109	0.886	0.906
31		17	11	47	9.4	0	0	8	1	0.017	0.000	0.000	0.557	14715	32109	0.803	0.827
32		33	11	114	15	0	0	19	4	0.030	0.000	0.000	0.615	16582	32109	0.820	0.843
33		23	11	105	12.4	0	0	10	1	0.008	0.000	0.000	0.657	20097	32109	0.949	0.953
34		19	11	71	9.8	0	0	7	2	0.024	0.000	0.000	0.603	17015	32109	0.869	0.879
35		28	11	74	12.8	0	0	15	4.4	0.048	0.000	0.000	0.553	13654	32109	0.742	0.778
36		8	10	29	5	0	1	1	0	0.000	0.000	0.029	0.545	16200	31472	0.942	0.944
37		26	10	104	6	0	3	7	3.4	0.029	0.000	0.026	0.666	17086	30274	0.840	0.849
38		19	10	55	7	4	2	9	2	0.029	0.057	0.029	0.590	14968	30274	0.822	0.842
39		16	10	54	7	0	2	13	1	0.016	0.000	0.031	0.606	17325	30274	0.933	0.945
40		23	10	73	5	10	3	13	2.4	0.026	0.107	0.032	0.672	16654	30274	0.799	0.823
41		28	10	103	11.5	1	4	14	1	0.008	0.008	0.033	0.620	17293	30274	0.913	0.922
42	A22	15	10	65	4	3	3	10	0	0.000	0.040	0.040	0.708	20400	30274	0.945	0.952
43		14	10	65	4	2	3	5	0	0.000	0.027	0.041	0.693	20314	30274	0.966	0.968
44		18	10	55	4.5	3	3	4	2.4	0.035	0.044	0.044	0.592	14380	30274	0.793	0.804
45		18	10	56	8	0	0	7	2.4	0.036	0.000	0.000	0.585	14680	30274	0.814	0.831
46		7	10	31	4	1	0	2	0	0.000	0.028	0.000	0.655	19543	31472	0.945	0.948
47		15	10	48	6	0	0	3	2.4	0.043	0.000	0.000	0.586	14256	30274	0.796	0.806
48		12	10	56	3	4	0	9	1	0.016	0.063	0.000	0.785	21900	30274	0.912	0.922

No	Appr	Time	Approach Width	Through-vehicles		Left-turning Vehicles		Right-turning Vehicles		Proportion of Turning Vehicles			Vehicle Type Effect	Observed SFR	Estimated Based SFR	Turning Effect	
		T	w	MC	PC	MC	PC	MC	PC	$p'_{PC,RT}$	$p'_{MC,LT}$	$p'_{PC,LT}$	f_{veh}	S	S_{0w}	f_1	f_{turn}
		[s]	[m]	[veh]	[veh]	[veh]	[veh]	[veh]	[veh]	[-]	[-]	[-]	[veh/h]	[veh/h]	[-]	[-]	[-]
		[1]	[2]	[15]	[16]	[17]	[18]	[19]	[20]	[21]	[22]	[23]	[24]	[25]	[26]	[27]	[28]
49		17	10	59	12	0	0	12	0	0.000	0.000	0.000	0.580	17576	30274	1.000	1.000
50		36	10	170	13.4	7	0	18	2	0.010	0.036	0.000	0.732	21040	30274	0.945	0.950
51		29	10	154	10	0	0	24	1	0.006	0.000	0.000	0.775	23462	30274	1.001	1.001
52		10	10	64	3	0	0	5	0	0.000	0.000	0.000	0.828	25920	30274	1.037	1.035
53		33	10	129	14	5	0	19	3	0.020	0.033	0.000	0.667	18545	30274	0.910	0.920
54		22	10	125	3	2	1	13	2	0.015	0.015	0.008	0.830	23891	30274	0.947	0.952
55		38	10	128	19.4	4	1	22	2	0.013	0.026	0.006	0.612	16712	30274	0.890	0.904
56		31	10	129	11	1	1	16	3	0.021	0.007	0.007	0.682	18697	30274	0.896	0.906
57		28	10	128	11	2	1	23	1	0.007	0.014	0.007	0.719	21343	30274	0.978	0.981
58		25	10	111	8.4	7	1	15	1	0.008	0.055	0.008	0.734	20650	30274	0.922	0.930
59		32	10	76	14	4	0	11	5.8	0.058	0.040	0.000	0.528	12465	30274	0.761	0.785
60		21	10	63	10	3	1	6	2	0.025	0.038	0.013	0.567	14571	30274	0.840	0.851
61		25	10	101	9	3	1.5	14	1.5	0.013	0.026	0.013	0.684	18720	30274	0.893	0.905
62		11	10	50	5	0	1	4	0	0.000	0.000	0.018	0.667	19636	30274	0.971	0.973
63		11	10	53	2	3	1	4	1	0.017	0.050	0.017	0.762	20945	30274	0.903	0.909
64		10	10	54	3	0	1	8	0	0.000	0.000	0.017	0.767	23760	30274	1.026	1.023
65		28	10	94	7	4	2	14	4.4	0.039	0.036	0.018	0.652	16123	30274	0.799	0.821
66		10	10	28	6	0	0	4	1	0.029	0.000	0.000	0.527	14040	30274	0.868	0.882
67		18	10	44	8	1	1	6	2.5	0.044	0.018	0.018	0.521	12500	30274	0.776	0.797
68		21	10	88	8	3	2	18	0	0.000	0.030	0.020	0.704	20400	30274	0.950	0.957
69		16	10	83	4	3	2	11	0	0.000	0.033	0.022	0.774	23175	30274	0.987	0.988
70		23	10	70	7	1	2	9	3.4	0.041	0.012	0.024	0.598	14463	30274	0.781	0.803
71	A23	12	9	23	5	0	0	0	2	0.067	0.000	0.000	0.462	9000	27522	0.709	0.709
72		12	9	33	4	0	0	0	2	0.051	0.000	0.000	0.565	11700	27522	0.752	0.752

No	Appr	Time	Approach Width	Through-vehicles		Left-turning Vehicles		Right-turning Vehicles		Proportion of Turning Vehicles			Vehicle Type Effect	Observed SFR	Estimated Based SFR	Turning Effect	
		T	w	MC	PC	MC	PC	MC	PC	$p'_{PC,RT}$	$p'_{MC,LT}$	$p'_{PC,LT}$	f_{veh}	S	S_{0w}	f_1	f_{turn}
		[s]	[m]	[veh]	[veh]	[veh]	[veh]	[veh]	[veh]	[-]	[-]	[-]	[veh/h]	[veh/h]	[-]	[-]	[-]
		[1]	[2]	[15]	[16]	[17]	[18]	[19]	[20]	[21]	[22]	[23]	[24]	[25]	[26]	[27]	[28]
73		19	9	45	8	0	0	0	3	0.054	0.000	0.000	0.505	10611	27522	0.764	0.764
74		15	9	43	8	0	0	2	1	0.019	0.000	0.000	0.545	12960	27522	0.859	0.864
75		10	9	27	8	0	0	1	0	0.000	0.000	0.000	0.474	12960	27522	0.994	0.994
76		12	9	34	6	0	0	0	1	0.024	0.000	0.000	0.539	12300	27522	0.828	0.828
77		7	9	33	3	0	0	2	0	0.000	0.000	0.000	0.717	19543	28611	0.950	0.953
78		16	9	52	8	0	0	0	1	0.016	0.000	0.000	0.575	13725	27522	0.867	0.867
79		13	9	39	6	0	0	3	1	0.022	0.000	0.000	0.583	13569	27522	0.837	0.847
80		21	9	58	11	0	0	2	2	0.028	0.000	0.000	0.529	12514	27522	0.856	0.860
81		15	9	38	8.5	0	0	2	1	0.021	0.000	0.000	0.510	11880	27522	0.840	0.847
82		25	9	113	12	0	0	3	0	0.000	0.000	0.000	0.681	18432	27522	0.983	0.984
83		8	9	23	6	0	0	2	0	0.000	0.000	0.000	0.508	13950	28611	0.957	0.960
84		10	9	26	8	0	0	0	0	0.000	0.000	0.000	0.459	12240	27522	0.968	0.968
85		13	9	50	5	0	0	0	1	0.018	0.000	0.000	0.651	15508	27522	0.865	0.865
86		7	9	30	4	0	0	0	0	0.000	0.000	0.000	0.630	17486	28611	0.971	0.971
87		10	9	44	5	0	0	0	0	0.000	0.000	0.000	0.662	17640	27522	0.968	0.968
88		15	9	62	8	0	0	0	0	0.000	0.000	0.000	0.636	16800	27522	0.959	0.959
89		13	9	28	5	0	0	0	2	0.057	0.000	0.000	0.500	9692	27522	0.704	0.704
90		8	9	42	3	0	0	0	0	0.000	0.000	0.000	0.750	20250	28611	0.944	0.944
91		14	9	70	5	0	0	1	0	0.000	0.000	0.000	0.752	19543	27522	0.943	0.944
92		12	9	59	5	0	0	0	0	0.000	0.000	0.000	0.719	19200	27522	0.970	0.970

Note. Own Table

C.6.3 Regression Results

The regression output gives the intercept values which reflect the effect of right-turning cars, left-turning motorcycles and left-turning cars.

$$f_1 = f_{RT,1} \cdot f_{LT,1} = \frac{1}{1 + a_1 . P'_{PC,RT}} \cdot \frac{1}{1 + b_1 . P'_{MC,LT} + c_1 . P'_{PC,LT}}$$

Parameter Estimates

Parameter	Estimate	Std. Error	95% Confidence Interval	
			Lower Bound	Upper Bound
a1	7.069	.237	6.598	7.540
b1	.003	.256	-.506	.513
c1	.720	.414	-.102	1.542

ANOVA[a]

Source	Sum of Squares	df	Mean Squares
Regression	70.045	3	23.348
Residual	.100	88	.001
Uncorrected Total	70.146	91	
Corrected Total	.575	90	

Dependent variable: y[a]

a. R squared = 1 - (Residual Sum of Squares) / (Corrected Sum of Squares) = .826.

Note. Own Tables

C.7 Data of Turning Effect with the Interference of Opposing Flows

C.7.1 Raw Data

Table C-19 gives information about raw data for defining the effect turning effect with the interference of opposing flows. Raw data include approach name, saturated green time, the number of through, left-turning, right-turning, vehicles passing the stop line during the observed time in accordance with vehicle types in each direction are illustrated from column [1] to column [15]. Besides, opposing through and opposing left-turning vehicles crossing the conflict area are given from column [16] to column [21].

Table C-19: Raw Data for Turning Effect Model (with the Interference of Opposing Flows)

No	Appr	Saturated Green Time	Appr. Width		Through-vehicles				Left-turning Vehicles				Right-turning Vehicles				Opposing Through-vehicles				Opposing Left-turning Vehicles	
		T	w	w_{OP}	MC	C	MV	HV	MC	C	MV	HV	MC	C	MV	HV	MC	C	MV	HV	MC	PC
		[s]	[m]	[m]	[veh]	[veh]	[veh]	[veh]	[veh]	[veh]	[veh]	[veh]	[veh]	[veh]	[veh]	[veh]	[veh]	[veh]	[veh]	[veh]	[veh]	[veh]
		[1]	[2]	[3]	[4]	[5]	[6]	[7]	[8]	[9]	[10]	[11]	[12]	[13]	[14]	[15]	[16]	[17]	[18]	[19]	[20]	[21]
1		14	12	11	82	2	0	0	7	0	0	0	2	1	0	0	43	2	0	0	10	0
2		40	12	11	150	15	0	0	28	0	0	0	9	2	0	0	146	11	0	0	34	0
3		10	12	11	53	5	0	0	3	0	0	0	4	0	0	0	37	3	0	0	4	0
4		28	12	11	105	11	0	0	12	0	0	0	10	1	0	0	45	3	0	0	42	0
5		26	12	11	102	9	0	0	25	0	0	0	7	0	0	0	90	5	0	0	25	0
6		16	12	11	64	6	0	0	12	0	0	0	6	1	0	0	74	3	0	0	7	0
7		35	12	11	130	10	0	0	10	0	0	0	4	3	0	0	151	8	0	0	49	0
8		35	12	11	100	11	0	2	24	0	0	0	5	1	0	0	101	5	1	0	46	0
9		35	12	11	140	9	0	0	24	0	0	0	14	3	0	0	127	10	0	0	41	0
10		25	12	11	128	6	0	0	16	0	0	0	13	0	0	0	49	1	1	0	28	0
11		34	12	11	133	4	0	2	21	0	0	0	15	0	0	0	136	10	0	0	48	0
12	A29	39	12	11	146	10	0	0	45	0	0	0	8	1	0	0	153	8	0	1	43	0
13		22	12	11	114	4	1	1	20	0	0	0	7	0	0	0	108	4	0	0	5	0
14		26	12	11	68	11	0	1	18	0	0	0	2	2	0	0	84	10	0	0	22	0
15		15	12	11	50	7	1	0	10	0	0	0	4	1	0	0	34	1	0	0	6	0
16		13	12	11	60	5	0	0	10	0	0	0	4	0	0	0	47	3	1	0	7	0
17		25	12	11	73	11	0	0	14	0	0	0	6	1	0	0	65	5	0	2	26	0
18		11	12	11	42	4	0	0	7	0	0	0	0	1	0	0	48	3	0	0	5	0
19		16	12	11	76	6	0	0	12	0	0	0	3	0	0	0	59	3	0	1	8	0
20		19	12	11	79	7	0	0	9	0	0	0	6	2	0	0	70	5	0	0	10	0
21		23	12	11	82	11	0	0	3	0	0	0	7	3	0	0	105	6	0	0	10	0
22		20	12	11	67	7	1	0	3	0	0	0	1	2	0	0	73	5	0	0	27	0
23		24	12	11	72	7	0	2	12	0	0	0	8	0	0	0	108	4	0	0	27	0

No	Appr	Saturated Green Time	Appr. Width		Through-vehicles				Left-turning Vehicles				Right-turning Vehicles				Opposing Through-vehicles				Opposing Left-turning Vehicles	
		T	w	w_{OP}	MC	C	MV	HV	MC	C	MV	HV	MC	C	MV	HV	MC	C	MV	HV	MC	PC
		[s]	[m]	[m]	[veh]	[veh]	[veh]	[veh]	[veh]	[veh]	[veh]	[veh]	[veh]	[veh]	[veh]	[veh]	[veh]	[veh]	[veh]	[veh]	[veh]	[veh]
		[1]	[2]	[3]	[4]	[5]	[6]	[7]	[8]	[9]	[10]	[11]	[12]	[13]	[14]	[15]	[16]	[17]	[18]	[19]	[20]	[21]
24		9	12	11	37	4	0	0	10	0	0	0	1	0	0	0	37	1	0	0	5	0
25		14	12	11	64	7	0	0	8	0	0	0	3	0	0	0	58	3	0	0	6	0
26		18	12	11	64	8	0	0	5	0	0	0	7	1	0	0	135	5	0	0	19	0
27		60	12	11	174	24	0	1	36	0	0	0	9	3	0	0	226	12	0	1	73	0
28		90	12	11	277	28	0	1	52	0	0	0	17	7	0	0	310	27	0	0	93	0
29		20	12	11	69	10	0	0	14	0	0	0	3	1	0	0	89	3	0	0	15	0
30		18	11	11	79	7	0	0	9	0	0	0	3	1	0	0	56	3	0	0	2	0
31		25	11	11	104	10	0	0	10	0	0	0	6	2	0	0	60	2	0	0	0	0
32		19	11	11	102	5	0	0	13	0	0	0	7	0	0	0	56	2	1	0	3	0
33		9	11	11	53	3	0	0	5	0	0	0	1	0	0	0	39	2	0	0	0	0
34		23	11	11	123	6	0	0	19	0	0	0	10	0	0	0	40	3	0	0	0	0
35		27	11	11	120	3	0	0	20	1	0	0	10	3	0	0	86	2	0	0	3	0
36		19	11	11	87	6	0	0	5	0	0	0	1	2	0	0	67	2	0	1	3	0
37	A31	30	11	11	129	6	1	0	31	0	0	0	7	2	0	0	68	2	0	1	3	0
38		10	11	11	47	5	0	0	3	0	0	0	3	0	0	0	33	1	0	0	0	0
39		35	11	11	142	11	0	0	23	0	0	0	13	2	0	0	82	4	0	1	6	0
40		10	11	11	37	7	0	0	5	0	0	0	3	0	0	0	19	1	0	0	0	0
41		26	11	11	105	6	0	0	12	0	0	0	6	3	0	0	78	4	0	1	1	1
42		27	11	11	122	10	0	0	13	0	0	0	17	1	0	0	89	4	0	0	2	0
43		34	11	11	129	11	0	0	13	0	0	0	22	3	0	0	114	4	0	1	2	0
44		25	11	11	109	8	0	0	13	0	0	0	13	2	0	0	72	4	0	0	2	0
45		36	11	11	170	10	0	0	26	0	0	0	22	1	0	0	101	6	0	0	5	0
46		22	11	11	93	6	0	0	16	0	0	0	9	2	0	0	41	5	0	0	2	0
47		28	11	11	103	11	0	0	16	0	0	0	14	1	1	0	76	2	0	0	1	0
48		29	11	11	130	7	0	0	26	0	0	0	10	2	0	0	98	3	0	0	3	0
49		18	11	11	105	4	0	0	15	0	0	0	8	0	0	0	58	0	0	0	0	0
50		21	11	11	117	3	0	0	12	0	0	0	11	1	0	0	82	5	0	0	3	0
51		25	11	11	126	9	0	0	9	0	0	0	14	1	0	0	95	5	0	0	3	0
52		41	11	11	248	6	0	0	29	0	0	0	13	2	0	0	152	10	0	0	2	0
53		14	11	11	68	6	0	0	8	0	0	0	6	0	0	0	55	2	0	0	0	0
54	A32	32	11	11	155	8	0	1	23	0	0	0	20	1	0	0	119	4	0	0	2	0
55		40	11	11	220	10	0	0	31	0	0	0	16	1	0	0	153	0	0	0	2	0
56		37	11	11	165	10	0	0	19	0	0	0	23	3	0	0	126	6	1	0	2	0
57		24	11	11	77	10	0	0	12	0	0	0	12	2	0	0	88	3	0	0	1	0
58		36	11	11	167	7	0	0	34	0	0	0	16	2	0	0	117	8	0	0	3	0
59		27	11	11	104	9	0	0	16	0	0	0	11	1	0	0	79	5	0	0	5	1
60		28	11	11	109	6	0	1	18	0	0	0	8	2	0	0	77	6	0	2	4	0
61		22	11	11	107	6	0	0	15	0	0	0	8	1	0	0	73	4	0	0	3	0
62		18	11	11	86	6	0	0	15	0	0	0	10	0	0	0	89	2	0	0	1	0
63		29	11	11	127	8	0	0	22	0	0	0	12	2	0	0	73	3	0	0	1	0

No	Appr	Saturated Green Time	Appr. Width		Through-vehicles				Left-turning Vehicles				Right-turning Vehicles				Opposing Through-vehicles				Opposing Left-turning Vehicles	
		T	w	w_{OP}	MC	C	MV	HV	MC	C	MV	HV	MC	C	MV	HV	MC	C	MV	HV	MC	PC
		[s]	[m]	[m]	[veh]	[veh]	[veh]	[veh]	[veh]	[veh]	[veh]	[veh]	[veh]	[veh]	[veh]	[veh]	[veh]	[veh]	[veh]	[veh]	[veh]	[veh]
		[1]	[2]	[3]	[4]	[5]	[6]	[7]	[8]	[9]	[10]	[11]	[12]	[13]	[14]	[15]	[16]	[17]	[18]	[19]	[20]	[21]
64		20	11	11	102	6	0	0	12	0	0	0	7	1	0	0	60	3	0	0	1	0
65		22	5	5	36	6	0	0	1	0	0	0	4	1	0	0	27	3	0	0	0	0
66		20	5	5	12	4	0	0	1	0	0	0	3	2	0	0	31	2	0	0	1	0
67		19	5	5	19	4	0	0	1	0	0	0	5	2	0	0	25	2	0	0	0	0
68		8	5	5	11	4	0	0	0	0	0	0	0	0	0	0	28	2	0	0	0	0
69		11	5	5	2	6	0	0	1	0	0	0	1	0	0	0	16	2	0	0	0	0
70		18	5	5	17	3	0	0	6	1	0	0	11	0	0	0	38	1	0	0	0	0
71		21	5	5	16	4	0	0	5	0	0	0	2	2	0	0	25	3	0	0	0	0
72		18	5	5	16	4	0	0	4	0	0	0	10	1	0	0	28	4	0	0	0	0
73		14	5	5	19	1	0	0	0	0	0	0	9	2	0	0	17	0	0	0	0	0
74		23	5	5	17	3	0	0	7	0	0	0	8	0	0	1	35	1	0	0	0	0
75		17	5	5	20	4	0	0	4	0	0	0	3	1	0	0	15	0	0	1	0	0
76		15	5	5	10	3	0	0	3	0	0	0	8	1	0	0	21	3	0	0	0	0
77		19	5	5	26	3	0	0	4	0	0	0	9	1	0	0	19	4	1	0	0	0
78		10	5	5	30	2	0	0	0	0	0	0	1	0	0	0	17	0	0	0	0	0
79		17	5	5	26	4	0	0	0	0	0	0	8	1	0	0	21	1	0	0	0	0
80		16	5	5	26	5	0	0	2	0	0	0	5	0	0	0	20	3	0	0	0	0
81		21	7	7	63	6	0	0	0	0	0	0	8	0	0	0	0	0	0	0	7	1
82		14	7	7	41	1	0	0	0	0	0	0	5	1	0	0	0	0	0	0	8	1
83		9	7	7	42	1	0	0	0	0	0	0	3	0	0	0	0	0	0	0	4	0
84		10	7	7	41	0	1	0	0	0	0	0	2	0	0	0	0	0	0	0	0	0
85		16	7	7	49	1	0	1	0	0	0	0	4	1	0	0	0	0	0	0	7	0
86		10	7	7	45	2	0	0	0	0	0	0	2	0	0	0	0	0	0	0	0	0
87		8	7	7	26	3	0	0	0	0	0	0	3	0	0	0	0	0	0	0	0	0
88		12	7	7	26	3	0	0	0	0	0	0	5	1	0	0	0	0	0	0	14	0
89		18	7	7	47	4	0	1	0	0	0	0	4	0	0	0	0	0	0	0	4	1
90	A34	22	7	7	60	5	0	0	0	0	0	0	7	1	0	0	0	0	0	0	21	1
91		6	7	7	24	0	1	0	0	0	0	0	3	0	0	0	0	0	0	0	0	0
92		9	7	7	36	3	0	0	0	0	0	0	2	0	0	0	0	0	0	0	0	0
93		21	7	7	62	7	0	0	0	0	0	0	10	0	0	0	0	0	0	0	11	0
94		10	7	7	32	1	0	0	0	0	0	0	6	0	0	0	0	0	0	0	7	1
95		12	7	7	51	1	1	0	0	0	0	0	0	0	0	0	0	0	0	0	0	0
96		5	7	7	24	0	0	0	0	0	0	0	1	0	0	0	0	0	0	0	1	0
97		13	7	7	33	3	0	0	0	0	0	0	4	1	0	0	0	0	0	0	15	0
98		22	7	7	81	4	0	0	0	0	0	0	10	0	0	0	0	0	0	0	8	1
99		10	7	7	43	0	0	0	0	0	0	0	1	1	0	0	0	0	0	0	6	0
100		13	7	7	50	1	0	0	0	0	0	0	3	0	0	0	0	0	0	0	13	1
101		18	9	9	72	4	0	0	20	0	0	0	4	0	0	0	49	1	0	0	0	0
102	A35	14	9	9	48	3	0	0	20	0	0	0	4	0	0	0	35	2	0	0	0	0
103		12	9	9	39	3	0	0	19	0	0	0	1	0	0	0	15	2	0	0	0	0

No	Appr	Saturated Green Time	Appr. Width		Through-vehicles				Left-turning Vehicles				Right-turning Vehicles				Opposing Through-vehicles				Opposing Left-turning Vehicles	
		T	w	w_{OP}	MC	C	MV	HV	MC	C	MV	HV	MC	C	MV	HV	MC	C	MV	HV	MC	PC
		[s]	[m]	[m]	[veh]	[veh]	[veh]	[veh]	[veh]	[veh]	[veh]	[veh]	[veh]	[veh]	[veh]	[veh]	[veh]	[veh]	[veh]	[veh]	[veh]	[veh]
		[1]	[2]	[3]	[4]	[5]	[6]	[7]	[8]	[9]	[10]	[11]	[12]	[13]	[14]	[15]	[16]	[17]	[18]	[19]	[20]	[21]
104		11	9	9	38	3	0	0	15	0	0	0	3	0	0	0	31	2	0	0	0	0
105		10	9	9	45	1	0	0	12	0	0	0	1	0	0	0	38	2	0	0	0	0
106		24	9	9	80	6	0	0	30	0	0	0	4	0	0	0	80	3	0	2	0	0
107		25	9	9	87	3	0	0	37	1	0	0	6	0	0	0	72	4	0	0	0	0
108		18	9	9	59	4	0	0	21	1	0	0	4	0	0	0	53	3	0	0	0	0
109		17	9	9	66	1	0	0	20	1	0	0	1	0	0	0	79	1	0	0	0	0
110		17	9	9	57	4	0	0	15	1	0	0	2	0	0	0	20	2	0	0	0	0
111		17	9	9	70	1	0	0	20	1	0	0	1	0	0	0	59	4	0	0	0	0
112		16	9	9	63	1	0	0	17	1	0	0	2	0	0	0	38	2	0	0	0	0
113		15	9	9	62	5	0	0	10	0	0	0	3	0	0	0	57	3	0	0	0	0
114		13	9	9	50	2	0	0	10	1	0	0	2	0	0	0	37	3	0	0	0	0
115		13	9	9	36	3	0	0	16	1	0	0	3	0	0	0	30	1	0	0	0	0
116		13	9	9	57	2	0	0	16	0	0	0	1	0	0	0	45	1	0	0	0	0
117		46	9	9	135	9	0	0	37	5	0	0	8	0	0	0	136	7	0	0	0	0
118		11	9	9	35	2	0	0	8	1	0	0	2	0	0	0	42	3	0	0	0	0
119		29	9	9	85	5	0	0	28	3	0	0	7	0	0	0	84	5	0	0	0	0
120		19	9	9	58	4	0	0	20	2	0	0	5	0	0	0	52	1	0	0	0	0
121		21	9	9	62	5	0	0	21	1	0	0	2	0	0	0	74	4	0	0	0	0
122		17	9	9	50	5	0	0	17	1	0	0	1	0	0	0	42	2	0	0	0	0
123		28	9	9	91	4	0	0	30	2	1	0	5	0	0	0	62	3	0	0	0	0
124		35	8	8	130	6	0	1	11	0	0	0	0	0	0	0	110	4	0	1	8	1
125		22	8	8	75	4	0	0	14	0	0	0	0	0	0	0	50	1	1	0	8	0
126		10	8	8	35	2	0	0	6	0	0	0	0	0	0	0	46	2	0	0	9	0
127		11	8	8	47	2	0	0	7	0	0	0	0	0	0	0	28	1	0	0	0	0
128		10	8	8	41	3	0	0	3	0	0	0	2	0	0	0	42	2	0	0	0	0
129		20	8	8	70	5	0	0	11	0	0	0	1	0	0	0	60	2	0	0	1	0
130		24	8	8	96	4	0	0	13	0	0	0	4	0	0	0	81	1	0	0	11	0
131		13	8	8	43	2	0	1	4	0	0	0	0	0	0	0	33	0	0	1	0	0
132		9	8	8	39	1	0	0	9	0	0	0	0	0	0	0	26	1	0	0	0	0
133		22	8	8	67	4	0	1	6	0	0	0	2	1	0	0	75	3	0	0	3	0
134	A36	31	8	8	102	4	0	1	7	0	0	0	5	0	0	0	95	6	0	0	11	3
135		11	8	8	45	1	0	0	10	0	0	0	0	0	0	0	29	0	0	0	4	0
136		17	8	8	64	4	0	0	8	0	0	0	0	0	0	0	46	4	0	0	1	0
137		8	8	8	28	2	0	0	7	0	0	0	1	0	0	0	25	0	0	0	1	0
138		24	8	8	85	3	0	0	14	0	0	0	3	0	0	0	66	3	0	0	9	2
139		12	8	8	57	1	0	0	3	0	0	0	1	0	0	0	37	1	0	0	7	1
140		25	8	8	91	5	0	0	11	0	0	0	0	0	0	0	70	4	0	0	10	0
141		31	8	8	117	3	0	0	24	0	0	0	0	1	0	0	98	4	0	0	14	0
142		13	8	8	33	0	0	1	9	0	0	0	0	0	0	0	31	1	0	0	5	2
143		14	8	8	43	3	0	0	4	0	0	0	0	1	0	0	30	0	0	0	4	0

No	Appr	Saturated Green Time	Appr. Width		Through-vehicles				Left-turning Vehicles				Right-turning Vehicles				Opposing Through-vehicles				Opposing Left-turning Vehicles	
		T	w	w_{OP}	MC	C	MV	HV	MC	C	MV	HV	MC	C	MV	HV	MC	C	MV	HV	MC	PC
		[s]	[m]	[m]	[veh]	[veh]	[veh]	[veh]	[veh]	[veh]	[veh]	[veh]	[veh]	[veh]	[veh]	[veh]	[veh]	[veh]	[veh]	[veh]	[veh]	[veh]
		[1]	[2]	[3]	[4]	[5]	[6]	[7]	[8]	[9]	[10]	[11]	[12]	[13]	[14]	[15]	[16]	[17]	[18]	[19]	[20]	[21]
144		14	8	8	47	3	0	0	7	0	0	0	1	0	0	0	51	2	0	0	6	0
145		20	8	8	80	3	1	0	8	0	0	0	0	0	0	0	55	1	0	0	2	0
146		11	8	8	39	2	0	0	8	0	0	0	1	0	0	0	39	1	0	0	2	0
147		18	8	8	66	5	0	0	3	0	0	0	2	0	0	0	23	0	0	0	6	0
148		13	8	8	47	3	0	0	4	0	0	0	2	0	0	0	40	3	0	0	3	1
149		7	8	8	27	2	0	0	3	0	0	0	0	0	0	0	18	1	0	0	2	0
150		14	8	8	57	4	0	0	6	0	0	0	4	0	0	0	51	1	0	0	0	0
151		18	8	8	69	3	0	0	10	0	0	0	2	0	0	0	46	4	0	0	6	0
152		11	8	8	50	2	0	0	2	0	0	0	0	0	0	0	34	0	0	0	2	0
153		12	8	8	41	2	0	0	10	0	0	0	0	0	0	0	53	1	0	0	6	0
154		8	8	8	32	1	0	0	7	0	0	0	0	0	0	0	21	0	0	0	2	0

Note. Own Table

C.7.2 Calculation Parameters

Calculated parameters computed from raw data in Table C-19 and are given through columns from [22] to [39] in Table C-20. Parameters in columns are estimated below:

$$[22] = \frac{[13]+[14]*1.5+[15]*2.4}{[4]+[5]+[6]\cdot 1.5+[7]\cdot 2.4+[8]+[9]+[10]\cdot 1.5+[11]\cdot 2.4+[13]+[14]\cdot 1.5+[15]\cdot 2.4};$$

$$[23] = \frac{[8]}{[4]+[5]+[6]\cdot 1.5+[7]\cdot 2.4+[8]+[9]+[10]\cdot 1.5+[11]\cdot 2.4+[13]+[14]\cdot 1.5+[15]\cdot 2.4};$$

$$[24] = \frac{[9]+[10]*1.5+[11]*2.4}{[4]+[5]+[6]\cdot 1.5+[7]\cdot 2.4+[8]+[9]+[10]\cdot 1.5+[11]\cdot 2.4+[13]+[14]\cdot 1.5+[15]\cdot 2.4}$$

$$[25] = \frac{[16]}{[1]}\cdot 3600;\ [26] = \frac{[17]+[18]*1.5+[19]*2.4}{[1]}\cdot 3600;\ [27] = \frac{[20]}{[1]}\cdot 3600;\ [28] = \frac{[21]}{[1]}\cdot 3600;$$

$$[29] = \frac{[4]}{[1]}\cdot 3600;\ [30] = \frac{[5]+[6]\cdot 1.5+[7]\cdot 2.4}{[1]}\cdot 3600$$

$$[31] = \frac{[16]+[17]+[18]\cdot 1.5+[19]\cdot 2.4}{[16]+([17]+[18]\cdot 1.5+[19]\cdot 2.4)\cdot 6}\cdot 3600 \; ; [32] = \frac{[4]+[5]+[6]\cdot 1.5+[7]\cdot 2.4}{[4]+([5]+[6]\cdot 1.5+[7]\cdot 2.4)\cdot 6}\cdot 3600$$

$$[33] = 3058\cdot[3]\cdot[31] \; ; \; [34] = 3058\cdot[2]\cdot[32]$$

$$[35] = \frac{[4]+[5]+[6]\cdot 1.5+[7]\cdot 2.4+[8]+[9]+[10]\cdot 1.5+[11]\cdot 2.4+[12]+[13]+[14]\cdot 1.5+[15]\cdot 2.4}{[4]+[8]+[12]+([5]+[6]\cdot 1.5+[7]\cdot 2.4+[9]+[10]\cdot 1.5+[11]\cdot 2.4+[13]+[14]\cdot 1.5+[15]\cdot 2.4)\cdot 6}$$

$$[36] = \frac{[4]+[5]+[6]\cdot 1.5+[7]\cdot 2.4+[8]+[9]+[10]\cdot 1.5+[11]\cdot 2.4+[12]+[13]+[14]\cdot 1.5+[15]\cdot 2.4}{[1]}\cdot 3600 \; ; \; [37] = 3058\cdot[2]$$

$$[38] = \frac{[36]-\frac{[12]\cdot 3600}{[1]}}{[37]\cdot[35]-\frac{[12]\cdot 3600}{[1]}} \; ; \; [39] = \frac{[12]\cdot 3600}{[1].[36]}+[38]\cdot\left(1-\frac{[12]\cdot 3600}{[1].[36]}\right)$$

Table C-20: Calculated Parameters for Turning Effect Model (with the Interference of Opposing Flows)

Proportion of Turning Vehicles			Opposing Through Volume	Opposing Left-turning Volume		Through-Volume		Adjustment Factor for Vehicle Types of Opposing Through Stream	Adjustment Factor for Vehicle Types of Targeted Through Stream	Opposing Through Saturation Flow Rate	Through Saturation Flow Rate	Adjustment Factor for Vehicle Types of Targeted Stream	Observed SFR	Estimated Based SFR	Turning Effect	
$p'_{PC,R1}$	$p'_{MC,L1}$	$p'_{PC,L1}$	$q_{MC,OPT}$	$q_{PC,OPT}$	$q_{MC,OPL}$	$q_{PC,OPL}$	$q_{MC,TH}$	$q_{PC,TH}$	$f_{veh,OPT}$	$f_{veh,TH}$	S_{OPT}	S_{TH}	f_{veh}	S	S_{0w}	f_2	$f_{turn,2}$
[-]	[-]	[-]	[veh/h]	[veh/h]	[veh/h]	[veh/h]	[veh/h]	[veh/h]					[-]	[veh/h]	[veh/h]	[-]	[-]
[22]	[23]	[24]	[25]	[26]	[27]	[28]	[29]	[30]	[31]	[32]	[33]	[34]	[35]	[36]	[37]	[38]	[39]
0.011	0.076	0.000	11,057	514	2,571.4	0.0	21,086	514.3	0.818	0.894	30,024	32,792	0.862	24,171	36,696	0.760	0.765
0.010	0.144	0.000	13,140	990	3,060.0	0.0	13,500	1,350.0	0.741	0.688	27,176	25,229	0.706	18,360	36,696	0.699	0.713
0.000	0.049	0.000	13,320	1,080	1,440.0	0.0	19,080	1,800.0	0.727	0.699	26,688	25,643	0.722	23,400	36,696	0.876	0.884
0.008	0.093	0.000	5,786	386	5,400.0	0.0	13,500	1,414.3	0.762	0.678	27,959	24,893	0.698	17,871	36,696	0.681	0.704
0.000	0.184	0.000	12,462	692	3,461.5	0.0	14,123	1,246.2	0.792	0.712	29,051	26,111	0.761	19,800	36,696	0.699	0.714
0.012	0.145	0.000	16,650	675	1,575.0	0.0	14,400	1,350.0	0.837	0.700	30,713	25,687	0.718	20,025	36,696	0.747	0.764
0.020	0.065	0.000	15,531	823	5,040.0	0.0	13,371	1,028.6	0.799	0.737	29,320	27,039	0.707	16,149	36,696	0.616	0.626
0.007	0.170	0.000	10,389	669	4,731.4	0.0	10,286	1,625.1	0.768	0.594	28,177	21,814	0.634	14,997	36,696	0.636	0.649

Proportion of Turning Vehicles			Opposing Through Volume	Opposing Left-turning Volume		Through-Volume		Adjustment Factor for Vehicle Types of Opposing Through Stream	Adjustment Factor for Vehicle Types of Targeted Through Stream	Opposing Through Saturation Flow Rate	Through Saturation Flow Rate	Adjustment Factor for Vehicle Types of Targeted Stream	Observed SFR	Estimated Based SFR	Turning Effect	
$p'_{PC,RT}$	$p'_{MC,LT}$	$p'_{PC,LT}$	$q_{MC,OPT}$	$q_{PC,OPT}$	$q_{MC,OPL}$	$q_{PC,OPL}$	$q_{MC,TH}$	$q_{PC,TH}$	$f_{veh,OPT}$	$f_{veh,TH}$	S_{OPT}	S_{TH}	f_{veh}	S	S_{0w}	f_2	$f_{turn,2}$
[-]	[-]	[-]	[veh/h]	[veh/h]	[veh/h]	[veh/h]	[veh/h]	[veh/h]					[-]	[veh/h]	[veh/h]	[-]	[-]
[22]	[23]	[24]	[25]	[26]	[27]	[28]	[29]	[30]	[31]	[32]	[33]	[34]	[35]	[36]	[37]	[38]	[39]
0.017	0.136	0.000	13,063	1,029	4,217.1	0.0	14,400	925.7	0.733	0.768	26,884	28,184	0.760	19,543	36,696	0.684	0.708
0.000	0.107	0.000	7,056	360	4,032.0	0.0	18,432	864.0	0.805	0.817	29,529	29,983	0.845	23,472	36,696	0.742	0.762
0.000	0.129	0.000	14,400	1,059	5,082.4	0.0	14,082	931.8	0.745	0.763	27,335	28,006	0.802	18,826	36,696	0.619	0.652
0.005	0.223	0.000	14,123	960	3,969.2	0.0	13,477	923.1	0.759	0.757	27,837	27,789	0.792	19,385	36,696	0.658	0.671
0.000	0.143	0.000	17,673	655	818.2	0.0	18,655	1,292.7	0.848	0.755	31,136	27,715	0.790	24,365	36,696	0.834	0.841
0.020	0.178	0.000	11,631	1,385	3,046.2	0.0	9,415	1,855.4	0.653	0.549	23,954	20,128	0.573	14,317	36,696	0.676	0.683
0.014	0.144	0.000	8,160	240	1,440.0	0.0	12,000	2,040.0	0.875	0.579	32,109	21,255	0.607	17,640	36,696	0.782	0.794
0.000	0.133	0.000	13,015	1,246	1,938.5	0.0	16,615	1,384.6	0.696	0.722	25,538	26,503	0.760	21,877	36,696	0.776	0.787
0.010	0.141	0.000	9,360	1,411	3,744.0	0.0	10,512	1,584.0	0.604	0.604	22,172	22,176	0.636	15,120	36,696	0.634	0.655
0.019	0.130	0.000	15,709	982	1,636.4	0.0	13,745	1,309.1	0.773	0.697	28,356	25,576	0.684	17,673	36,696	0.705	0.705
0.000	0.128	0.000	13,275	1,215	1,800.0	0.0	17,100	1,350.0	0.705	0.732	25,856	26,867	0.764	21,825	36,696	0.773	0.780
0.021	0.093	0.000	13,263	947	1,894.7	0.0	14,968	1,326.3	0.750	0.711	27,522	26,081	0.696	19,516	36,696	0.753	0.768
0.030	0.030	0.000	16,435	939	1,565.2	0.0	12,835	1,721.7	0.787	0.628	28,888	23,059	0.602	16,591	36,696	0.738	0.755
0.025	0.037	0.000	13,140	900	4,860.0	0.0	12,060	1,530.0	0.757	0.640	27,789	23,479	0.608	14,670	36,696	0.655	0.659
0.000	0.125	0.000	16,200	600	4,050.0	0.0	10,800	1,770.0	0.848	0.587	31,136	21,534	0.638	15,570	36,696	0.647	0.675
0.000	0.196	0.000	14,800	400	2,000.0	0.0	14,800	1,600.0	0.884	0.672	32,429	24,665	0.722	20,800	36,696	0.782	0.786
0.000	0.101	0.000	14,914	771	1,542.9	0.0	16,457	1,800.0	0.803	0.670	29,453	24,579	0.701	21,086	36,696	0.814	0.821
0.013	0.064	0.000	27,000	1,000	3,800.0	0.0	12,800	1,600.0	0.848	0.643	31,136	23,590	0.654	17,000	36,696	0.690	0.716
0.013	0.150	0.000	13,560	864	4,380.0	0.0	10,440	1,584.0	0.770	0.603	28,239	22,124	0.628	14,904	36,696	0.638	0.651
0.019	0.142	0.000	12,400	1,080	3,720.0	0.0	11,080	1,216.0	0.714	0.669	26,200	24,555	0.672	15,336	36,696	0.611	0.628
0.011	0.149	0.000	16,020	540	2,700.0	0.0	12,420	1,800.0	0.860	0.612	31,552	22,473	0.638	17,460	36,696	0.740	0.748
0.010	0.094	0.000	11,200	600	400.0	0.0	15,800	1,400.0	0.797	0.711	26,819	23,908	0.712	19,800	33,638	0.822	0.827
0.016	0.079	0.000	8,640	288	0.0	0.0	14,976	1,440.0	0.861	0.695	28,966	23,383	0.688	19,008	33,638	0.815	0.823
0.000	0.108	0.000	10,611	663	568.4	0.0	19,326	947.4	0.773	0.811	25,993	27,267	0.836	24,063	33,638	0.849	0.857
0.000	0.082	0.000	15,600	800	0.0	0.0	21,200	1,200.0	0.804	0.789	27,042	26,531	0.805	24,800	33,638	0.914	0.916
0.000	0.128	0.000	6,261	470	0.0	0.0	19,252	939.1	0.741	0.811	24,939	27,291	0.840	24,730	33,638	0.867	0.876
0.020	0.136	0.007	11,467	267	400.0	0.0	16,000	400.0	0.898	0.891	30,206	29,982	0.818	20,933	33,638	0.749	0.765
0.020	0.050	0.000	12,695	834	568.4	0.0	16,484	1,136.8	0.764	0.756	25,715	25,434	0.716	19,137	33,638	0.793	0.795
0.012	0.183	0.000	8,160	528	360.0	0.0	15,480	900.0	0.767	0.784	25,799	26,388	0.788	21,180	33,638	0.793	0.801
0.000	0.055	0.000	11,880	360	0.0	0.0	16,920	1,800.0	0.872	0.675	29,325	22,717	0.699	20,880	33,638	0.883	0.889
0.011	0.129	0.000	8,434	658	617.1	0.0	14,606	1,131.4	0.734	0.736	24,698	24,743	0.746	19,646	33,638	0.771	0.786
0.000	0.102	0.000	6,840	360	0.0	0.0	13,320	2,520.0	0.800	0.557	26,910	18,735	0.598	18,720	33,638	0.927	0.931
0.024	0.095	0.000	10,800	886	138.5	138.5	14,538	830.8	0.725	0.787	24,390	26,481	0.746	18,277	33,638	0.719	0.732
0.007	0.089	0.000	11,867	533	266.7	0.0	16,267	1,333.3	0.823	0.725	27,684	24,397	0.748	21,733	33,638	0.851	0.866

Proportion of Turning Vehicles			Opposing Through Volume	Opposing Left-turning Volume		Through-Volume		Adjustment Factor for Vehicle Types of Opposing Through Stream	Adjustment Factor for Vehicle Types of Targeted Through Stream	Opposing Through Saturation Flow Rate	Through Saturation Flow Rate	Adjustment Factor for Vehicle Types of Targeted Stream	Observed SFR	Estimated Based SFR	Turning Effect	
$p'_{PC,RT}$	$p'_{MC,LT}$	$p'_{PC,LT}$	$q_{MC,OPT}$	$q_{PC,OPT}$	$q_{MC,OPL}$	$q_{PC,OPL}$	$q_{MC,TH}$	$q_{PC,TH}$	$f_{veh,OPT}$	$f_{veh,TH}$	S_{OPT}	S_{TH}	f_{veh}	S	S_{0w}	f_2	$f_{turn,2}$
[-]	[-]	[-]	[veh/h]	[veh/h]	[veh/h]	[veh/h]	[veh/h]	[veh/h]					[-]	[veh/h]	[veh/h]	[-]	[-]
[22]	[23]	[24]	[25]	[26]	[27]	[28]	[29]	[30]	[31]	[32]	[33]	[34]	[35]	[36]	[37]	[38]	[39]
0.019	0.083	0.000	12,071	678	211.8	0.0	13,659	1,164.7	0.790	0.718	26,575	24,150	0.718	18,847	33,638	0.757	0.787
0.015	0.098	0.000	10,368	576	288.0	0.0	15,696	1,152.0	0.792	0.745	26,630	25,068	0.744	20,880	33,638	0.821	0.837
0.005	0.126	0.000	10,100	600	500.0	0.0	17,000	1,000.0	0.781	0.783	26,272	26,325	0.806	22,900	33,638	0.831	0.847
0.017	0.137	0.000	6,709	818	327.3	0.0	15,218	981.8	0.648	0.767	21,794	25,815	0.759	20,618	33,638	0.796	0.810
0.019	0.121	0.000	9,771	257	128.6	0.0	13,243	1,414.3	0.886	0.675	29,816	22,691	0.685	18,836	33,638	0.803	0.821
0.012	0.158	0.000	12,166	372	372.4	0.0	16,138	869.0	0.871	0.797	29,288	26,793	0.795	21,724	33,638	0.803	0.814
0.000	0.121	0.000	11,600	0	0.0	0.0	21,000	800.0	1.000	0.845	33,638	28,423	0.868	26,400	33,638	0.898	0.904
0.008	0.090	0.000	14,057	857	514.3	0.0	20,057	514.3	0.777	0.889	26,130	29,900	0.878	24,686	33,638	0.825	0.838
0.007	0.062	0.000	13,680	720	432.0	0.0	18,144	1,296.0	0.800	0.750	26,910	25,229	0.761	22,896	33,638	0.886	0.896
0.007	0.102	0.000	13,346	878	175.6	0.0	21,776	526.8	0.764	0.894	25,705	30,085	0.882	26,166	33,638	0.878	0.883
0.000	0.098	0.000	14,143	514	0.0	0.0	17,486	1,542.9	0.851	0.712	28,617	23,935	0.746	22,629	33,638	0.896	0.903
0.005	0.121	0.000	13,388	450	225.0	0.0	17,438	1,170.0	0.860	0.761	28,933	25,592	0.786	23,558	33,638	0.881	0.892
0.004	0.118	0.000	13,770	0	180.0	0.0	19,800	900.0	1.000	0.821	33,638	27,631	0.835	25,020	33,638	0.885	0.892
0.015	0.096	0.000	12,259	730	194.6	0.0	16,054	973.0	0.781	0.778	26,261	26,163	0.772	21,405	33,638	0.808	0.828
0.020	0.119	0.000	13,200	450	150.0	0.0	11,550	1,500.0	0.858	0.635	28,878	21,361	0.653	16,950	33,638	0.751	0.777
0.010	0.162	0.000	11,700	800	300.0	0.0	16,700	700.0	0.758	0.833	25,483	28,005	0.834	22,600	33,638	0.794	0.808
0.008	0.123	0.000	10,533	667	666.7	133.3	13,867	1,200.0	0.771	0.715	25,923	24,058	0.738	18,800	33,638	0.742	0.762
0.015	0.131	0.000	9,900	1,389	514.3	0.0	14,014	1,080.0	0.619	0.737	20,828	24,775	0.737	18,694	33,638	0.744	0.758
0.008	0.116	0.000	11,945	655	490.9	0.0	17,509	981.8	0.794	0.790	26,702	26,581	0.797	22,418	33,638	0.828	0.838
0.000	0.140	0.000	17,800	400	200.0	0.0	17,200	1,200.0	0.901	0.754	30,308	25,366	0.796	23,400	33,638	0.864	0.875
0.013	0.138	0.000	9,062	372	124.1	0.0	15,766	993.1	0.835	0.771	28,093	25,949	0.774	21,228	33,638	0.804	0.818
0.008	0.099	0.000	10,800	540	180.0	0.0	18,360	1,080.0	0.808	0.783	27,169	26,325	0.785	23,040	33,638	0.866	0.873
0.023	0.023	0.000	4,418	491	0.0	0.0	5,891	981.8	0.667	0.583	10,193	8,919	0.578	7,855	15,290	0.879	0.889
0.105	0.053	0.000	5,580	360	180.0	0.0	2,160	720.0	0.767	0.444	11,734	6,796	0.423	3,960	15,290	0.577	0.635
0.077	0.038	0.000	4,737	379	0.0	0.0	3,600	757.9	0.730	0.535	11,158	8,178	0.508	5,874	15,290	0.722	0.767
0.000	0.000	0.000	12,600	900	0.0	0.0	4,950	1,800.0	0.750	0.429	11,468	6,553	0.429	6,750	15,290	1.030	1.030
0.000	0.111	0.000	5,236	655	0.0	0.0	655	1,963.6	0.643	0.211	9,829	3,219	0.250	3,273	15,290	0.843	0.858
0.000	0.222	0.037	7,600	200	0.0	0.0	3,400	600.0	0.886	0.571	13,553	8,737	0.655	7,600	15,290	0.691	0.780
0.074	0.185	0.000	4,286	514	0.0	0.0	2,743	685.7	0.651	0.500	9,956	7,645	0.492	4,971	15,290	0.645	0.670
0.040	0.160	0.000	5,600	800	0.0	0.0	3,200	800.0	0.615	0.500	9,409	7,645	0.583	7,000	15,290	0.723	0.802
0.091	0.000	0.000	4,371	0	0.0	0.0	4,886	257.1	1.000	0.800	15,290	12,232	0.674	7,971	15,290	0.708	0.793
0.082	0.238	0.000	5,478	157	0.0	0.0	2,661	469.6	0.878	0.571	13,425	8,737	0.581	5,854	15,290	0.603	0.688
0.034	0.138	0.000	3,176	508	0.0	0.0	4,235	847.1	0.592	0.545	9,049	8,340	0.561	6,776	15,290	0.773	0.794
0.059	0.176	0.000	5,040	720	0.0	0.0	2,400	720.0	0.615	0.464	9,409	7,099	0.556	6,000	15,290	0.621	0.742
0.029	0.118	0.000	3,600	1,042	0.0	0.0	4,926	568.4	0.471	0.659	7,204	10,078	0.683	8,147	15,290	0.738	0.793

Proportion of Turning Vehicles			Opposing Through Volume	Opposing Left-turning Volume		Through-Volume		Adjustment Factor for Vehicle Types of Opposing Through Stream	Adjustment Factor for Vehicle Types of Targeted Through Stream	Opposing Through Saturation Flow Rate	Through Saturation Flow Rate	Adjustment Factor for Vehicle Types of Targeted Stream	Observed SFR	Estimated Based SFR	Turning Effect	
$p'_{PC,RT}$	$p'_{MC,LT}$	$p'_{PC,LT}$	$q_{MC,OPT}$	$q_{PC,OPT}$	$q_{MC,OPL}$	$q_{PC,OPL}$	$q_{MC,TH}$	$q_{PC,TH}$	$f_{veh,OPT}$	$f_{veh,TH}$	S_{OPT}	S_{TH}	f_{veh}	S	S_{0w}	f_2	$f_{turn,2}$
[-]	[-]	[-]	[veh/h]	[veh/h]	[veh/h]	[veh/h]	[veh/h]	[veh/h]					[-]	[veh/h]	[veh/h]	[-]	[-]
[22]	[23]	[24]	[25]	[26]	[27]	[28]	[29]	[30]	[31]	[32]	[33]	[34]	[35]	[36]	[37]	[38]	[39]
0.000	0.000	0.000	6,120	0	0.0	0.0	10,800	720.0	1.000	0.762	15,290	11,650	0.767	11,880	15,290	1.013	1.012
0.032	0.000	0.000	4,447	212	0.0	0.0	5,506	847.1	0.815	0.600	12,459	9,174	0.609	8,259	15,290	0.861	0.890
0.000	0.061	0.000	4,500	675	0.0	0.0	5,850	1,125.0	0.605	0.554	9,254	8,464	0.603	8,550	15,290	0.917	0.928
0.000	0.000	0.000	0	0	1,200.0	171.4	10,800	1,028.6	1.000	0.697	20,794	14,493	0.720	13,200	20,794	0.870	0.884
0.023	0.000	0.000	0	0	2,057.1	257.1	10,543	257.1	1.000	0.894	20,794	18,582	0.828	12,343	20,794	0.694	0.726
0.000	0.000	0.000	0	0	1,600.0	0.0	16,800	400.0	1.000	0.896	20,794	18,628	0.902	18,400	20,794	0.980	0.981
0.000	0.000	0.000	0	0	0.0	0.0	14,760	540.0	1.000	0.850	20,794	17,675	0.856	16,020	20,794	0.896	0.901
0.019	0.000	0.000	0	0	1,575.0	0.0	11,025	765.0	1.000	0.755	20,794	15,701	0.723	12,915	20,794	0.850	0.861
0.000	0.000	0.000	0	0	0.0	0.0	16,200	720.0	1.000	0.825	20,794	17,146	0.831	17,640	20,794	1.022	1.021
0.000	0.000	0.000	0	0	0.0	0.0	11,700	1,350.0	1.000	0.659	20,794	13,705	0.681	14,400	20,794	1.019	1.017
0.033	0.000	0.000	0	0	4,200.0	0.0	7,800	900.0	1.000	0.659	20,794	13,705	0.636	10,500	20,794	0.767	0.800
0.000	0.000	0.000	0	0	800.0	200.0	9,400	1,280.0	1.000	0.625	20,794	13,003	0.642	11,480	20,794	0.851	0.861
0.015	0.000	0.000	0	0	3,436.4	163.6	9,818	818.2	1.000	0.722	20,794	15,018	0.709	11,945	20,794	0.795	0.814
0.000	0.000	0.000	0	0	0.0	0.0	14,400	900.0	1.000	0.773	20,794	16,068	0.792	17,100	20,794	1.043	1.039
0.000	0.000	0.000	0	0	0.0	0.0	14,400	1,200.0	1.000	0.722	20,794	15,018	0.732	16,400	20,794	1.081	1.078
0.000	0.000	0.000	0	0	1,885.7	0.0	10,629	1,200.0	1.000	0.663	20,794	13,796	0.693	13,543	20,794	0.932	0.940
0.000	0.000	0.000	0	0	2,520.0	360.0	11,520	360.0	1.000	0.868	20,794	18,058	0.886	14,040	20,794	0.730	0.772
0.000	0.000	0.000	0	0	0.0	0.0	15,300	750.0	1.000	0.811	20,794	16,856	0.811	16,050	20,794	0.952	0.952
0.000	0.000	0.000	0	0	720.0	0.0	17,280	0.0	1.000	1.000	20,794	20,794	1.000	18,000	20,794	0.861	0.866
0.027	0.000	0.000	0	0	4,153.8	0.0	9,138	830.8	1.000	0.706	20,794	14,678	0.672	11,354	20,794	0.796	0.816
0.000	0.000	0.000	0	0	1,309.1	163.6	13,255	654.5	1.000	0.810	20,794	16,834	0.826	15,545	20,794	0.895	0.906
0.023	0.000	0.000	0	0	2,160.0	0.0	15,480	0.0	1.000	1.000	20,794	20,794	0.900	16,200	20,794	0.863	0.866
0.000	0.000	0.000	0	0	3,600.0	276.9	13,846	276.9	1.000	0.911	20,794	18,938	0.915	14,954	20,794	0.776	0.788
0.000	0.208	0.000	9,800	200	0.0	0.0	14,400	800.0	0.909	0.792	25,576	22,272	0.833	20,000	28,134	0.848	0.854
0.000	0.282	0.000	9,000	514	0.0	0.0	12,343	771.4	0.787	0.773	22,148	21,740	0.833	19,286	28,134	0.814	0.824
0.000	0.311	0.000	4,500	600	0.0	0.0	11,700	900.0	0.630	0.737	17,714	20,730	0.805	18,600	28,134	0.819	0.822
0.000	0.268	0.000	10,145	655	0.0	0.0	12,436	981.8	0.767	0.732	21,591	20,598	0.797	19,309	28,134	0.854	0.862
0.000	0.207	0.000	13,680	720	0.0	0.0	16,200	360.0	0.800	0.902	22,507	25,375	0.922	21,240	28,134	0.816	0.820
0.000	0.259	0.000	12,000	1,170	0.0	0.0	12,000	900.0	0.692	0.741	19,481	20,858	0.800	18,000	28,134	0.794	0.801
0.000	0.289	0.008	10,368	576	0.0	0.0	12,528	432.0	0.792	0.857	22,272	24,115	0.870	19,296	28,134	0.780	0.790
0.000	0.247	0.012	10,600	600	0.0	0.0	11,800	800.0	0.789	0.759	22,190	21,354	0.781	17,800	28,134	0.803	0.812
0.000	0.227	0.011	16,729	212	0.0	0.0	13,976	211.8	0.941	0.931	26,479	26,180	0.899	18,847	28,134	0.743	0.746
0.000	0.195	0.013	4,235	424	0.0	0.0	12,071	847.1	0.688	0.753	19,342	21,187	0.760	16,729	28,134	0.778	0.784
0.000	0.217	0.011	12,494	847	0.0	0.0	14,824	211.8	0.759	0.934	21,354	26,283	0.903	19,694	28,134	0.773	0.776
0.000	0.207	0.012	8,550	450	0.0	0.0	14,175	225.0	0.800	0.928	22,507	26,095	0.894	18,900	28,134	0.747	0.753

Proportion of Turning Vehicles			Opposing Through Volume	Opposing Left-turning Volume		Through-Volume		Adjustment Factor for Vehicle Types of Opposing Through Stream	Adjustment Factor for Vehicle Types of Targeted Through Stream	Opposing Through Saturation Flow Rate	Through Saturation Flow Rate	Adjustment Factor for Vehicle Types of Targeted Stream	Observed SFR	Estimated Based SFR	Turning Effect	
$p'_{PC,RT}$	$p'_{MC,LT}$	$p'_{PC,LT}$	$q_{MC,OPT}$	$q_{PC,OPT}$	$q_{MC,OPL}$	$q_{PC,OPL}$	$q_{MC,TH}$	$q_{PC,TH}$	$f_{veh,OPT}$	$f_{veh,TH}$	S_{OPT}	S_{TH}	f_{veh}	S	S_{0w}	f_2	$f_{turn,2}$
[-]	[-]	[-]	[veh/h]	[veh/h]	[veh/h]	[veh/h]	[veh/h]	[veh/h]					[-]	[veh/h]	[veh/h]	[-]	[-]
[22]	[23]	[24]	[25]	[26]	[27]	[28]	[29]	[30]	[31]	[32]	[33]	[34]	[35]	[36]	[37]	[38]	[39]
0.000	0.130	0.000	13,680	720	0.0	0.0	14,880	1,200.0	0.800	0.728	22,507	20,489	0.762	19,200	28,134	0.892	0.896
0.000	0.159	0.016	10,246	831	0.0	0.0	13,846	553.8	0.727	0.839	20,461	23,596	0.813	18,000	28,134	0.782	0.789
0.000	0.286	0.018	8,308	277	0.0	0.0	9,969	830.8	0.861	0.722	24,226	20,319	0.747	16,338	28,134	0.768	0.780
0.000	0.213	0.000	12,462	277	0.0	0.0	15,785	553.8	0.902	0.855	25,375	24,056	0.884	21,046	28,134	0.845	0.847
0.000	0.199	0.027	10,643	548	0.0	0.0	10,565	704.3	0.803	0.762	22,602	21,435	0.735	15,183	28,134	0.726	0.737
0.000	0.174	0.022	13,745	982	0.0	0.0	11,455	654.5	0.750	0.787	21,100	22,148	0.762	15,709	28,134	0.724	0.736
0.000	0.231	0.025	10,428	621	0.0	0.0	10,552	620.7	0.781	0.783	21,964	22,018	0.762	15,890	28,134	0.730	0.745
0.000	0.238	0.024	9,853	189	0.0	0.0	10,989	757.9	0.914	0.756	25,708	21,272	0.748	16,863	28,134	0.792	0.804
0.000	0.236	0.011	12,686	686	0.0	0.0	10,629	857.1	0.796	0.728	22,392	20,489	0.752	15,600	28,134	0.733	0.739
0.000	0.233	0.014	8,894	424	0.0	0.0	10,588	1,058.8	0.815	0.688	22,924	19,342	0.712	15,671	28,134	0.780	0.783
0.000	0.233	0.027	7,971	386	0.0	0.0	11,700	514.3	0.813	0.826	22,859	23,241	0.781	17,164	28,134	0.775	0.783
0.000	0.074	0.000	11,314	658	822.9	102.9	13,371	864.0	0.784	0.767	19,189	18,768	0.781	15,367	24,464	0.805	0.805
0.000	0.151	0.000	8,182	409	1,309.1	0.0	12,273	654.5	0.808	0.798	19,759	19,522	0.823	15,218	24,464	0.756	0.756
0.000	0.140	0.000	16,560	720	3,240.0	0.0	12,600	720.0	0.828	0.787	20,246	19,259	0.811	15,480	24,464	0.780	0.780
0.000	0.125	0.000	9,164	327	0.0	0.0	15,382	654.5	0.853	0.831	20,866	20,318	0.848	18,327	24,464	0.883	0.883
0.000	0.064	0.000	15,120	720	0.0	0.0	14,760	1,080.0	0.815	0.746	19,934	18,244	0.766	17,640	24,464	0.939	0.942
0.000	0.128	0.000	10,800	360	180.0	0.0	12,600	900.0	0.861	0.750	21,066	18,348	0.777	15,660	24,464	0.822	0.824
0.000	0.115	0.000	12,150	150	1,650.0	0.0	14,400	600.0	0.943	0.833	23,058	20,387	0.854	17,550	24,464	0.835	0.841
0.000	0.078	0.000	9,138	665	0.0	0.0	11,908	1,218.5	0.747	0.683	18,271	16,709	0.700	14,234	24,464	0.831	0.831
0.000	0.184	0.000	10,400	400	0.0	0.0	15,600	400.0	0.844	0.889	20,642	21,746	0.907	19,600	24,464	0.883	0.883
0.012	0.075	0.000	12,273	491	490.9	0.0	10,964	1,047.3	0.839	0.696	20,518	17,037	0.690	13,484	24,464	0.795	0.800
0.000	0.061	0.000	11,032	697	1,277.4	348.4	11,845	743.2	0.771	0.772	18,862	18,888	0.790	13,982	24,464	0.715	0.727
0.000	0.179	0.000	9,491	0	1,309.1	0.0	14,727	327.3	1.000	0.902	24,464	22,066	0.918	18,327	24,464	0.816	0.816
0.000	0.105	0.000	9,741	847	211.8	0.0	13,553	847.1	0.714	0.773	17,474	18,904	0.792	16,094	24,464	0.831	0.831
0.000	0.189	0.000	11,250	0	450.0	0.0	12,600	900.0	1.000	0.750	24,464	18,348	0.792	17,100	24,464	0.880	0.883
0.000	0.137	0.000	9,900	450	1,350.0	300.0	12,750	450.0	0.821	0.854	20,095	20,901	0.875	15,750	24,464	0.730	0.738
0.000	0.049	0.000	11,100	300	2,100.0	300.0	17,100	300.0	0.884	0.921	21,619	22,522	0.925	18,600	24,464	0.819	0.822
0.000	0.103	0.000	10,080	576	1,440.0	0.0	13,104	720.0	0.787	0.793	19,259	19,409	0.811	15,408	24,464	0.777	0.777
0.007	0.166	0.000	11,381	465	1,625.8	0.0	13,587	348.4	0.836	0.889	20,454	21,746	0.879	16,839	24,464	0.783	0.783
0.000	0.203	0.000	8,585	277	1,384.6	553.8	9,138	664.6	0.865	0.747	21,158	18,271	0.787	12,295	24,464	0.638	0.638
0.020	0.078	0.000	7,714	0	1,028.6	0.0	11,057	771.4	1.000	0.754	24,464	18,448	0.718	13,114	24,464	0.746	0.746
0.000	0.123	0.000	13,114	514	1,542.9	0.0	12,086	771.4	0.841	0.769	20,581	18,818	0.795	14,914	24,464	0.764	0.768
0.000	0.086	0.000	9,900	180	360.0	0.0	14,400	810.0	0.918	0.790	22,459	19,320	0.804	16,650	24,464	0.846	0.846
0.000	0.163	0.000	12,764	327	654.5	0.0	12,764	654.5	0.889	0.804	21,746	19,667	0.833	16,364	24,464	0.799	0.803
0.000	0.041	0.000	4,600	0	1,200.0	0.0	13,200	1,000.0	1.000	0.740	24,464	18,093	0.752	15,200	24,464	0.822	0.827

Proportion of Turning Vehicles			Opposing Through Volume	Opposing Left-turning Volume		Through-Volume		Adjustment Factor for Vehicle Types of Opposing Through Stream	Adjustment Factor for Vehicle Types of Targeted Through Stream	Opposing Through Saturation Flow Rate	Through Saturation Flow Rate	Adjustment Factor for Vehicle Types of Targeted Stream	Observed SFR	Estimated Based SFR	Turning Effect	
$p'_{PC,RT}$	$p'_{MC,LT}$	$p'_{PC,LT}$	$q_{MC,OPT}$	$q_{PC,OPT}$	$q_{MC,OPL}$	$q_{PC,OPL}$	$q_{MC,TH}$	$q_{PC,TH}$	$f_{veh,OPT}$	$f_{veh,TH}$	S_{OPT}	S_{TH}	f_{veh}	S	S_{0w}	f_2	$f_{turn,2}$
[-]	[-]	[-]	[veh/h]	[veh/h]	[veh/h]	[veh/h]	[veh/h]	[veh/h]					[-]	[veh/h]	[veh/h]	[-]	[-]
[22]	[23]	[24]	[25]	[26]	[27]	[28]	[29]	[30]	[31]	[32]	[33]	[34]	[35]	[36]	[37]	[38]	[39]
0.000	0.074	0.000	11,077	831	830.8	276.9	13,015	830.8	0.741	0.769	18,137	18,818	0.789	15,508	24,464	0.798	0.805
0.000	0.094	0.000	9,257	514	1,028.6	0.0	13,886	1,028.6	0.792	0.744	19,367	18,191	0.762	16,457	24,464	0.883	0.883
0.000	0.090	0.000	13,114	257	0.0	0.0	14,657	1,028.6	0.912	0.753	22,318	18,424	0.780	18,257	24,464	0.954	0.957
0.000	0.122	0.000	9,200	800	1,200.0	0.0	13,800	600.0	0.714	0.828	17,474	20,246	0.848	16,800	24,464	0.806	0.810
0.000	0.037	0.000	11,127	0	654.5	0.0	16,364	654.5	1.000	0.839	24,464	20,518	0.844	17,673	24,464	0.856	0.856
0.000	0.189	0.000	15,900	300	1,800.0	0.0	12,300	600.0	0.915	0.811	22,391	19,848	0.841	15,900	24,464	0.773	0.773
0.000	0.175	0.000	9,450	0	900.0	0.0	14,400	450.0	1.000	0.868	24,464	21,245	0.889	18,000	24,464	0.828	0.828

Note. Own Table

C.7.3 Regression Results

The regression output gives the value of intercepts which reflect the effect of right-turning cars, left-turning motorcycles and left-turning cars.

$$f_2 = f_{RT,2} \cdot f_{LT,2} \cdot f_{OPL,2}$$

$$f_{RT,2} = \frac{1}{1 + a_1 P'_{PC,RT}}$$

$$f_{LT,2} = 1 - \frac{a_2 \cdot p'_{MC,LT} + b_2 \cdot p'_{PC,LT}}{1 + (a_2 \cdot p'_{MC,LT} + b_2 \cdot p'_{PC,LT}) \cdot (c_2 + \frac{d_2 \cdot q_{MC,OPT} + e_2 \cdot q_{PC,OPT}}{S_{OPT}})}$$

$$f_{OPL,2} = 1 - \frac{(a_3 \cdot q_{MC,OPL} + b_3 \cdot q_{PC,OPL}) \cdot (c_3 + \frac{d_3 \cdot q_{MC,TH} + e_3 \cdot q_{PC,TH}}{S_{TH}})}{1 + (a_3 \cdot q_{MC,OPL} + b_3 \cdot q_{PC,OPL})}$$

Parameter Estimates

Parameter	Estimate	Std. Error	95% Confidence Interval	
			Lower Bound	Upper Bound
a1	4.464	.279	3.912	5.016
b2	133.187	147.957	-159.279	425.652
c2	4.885	.613	3.674	6.096
a2	2.016	.256	1.510	2.522
d2	-1.428	1.112	-3.626	.771
e2	-15.179	7.114	-29.241	-1.116
a3	.729	.281	.173	1.285
b3	9.351	4.926	-.386	19.087
c3	.788	.149	.493	1.082
e3	-.359	.566	-1.477	.759
d3	-.650	.149	-.946	-.355

ANOVA[a]

Source	Sum of Squares	df	Mean Squares
Regression	99.267	11	9.024
Residual	.146	143	.001
Uncorrected Total	99.413	154	
Corrected Total	1.325	153	

Dependent variable: f_2

a. R squared = 1 - (Residual Sum of Squares) / (Corrected Sum of Squares) = .889.

Note. Own Tables

D Data of Effective Green Time Model

Figure D-1 depicts a method which is used to calculate the components to the effective green time.

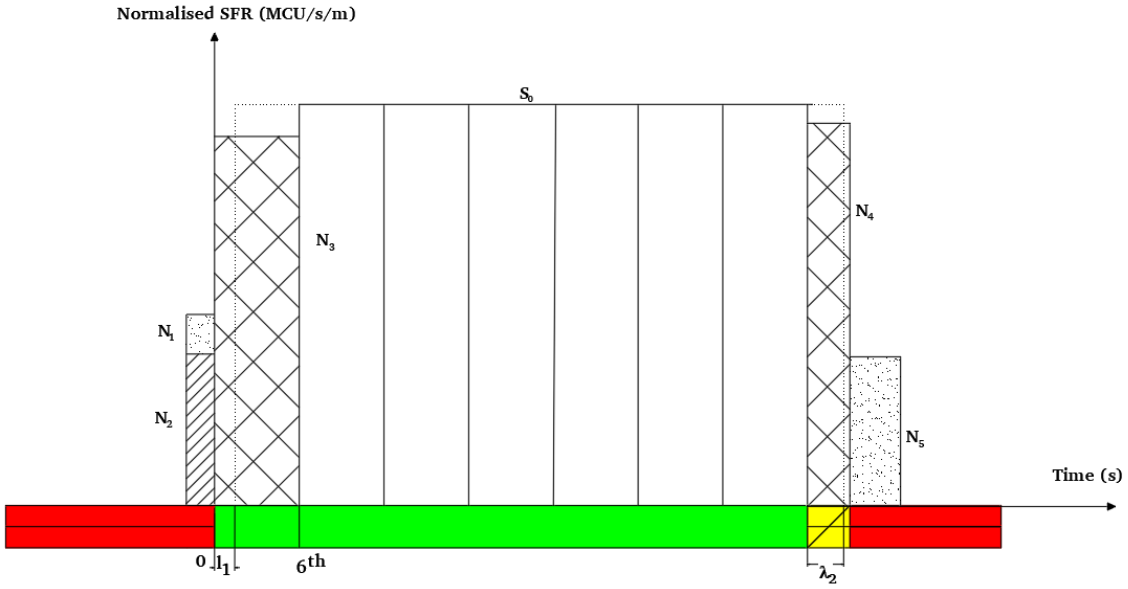

Figure D-1: Effective Green Time Model

Note. Own Graph

D.1 Data of Start-up Lost Time Calculation

Data were collected for estimating the number of motorcycles passing the stop line during the different periods. Figure D-1 and Table D-1 give information about observed data and how they are measured. All data are illustrated from column [1] to column [10]. Each data is expressed as follows:

[1] = Approach width
[2] = Number of motorcycles stopping over the stop line during the red time
[3] = Number of motorcycles passing the stop line during the red time
[4] = Number of motorcycles departing over the stop line during the first 6-second green period

[1]: [2], [3], [4] were observed from field survey

$$[5]=\frac{[2]}{[1]};[6]=\frac{[3]}{[1]};[7]=\frac{[4]}{[1]}$$

$$[8]=\frac{S_0}{3600}=\frac{3058}{3600}=0.849 \text{ (mcu/s)}$$

$$[9]=6-\frac{[7]}{[8]};\ [10]=6-\frac{[5]+[6]+[7]}{[8]}$$

Table D-1: Raw Data and Calculated Parameters for Start-up Lost Time Model

	Approach Width	Number of Motorcycles			Number of Motorcycles of a 1 m wide Approach			SFR of a 1 m Wide Approach	Start-up Lost time	
	w	n_1	n_2	n_3	N_1	N_2	N_3	S_0	$l_{1,nor}$	$l_{1,max}$
No.	[m]	[mcu]	[mcu]	[mcu]	[mcu/m]	[mcu/m]	[mcu/m]	[mcu/(s*m)]	[s]	[s]
	[1]	[2]	[3]	[4]	[5]	[6]	[7]	[8]	[9]	[10]
1	9.00	2	18	27	0.222	2.000	3.000	0.849	2.47	-0.15
2	9.00	0	12	37	0.000	1.333	4.111	0.849	1.16	-0.41
3	9.00	8	10	30	0.889	1.111	3.333	0.849	2.08	-0.28
4	9.00	4	15	28	0.444	1.667	3.111	0.849	2.34	-0.15
5	9.00	4	15	28	0.444	1.667	3.111	0.849	2.34	-0.15
6	9.00	2	10	33	0.222	1.111	3.667	0.849	1.68	0.11
7	9.00	7	17	26	0.778	1.889	2.889	0.849	2.60	-0.54
8	9.00	9	12	26	1.000	1.333	2.889	0.849	2.60	-0.15
9	9.00	1	9	44	0.111	1.000	4.889	0.849	0.24	-1.06
10	9.00	4	9	33	0.444	1.000	3.667	0.849	1.68	-0.02
11	9.00	3	5	33	0.333	0.556	3.667	0.849	1.68	0.64
12	9.00	9	10	27	1.000	1.111	3.000	0.849	2.47	-0.02
13	9.00	6	9	28	0.667	1.000	3.111	0.849	2.34	0.38
14	9.00	1	16	29	0.111	1.778	3.222	0.849	2.21	-0.02
15	9.00	1	19	27	0.111	2.111	3.000	0.849	2.47	-0.15
16	9.00	3	5	30	0.333	0.556	3.333	0.849	2.08	1.03
17	9.00	5	3	42	0.556	0.333	4.667	0.849	0.51	-0.54
18	9.00	2	3	31	0.222	0.333	3.444	0.849	1.95	1.29
19	9.00	1	5	29	0.111	0.556	3.222	0.849	2.21	1.42
20	9.00	2	10	27	0.222	1.111	3.000	0.849	2.47	0.90
21	9.00	7	5	30	0.778	0.556	3.333	0.849	2.08	0.51
22	9.00	4	20	40	0.444	2.222	4.444	0.849	0.77	-2.37
23	9.00	9	11	42	1.000	1.222	4.667	0.849	0.51	-2.11
24	4.00	7	0	12	1.750	0.000	3.000	0.849	2.47	0.41
25	4.00	2	2	18	0.500	0.500	4.500	0.849	0.70	-0.47
26	4.00	1	0	15	0.250	0.000	3.750	0.849	1.59	1.29
27	4.00	2	5	12	0.500	1.250	3.000	0.849	2.47	0.41
28	4.00	0	0	15	0.000	0.000	3.750	0.849	1.59	1.59
29	4.00	1	0	15	0.250	0.000	3.750	0.849	1.59	1.29
30	4.00	0	1	14	0.000	0.250	3.500	0.849	1.88	1.59
31	4.00	1	0	13	0.250	0.000	3.250	0.849	2.17	1.88
32	4.00	2	3	15	0.500	0.750	3.750	0.849	1.59	0.11
33	4.00	2	0	14	0.500	0.000	3.500	0.849	1.88	1.29
34	4.00	2	0	12	0.500	0.000	3.000	0.849	2.47	1.88
35	4.00	2	1	12	0.500	0.250	3.000	0.849	2.47	1.59
36	4.00	0	3	13	0.000	0.750	3.250	0.849	2.17	1.29
37	4.00	2	1	16	0.500	0.250	4.000	0.849	1.29	0.41
38	4.00	2	4	12	0.500	1.000	3.000	0.849	2.47	0.70
39	4.00	0	2	18	0.000	0.500	4.500	0.849	0.70	0.11

No.	Approach Width	Number of Motorcycles			Number of Motorcycles of a 1 m wide Approach			SFR of a 1 m Wide Approach	Start-up Lost time	
	w	n_1	n_2	n_3	N_1	N_2	N_3	S_0	$l_{1,nor}$	$l_{1,max}$
	[m]	[mcu]	[mcu]	[mcu]	[mcu/m]	[mcu/m]	[mcu/m]	[mcu/(s*m)]	[s]	[s]
	[1]	[2]	[3]	[4]	[5]	[6]	[7]	[8]	[9]	[10]
40	4.00	5	1	14	1.250	0.250	3.500	0.849	1.88	0.11
41	4.00	2	5	17	0.500	1.250	4.250	0.849	1.00	-1.06
42	4.00	0	1	15	0.000	0.250	3.750	0.849	1.59	1.29
43	4.00	0	0	17	0.000	0.000	4.250	0.849	1.00	1.00
44	4.00	0	1	17	0.000	0.250	4.250	0.849	1.00	0.70
45	4.00	1	0	13	0.250	0.000	3.250	0.849	2.17	1.88
46	4.00	5	1	13	1.250	0.250	3.250	0.849	2.17	0.41
47	4.00	1	0	16	0.250	0.000	4.000	0.849	1.29	1.00
48	4.00	2	0	16	0.500	0.000	4.000	0.849	1.29	0.70
49	4.00	0	0	13	0.000	0.000	3.250	0.849	2.17	2.17
50	4.00	0	0	12	0.000	0.000	3.000	0.849	2.47	2.47

Note. Own Table

Distributions start-up lost time are drawn in Figure D-2 and Figure D-3.

Bin	Frequency	umulative %
0	0	0.00%
0.5	1	2.00%
1	8	18.00%
1.5	4	26.00%
2	12	50.00%
2.5	23	96.00%
3	2	100.00%
More	0	100.00%

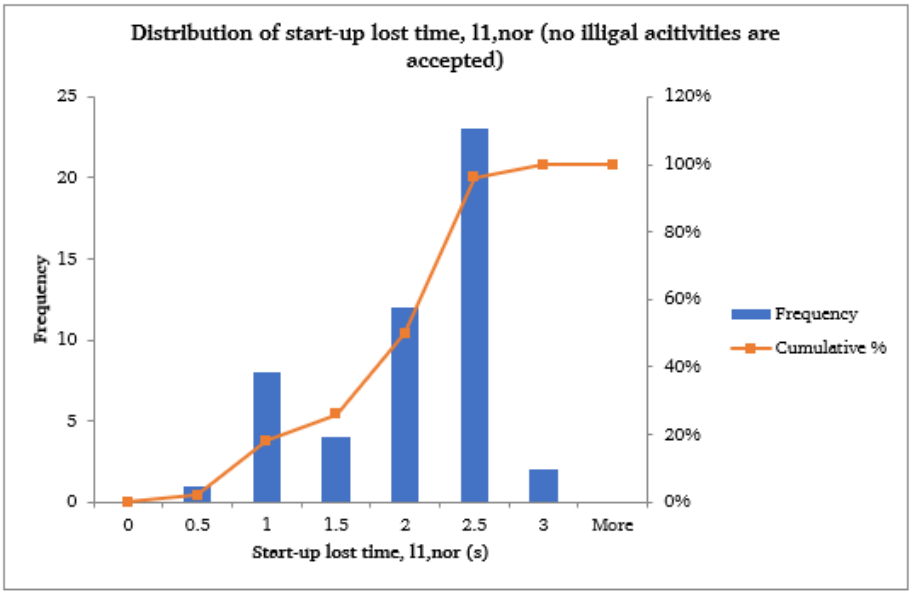

Figure D-2: Distribution of Start-up Lost time, no Illegal Activities are considered

Note. Own Table and Graph

Bin	Frequency	umulative %
-2.5	0	0.00%
-2	2	4.00%
-1.5	0	4.00%
-1	2	8.00%
-0.5	2	12.00%
0	11	34.00%
0.5	9	52.00%
1	8	68.00%
1.5	8	84.00%
2	6	96.00%
2.5	2	100.00%
More	0	100.00%

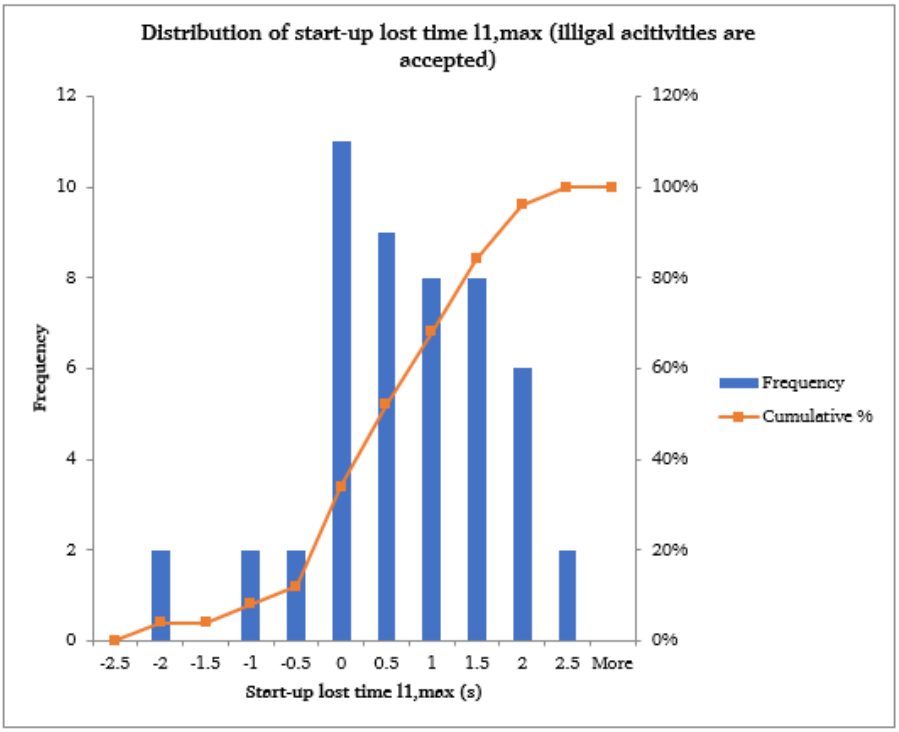

Figure D-3. Distribution of Start-up Lost Time, Illegal Activities are considered

Note. Own Table and Graph

D.2 Data of Green End-lag Time Calculation

Table C-22, Figure C-5 give information about observed data and how they are estimated. All the data are illustrated from column [1] to column [8]. Each data is expressed as follows:

[1] = Approach Width
[2] = Number of motorcycles stopping over the stop line during the red time
[3] = Number of motorcycles passing the stop line during the red time
[4] = Number of motorcycles departing over the stop line during the first 6-second green period

[1]: [2], [3], [4] were observed from field survey

$$[5]=\frac{[2]}{[1]};[6]=\frac{[3]}{[1]};[7]=\frac{[4]}{[1]}$$

$$[8]=\frac{S_0}{3600}=\frac{3058}{3600}=0.849 \text{ (mcu/s)}$$

$$[9]=6-\frac{[7]}{[8]};\ [10]=6-\frac{[5]+[6]+[7]}{[8]}$$

Table D-2: Raw Data and Calculated Parameters for Start-up Lost Time Model

No.	Approach Width	Number of Motorcycles		Number of Motorcycles of a 1 m wide Approach		SFR of a 1 m wide Approach	Green End-lag Time	
	w	n_4	n_5	N_4	N_5	S_0	$\lambda_{2,nor}$	$\lambda_{2,\max}$
	[m]	[mcu]	[mcu]	[mcu/m]	[mcu/m]	[mcu/(s*m)]	[s]	[s]
	[1]	[2]	[3]	[4]	[5]	[6]	[7]	[8]
1	9.00	18	6	2.039	0.667	0.849	2.40	3.18
2	9.00	18	5	2.039	0.556	0.849	2.40	3.05
3	9.00	18	1	2.039	0.111	0.849	2.40	2.53
4	9.00	18	2	2.039	0.222	0.849	2.40	2.66
5	9.00	18	2	2.039	0.222	0.849	2.40	2.66
6	9.00	18	7	2.039	0.778	0.849	2.40	3.32
7	9.00	18	5	2.039	0.556	0.849	2.40	3.05
8	9.00	18	4	2.039	0.444	0.849	2.40	2.92
9	9.00	18	8	2.039	0.889	0.849	2.40	3.45
10	9.00	18	2	2.039	0.222	0.849	2.40	2.66
11	9.00	18	1	2.039	0.111	0.849	2.40	2.53
12	9.00	18	3	2.039	0.333	0.849	2.40	2.79
13	9.00	18	3	2.039	0.333	0.849	2.40	2.79
14	9.00	18	2	2.039	0.222	0.849	2.40	2.66
15	9.00	18	7	2.039	0.778	0.849	2.40	3.32
16	9.00	18	2	2.039	0.222	0.849	2.40	2.66
17	9.00	18	3	2.039	0.333	0.849	2.40	2.79
18	9.00	18	1	2.039	0.111	0.849	2.40	2.53
19	9.00	18	4	2.039	0.444	0.849	2.40	2.92
20	9.00	18	12	2.039	1.333	0.849	2.40	3.97
21	9.00	18	4	2.039	0.444	0.849	2.40	2.92
22	9.20	19	0	2.039	0.000	0.849	2.40	2.40
23	9.20	19	0	2.039	0.000	0.849	2.40	2.40
24	9.20	19	2	2.039	0.217	0.849	2.40	2.66
25	9.20	19	6	2.039	0.652	0.849	2.40	3.17
26	9.20	19	0	2.039	0.000	0.849	2.40	2.40
27	9.20	19	3	2.039	0.326	0.849	2.40	2.78
28	9.20	19	0	2.039	0.000	0.849	2.40	2.40
29	9.20	19	5	2.039	0.543	0.849	2.40	3.04
30	9.20	19	5	2.039	0.543	0.849	2.40	3.04
31	9.20	19	3	2.039	0.326	0.849	2.40	2.78
32	9.20	19	1	2.039	0.109	0.849	2.40	2.53
33	9.20	19	6	2.039	0.652	0.849	2.40	3.17
34	9.20	19	1	2.039	0.109	0.849	2.40	2.53
35	9.20	19	0	2.039	0.000	0.849	2.40	2.40
36	9.20	19	3	2.039	0.326	0.849	2.40	2.78
37	9.20	19	8	2.039	0.870	0.849	2.40	3.42
38	9.20	19	1	2.039	0.109	0.849	2.40	2.53
39	9.20	19	5	2.039	0.543	0.849	2.40	3.04
40	9.20	19	3	2.039	0.326	0.849	2.40	2.78
41	9.20	19	1	2.039	0.109	0.849	2.40	2.53
42	9.20	19	3	2.039	0.326	0.849	2.40	2.78

Note. Own Table

Distributions green end-lag time (in case of illegal activities are considered) are drawn in Figure D-4.

Bin	Frequency	Cumulative %
2	0	0.00%
2.5	5	11.90%
3	24	69.05%
3.5	12	97.62%
4	1	100.00%
More	0	100.00%

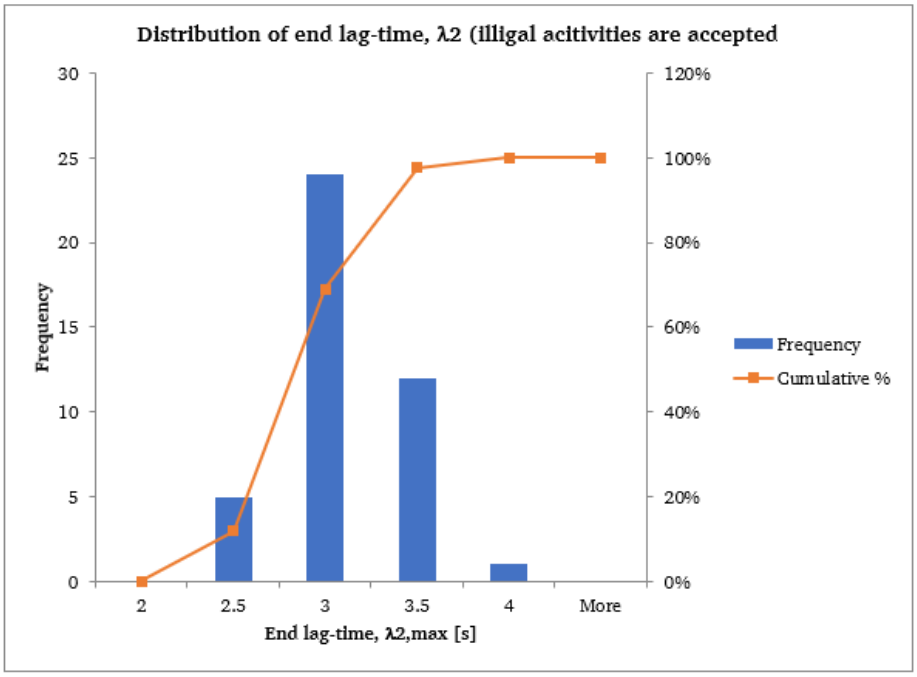

Figure D-4. Distribution of Green End-lag Time, Illegal Activities are considered

Note. Own Graph